Sheffield Hallam University

A Sheffield Hallam University thesis

ProQuest Number: 10694264

ProQuest 10694264

A DIELECTRIC STUDY OF SYSTEMS

EXHIBITING MOLECULAR ASSOCIATION

BY

MICHAEL HUGH BOYLE

This thesis has been submitted in partial fulfilment
of the requirements for the award of the Degree of
Doctor of Philosophy of the Council for National
Academic Awards.
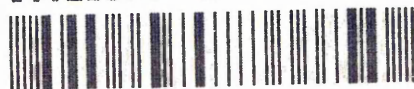
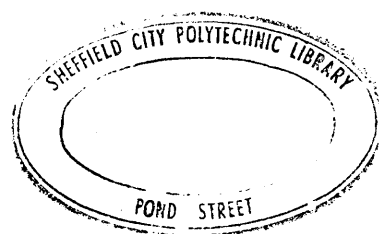Sheffield City Polytechnic
July 1979

ABSTRACT

A dielectric study of systems exhibiting molecular
association by Michael H Boyle.

Time domain spectroscopic methods have been developed
and in combination with bridge methods have provided
interpretable data on selected alcohol-water systems and
micellar solutions of nonionic surfactants.

Dielectric relaxation studies have shown that addition of
water to an alcohol causes a reduction in the relaxation
time of the principal dispersion which for all compositions
is Debye-type. The relaxation behaviour has been inter-
preted using a model based on hydrogen-bond rupture and
subsequent dipole reorientation. The possibility of
relaxation times being modified by the formation of
associated species has been examined.

Static permittivites of the polyoxyethylene dodecyl
ether surfactants $C_{12}E_n$ (n = 4, 6 and 8) and Brij 30 in
binary mixtures with water are interpreted as originating
from normal micelles at all compositions. In $C_{12}E_4$ and
Brij 30 mixtures, the behaviour at higher surfactant
concentrations is most successfully described by hetero-
geneous mixture equations for spherical dispersions;
deviations at low surfactant concentration are attributed
to either oblate spheroidal micelle shape or secondary
aggregation of micelles. Axial ratios for oblate
spheroids have been calculated using equations derived
in this work. In mixtures containing higher n-ethylene
oxides, the heterogeneous mixture approach becomes
progressively less applicable because of smaller micelle
size and an increasing contribution of molecular
association between surfactant headgroups and water.

Static permittivities of $C_{12}E_4$ and Brij 30 in ternary
mixtures with water and an n-alkane are attributed to
normal micelles at some compositions and inverted micelles
at others. Results for microemulsions of $C_{12}E_4$ have been
interpreted as indicating micellar inversion in which
normal spherical micelles change to oblate spheroidal
with increasing temperature and then invert to form prolate
spheroidal and finally spherical inverted micelles. Axial
ratios for both types of spheroidal shape have been
calculated.

CHAPTER 3 : Experimental

Chapter 1 Introduction

1.1 Alcohol-water mixtures – Introduction

Since the explicit recognition of the existence of the hydrogen bond, there has appeared a very extensive number of papers dealing with such bonding (1). In alcohols, H-bonding frequently leads to the association of molecules into clusters ranging from dimeric complexes up to large chain-like structures.

In pure alcohols, complex equilibria exist between single, unassociated molecules commonly referred to as monomers, and a large number of H-bonded species, both of the open linear and closed cyclic type referred to as multimers (2). A number of authors have suggested specific association complexes for the pure alcohols involving small sized clusters such as the tetramer (3, 4) but the weight of evidence is now in favour of association involving long chains (5, 6). Studies of alcohol-water mixtures have led to the suggestion of small complexes involving four alcohol molecules and one water molecule in some alcohol-water mixtures (7, 8). In contrast to alcohol-water mixtures, molecular association in binary and ternary mixtures involving surfactants leads to micelle formation involving aggregation of a large number of molecules (9, 10, 11, 12).

This thesis describes an attempt to gain more information on molecular association using dielectric methods, where the associated mixtures under investigation have been:

(1) alcohol-water mixtures,

(2) micellar solutions of non-ionic surfactants in binary mixtures with water and ternary mixtures with hydrocarbons and water.

1.1.1 Alcohols

A variety of techniques including dielectric methods have been applied to the study of liquid alcohols. In dielectric studies, information on molecular association has been obtained from two basic aspects, namely:

(i) Static permittivity, and

(ii) Dielectric relaxation.

1.1.1.1 Static Permittivity

Association between molecules arises from short range interactions due to H-bonding with near neighbours. Such interactions were neglected in the earlier theories of Debye (13) and Onsager (14), but were included in the later theory of Kirkwood (15).

In order to account for short range interactions, Kirkwood introduced a dimensionless correlation parameter 'g', the so called g-factor, which indicates an average parallel orientation of

neighbouring dipoles when g > 1, whereas an
average anti-parallel orientation is indicated by
g < 1.

An open linear chain will give g > 1 whereas a
closed structure will give g < 1.

Chain dimer structures for alcohols are
illustrated in Figure 1.

Figure 1
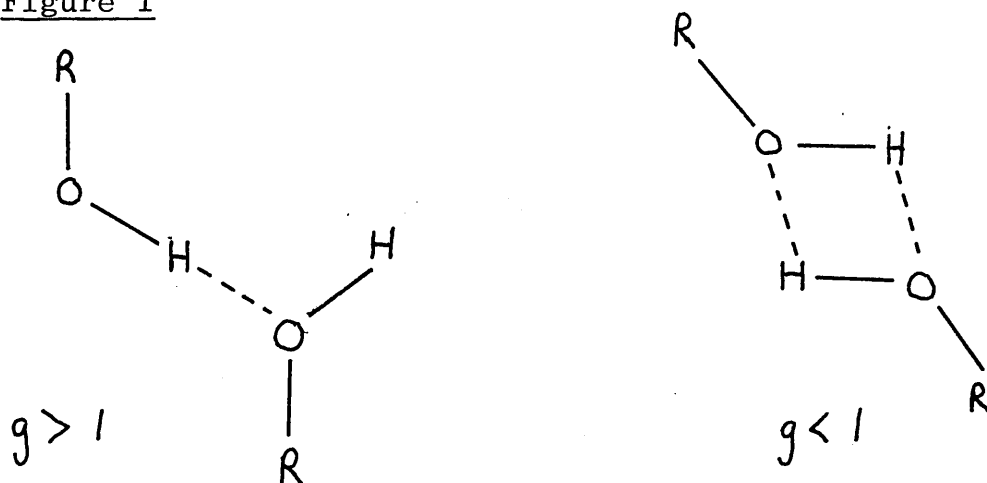
The Kirkwood-Fröhlich equation (Chapter 2
equation $\boxed{2.3}$) has been used to determine g-values
for alcohols. The values obtained will be subject
to some error due to uncertainty concerning the
appropriate value of ε_∞. In the extensive early
determinations of Dannhauser and Cole (16), a
"somewhat arbitrary" choice of ε_∞ = 2.4 was
adopted as a "reasonable compromise" between the
value given by the high frequency limiting value
of the principal dispersion, and that given by

- 3 -

n^2 (n = refractive index). In later works, the
value selected has ranged between 1.0 n^2 (17)
and 1.1 n^2 (18).

Garg and Smyth (19) studied C_3 to C_{10} n-alcohols
over a range of frequencies up to 136 GHz.
Comparison of the interpolated ε_∞ values with
refractive index data by the same authors
indicates that the assumption that ε_∞ = kn^2
where k lies between 1.0 and 1.1 is justified,
although the scarcity of high frequency data
points gives some uncertainty. In contrast,
results for the secondary alcohol cyclohexanol
(20) suggest a rather higher value for ε_∞, and in
the absence of detailed experimental relaxation
data for alcohols other than the normal type, it
is possible that the ε_∞ values for such alcohols
may be significantly in error. However, despite
this uncertainty in ε_∞, it is well established that
for the n-alcohols g is significantly greater
than unity, being typically within the range 2.5
to 3.1 at room temperature (16, 18, 21),
indicating extensive self-association of the
open linear type.

Similarly high g-values have been reported for
other alcohols such as the secondary alcohol
cyclohexanol (17) indicating similar association.

Tertiary butanol has $g = 2.12$ at 25° C (18) indicating some degree of steric hindrance to linear association. In contrast, for more sterically hindered alcohols such as the octanol isomers 2 methyl- and 3 methyl 4 heptanol values of $g \simeq 1$ and $g < 1$ have been reported (22), indicating the presence of closed structures

Many authors have suggested that the behaviour of the n-alcohols and other unhindered ones such as the secondary alcohol cyclohexanol is most satisfactorily explained on the basis of association involving long chains of indefinite length (eg 6, 16, 17).

Using a method for calculating the g-factor which was an extension of the earlier work of Oster and Kirkwood (23), Dannhauser and Cole (16) considered a model of infinite chains of doubly H-bonded molecules.

It was assumed that there exists a distribution of chains of varying lengths governed by the association equilibria:

$$(ROH)_n + (ROH) \rightleftharpoons (ROH)_{n+1}$$
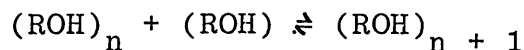
with equilibrium concentrations governed by an equilibrium constant K given by

$$K = \frac{C_{n+1}}{C_n C_1} = \frac{1}{C_0} \exp\left(\frac{\Delta H - T\Delta S}{RT}\right)$$

where C_n = concentration of polymer

$\quad\quad C_o$ = gross monomer concentration

$\quad\quad \Delta H$ = activation enthalpy

and $\quad \Delta S$ = activation entropy

The authors obtained the following approximate expression for the mean g-value of an n-membered chain, $\bar{g}_n$, in which the group moments along the O-H and O-R bonds were 1.55 D and 1.20 D respectively with the ROH bond angle = 105°:

$$\bar{g}_n = 2.40 + \frac{2.00}{n} \quad (n > 1)$$

$$\text{and } g_1 = 1$$

The mean g-factor $\bar{g}$ was then given by

$$\bar{g} = \frac{1}{C_o} \sum_{n=1}^{\infty} n\bar{g}_n C_n = 2.39 - 2.00\alpha^{\frac{1}{2}} + 0.61\alpha$$

where α is defined by $\dfrac{C_1}{C_o} = (1 - KC_o\alpha)^2$

For ΔH in the range 25 to 35 k J mol^{-1} and ΔS in the range 65 to 105 J mol^{-1}K^{-1}, they reported that the temperature dependence of g in butyl alcohols was satisfactorily accounted for, but the low temperature value of g = 2.39 for 1 butanol was too low, even when the uncertainty in the experimental value of g due to uncertainty in ε_∞ was included.

They suggested that this discrepancy in g was at least partly due to the "crude assumptions" of the

model with the assumption that K is independent of n being particularly doubtful.

In a subsequent paper, Dannhauser and Bahe (18) reported g values for C_1, C_2 and C_3 alcohols in addition to the C_4 data and values for all the alcohols were given for a wide range of temperatures. For MeOH, the values of ΔH and ΔS were rather lower than for the other alcohols and for all the alcohols, the authors noted that the ΔS values were considerably more negative than those given by Pimentel and McClellan (1). Although this discrepancy was noted, it was not discussed. The success in giving the correct temperature dependence of g is considered significant but the discrepancies between both the low temperature values of g with experimental values and that of ΔS with literature data reveals limitations in the approach.

An alternative approach favoured by some authors has been one based on a smaller association complex of specific size. Fletcher (4) favoured an open tetramer and Bordewijk et al (3) favoured a closed tetramer where the g value is greater than unity because the hydroxyl groups are not all in the same plane. It should be noted that, in contrast with the chain association model, neither

Fletcher nor Bordewijk et al calculated g-values
for these specific sized complexes. In addition,
the more recent work of Bordewijk et al (24)
favoured a large open structure of unspecified
size for pure alcohols.

As dilution of alcohols in non-polar solvents
reduces the self-association of the alcohol, such
studies have been extensively performed in order
to gain information on possible association
complexes. The experimental data for diluted
alcohols appears to be adequately accounted for
by association models involving equilibria of
monomers, dimers, trimers and possibly tetramers.
(4, 24, 25, 26).

It is considered that whilst there is much detail
concerning association complexes in alcohols still
to be resolved, the weight of evidence is
essentially in favour of the long chain model for
unhindered alcohols, whereas when steric hindrance
is significant, association is often limited to
small closed complexes such as dimers, trimers and
tetramers. Further, dilution of unhindered alcohols
in non-polar solvents also reduces association to
similar small size complexes.

1.1.1.2 Dielectric Relaxation

Relaxation studies have revealed that the dielec-

tric dispersion of unhindered alcohols may be described by three relaxation times, τ_1, τ_2 and τ_3 where $\tau_1 > \tau_2 > \tau_3$ (19, 20). The principal dispersion is due to the τ_1 process and if A_1, A_2 and A_3 represent the amplitudes of each dispersion, it is generally assumed that these three regions describe the entire dipolar relaxation behaviour of the alcohol, ie

$$A_1 + A_2 + A_3 = \varepsilon_S - \varepsilon_\infty$$

where ε_∞ is the high frequency limiting value of the dispersion. The highest frequency dispersion region (ie τ_3) is generally attributed to reorientation of the OH groups in free monomers around the C-O bond (19).

There is some disagreement concerning the cause of the τ_2 dispersion. Garg and Smyth (20), Jakusek and Sobczyk (27) and Crossley (28) have suggested that it is due to monomer rotation but Glasser et al (29) suggested that τ_2 is a mean of monomer values with either small multimers or a polymer chain segment such as an -OR group rotating about its bond.

By far the most pronounced dispersion is that associated with the τ_1 process and at present the interpretation is the least clear. For the n-alcohols τ_1 increases regularly with increasing alkyl chain length, ranging from

54.4 ps for MeOH (30) to 2.019 ns for 1 decanol
at 20° C (19) and the dispersion is Debye-type
(single relaxation time). Sterically-hindered
alcohols such as 3 methyl 4 heptanol do not
exhibit the τ_1 relaxation and it is thus sensitive
to the steric environment of the OH group.

There are two basic approaches in the explanation
of the τ_1 dispersion. The first is based on chain
like association following the model of Kauzmann (31
-33) which considered dielectric relaxation in
terms of H-bond rupture followed by rotation of
monomers, where H-bond rupture is the rate
determining step. Dannhauser and Flueckinger (5)
studied isomeric methylheptanols and observed
Debye-type relaxation for all the liquids studied
but the activation energies for the dispersion
were found to be sensitive functions of the isomer
structure. This led them to conclude that H-bond
rupture is not the rate determining step but
rather a prerequisite for dipolar reorientation.
They suggested that, because the local structure
remains on average chain-associative, dipolar
reorientation is, of necessity, co-operative and
occurs relatively infrequently; but when it does
occur they suggested that the orientation rate is
dependent on both the shape and size of the
molecule since both of these properties will

affect the interaction between a molecule and its near neighbours. Campbell et al (34) suggested that on the basis of the Dannhauser and Fleuckinger model (5), a monotonous shortening of τ_1 on dilution would be expected due to reduced molecular association but for C_2 to C_6 alcohols in cyclohexane, these authors observed an initial lengthening of τ_1 on dilution. They added that co-operative effects by the solvent would not be expected since in cyclohexane solute – solvent interactions were minimal. An initial increase of τ on dilution was also reported by Sagal (35) for ethanol in cyclohexane, Hanna (36) for 1 butanol in tetralin and decalin, van den Berg et al (37) for 1 butanol in hexane and tetrachloromethane and Komooka (38) for 1 hexanol in cyclohexane. In contrast, both 1 propanol and 1 butanol exhibited a monotonous fall in τ_1 on dilution in the more electron donating solvents 1, 4 dioxane, benzene, chlorobenzene and pyridine (39). Sagal (35) suggested that the observed behaviour could be explained on a model where H-bond rupture and dipole reorientation occur when a monomer molecule approaches the associated chain with its oxygen favourably orientated for a 'switch', where the oxygen may be present in a monomer or at the end of a chain structure.

Figure 2

Switch Model
of Sagal (35)

R ── O

R

O

H

H

O ── H

R
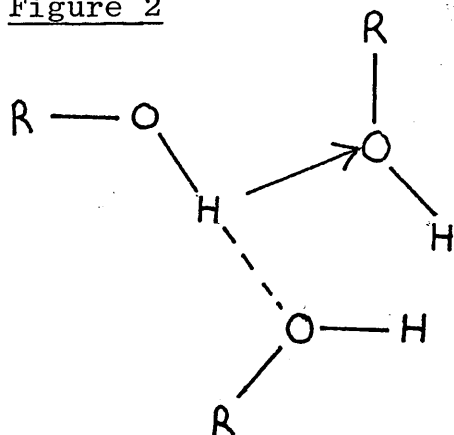
The initial lengthening of τ_1 was attributed to a solvent-screening effect giving increased resistance to rotation due to the presence of more bulky cyclohexane molecules.

A similar 'switch' interpretation was suggested by Campbell et al (34), but these authors suggested that in the pure alcohol, the linearly associated chains become entangled which thus increases the proximity of all molecular species enabling the switch to be more rapid. With initial dilution, the chains become less entangled without becoming shortened, thus increasing τ_1. On further dilution, there is an increase in the fraction of unbonded oxygen atoms as the chain structure is broken thus again reducing τ_1.

The results of van den Berg et al (37) revealed

an increase in τ on dilution to approximately
0.5 mf of alcohol and that over the range of
concentrations in which τ increased, the
g-factor remained constant at the pure alcohol
value. Below 0.5 mf of alcohol, both τ and g
decreased. The authors suggested that the close
correspondence between τ and g indicated that the
dielectric relaxation was due to linear multimers,
but the authors did not make proposals concerning
the size of such multimers.

Campbell et al (34) made no reference to the data
of van den Berg et al but the observed relation
between g and τ could be accounted for on the
"entangled-chain" model if the behaviour over the
range of concentrations from pure alcohol down to
0.5 mf is attributed to chains becoming less
entangled in such a way that the net association
between entangled chains is such that the g-factor
is unaffected. This is not an unreasonable prop-
osal since entangled chains would not be
expected to produce a highly ordered lattice-type
structure, thus in some regions an increase in g
will occur, whereas in others there will be a
reduction in g so that, on average, the net change
in g is zero. Further, since the g-values of pure
alcohols can be adequately accounted for without
reference to entangled chains, it seems reasonable

to assume that such entangled chains do not affect the measured average g-factor.

The 'solvent screening' proposal of Sagal (35) is considered more difficult to reconcile with the data of van den Berg et al (37) since if such screening is the cause of the observed initial increase in τ on dilution, it would be reasonable to expect that the g-factor would be affected due to reduced association which is not in accord with the experimental data.

The other approach in explaining the τ_1 dispersion has been due to Bordewijk et al (3) who suggested that the only associated species in the pure alcohol is a highly polar cyclic tetramer which is retained during reorientation. This model satisfactorily accounts for the Debye-type relaxation of the τ_1 process but it was disputed by Campbell et al (34) on the basis of observed similar relaxation times for C_2 to C_{10} n-alcohols diluted to below 0.3 mf in a non-polar solvent (34, 19) where the principal dispersion was Debye-type down to quite low concentrations. These authors suggested that, since several associated polar species are likely to exist in similar proportion at these low concentrations, their observations "throw considerable doubt" on

Bordewijk's hypothesis.

It should be added that the presence of similar proportions of several associated polar species at low concentrations has been confirmed by infra red data (4).

It is considered that, although the mechanism of the τ_1 dispersion is not yet fully accounted for, since the existence of self-association involving long chains is reasonably firmly established, a mechanism of H-bond rupture, and thus chain breakage, followed by reorientation is at present the most satisfactory. A model based on the 'switch' proposal of Sagal seems particularly suitable with the entangled-chains suggestions of Campbell et al (34) rather than solvent screening being preferred.

1.1.2 Water

The dielectric properties of water have been extensively studied and have been considered in detail in recent treatises by Hasted (40) and Grant et al (42).

1.1.2.1 Static Permittivity ε_s

The static permittivity of water is accurately described by the expression

$$\varepsilon_s = 87.740 - 0.4008T + 9.398 \times 10^{-4}T^2 - 1.410 \times 10^{-6}T^3$$

where T is the temperature in $^{\circ}$C (43).

It is well established that liquid water has a high degree of short range order and thus, since ε_s is high, the Kirkwood g-factor would be expected to be substantially higher than unity. Determination of g-values using the Kirkwood-Fröhlich equation [2.3] has posed considerable difficulty however, since at present the appropriate value of ε_∞ is still unresolved. If the value corresponding to the high frequency limit of the principal dispersion is adopted following Hill (44), a value of $g \simeq 1$ at 25° C is obtained which, as Grant et al (42) noted, is rather unlikely.

Zafar et al (45) proposed that a second relaxation process occurs in the far infra-red region which had a value of ε_∞ of 1.8 ($= n^2$). When equation [2.3] is applied, a value of $g = 2.8$ is obtained. However, Afsar and Hasted (46) have suggested that the dielectric behaviour in the far infra-red region is better explained in terms of a resonance absorption process, rather than one of relaxation, thus the value of ε_∞ must be regarded as still undetermined.

Theoretical approaches to account for the magnitude of ε_s and its temperature dependence,

together with g-factor estimations, have been applied by a number of authors.

X-ray studies by Bernal and Fowler (47) established that water molecules, like ice, are tetrahedrally H-bonded. Two basic types of approach commonly adopted to describe liquid water behaviour have been

(i) the bond bending model (47, 48), and

(ii) characterisation of water by a significant number of broken bonds together with the presence of some zero bonded molecules (49, 50).

Pople (48) developed a model in which the majority of H bonds were regarded as distorted rather than being broken. He assumed that all molecules in liquid water are H-bonded to 4 neighbours each at a fixed distance $\bar{R}_O$. The nearest neighbour was thus constrained to be $\bar{R}_O$ distant from the central molecule, but the distances from the central molecule to the second, third and further neighbours will be dependent on the extent of bond-bending. This is illustrated in figure 3.

Figure 3
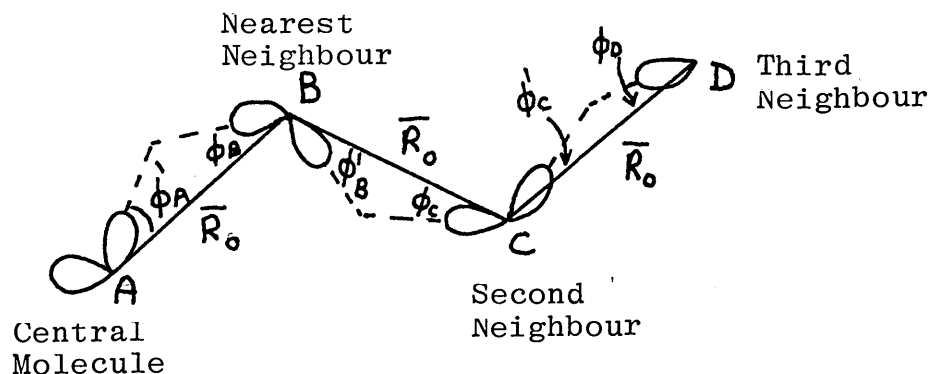
Each lobe represents either an O-H bond or a lone
pair of electrons. He further assumed that each
water molecule is exactly tetrahedral so that the
angles between O-H bond directions and lone pair
directions are all arc cos $(-\frac{1}{3})$. On this model
an H-bond is considered undistorted when both the
O-H of a donor water molecule and the lone pair
to which it is H-bonded lie along the oxygen-oxygen
line of the two molecules, giving zero bond-
bending energy when all the H_2O--H_2O--H_2O angles
are tetrahedral as in ice I. When either the lone
pair direction or the O-H bond direction depart
from the oxygen-oxygen line by an angle $\emptyset$ the bond
is distorted, giving an increase in the energy of
the system ΔU given by:

$$\Delta U = k_\emptyset (1 - \cos \emptyset)$$

where $k_\emptyset$ is called the H-bond bending force
constant. The radial distribution function of

the second and third neighbours was derived by

statistical mechanics and analytical geometry

and the value of $k_\emptyset$ which gave the best fit with

X-ray diffraction data was selected. Application

of the Kirkwood theory to this model predicted a

temperature dependence of ε_s in close agreement

with experiment but the absolute values of ε_s

were too low. This discrepancy has been

attributed to neglect of the field contribution

from further neighbours and revised calculations

by Eisenberg and Kauzmann (51) have given ε_s

values in close agreement with the experimental

ones. Pople also obtained satisfactorily high

g-factor values of 2.60 at 0° C falling to 2.46

at 83° C.

Using a model of water characterised by a

significant proportion of broken bonds, Haggis et

al (50) considered water as a statistical assembly

of molecules forming 0, 1, 2, 3 and 4 bonds with

surrounding neighbours. By assuming that the

probability of H-bond forming or breaking is the

same for all bonds, with the probability of a

given type of bond, i-j, being broken given by

$m_{ij} f_1(T) \exp\left[\frac{-\Delta H}{RT}\right]$ where $f_1(T)$ is a function

and m_{i-j} is the number of bonds of type i-j between two water aggregates

of temperature only. The probability of a given

bond being formed at the same time was given by

$n_{i-1} \cdot n_{j-1} f_2(T,p)$ where $f_2(T,p)$ is a function

both of the temperature and the condition of the

surrounding water molecules. Under equilibrium:

$$m_{ij} f_1(T) \exp \left(\frac{-\Delta H}{RT} \right) = n_{i-1} \cdot n_{j-1} f_2(T,p)$$

Following Pauling (52), the authors considered

that the latent heat of vaporisation, L, is made

up of two parts, the heat necessary to overcome

the van der Waals forces (W) and the heat

required to break the remaining H bonds, of which

there are two per molecule; giving:

$$p = 100 \left(1 - \frac{L-W}{2\Delta H} \right)$$

The value of p at $0°$ C was obtained using dielectric

data and assuming the van der Waals forces were

temperature invariant, using $\Delta H = 19$ k J mol^{-1},

both the value of ε_s and its temperature

dependence could be accounted for. G-factor

values were calculated for the four types of

associated structures with a value of g = 2.81 at $0°C$

being obtained for the four molecule complex.

Recent developments have been molecular dynamics

calculations by Rahman and Stillinger (53) on a

sample of water containing 216 rigid molecules

with the assumption that each oxygen atom is

surrounded by a tetrahedral arrangement of four

point charges. At the single temperature of

$34.3°$ C, these authors obtained a value of

g = 2.72.

All the theoretical approaches considered here give g-values substantially higher than unity as expected from the well-established high degree of correlation in the liquid. The values are also notably similar to the value of 2.8 at $25°C$ obtained from equation $\boxed{2.3}$ when the value of ε_∞ of 1.8 given by Zafar et al (48) is used.

1.1.2.2 Dielectric Relaxation

The dielectric relaxation of water is characterised by a relaxation time τ of 9.3 ps at $20°$ C which exhibits a small distribution of values with the relaxation time spread parameter $\alpha = 0.013$ (equation $\boxed{2.8}$) at this temperature (41).

Grant et al (42) suggested that the value of τ indicates that it is related to the movement of individual molecules rather than clusters. These authors added that the molecular dynamics calculations of Rahman and Stillinger (53), which used a model based on individual molecules, gave a value of $\tau = 6.7$ ps at $34.3°$ C, which compares very favourably with the experimental value of 5.6 ps thus giving further support to the monomer reorientation interpretation.

Grant and Sheppard (54) have suggested that the small distribution of relaxation times could be explained using a bond breaking model in which

the distribution is attributed to different H
bond strengths between symmetrically and
asymmetrically two-bonded water molecules, where
in the symmetrical case the H-bonding involves
either both protons or both orbitals associated
with lone pair electrons whereas in the
asymmetrical case the H-bonds are one of each
type. The dielectric relaxation was attributed
to the rate formation of one-bonded molecules
from two-bonded molecules.

1.1.3 Alcohol-water Mixtures

1.1.3.1 Static Permittivity ε_s

Since the static permittivity of water is higher
than that of any of the alcohols, using simple
additivity rules, it would be expected that the
addition of water to alcohols would result in a
steadily increasing value of ε_s as the water
content is increased. This behaviour was
observed by Akerlof (55) and Decroocq (56) in
methanol, ethanol and n-propanol-water mixtures.
However, work on longer alkyl chain alcohols has
revealed a fall in permittivity with increasing
water content and, in some cases, the presence
of a minimum value for ε_s .

This effect was observed by Brown and Ives (7) in
t-butanol water mixtures, Lawrence et al (8) in
cylcohexanol-water mixtures, and D'Aprano (57)

in 1-pentanol-water mixtures. Brown and Ives suggested that the effect was due to the formation of a relatively long life water-centred aggregate in which four alcohol molecules are H-bonded to one water molecule (4A/W). This interpretation was also favoured by Lawrence et al from viscosity, nmr and dielectric data. The latter authors reported dipole moment calculations based on the assumption of free rotation of the alcohol molecules about the H-bonds connecting them to the central water molecule which revealed that a decrease in ε_s occurs with addition of water, when linear multimers larger than tetramers are present in the anhydrous alcohol; but if the multimers are cyclic, the formation of the 4A/W complex leads to an increase in ε_s. Using this approach, these authors were able to satisfactorily account for the variation of ε_s with water content for a number of alcohols, together with its temperature dependence. The water-centred 4A/W complex model was also favoured by Lippold and Adel (58) from dielectric, viscosity and nmr studies of n-octanol-water mixtures.

Tjia (59) disputed the 4A/W complex model and suggested that the divergence of the behaviour of ε_s upon the addition of water to different alcohols was due to differences in the structure

of the corresponding complexes. In contrast
to the monotonous increase in ε_s when water is
added to ethanol, Tjia observed that, at low
temperatures, the addition of water to mixtures
of ethanol with the non-polar solvent
methylcyclopentane caused an initial reduction
in ε_s. This was interpreted as indicating that
the type of complex is highly sensitive to the
density of hydroxyl groups of alcohol molecules
and that allowance should be made for the
existence of at least two kinds of complex. It
was suggested that one complex gave rise to a
relatively high dipole moment and the other a
relatively low dipole moment where the former
dominates at high densities of hydroxyl groups
of alcohol molecules. This dominance of the
former at high densities led Tjia to conclude
that it contains more alcohol molecules than the
low moment type.

Tjia suggested that the high dipole moment
complex was one containing two α multimers
(ie multimers with g > 1) joined by one water
molecule with their dipole moments aligning.
He added that proposed forms of the association
complexes were highly speculative due primarily
to uncertainty concerning the structure of the
α multimers.

In the absence of a proposed structure for the
α multimers, the suggestion of an aggregate in
which two such multimers are joined by one water
molecule is considered unsatisfactory.

Hasted (40, 41) has calculated g-values for a
number of alcohol-water mixtures by assuming
that $g_1 = g_2 = g$ in equation $[2.6]$ and using
early experimental values for the static
permittivity, refractive index and gas-phase
dipole moment data. He noted that the theory had
limitations due to neglect of cross-correlation
terms arising from the correlation of dipoles
of species 2 with those of species 1.

The calculations revealed that for methanol-
water mixtures, as the alcohol content is
increased from zero, the g-factor increases to a
maximum at approximately 0.4 mole fraction (mf)
of alcohol at 20° C with a shift to lower mf at
higher temperatures. N-propanol-water mixtures
exhibited a minimum in the g-factor at
approximately 0.5 mf whereas t butanol-water
mixtures exhibited a progressive fall in g with
added alcohol to 0.6 mf above which g remained
almost constant.

The results for methanol-water mixtures were
interpreted as indicating a structure-making effect

which maximises the g-factor. Conversely for
the propanol-water mixtures, a structure-breaking
effect which is most pronounced at about 0.5 mf
was suggested.

In view of the fact that alcohol-water mixtures
contain two highly associated components, neglect
of cross-correlation terms is probably an unjustified
assumption which makes the results of the
calculations open to some doubt. This view is
strengthened by the proposals given by various
authors for the existence of a 4A/W complex which
indicates the importance of cross-correlation
effects.

1.1.3.2 Dielectric Relaxation

The relaxation behaviour of mixtures of polar
liquids has been discussed by Davies (60). The
author suggested that, if the relaxation process
consists in single molecule reorientation, a
binary polar mixture should show separate
absorption centres corresponding to the
relaxation times of the two components. Further,
if the volume participating in the molecular
relaxation was sufficiently large to have a
composition indistinguishable from the overall
average, then only a single absorption effect would
be observed. This interpretation was proposed by

Schallamach (61) from dielectric dispersion
studies of a number of binary mixtures of polar
liquids.

Only one relaxation process was observed if both
components were associated or if both were
unassociated whereas mixtures of an associated
with an unassociated liquid exhibited two separate
relaxations. Davies (60) noted that the results
conformed to a general pattern in that the more
compatible pairs of liquids, eg two alcohols, two
ethers, bromide and aldehyde, appeared to merge
molecularly, thus giving the observed single
relaxation whereas the less compatible mixtures of
an alcohol with a bromide or an alcohol with an
ether could exhibit molecular segregation due to
the strong self-association of the alcohol
molecules thus giving two separate relaxations.

However, Schallamach's results were obtained only
for a restricted frequency range and in order to
traverse the dispersion region, the measurements
were performed over a range of temperatures. This
procedure was rightly criticised by Davies (60)
on the basis that varying temperature also varies
permittivity, viscosity and solubility values.
In particular, it was suggested that the range of
temperatures used would have probably exceeded the

solubility limit for mixtures such as 1 propanol with isoamyl bromide, thus causing phase separation effects.

Daumezon and Heitz (62) studied binary mixtures of an alcohol with an alkyl halide at temperatures between 120 and 160 K and similarly observed two separate relaxations, thus confirming the observations of Schallamach for such mixtures. These authors attributed the Debye-type lower frequency dispersion to relaxation of the alcohol and the higher frequency dispersion, which was not Debye-type, was attributed to a co-operative process between a weakly associated species involving alkali halide molecules and alcohol monomers.

Studies of mixtures of alcohols by Denney and Cole (63) and Bordewijk et al (3) did not reveal resolution of component features but simply a progressive shift from characteristics of the one alcohol to those of the other, thus indicating that these mixtures could be considered to have effectively provided a single environment.

If such behaviour were exhibited by alcohol-water mixtures, the principal dispersion should exhibit a progressive decrease in relaxation time with increasing water content. This behaviour has

been reported by Chekalin and Shakhparonov in methanol and 1 propanol-water mixtures (64, 65). Similarly, Peyrelasse (66) observed the effect in methanol-water mixtures. Chekalin et al attributed the relaxation to two single Debye-type dispersions and interpreted the dielectric behaviour using a chain association model where water molecules replaced alcohol molecules in the H-bonded chain. Their chain model for the alcohol-water mixture exhibited the unusual feature of an alcohol oxygen atom being involved in H-bonding to the hydrogen atoms of two other molecules. These results of Chekalin et al also showed that addition of water produced an increase in the relaxation time of the higher frequency τ_2 dispersion. This effect was not commented upon.

Peyrelasse (66) considered that the principal dispersion was more accurately described by a Cole-Cole arc relation (equation $\boxed{2.8}$) with parameter α exhibiting a maximum value of 0.083 at about 65% by weight of alcohol (corresponding to about 0.5 mf). The author noted that this peak in α occurred at a similar composition to the peak at 0.4 mf of alcohol in the g-factor for methanol-water mixtures calculated by Hasted (41).

This approximate correlation of the peak in α

with the peak in g led Peyrelasse to conclude that addition of methanol to water increases the molecular association. In the absence of other $data$ in which a maximum in the spread of relaxation times, α, is related to molecular correlation, g, this proposal is considered unacceptable.

Tjia (59) observed a fall in relaxation time for alcohol-water mixtures of 1, 2, 3 and 4 heptanol on the addition of water up to 0.15 mf. The principal dispersion for 1 heptanol-water mixtures was Debye type but the 2, 3 and 4 heptanol-water mixtures exhibited Cole-Davidson skewed-arc behaviour where the β-parameter decreased monotonously with increasing water content. In order to interpret the relaxation behaviour, Tjia suggested two possibilities. In the first case, he considered his results could be explained on the basis of cyclic alcohol-water complexes of varying size. Alternatively, the results were considered to be due to dielectric friction effects associated with dipole-dipole interactions in linear structures based on a proposal that in alcohol-water mixtures which exhibit a fall in static permittivity ε_s on addition of water, such as the heptanols at higher temperatures, a decrease in the energy of the

dipole-dipole interaction also occurs. This was suggested as being quite plausible on the basis that the dipole-dipole interaction energy contributes to the activation energy ΔG and using a Kauzmann type relation (31): $\tau = \tau_0 \exp \left(\frac{\Delta G}{kT} \right)$ a decrease in ΔG would be accompanied by a fall in relaxation time τ which is in agreement with Tjia's experimental observations. He considered that a fall in ε_S is likely to cause the dipolar reorientation to be less hindered, giving a reduction in friction on the dipole. It was pointed out that this approach would also account for the observed properties of ethanol-water mixtures where addition of water causes a monotonous increase in ε_S and Hassion and Cole (21) had reported a monotonous increase in relaxation time τ on addition of water to ethanol up to 5% by mass.

An increase in τ on addition of water was also reported by Sarojini (67) in methanol-, ethanol-, 2 propanol- and 1 butanol-water mixtures up to approximately 4% by volume of water, with the effect being most pronounced in the 1 butanol mixtures. These mixtures also exhibit a monotonous increase in ε_S on addition of water, giving further support for Tjia's dielectric friction interpretation.

However, the relaxation data of Sarojini for methanol-water mixtures is in disagreement with the more recent data of Chekalin et al (64) and Peyrelasse (66). Further, more recent measurements by Buck (68) revealed a decrease in τ as water is added to ethanol which is in disagreement with the results of Hassion and Cole (21) and Sarojini (67). More recent measurements have thus established that addition of water to both methanol and ethanol reduces the relaxation time. Since it is well established that for both of these alcohols, addition of water also increases the static permittivity ε_S, it would appear that the relationship between τ and ε_S proposed by Tjia on the basis of dielectric friction is incorrect.

The more recent measurements on methanol and ethanol-water mixtures, in which addition of water causes a reduction in relaxation time, are in accord with those of Chekalin and Shakhparonov for 1-propanol-water and Tjia for 1, 2, 3 and 4 heptanol-water mixtures and it appears that addition of water to alcohols causes a reduction in relaxation time regardless of whether the static permittivity increases or decreases on addition of water.

The only exception to this trend is the data of

Tjia (59) on 3 heptanol-water mixtures at the low
temperatures $- 60^{\circ}$ and $- 70^{\circ}C$, particularly the
$- 70^{\circ}$ data. At these temperatures, Tjia observed
a minimum in ε_S and obtained values of τ which
remained almost constant with water content over
the range 0.02 to 0.15 mf of water. In contrast,
at higher temperatures where a minimum in ε_S was
not exhibited, a steady decrease in τ with
increasing water content was observed. The author
suggested that the different relaxation behaviour
of the 3 heptanol-water mixtures at low temperatures
could have been due to the mixture being no longer
homogeneous, which is clearly a possibility at
temperatures of $- 60^{\circ}$ and $- 70^{\circ}$ C.

1.1.3.3 <u>Summary</u>

Since particularly strong support for a specific
association complex (4A/W) arose from studies of
t butanol- and cyclohexanol-water mixtures in
which a minimum in ε_S is observed (7, 8), it was
considered that dielectric relaxation studies on
aqueous mixtures of these two alcohols might give
further information on the proposed (4A/W) complex.

In addition, since it has been suggested that
steric factors limit the association in t butanol
to small size complexes (69), which is in contrast
with cyclohexanol for which chain-like association

has been proposed (17), it was considered that
the dielectric relaxation of aqueous mixtures of
these two alcohols might exhibit significantly
different behaviour.

It was therefore decided to study the dielectric
relaxation of alcohol-water mixtures of both
t butanol and cyclohexanol. Since the experi-
mental data of Sarojini (67) for both methanol-
and ethanol-water mixtures appears to be in error,
it was considered possible that her data for
1 butanol-water mixtures might also be erroneous.
In view of this, it was decided to include some
studies of the relaxation of 1 butanol-water
mixtures. In addition, some measurements on
1 heptanol-water mixtures have been included in
order to confirm or otherwise the trend revealed
in the lower temperature studies of Tjia (59).

1.2 <u>Micellar solutions of non-ionic surfactants in</u>
    <u>binary mixtures with water and ternary mixtures</u>
    <u>with water and hydrocarbons</u>

1.2.1 <u>Introduction</u>

In dilute aqueous solution, the behaviour of non-
ionic surface active agents (surfactants) often
resembles that of simple organic molecules, but
at higher concentrations of surfactant, pronounced
deviation from this simple behaviour occurs (9, 10).
Examples of physical properties which have been

found to be exhibiting these deviations are inter-facial tension, viscosity, electrical conductivity and specific heat (9).

The well-defined, but not abrupt, changes are attributed to the association of molecules into micelles and the concentration of surfactant at which micelles appear is known as the critical micelle concentration (CMC). The micelle may be anionic, cationic, zwitterionic or non-ionic, depending on the chemical structure of the surfactant.

Non-ionic surfactants are characterised by CMC values that are typically about a factor of 100 lower than ionic surfactants containing comparable oleophilic groups. This is due to the absence of the counterion layer which reduces the electro-static repulsion between the charged surfactant headgroups at the micelle-solvent interface in ionic surfactants. Commercial non-ionic surfactants such as those with a polar headgroup based on ethylene oxide contain a range of ethylene oxide group sizes and are thus termed polydisperse in contrast to the monodisperse pure surfactant.

Becher (11) has pointed out that, although a large number of non-ionic surfactants prepared by

commercial processes are polydisperse, "it is
to be expected that their properties will be close
to that of the homogeneous compound having the
composition of the mean". However, Shinoda et al
(10) have pointed out that impurity and poly-
dispersity effects introduce a certain degree of
ambiguity into the determination of surfactant
properties and suggested that experiments with pure
materials or mixtures 'of known composition would be
"highly desirable". Further, Shinoda and Kunieda
(70) have shown that solubilisation of oil (or
water) is higher when the surfactant is monodisperse
than when it is in a polydisperse form.

1.2.2   Micellar Structure

Surfactants are characterised by a polar headgroup
which has hydrophilic properties, and is thus at
the micelle-water interface in an aqueous solution
of a surfactant and, further, these headgroups
will be hydrated by a number of water molecules.
The other part of a surfactant molecule is
typically a hydrocarbon chain which will therefore
have oleophilic properties.

It would be thus expected that in an aqueous
mixture containing a small proportion of surfactant
which is in excess of the CMC, a representative
spherical micellar structure would be as in

figure 4. (9).

Figure 4

Aqueous Continuous Phase

Polar Headgroup
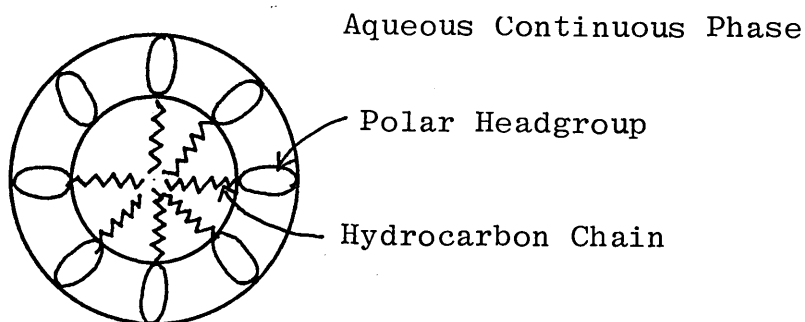
Hydrocarbon Chain

The hydrocarbon (oily) portion of the surfactant
is inside the micelle which may be thus referred
to as an oil-in-water (O/W) structure. Such a
micellar structure is called a normal micelle,
whereas an arrangement in which the polar head-
groups are at the centre is called an inverted
micelle. Whilst an inverted micelle would not be
expected in a binary mixture of surfactant and
water at low surfactant concentration, in ternary
mixtures with a hydrocarbon as the third component
such inverted structures would be possible. In
non-ionic surfactants, reduced H-bonding causes the
hydrophilic behaviour of the polar headgroup to
decrease rapidly at higher temperatures and is
accompanied by dehydration. This causes an increase
in the aggregation number of the micelle and
produces "giant" micelles (10, 11). Above a certain
temperature known as the cloud point, the mixture
turns turbid and at a somewhat higher temperature it

begins to separate into two phases (11). This turbidity is generally attributed to reorganisation, growth and eventual bursting of the micelles associated with dehydration of the polar headgroup (71) which is followed by the formation of a separate surfactant-rich phase.

1.2.3 Micellar Shape

Although many authors have assumed that micelles are spherical in shape (eg 9, 10, 72, 73), Tanford et al (74) have reported that for aqueous solutions of polyethylene glycol dodecyl ethers ($C_{12}E_n$) where n $\geqslant$ 8, comparison of calculated and observed Stokes radii revealed an oblate spheroidal shape with axial ratios ranging from 1.5:1 for $C_{12}E_{23}$ up to 2.5:1 for $C_{12}E_8$. Theoretical calculations of micellar free energy by Tanford (75) also favoured an oblate spheroidal shape.

Tanford et al (74) also suggested that for aqueous solutions of $C_{12}E_n$ where n < 8, a distinctly different mode of association believed to be the result of secondary aggregation occurs. These authors reported the work of Elworthy and Macfarlane (76) and Attwood (77) in support of this interpretation. Tanford et al (74) added that this secondary aggregation effect was strongly temperature dependent since $C_{12}E_6$, which formed

large aggregates at 25° C or above only formed single micelles at 5° C (78, 79).

Secondary aggregation effects rather than an increased aggregation number as the cloud point is reached were suggested by Staples and Tiddy (80) from nmr studies of $C_{12}E_6$ micelles. The authors differed in respect of whether or not the secondary aggregation involves association of polyoxyethylene chains between different micelles. Such association was favoured by Tanford et al but Staples and Tiddy reported that calculations of the average distance between micelles gave a figure which was too large for association to occur. These authors instead suggested an interpretation based on the change in the balance between hydration forces and van der Waals forces. The hydration force arises due to the attraction between the polar headgroups and water and gives a repulsive force between the oily aggregates whereas the van der Waals force causes an attraction between the oily aggregates. The authors suggested that since dehydration of non-ionic surfactants occurs when the temperature is increased, the hydration-repulsion force will also decrease with increasing temperature. This change of hydration-repulsion force was suggested as causing a balance between this force and the van der Waals force at the cloud point, resulting in

secondary aggregation. It was added that similar effects should occur in all pure non-ionic surfactants with water just below the cloud point.

Bostock et al (81) have shown, from nmr studies of self diffusion in aqueous solutions of $C_{12}E_6$ with mass fractions of surfactant between 0.1 and 1, that normal micelles are present at all compositions including the pure surfactant. In contrast, Friberg et al (86) reported that in surfactant-rich aqueous solutions of $C_{12}E_4$, no micelles had been detected. In the absence of details of the experimental methods used, it is difficult to evaluate the assertion of an absence of micelles. It is possible that failure to identify micelles could have been due to the micellar structures being of small size and thus outside the measurement limits of the technique used by Friberg et al.

In contrast to possible small micelles in surfactant-rich solutions, Bostock (83) has reported that, in water-rich solutions of the surfactant $C_{12}E_4$ and its commercial counterpart Brij 30, which has an average alkyl chain length of twelve and an average ethylene oxide chain length of four, large micelles occur. In addition, some marked differences between $C_{12}E_4$ and Brij 30

have been reported in both binary mixtures with water and ternary mixtures with heptane.

1.2.4 Microemulsions

Ternary mixtures containing a surfactant, water and an oily component often form an optically transparent liquid phase. With non-ionic surfactants, the clear phase is often observed over appreciable composition ranges (82, 84, 85, 86, 87).

A representative phase diagram is given in figure 5.

Figure 5

[Based on (82)]

Oil

$/\!/\!/$ ≡ 20° C

$/\,/\,/$ ≡ 40° C

Water $C_{12}E_n$ ($\bar{n}$ = 4)
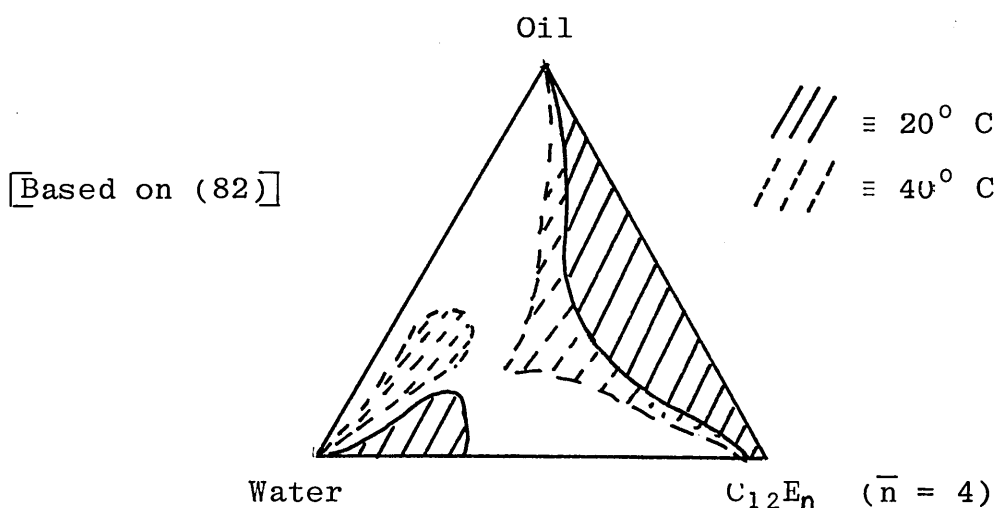
Some of the clear phases contain normal micelles (W/O) and others contain inverted micelles (O/W). In ternary systems containing appreciable proportions of both oil and water where the micelles become very large, these clear phases are frequently referred to as microemulsions, following the proposal of Schulman (88). Although micro-emulsions of both ionic and non-ionic surfactants

are currently attracting much interest, there is
still "disagreement, confusion and controversy"
(89) concerning use of the title microemulsions.
Shah et al (89) suggested that this is due to a
lack of complete characterisation of the molecular
association and aggregation in such systems. In
order to show the relative order of the size of the
dispersed phase in various systems, the authors
proposed a classification of droplet size as
follows:

Molecular solutions   : size 0 to 1 nm

Micellar solutions   : size 1 nm to 10 nm

Microemulsions   : size 10 nm to 100 nm

Colloidal dispersions : size 100 nm to 1 μm

Macroemulsions   : size 1 μm to 10 μm

For microemulsions, Friberg (90) proposed that the
droplet sizes be in the range 20 to 80 nm, whereas
Prince (91) proposed 10 nm to 200 nm. Thus,
although there is some disagreement about the
precise upper and lower limits for the size of the
dispersed phase, there is a consensus that droplet
sizes are substantially larger than those of
micellar solutions.

There have been two basic approaches in the theory
of microemulsion stability, and these have been
discussed in the review by Prince (91). One
theory considers a microemulsion as a two phase

- 42 -

system, resembling an emulsion in being thermo-
dynamically unstable (92), where the surfactant
is adsorbed between two mutually insoluble liquids
causing one liquid to be spontaneously dispersed
in the other due to transient interfacial forces
(93, 94). The other theory considers a micro-
emulsion to be a thermodynamically stable one phase
system of swollen micelles where the surfactant
organises itself into colloidal aggregates which,
under appropriate conditions, can bind water or
oil (95, 96). A recent article by Crooks (97)
suggested that, at present, the experimental
evidence favours the swollen micellar approach.
Prince (91) noted that either theory "can and is
being used" to formulate microemulsions.

Emulsions stabilised with non-ionic surfactants
such as polyethylene glycol alkyl ethers generally
form O/W emulsions at low temperatures and W/O
emulsions at higher temperatures (87, 98), and
there is thus a temperature at which the emulsion
type changes. This temperature is usually referred
to as the phase inversion temperature (PIT). Phase
inversion effects have also been reported in micro-
emulsions (84, 86, 87). In addition to O/W and W/O
micellar structures, Shinoda et al (70, 87, 99-
102 have reported that, at temperatures close to the
PIT, another isotropic liquid phase may be obtained.

This phase is called the surfactant phase and is observed as an isolated region, corresponding to about 10% by mass of surfactant, in the three component phase diagrams (82, 84, 85). Shinoda and Kunieda (87) suggested that the surfactant phase consists of lamellae of water and hydrocarbon with the surfactant as the continuous phase. From studies of ternary mixtures of the surfactants polyethylene glycol dodecyl ether ($C_{12}E_n$), Friberg et al (86) suggested that the presence of spherical micelles, in addition to planar structures, in the isotropic surfactant phase could not be ruled out. These authors considered that their results could be broadly accounted for by considering that in both normal and inverted micellar solutions, the micelles were spherical. However, the authors also observed anomalous hydrocarbon solubilisation behaviour and this was attributed to deviations from spherical shape.

1.2.5 <u>Dielectric Properties</u>

1.2.5.1 <u>Ionic Surfactants</u>

In contrast to alcohols and water, the dielectric properties of aqueous mixtures of surfactants have received very little attention and where studies have been reported, they have been primarily on ionic surfactants (103, 104, 105, 106, 107). Due to the presence of the counterion layer between

the polar headgroup of the surfactant and the
continuous aqueous phase, substantial
differences between the dielectric behaviour of
ionic and non-ionic surfactant micellar mixtures
would be expected.

In micellar solutions of anionic surfactants, a
typical structure will be as given in figure 6,
(9).

Figure 6

Aqueous
Bulk Phase

Counterions

$d_1 \equiv$ core 10 - 28 $\overset{o}{A}$

$d_2 \equiv$ Stern layer
up to a few $\overset{o}{A}$

$d_3 \equiv$ Gouy-Chapman
double layer
up to a few
hundred $\overset{o}{A}$
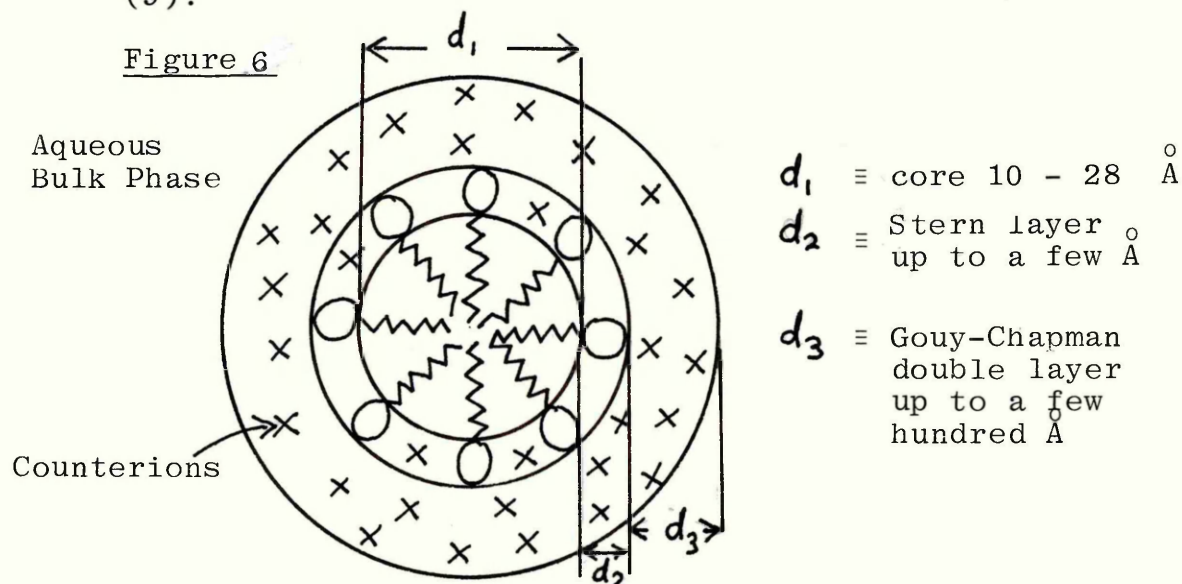
The thick double layer would be expected to
give an important and possibly dominating
contribution to the dielectric properties. The
electrical properties of counterion layers have
been considered in detail by O'Konski (108) who
showed that such layers can cause pronounced
dielectric dispersion effects.

1.2.5.1.1 Binary Mixtures with Water

Kaatze et al (103) studied aqueous solutions
of n-alkyl amine hydrochlorides as ionic

- 45 -

surfactants above the CMC at 25° C in the
frequency range 5 to 37 GHz with surfactant
concentrations typically in the range 0.2 to
2.7 mol l^{-1}. The extrapolated static
permittivity, ε_s, decreased with increased
surfactant concentration, falling from 76.1 at
0.2 mol l^{-1} to 34.0 at 2.71 mol l^{-1} for OcACl.
The authors reported that with concentrations
below about 1.5 mol l^{-1}, the ε_s values agreed
with the "commonly expected" respective ε
values for the mixture but the mixture
relation used was not quoted except that it was
stated as being applicable to "non-polar,
spherically shaped solute particles which do not
strongly interact with the solvent".

However, from the later works of Kaatze et al
(109, 110) on the dielectric properties of
aqueous solutions of polyethylene glycols where
n = 1 to 14,000, it is evident that the mixture
equation used was a modified form of the
Rayleigh equation for a heterogeneous mixture,
(equation [2.14] in Chapter 2), in which an
adjustable empirical parameter was included.
It should be noted that these heterogeneous
mixture equations assume complete absence of
molecular association between the two or more
components of the mixture. In the binary

mixture case, such a mixture is considered as a dispersion of globules of one component in the continuous medium formed by the other component. In the general case in which the two components differ from each other in terms of permittivity and conductivity, polarisation occurs due to accumulation of charge at the interface between the two components. This interfacial polarisation is often called the Maxwell-Wagner effect.

At higher concentrations of all the surfactants and, in addition, for all solutions of DoTACl which was studied at concentrations down to 0.4 mol l^{-1}, Kaatze et al (103) reported that the measured ε_s values were lower than the calculated values. Using an approach based on the heterogeneous mixture equation of Polder and Van Santen (equation [2.49] in Chapter 2), the authors reported that the experimental values agreed with theoretical values if an oblate spheriodal shape of axial ratio approximately 3:1 was assumed. The authors reported that other data on DoTACl (111, 112) supported the 3:1 value. The adjustable parameter used in the more recent reports of Kaatze et al (109, 110) was not referred to and so it is presumed that it was not applied to this experimental

data.

The dielectric relaxation data was considered
to be most accurately described by a model
based on two Debye-type relaxations with times
τ_p and τ_q. The τ_q value was approximately four
times longer than that of free water, whereas
the τ_p value was slightly smaller than that of
free water. The authors reported that extensive
earlier studies of aqueous solutions of monomers
had not revealed τ values similar to τ_q and
they attributed it to the porous structure of
the micellar surface producing a relatively long
bound water dispersion. The τ_p dispersion was
attributed to effects of weak electric fields
acting near the micellar surface modifying the
free water relaxation.

It is worthy of note that Kaatze et al (109, 110)
favoured use of a heterogeneous mixture equation
in studies of aqueous solutions of polyethylene
glycols. Since such solutions are not micellar
and, in the case of ethylene glycol particularly,
association between individual molecules would
be expected, description based on a heterogeneous
mixture equation is surprising. Nevertheless,
since the authors reported good agreement with
experimental values when the adjustable parameter

had the same value of 0.728 for all polymers (n = 1 to 600,000), the use of such an approach does seem to be justified.

Cavell (107) studied cationic micelles in aqueous solutions of tetradecyl trimethyl ammonium bromide (TTAB) with TTAB concentrations in the range from zero up to 800 mol m^{-3} at 20° C in the frequency range 0.35 to 35 GHz. The static permittivity ε_S exhibited anomalous effects in giving a maximum value of 92.0 at 200 mol m^{-3}. This effect was not commented upon.

The dielectric relaxation was analysed in terms of two relaxation times τ_1 and τ_2 where the faster τ_1 dispersion contained a small distribution of relaxation times which remained constant around 9.5 ps for all concentrations of TTAB. The τ_2 dispersion was Debye-type and decreased with increasing concentration of TTAB above 50 mol m^{-3} from 596 ps at 50 mol m^{-3} to 202 ps at 800 mol m^{-3}. The τ_1 dispersion was attributed to relaxation of the slightly bound solvent water and the τ_2 dispersion was interpreted using a model of Schwarz (113) based on a frequency dependent surface admittance of the assumed spherical counterion layer. Using micellar size values for TTAB given by Tartar

(114) and known mobilities of bromide ions, the equation of Schwarz was found to give a value for τ_2 which was a factor of two lower than the experimental value at the highest concentration.

The reduction of τ_2 with increasing water content was attributed to an increase in the thickness of the electrical double layer, which in the model of Schwarz had been assumed to be of negligible thickness compared with that of the radius of the dispersed globule. The author used his experimental data to calculate a value for the radius, r, of the micelle which included the double layer and obtained a small fall in r with increasing TTAB content where the values of r were approximately 50% higher than the value given by Tartar.

Beard et al (105) studied micellar solutions of SDS (sodium dodecyl sulphate) in water with SDS concentrations of up to 12 g l^{-1} at 25° C in the frequency range 500 kHz to 1.5 GHz. The static permittivity increased with increasing SDS concentration following an approximately linear relationship. The dielectric relaxation revealed Cole-Cole arc type behaviour with parameter $\alpha = 0.19$ and a relaxation time, τ, of approximately 1×10^{-9} s. Both α and τ remained

constant over the range of concentrations studied.

The variation of ε_S with concentration was discussed in the context of the observed linear increase of the dielectric increment $\Delta\varepsilon$ ($=\varepsilon_S - \varepsilon_\infty$) with SDS concentration. The authors stated that the observed dielectric properties were characteristic of a heterogeneous dielectric relaxation for an inhomogeneous boundary of bound water between the hydrocarbon core of the micelle and the bulk water. The measured α value was noted as being close to the value of 0.2 obtained by Grant (115) for bound water in bovine serum albumen, where in the SDS solutions the heterogeneous relaxation was not handicapped by the much larger dipolar relaxation of the core.

The authors considered a number of approaches to the dielectric properties of spherical particles surrounded by a shell and found the approach of O'Konski (108) to be of particular interest. The O'Konski model enabled the dielectric increment to be satisfactorily accounted for but gave τ values approximately a factor of 100 larger than the measured ones. The authors suggested that this could be due to a contribution by the

reactive component of the conductive shell
which was neglected in O'Konski's theory. In
this case, since the shell contained both ions
and water with a permittivity greater than that
of the core, it was considered that an analysis
based on bound water would be useful. Two such
approaches were used. The first followed a model
by Grant (115) for protein hydration based on a
dielectric mixture formula. The second followed
a shell model after Schwan (116) where the
behaviour of the hydrocarbon core, water shell
and surrounding electrolyte were considered in
terms of a Maxwell-Wagner type dispersion. Using
the experimental data for τ and $\Delta\varepsilon$ in the approach
following Schwan and assuming that the radius of
the spherical micelle core did not exceed that
of the straight dodecyl chain, the authors ob-
tained a value of 6.6 g H_2O/g SDS for the number
of grams of bound water per gram of SDS in the
micelle, compared with a value of 25 g H_2O/g SDS
given by the Grant model. It should be noted
that even with the lower figure of 6.6 g H_2O/g
SDS, a rather high figure of 100 water molecules
per molecule of SDS is obtained.

1.2.5.1.2 Ternary Mixtures with Water and a Hydrocarbon

Eicke and Christen (117) studied micellar
solutions of the ionic surfactant Aerosol AY

(sodium di 2 pentyl sulphosuccinate) in benzene
containing solubilised water. They reported
that studies using a number of techniques
indicated that the Aerosol AY with benzene
micellar solution involved aggregations of simi-
lar size and that the micelles contained sub-
units of trimer complexes. Eicke and Shepherd
(104) studied the dielectric relaxation of
Aerosol AY in benzene with solubilised water at
20° C in the frequency range 200 kHz to 10 MHz.
The static permittivity increased from 5 without
water up to 27 at 6.3% by volume of water and
followed an approximately quadratic relationship
$\left(\frac{\Delta \varepsilon_s}{\Delta \emptyset} \simeq 2 \text{ where } \emptyset = \text{volume fraction of water} \right)$.
Dielectric relaxation was observed exhibiting
Cole-Davidson type dispersion with parameter β
increasing from 0.33 without water up to 0.45
at 6.3% of water. The relaxation time τ fell
from $3.8.10^{-7}$ s to $6.3.10^{-8}$ s at 2.7% of water
and then remained constant up to the 6.3% value.
At higher water content, both the permittivity
and conductivity became unstable.

The authors used an approximate equation derived
from the equation of Kirkwood where the dielec-
tric increment ($\varepsilon_s - \varepsilon_\infty$) was considered to be
proportional to the product of the concentration
and square of the dipole moment of the polar

units, in order to obtain an aggregation number, n, for the hydrated micelles. From the experimental data, a value of n = 2 was obtained, indicating aggregation of micelles into pairs.

This aggregation of micelles into pairs was suggested as being the cause of the observed variation of ϵ_s with increasing water content. The instability above 6.3% by volume of water was attributed to further aggregation of micelle pairs into higher aggregates. The authors added that approximate confirmation of the micelle pair interpretation was given by apparent molecular weight data.

The dielectric relaxation was attributed to orientation of the micelle and the authors reported that when viscosity data was substituted into the Debye equation for relaxation time, a micelle size of comparable value to that determined from both geometrical considerations and from partial specific volume and diffusion coefficient data was obtained.

The reduction of τ on addition of water was attributed to stabilisation of the micelle by water causing denser packing and thus allowing faster reorientation in the applied field. This interpretation is open to dispute since it would

not be expected that addition of water to an inverted micelle would cause a reduction in micellar size.

The observed Cole-Davidson type dispersion was simply attributed to micellar aggregation and deviation from spherical shape without further justification. Eicke et al (118) reported that high field studies on Aerosol OT (sodium di 2 ethyl hexyl sulphosuccinate) at 22° C revealed two superimposed relaxation processes. These were attributed to separate orientation polarisation effects with the higher frequency relaxation due to the trimer sub-units of the micelle and the lower frequency one due to whole micelles. In view of the sparse high frequency data of Eicke and Shepherd (104), it could easily be argued that their results were due to separate Debye-type dispersions rather than the Cole-Davidson type and thus the interpretation based on aggregation and non-spherical shape must be treated with some caution.

Clausse et al (119) used the ionic surfactant potassium oleate with 1 hexanol as co-surfactant in dielectric studies of microemulsions of water in hexadecane. Temperatures were not stated. The authors reported that microemulsions could be

prepared for mass fractions of water, p, up to
0.32 above which turbidity and instability was
observed. The static permittivity increased
linearly from approximately 4 at p = 0 to 8 at
p = 0.2 above which it increased rapidly to
approximately 80 at p = 0.3 and giving values in
excess of 100 at concentrations close to p = 0.32.
The one dielectric relaxation curve given in the
report was for p = 0.308 for which the static
permittivity was approximately 90. Although the
measurement temperature was not stated, it is
evident from a study of the report that it was
approximately room temperature, for which pure
water has a permittivity of less than 80.

For values of p < 0.2, dielectric dispersion was
not observed but at higher values of p a
pronounced dispersion occurred. The dielectric
relaxation parameters were not quoted but from
inspection of their results a value of
$\tau \simeq 5 \times 10^{-8}$ s has been calculated by this author.
The dielectric behaviour for p > 0.2 did not
agree with predicted values given by equations
due to Hanai (120) for water in oil emulsions.
The authors suggested that for p < 0.2, the
dispersed water could be considered as solubilised
within the polar headgroups of the surfactant
molecules and that the solutions should be called

hydrated micelles, rather than microemulsions. The concentration dependence of ε_s in the range p = 0 to 0.2 was not commented on.

For p > 0.2, the authors suggested that most of the water molecules gathered into minute droplets surrounded by an interfacial film which was dispersed within the system and could thus be defined as a water-in-oil (W/O) microemulsion.

The dielectric relaxation was attributed to interfacial polarisation effects "similar to those observed in emulsions". They added that high conductivity observed in the microemulsions indicated that some of the water remained "free".

This interpretation of the dielectric behaviour on the basis of similarity to interfacial polarisation effects observed in emulsions is open to dispute since the literature data for emulsions reveals static permittivity values that are lower than those for pure water (120 to 127) with the only exception being a W/O dispersion in which the volume fraction of the dispersed phase was greater than 0.6 (121).

In order to account for the observed high static permittivity values on the basis of interfacial polarisation, it would be necessary to use an

approach based on that of Schwarz (113) where
the dielectric behaviour is related to counterion
effects. The observed high conductivity of the
microemulsions is compatible with such a model.

Sjoblom and Friberg (128) studied W/O micro-
emulsions of potassium oleate with potassium
ethylate in ethanol as co-surfactant in hexadecane
using light scattering and electron microscopy
methods. They reported that, in the concentration
range corresponding to the p < 0.2 range studied
by Clausse et al (119), no micelles were present
and it was suggested that this absence of micelles
was the reason for the absence of dielectric
relaxation in such mixtures.

More detailed studies of water in hexadecane
microemulsions using the same surfactants as those
used by Clausse et al (119) at mass fraction of
water p = 0.310 have been reported by Peyrelasse
et al (106). The dielectric behaviour was studied
at a number of temperatures between 20° and
32.5° C in the frequency range 5 kHz to 2 GHz.
The static permittivity data exhibited anomalous
effects, giving a maximum ε_s value of 69.1 at
25° C. Further, the lowest ε_s value obtained
was 40.0 at 20° C.

Anomalous relaxation behaviour was also observed in that a maximum value in the relaxation time τ was obtained at 25° C. Thus at the temperature where ε_s was a maximum, τ was also a maximum. The dielectric dispersion was Cole-Cole arc type with parameter α falling from 0.36 at 20° to 0.27 at 32.5° C.

The authors suggested that since the dielectric dispersion was of a Cole-Cole arc type, it arises from interfacial polarisation phenomena similar to those observed in emulsions. They added that the peculiar dependence of ε_s and τ upon temperature indicated that the dielectric behaviour could be more related to surface admittance effects associated with the surfactant/ co-surfactant shell surrounding the water-swollen micelles.

It should be pointed out that conformation with a Cole-Cole arc representation of the dielectric dispersion does not of itself provide support for an interfacial polarisation interpretation, but in view of the presence of the counterion layer, such polarisation effects are to be expected.

Senatra and Guibilaro (129, 130) studied water in dodecane microemulsions using the same surfactant/

co-surfactant as Clausse et al (119). For mass
fractions of water, p, up to $\simeq$ 0.3, stable
isotropic solutions were obtained and for p > 0.3
turbidity and instability were observed in
qualitative agreement with the observations of
Clausse et al. However for p > 0.7 stable
isotropic solutions were again obtained. The
authors suggested that for p > 0.7, the micro-
emulsions were of the O/W type, since they were
characterised by high static permittivity and
high conductivity. Further, at mass fraction
p = p_c = 0.625, both $\varepsilon`$ and $\varepsilon``$ diverged to
infinity and at values of p close to p_c both
W/O and O/W dispersions were reported as co-
existing where only one dispersion was stable
with the other being metastable with life-times
of the order of a few days. The dielectric
behaviour for p close to p_c revealed maxima in
both the real and imaginary component of the
permittivity ($\varepsilon`$ and $\varepsilon``$) where the magnitude of
both $\varepsilon`$ and $\varepsilon``$ exhibited a steady increase as the
frequency was reduced to its lowest value of
16 kHz. The authors suggested that, since similar
behaviour is observed in some nematic liquid
crystals, the observation of such behaviour at
values of p close to p_c could be due to a similar
nematic liquid crystalline phase.

1.2.5.2 Non-ionic surfactants

1.2.5.2.1 Binary Mixtures with Water

The only literature data on the dielectric properties of mixtures of non-ionic surfactants with water is the relaxation study of dimethyl ethers of ethylene, diethylene and triethylene glycols reported by Kaatze (110). As in the studies of polyethylene glycols reported in the same paper, investigation was restricted to one composition only at a volume fraction of water of 0.93. The static permittivity values of these solutions were lower than those of the ethylene glycols but the relaxation times were very similar. The lower static permittivity values of the surfactant solutions were not commented upon, neither were the structural differences between the surfactants and the polyethylene glycols considered.

1.2.5.2.2 Ternary Mixtures with Water and a Hydrocarbon

There have been few investigations of ternary mixtures of non-ionic surfactants and these have all been with commercial products.

Clausse et al (131) used the non-ionic surfactants Tween 20 and Span 20 as emulsifiers in studies of benzene in water microemulsions. The dielectric properties were studied at 20° C in

the frequency range 100 kHz to 5 MHz.
Dielectric dispersion was not observed. The
dielectric behaviour was attributed to inter-
facial polarisation and the experimental data
gave good agreement with theoretical values
given by equations of Hanai (120, 121) for oil
in water (O/W) emulsions. Deviations between
theory and experiment were observed at low
volume fractions of the dispersed phase when
the mass fraction of the surfactants was 15%
Tween and 1% Span, and also when the fraction
was 10% Tween and 1% Span. When the mass
fraction was reduced to 5% Tween and 1% Span,
deviations were not observed. The authors
suggested two possibilities for the observed
deviations. There could be a contribution by
the polar group of the surfactant in the shell
of the dispersed globule, particularly when the
size of the dispersed globule was small and this
effect could be greater at higher surfactant
concentration. The other possibility suggested
was that in the continuous aqueous phase,
micelles of the surfactant might be formed. Since
the concentration of surfactant in the aqueous
phase was kept constant, the authors pointed out
that the concentration of surfactant molecules
available for micelle formation would be greater

as the volume $\overset{\text{fraction}}{\wedge}$ of the dispersed phase was reduced. It should be added that in the continuous aqueous phase, micelles of the surfactant must of necessity be formed. Possibly the authors were implying that in addition to swollen micelles which are oil (benzene) centred, there are other micelles present consisting solely of the surfactant alone. This is considered unlikely and indeed unnecessary to postulate, since the first proposal seems quite reasonable.

These authors suggested that extension of the studies to the higher frequencies utilised by Beard et al (105) could check the validity of the qualitative explanations proposed. How such an extension in frequency range would check the validity is not entirely clear but presumably such a study would confirm or otherwise the absence of dielectric dispersion in O/W microemulsions since the Hanai equations for O/W dispersions predict negligible dispersion, although Clausse et al appeared to imply that dielectric relaxation might well be observed at higher frequencies simply because such an effect occurred with the ionic surfactant SDS.

Peyrelasse et al (132) used the non-ionic
surfactant Octarox, which is composed of blends
of polyoxyethylene octyl phenyl ethers, as
surfactant for microemulsions of water in
undecane. The dielectric properties of a
mixture containing 2.5 g of water, 15 g of
undecane and 2 g of Octarox were studied in the
temperature range 25° to 40° C in the frequency
range 400 Hz to 3 MHz with an additional spot
frequency measurement at 2.1 GHz. The authors
published the dielectric data for the 30.2° C
measurements. A static permittivity value of
17.5 was obtained and a pronounced dielectric
dispersion was observed with $\varepsilon_\infty \simeq 3.4$.
Relaxation parameters were not quoted but
inspection of the published data reveals that
the dispersion was of the Cole-Cole arc type with
parameter α approximately 0.5. The relaxation
time τ was about 2×10^{-7} s. The authors added
that the dispersion was of the Cole-Cole arc
type over the whole temperature range studied.
Interpretation of the dielectric behaviour was
not given.

1.2.5.3 <u>Summary</u>

Hanai (120) pointed out that, whilst solutions of
simple molecules and some polymers are considered
on the basis of the dielectric theory of polar

molecules, and emulsions are considered on the
basis of the dielectric theory of heterogeneous
systems, "there is no established approach to the
dielectric properties of systems such as inverted
micellar solutions and microemulsions". Although
that assertion was made about a decade ago, a
survey of more recent studies suggests that it
is still applicable, as is indicated in the
following summary of recent work.

Kaatze et al (103) have attributed the dielectric
relaxation of binary mixtures of an ionic
surfactant with water to orientation polarisation
whereas Cavell (107) and Beard et al (105) have
favoured an interfacial polarisation approach.
Similarly in ternary mixtures of an ionic surfact-
ant with water and a hydrocarbon Eicke et al (104)
have proposed orientation polarisation, whereas
Clausse et al (119) and Peyrelasse et al (106)
have favoured an interfacial mechanism.

In non-ionic surfactants, the absence of the
counterion layer should considerably simplify
interpretation of dielectric properties but the
very limited experimental data available precludes
identification of the most suitable approach.

In binary mixtures with water, the only published
data is for polyethylene glycol dimethylethers at one

composition (110) and the author made no reference to micellar behaviour. In ternary mixtures of a commercial non-ionic surfactant with water and benzene, Clausse et al (131) favoured an interfacial polarisation approach and the agreement between the experimental data at low proportions of surfactant with values given by the equation of Hanai for an O/W dispersion (120) is worthy of note.

It was considered that a study of the dielectric properties of binary mixtures of a non-ionic surfactant with water over a range of compositions would be instructive. In view of the proposals concerning micellar shape and size, together with secondary aggregation effects, for aqueous solutions of polyethylene glycol dodecyl ethers (74, 80, 81, 83, 85), these solutions seemed to be particularly worthy of investigation.

It was therefore decided to study the dielectric behaviour of aqueous solutions of the surfactants $C_{12}E_4$, $C_{12}E_6$, $C_{12}E_8$ and Brij 30 over the whole composition range. In addition, aqueous solutions of tetra ethylene glycol (E_4) were studied over the whole composition range in order to gain information on the properties of a mixture which contains the E_4 polar groups only

and would thus not be expected to form micellar
aggregates.

It was also decided to study the dielectric
properties of ternary mixtures of the surfactants
$C_{12}E_4$ and Brij 30 with water and a hydrocarbon
since the results of phase diagram and electrical
conductivity studies by Bostock (83) had revealed
considerable complexity and suggested the occur-
rence of normal micelles in some compositions and
inverted micelles in others.

Chapter 2 Theory

The dielectric properties of alcohol-water mixtures would be expected to be more satisfactorily described by molecular theories of homogeneous mixtures or solutions, whereas those of micellar and microemulsion systems may be more satisfactorily described by a macroscopic heterogeneous mixture approach. The theories of both homogeneous and heterogeneous mixtures are considered in this chapter. Existing theoretical equations for heterogeneous mixtures have been extended to concentrated spheroidal dispersions.

2.1 Dielectric theory of homogeneous mixtures

These have been reviewed by a number of authors. The treatise by Hill (60) is particularly worthy of note.

2.1.1 Static Permittivity ε_s

2.1.1.1 Pure Liquids

Debye (13) considered a microscopic spherical region surrounding a molecule in the dielectric which was large compared with molecular dimensions. By assuming that the field inside the sphere was zero and that local directional forces could be neglected, he obtained the equation

$$\frac{\varepsilon_s - 1}{\varepsilon_s + 2} = \frac{N_A}{3\varepsilon_o \nu} \left(\alpha + \frac{\mu^2}{3kT} \right) \qquad [2.1]$$

where N_A is Avogadro's number

$\quad \varepsilon_o$ is the permittivity of free space

$\quad \nu$ is the molar volume

$\quad k$ is the Boltzmann's constant

μ is the dipole moment

and α is the distortion polarisability

The later theory of Onsager (14) represented a molecule
as a point dipole in a spherical cavity of molecular
size, but local directional forces were again neglected.
Subsequent theories of Kirkwood (15) and Fröhlich (133)
included these local forces. Kirkwood treated unpolar-
isable point dipoles and obtained the equation:

$$\frac{(\varepsilon_S - 1)(2\varepsilon_S + 1)}{3\varepsilon_S} = \frac{N_A}{\varepsilon_0 v} \left(\frac{g\mu^2}{3kT}\right) \qquad [2.2]$$

where g is a dimensionless quantity called the Kirkwood
g-factor which is included to take account of local
directional forces.

Fröhlich (133) included the distortion polarisation
contribution by considering the non-polarisable dipoles to
be embedded in a medium of permittivity ε_∞. Using the
relation

$$\mu_g = \left(\frac{3}{\varepsilon_\infty + 2}\right) \mu$$

where μ_g is the gas phase dipole moment (60), the Kirkwood-
Fröhlich equation was obtained:

$$\frac{(\varepsilon_S - \varepsilon_\infty)(2\varepsilon_S + \varepsilon_\infty)}{\varepsilon_S (\varepsilon_\infty + 2)^2} = \frac{N_A g\mu_g^2}{9\varepsilon_0 v kT} \qquad [2.3]$$

This is a standard equation applicable to single component
liquids.

2.1.1.2 Extension of Kirkwood theory to liquid mixtures

Oster (134) used the original form of the Kirkwood equation [2.2] assuming that the net polarisation P is given by the sum of the two components P_1 and P_2 according to the ideal mixing equation

$$P = x_1 P_1 + x_2 P_2$$

where x_1, x_2 are the respective molar fractions of components '1' and '2'. Application of the Oster approach gives:

$$\frac{(\varepsilon_S - 1)(2\varepsilon_S + 1)\nu}{\varepsilon_S} = \frac{(\varepsilon_{S1} - 1)(2\varepsilon_{S1} + 1)x_1\nu_1}{\varepsilon_{S1}} + \frac{(\varepsilon_{S2} - 1)(2\varepsilon_{S2} + 1)x_2\nu_2}{\varepsilon_{S2}}$$

[2.4]

Assuming additivity of volumes, the molar volume of the mixture, ν, can be written as $\nu = x_1\nu_1 + x_2\nu_2$ and if ε_S, ε_{S1} and $\varepsilon_{S2} \gg 1$ then

$$\varepsilon_S = \frac{\varepsilon_{S1} x_1\nu_1 + \varepsilon_{S2} x_2\nu_2}{x_1\nu_2 + x_2\nu_2}$$

or $\varepsilon_S = \varepsilon_{S1} \phi_1 + \varepsilon_{S2} \phi_2$ [2.5]

where ϕ_1 and ϕ_2 are the volume fractions of components '1' and '2'.

The Oster apprach can be similarly applied to the Kirkwood-Fröhlich equation by writing

$$\frac{(\varepsilon_S - \varepsilon_\infty)(2\varepsilon_S + \varepsilon_\infty)}{\varepsilon_S} = \frac{N_A}{\varepsilon_0 \nu kT} (x_1 g_1 \mu_1^2 + x_2 g_2 \mu_2^2)$$

[2.6]

where the subscripts '1' and '2' refer to the components '1' and '2'.

2.1.2 Dielectric Relaxation : Macroscopic Relaxation Time τ

2.1.2.1 Debye-type dispersion

It is assumed that when an electric field E is applied, the distortion polarisation P_1 is established instantaneously compared with the dipolar reorientation and that the dipolar part of the polarisation P_2 obeys a rate equation of the form:

$$\frac{dP_2}{dt} = \frac{P - P_1 - P_2}{\tau}$$

where P is the equilibrium value of the total polarisation and τ is the macroscopic relaxation time.

Writing $P = \varepsilon_0(\varepsilon_S - 1)E$

$$P_1 = \varepsilon_0(\varepsilon_\infty - 1)E$$

and $\quad P_2 = \varepsilon_0(\varepsilon^* - 1)E$

the following expression for the complex permittivity ε^*, $(=\varepsilon` - j\varepsilon``)$ is obtained:

$$\varepsilon^* = \varepsilon_\infty + \frac{\varepsilon_S - \varepsilon_\infty}{1 + j\omega\tau} \qquad \boxed{2.7}$$

A plot of $\varepsilon``$ plotted against $\varepsilon`$ produces a semi-circle of radius $\dfrac{\varepsilon_S - \varepsilon_\infty}{2}$ with a centre at $\left[\dfrac{\varepsilon_S + \varepsilon_\infty}{2}, 0\right]$.

Dielectric relaxation for which such a semi-circle is obtained is termed Debye-type.

2.1.2.2 Cole-Cole arc type dispersion

Many examples are found in practice which give a broader dispersion with a lower value of $\varepsilon``_{max}$ than the Debye-type. For such dispersions, Cole and Cole (135) suggested the empirical equation:

$$\varepsilon^* = \varepsilon_\infty + \frac{\varepsilon_S - \varepsilon_\infty}{1 + (j\omega\tau)^{1-\alpha}} \qquad [2.8]$$

where $0 \leq \alpha < 1$

This is termed Cole-Cole arc type dispersion and is attributed to a symmetrical distribution of relaxation times about a mean value.

2.1.2.3 Cole-Davidson skewed-arc type dispersion

Cole and Davidson (136) observed that the dielectric dispersion of glycerol gave a skewed-arc when $\varepsilon^{''}$ was plotted against $\varepsilon^{'}$. These authors suggested the empirical equation:

$$\varepsilon^* = \varepsilon_\infty + \frac{\varepsilon_S - \varepsilon_\infty}{(1 + j\omega\tau)^\beta} \qquad [2.9]$$

where $0 < \beta \leq 1$

The skewed-arc behaviour is attributed to a distribution of relaxation times with mechanisms of decreasing importance extending to the high frequency side of the dispersion.

In many liquids including the alcohols, the dielectric dispersion is best described by Debye-type relaxation involving more than one relaxation time, although in practice, distinction between multiple Debye-type relaxations and Cole-Davidson type dispersion is difficult due to sparseness of data points.

2.1.3 Molecular Relaxation Time

As the reaction field, which is set up in the Onsager cavity by the polarisation which the dipole induces in its

surroundings, does not follow precisely in phase with
either the applied field or the dipole motion, the macro-
scopic relaxation time τ obtained from experimental
measurements is not the same as the time constant for
molecular dipole relaxation, $\tau^{'}$.

A number of theoretical equations are available, giving
relationships between $\tau^{'}$ and τ. The simpler ones are
listed below.

$$\tau^{'} = \left(\frac{\varepsilon_{\infty} + 2}{\varepsilon_{s} + 2}\right)\tau \qquad\qquad [2.10] \quad (13)$$

$$\tau^{'} = \left(\frac{2\varepsilon_{s} + \varepsilon_{\infty}}{3\varepsilon_{s}}\right)\tau \qquad\qquad [2.11] \quad (137,138)$$

and $\quad \tau^{'} = \frac{3\varepsilon_{s}\varepsilon_{\infty}(2\varepsilon_{s} + \varepsilon_{\infty})}{2\varepsilon_{s}^{3} + 6\varepsilon_{s}^{2}\varepsilon_{\infty} + \varepsilon_{\infty}^{3}}\cdot\tau \qquad [2.12] \quad (139)$

The above equations reveal that $\tau^{'}$ should be generally
smaller than τ and thus care should be exercised when the
macroscopic relaxation time τ is interpreted in terms of
molecular orientation.

2.2 Dielectric theory of heterogeneous mixtures

In heterogeneous mixtures, it is assumed that there is no
molecular association between the two or more components
of the mixture.

A binary heterogeneous mixture is considered as a dispersion
of globules of one component in the continuous medium formed
by the other component, and it is usually assumed that the
dispersed component contains spherical or, more generally,

spheroidal globules.

The dielectric properties of heterogeneous mixtures have received much less attention than those of homogeneous liquids but extensive reviews have been given by van Beek (140) and Hanai (120). Of these two, the former is the more comprehensive.

2.2.1 Spherical dispersions : Static permittivity

Rayleigh (141) calculated the permittivity of a dispersion of spherical particles by considering the electrostatic field in a mixture where the spherical particles have uniform radius and are arranged regularly at the lattice points of a simple cubic lattice in a continuous medium.

For a volume fraction ϕ of dispersed phase of permittivity ε_2 in a continuous phase of permittivity ε_1, Rayleigh derived an expression for the permittivity of the mixture, ε, given by:

$$\varepsilon = \varepsilon_1 \left[1 + \frac{3\phi}{\dfrac{\varepsilon_2 + 2\varepsilon_1}{\varepsilon_2 - \varepsilon_1} - \phi - 1.65 \dfrac{(\varepsilon_2 - \varepsilon_1)}{\varepsilon_2 + \frac{4}{3}\varepsilon_1} \cdot \phi^{10/3}} \right] \quad [2.13]$$

For $\phi \ll 1$ [2.13] reduces to

$$\frac{\varepsilon - \varepsilon_1}{\varepsilon + 2\varepsilon_1} = \frac{\varepsilon_2 - \varepsilon_1}{\varepsilon_2 + 2\varepsilon_1} \cdot \phi \qquad [2.14]$$

This is sometimes referred to as Wiener's equation (142) but it is also one of the equations derived by Wagner (discussed later). In this work [2.14] will be termed the Rayleigh equation. Rayleigh considered that [2.14] should

be only applicable to low values of $\emptyset$ and van Beek has
suggested that $\boxed{2.14}$ should be only applicable to volume
fractions of dispersed phase $\emptyset < 0.2$.

Other forms of $\boxed{2.13}$ have also been reported. Runge (143)
corrected for a factor $\left(\dfrac{1}{\pi}\right)$ in the full Rayleigh equation by
replacing the factor 1.65 by 0.525. Meredith and Tobias
(144) used a different potential function for the electro-
static field and, by considering higher terms in the series
expansion for the potential in the continuous phase,
obtained the expression:

$$\varepsilon = \varepsilon_1 \left[\frac{\dfrac{2\varepsilon_1 + \varepsilon_2}{\varepsilon_2 - \varepsilon_1} + 2\emptyset - 1.227 \dfrac{2\varepsilon_1 + \varepsilon_2}{4\varepsilon_1 + 3\varepsilon_2} \emptyset^{7/3} - 6.399 \dfrac{\varepsilon_2 - \varepsilon_1}{4\varepsilon_1 + 3\varepsilon_2} \emptyset^{10/3}}{\dfrac{2\varepsilon_1 + \varepsilon_2}{\varepsilon_2 - \varepsilon_1} - \emptyset - 1.227 \dfrac{2\varepsilon_1 + \varepsilon_2}{4\varepsilon_1 + 3\varepsilon_2} \emptyset^{7/3} - 2.718 \dfrac{\varepsilon_2 - \varepsilon_1}{4\varepsilon_1 + 3\varepsilon_2} \emptyset^{10/3}} \right]$$

$$\boxed{2.15}$$

Bruggeman (145) extended the Rayleigh equation $\boxed{2.14}$ to
more concentrated dispersions by assuming that the equation
holds for infinitesimally small increments of concentration
of the disperse phase and that the final high concentration
of disperse phase is attained by a succession of these
processes. This was performed by putting $\varepsilon_1 \rightarrow \varepsilon$ and
$\varepsilon \rightarrow \varepsilon + \Delta\varepsilon$. The volume fraction term was found by writing
that the change in concentration $\Delta\emptyset`$ between stages i and
i + 1 is given by:

$$\Delta\emptyset` = \frac{V\emptyset` + \Delta V_2}{V + \Delta V_2} - \emptyset` = \frac{\Delta V_2}{V + \Delta V_2}(1 - \emptyset`)$$

where V is the total volume

ΔV_2 is the infinitesimal amount of added disperse

phase

and $\emptyset^i$ is the concentration at stage i.

On assuming Rayleigh's equation [2.14] holds for

infinitesimal incrementation, we can write $\emptyset = \dfrac{\Delta V_2}{V + \Delta V_2}$

giving $\emptyset = \dfrac{\Delta \emptyset^i}{1 - \emptyset^i}$.

Replacing ε_1 by ε, ε by $\varepsilon + \Delta\varepsilon$ and $\emptyset$ by $\dfrac{\Delta \emptyset^i}{1 - \emptyset^i}$ gives

$$\frac{2\varepsilon + \varepsilon_2}{3\varepsilon(\varepsilon - \varepsilon_2)} \Delta\varepsilon = \frac{-\Delta \emptyset^i}{1 - \emptyset^i}$$

Integrating ε between the limits ε_1 and ε and $\emptyset^i$ between 0

and $\emptyset$ gives

$$\frac{\varepsilon - \varepsilon_2}{\varepsilon_1 - \varepsilon_2} \left(\frac{\varepsilon_1}{\varepsilon}\right)^{1/3} = 1 - \emptyset \qquad\qquad [2.16]$$

which is the Bruggeman equation.

A different approach was taken by Looyenga (146) who

assumed that on mixing two components ε_1 and ε_2, the

infinitesimal changes in the Rayleigh equation are of the

type $\varepsilon_1 \to \varepsilon - \Delta\varepsilon$ and $\varepsilon_2 \to \varepsilon + \Delta\varepsilon$.

Applying a binomial expansion leads to

$$\emptyset^i = \frac{1}{2} + \frac{\Delta\varepsilon}{2(3\varepsilon - 2\Delta\varepsilon)}$$

The volume fractions $\emptyset(\varepsilon)$ at ε, $\varepsilon - \Delta\varepsilon$ and $\varepsilon + \Delta\varepsilon$ were

expanded in a Taylor's series form to the second derivative,

by considering the mixture as composed of a volume fraction

$(1 - \emptyset^i)$ with a permittivity $(\varepsilon - \Delta\varepsilon)$ and fraction $\emptyset^i$ with

permittivity $(\varepsilon + \Delta\varepsilon)$ where

$$\emptyset(\varepsilon) = (1 - \emptyset^i).\emptyset(\varepsilon - \Delta\varepsilon) + \emptyset^i.\emptyset(\varepsilon + \Delta\varepsilon)$$

Using the Taylor's series form for $\phi(\varepsilon - \Delta\varepsilon)$ and $\phi(\varepsilon - \Delta\varepsilon)$ gives

$$\phi^{\backprime} = \frac{1}{2} - \frac{1}{4} \Delta\varepsilon \frac{d^2\phi/d\varepsilon^2}{d\phi/d\varepsilon} \qquad\qquad [2.16a]$$

Combining the two equations for $\phi^{\backprime}$ leads to the differential equation $3\varepsilon \frac{d^2\phi}{d\varepsilon^2} + 2 \frac{d\phi}{d\varepsilon} = 0$ and applying boundary conditions: $\varepsilon = \varepsilon_1$ when $\phi = 0$ and $\varepsilon = \varepsilon_2$ when $\phi = 1$ gives

$$\varepsilon = \left[(\varepsilon_2{}^{1/3} - \varepsilon_1{}^{1/3})\phi + \varepsilon_1{}^{1/3} \right]^3 \qquad\qquad [2.17]$$

which is the Looyenga equation. (It should be noted that this was independently derived by Landau and Lifshitz (147)).

An equation of rather similar form was derived by Kraszewski et al (148) for a multi-layer suspension by assuming that a layer of the suspension could be considered as a sum of an infinite number of alternate layers of permittivity ε_1 and ε_2. By assuming that the propagation constant γ_m of a plane electromagnetic wave through the suspension is given by $\gamma_m = \gamma_1 t_1 + \gamma_2 t_2$ where t_1 and t_2 represent the thickness of the component layers, they obtained the equation

$$\varepsilon = \left[(\varepsilon_2{}^{\frac{1}{2}} - \varepsilon_1{}^{\frac{1}{2}})\phi + \varepsilon_1{}^{\frac{1}{2}} \right]^2 \qquad\qquad [2.18]$$

A completely different approach was used by Böttcher (149) who considered the disperse system to be a close aggregate of two kinds of spherical globules. He assumed that the electric field E_2 inside a sphere of the component of

permittivity ε_2 exerted by its inhomogeneous surroundings is equivalent to that of the sphere placed in a homogeneous dielectric of permittivity ε.

According to electrostatic theory (149), E_2 is given by $E_2 = \dfrac{3\varepsilon}{2\varepsilon + \varepsilon_2}$ .E where E is the electric field at an infinite distance from the sphere. Similarly for the spheres of permittivity ε_1, $E_1 = \dfrac{3\varepsilon}{2\varepsilon + \varepsilon_1}$.E and the total polarisation per unit volume of the mixture is given by

$$P = \varepsilon_0(\varepsilon - 1)E = (1 - \phi)\varepsilon_0(\varepsilon_1 - 1)E_1 + \phi\varepsilon_0(\varepsilon_2 - 1)E_2$$

giving

$$\frac{\varepsilon - \varepsilon_1}{3\varepsilon} = \frac{\varepsilon_2 - \varepsilon_1}{\varepsilon_2 + 2\varepsilon}.\phi \qquad\qquad [2.19]$$

which is Böttcher's equation.

The range of ϕ values for which the equations for higher concentrations of dispersed phase should be applicable is not fully established but comparison between experimental values for emulsions with values given by the equations of Hanai, one of which is identical with the Bruggeman equation, discussed in the following section, (120, 121, 150, 151) reveals that the Bruggeman equations can be applicable for volume fractions of dispersed phase ϕ up to approximately 0.8. Mandel (152) suggested that $[2.19]$ should be applicable for ϕ up to 0.2.

2.2.2 Dielectric relaxation of spherical dispersions : Interfacial polarisation

When either or both of the components of a binary mixture has a significant conductivity component, dielectric

dispersion behaviour may be observed. This dispersion is
known as the Maxwell-Wagner effect. Maxwell (153)
considered a two layer system of permittivities ε_1 and ε_2,
with conductivities σ_1 and σ_2 and derived equations for
the high frequency limiting value of the permittivity ε_∞,
the low frequency limiting value ε_s, the relaxation time
τ and the conductivity σ.

Wagner (154) presented a dielectric theory for a disperse
system of a large number of spherical particles sparsely
distributed in a continuous medium. By considering the
complex potential due to a dispersion of spheres of
permittivity ε_2 in a continuous medium of permittivity ε_1,
the following relation was obtained:

$$\frac{\varepsilon^* - \varepsilon_1^*}{\varepsilon^* + 2\varepsilon_1^*} = \frac{\varepsilon_2^* - \varepsilon_1^*}{\varepsilon_2^* + 2\varepsilon_1^*} \cdot \emptyset \qquad [2.20]$$

where ε^* is the permittivity of the mixture. This is the
same as the Rayleigh equation $[2.14]$ except that the
permittivities are expressed in complex form.

Solution of $[2.20]$ gives a Debye-type dispersion of
relaxation time τ given by

$$\tau = \varepsilon_0 \frac{[2\varepsilon_1 + \varepsilon_2 - \emptyset(\varepsilon_2 - \varepsilon_1)]}{2\sigma_1 + \sigma_2 - \emptyset(\sigma_2 - \sigma_1)} \qquad [2.21]$$

where σ_1, σ_2 are the conductivities of components '1' and
'2'.

The high and low frequency limiting values of the
permittivity ε_∞ and ε_s are:

$$\varepsilon_\infty = \varepsilon_1 \frac{2\varepsilon_1 + \varepsilon_2 + 2\phi(\varepsilon_2 - \varepsilon_1)}{2\varepsilon_1 + \varepsilon_2 - \phi(\varepsilon_2 - \varepsilon_1)} \qquad [2.22]$$

and

$$\varepsilon_S = \varepsilon_1 \frac{2\sigma_1 + \sigma_2 + 2\phi(\sigma_2 - \sigma_1)}{2\sigma_1 + \sigma_2 - \phi(\sigma_2 - \sigma_1)} + 3\phi \, \sigma_1 \frac{(2\sigma_1 + \sigma_2)(\varepsilon_2 - \varepsilon_1) - (2\varepsilon_1 + \varepsilon_2)(\sigma_2 - \sigma)}{\{2\sigma_1 + \sigma_2 - \phi(\sigma_2 - \sigma_1)\}^2}$$

$$[2.23]$$

It can be seen that equation $[2.22]$ is the same as the Rayleigh equation $[2.14]$ and thus the above equations should be similarly applicable to $\phi < 0.2$.

Hanai (120) extended the Wagner theory to higher concentrations of disperse phase using a method similar to that of Bruggeman by proposing that during the infinitesimal increases in concentration $\varepsilon_1^* \to \varepsilon^*$ and $\varepsilon^* \to \varepsilon^* + \Delta\varepsilon^*$ with $\phi = \frac{\Delta\phi}{1 - \phi}$ giving the equation

$$\frac{2\varepsilon^* + \varepsilon_2^*}{3\varepsilon^*(\varepsilon^* - \varepsilon_2^*)} \Delta\varepsilon^* = \frac{-\Delta\phi}{1 - \phi}$$

He showed that this expression integrated to:

$$\frac{\varepsilon^* - \varepsilon_2^*}{\varepsilon_1^* - \varepsilon_2^*} \left(\frac{\varepsilon_1^*}{\varepsilon^*}\right)^{1/3} = 1 - \phi \qquad [2.24]$$

which is the Bruggeman equation for spheres in complex form.

The complex quantities were expressed as

$$\varepsilon^* - \varepsilon_2^* = \left[(\varepsilon - \varepsilon_2)^2 + (\gamma - \gamma_2)^2\right]^{\frac{1}{2}} \exp\left[-j \arctan\left(\frac{\gamma - \gamma_2}{\varepsilon - \varepsilon_2}\right)\right]$$

where γ is the dielectric loss,

$$\varepsilon_1^* - \varepsilon_2^* = \left[(\varepsilon_1 - \varepsilon_2)^2 + (\gamma_1 - \gamma_2)^2\right]^{\frac{1}{2}} \exp\left[-j \arctan\left(\frac{\gamma_1 - \gamma_2}{\varepsilon_1 - \varepsilon_2}\right)\right]$$

$$\varepsilon_1{}^* = \left(\varepsilon_1{}^2 + \gamma_1{}^2\right)^{\frac{1}{2}} \exp\left[-\ j\ \text{arc tan}\left(\frac{\gamma_1}{\varepsilon_1}\right)\right]$$

and

$$\varepsilon^* = \left(\varepsilon^2 + \gamma^2\right)^{\frac{1}{2}} \exp\left[-\ j\ \text{arc tan}\left(\frac{\gamma}{\varepsilon}\right)\right]$$

Substitution into equation [2.24] and separation of real and imaginary terms together with use of the relation

$$\text{tan } (A - B) = \frac{\text{tan } A\ -\ \text{tan } B}{1\ -\ \text{tan } A\ \text{tan } B} \quad \text{gave:}$$

$$\frac{\left[(\varepsilon - \varepsilon_2)^2 + (\gamma - \gamma_2)^2\right]}{\left[(\varepsilon_1 - \varepsilon_2)^2 + (\gamma_1 - \gamma_2)^2\right]} \frac{(\varepsilon_1{}^2 + \gamma_1{}^2)^{\frac{1}{3}}}{(\varepsilon^2 + \gamma^2)^{\frac{1}{3}}} = (1 - \emptyset)^2 \quad [2.24a]$$

and

$$\text{arc tan}\left(\frac{\varepsilon\gamma_1 - \varepsilon_1\gamma}{\varepsilon\varepsilon_1 + \gamma\gamma_1}\right) = 3\ \text{arc tan}\left[\frac{(\varepsilon - \varepsilon_2)(\gamma_1 - \gamma_2) - (\varepsilon_1 - \varepsilon_2)(\gamma - \gamma_2)}{(\varepsilon - \varepsilon_2)(\varepsilon_1 - \varepsilon_2) + (\gamma - \gamma_2)(\gamma_1 - \gamma_2)}\right]$$

$$[2.24b]$$

Hanai stated without justification that [2.24b], which is of the form arc tan A = 3 arc tan B, could be written in the simplified form:

$$A = \frac{B(3 - B^2)}{1 - 3B^2} \qquad [2.24c]$$

Investigation by this author has shown that, in order to obtain [2.24c], the arc tan X functions have been expressed in the series expansion form using the first two terms only, ie

$$\text{arc tan } X = X - \frac{X^3}{3}$$

Neglect of the terms for higher power of X is open to criticism since the series expansion is only rapidly convergent for $X \leqslant 0.5$, whereas in [2.24b] values of X up to 2π are possible.

Applying the series expansion to A and B in $\boxed{2.24c}$ reveals a further assumption made by Hanai:

We have $A - \dfrac{A^3}{3} = 3B - B^3$

ie $\qquad A\left(1 - \dfrac{A^2}{3}\right) = B(3 - B^2)$

or $\qquad A = \dfrac{B(3 - B^2)}{1 - A^2/3}$ $\qquad\qquad\qquad \boxed{2.24d}$

In order to obtain $\boxed{2.24c}$ we must put:

$$\frac{A^2}{3} = 3B^2$$

ie $\qquad A = 3B$

which is only valid for small values of A and B. Thus the upper limit for A and B for the series expressions to be rapidly convergent will be somewhat lower than the 0.5 figure already quoted.

Using a solution of $\boxed{2.24b}$ based on $\boxed{2.24c}$, Hanai obtained the following cumbersome expression for the "general solution" of $\boxed{2.24}$:

$$(\varepsilon\gamma_1 - \varepsilon_1\gamma)\Big[(\varepsilon - \varepsilon_2)(\varepsilon_1 - \varepsilon_2)+(\gamma - \gamma_2)(\gamma_1 - \gamma_2)\Big]\Bigg\{\Big[(\varepsilon - \varepsilon_2)(\varepsilon_1 - \varepsilon_2) +$$

$$(\gamma - \gamma_2)(\gamma_1 - \gamma_2)\Big]^2 - 3\Big[(\varepsilon - \varepsilon_2)(\gamma_1 - \gamma_2)-(\gamma - \gamma_2)(\varepsilon_1 - \varepsilon_2)\Big]^2\Bigg\} =$$

$$(\varepsilon\varepsilon_1 + \gamma\gamma_1)\Big[(\varepsilon - \varepsilon_2)(\gamma_1 - \gamma_2)-(\gamma - \gamma_2)(\varepsilon_1 - \varepsilon_2)\Big]\Bigg\{3\Big[(\varepsilon - \varepsilon_2)(\varepsilon_1 - \varepsilon_2) +$$

$$(\gamma - \gamma_2)(\gamma_1 - \gamma_2)\Big]^2 - \Big[(\varepsilon - \varepsilon_2)(\gamma_1 - \gamma_2) - (\gamma - \gamma_2)(\varepsilon_1 - \varepsilon_2)\Big]^2\Bigg\} \quad \boxed{2.24e}$$

Noting that the γ terms represent the dielectric loss $\left(= \dfrac{\sigma}{j\omega\varepsilon_0}\right)$, at high frequencies $\varepsilon_1 \gg \gamma_1$, $\varepsilon_2 \gg \gamma_2$ and $\varepsilon \gg \gamma$ ($\varepsilon = \varepsilon_\infty$) [2.24a] will then reduce to

$$\frac{\varepsilon_\infty - \varepsilon_2}{\varepsilon_1 - \varepsilon_2} \left(\frac{\varepsilon_1}{\varepsilon}\right)^{1/3} = 1 - \phi \qquad\qquad [2.25]$$

which is the Bruggeman equation and [2.24e] reduces to

$$\sigma_\infty \left[\frac{3}{\varepsilon_\infty - \varepsilon_2} - \frac{1}{\varepsilon_\infty}\right] = 3\left[\frac{\sigma_1 - \sigma_2}{\varepsilon_1 - \varepsilon_2} + \frac{\sigma_2}{\varepsilon_\infty - \varepsilon_2}\right] - \frac{\sigma_1}{\varepsilon_1} \qquad [2.26]$$

At low frequencies $\gamma_1 \gg \varepsilon_1$, $\gamma_2 \gg \varepsilon_2$ and $\gamma \gg \varepsilon$ ($\varepsilon = \varepsilon_s$) giving

$$\varepsilon_s \left[\frac{3}{\sigma_s - \sigma_2} - \frac{1}{\sigma_s}\right] = 3\left[\frac{\varepsilon_1 - \varepsilon_2}{\sigma_1 - \sigma_2} + \frac{\varepsilon_2}{\sigma_s - \sigma_2}\right] - \frac{\varepsilon_1}{\sigma_1} \qquad [2.27]$$

and

$$\frac{\sigma_s - \sigma_2}{\sigma_1 - \sigma_2} \left(\frac{\sigma_1}{\sigma_s}\right)^{1/3} = 1 - \phi \qquad\qquad [2.28]$$

It should be added that in both the high and low frequency limiting cases considered above, the denominator terms in the arc tan X expressions will be much larger than the numerator terms, and thus the expansion used to obtain [2.24c] will be valid.

Hanai considered two special cases.

(a) $\sigma_1 \gg \sigma_2$ which is termed an oil in water O/W dispersion since water would be expected to exhibit a substantially higher conductivity than an oily component.

In this case [2.25] is unchanged but [2.26] to [2.28] reduce to:

$$\frac{\sigma_\infty}{\sigma_1} = \frac{\epsilon_\infty(\epsilon_\infty - \epsilon_2)(2\epsilon_1 + \epsilon_2)}{\epsilon_1(\epsilon_1 - \epsilon_2)(2\epsilon_\infty + \epsilon_2)} \qquad [2.28a]$$

$$\epsilon_S = \sigma_S \frac{3\epsilon_2\sigma_1 + (2\epsilon_1 - 3\epsilon_2)\sigma_S}{\sigma_1(2\sigma_S + \sigma_2)} \qquad [2.28b]$$

and

$$\frac{\sigma_S - \sigma_2}{\sigma_1}\left(\frac{\sigma_1}{\sigma_S}\right)^{1/3} = 1 - \emptyset \qquad [2.28c]$$

In the case of $\sigma_S \gg \sigma_2$, the equations further reduce to

$$\epsilon_S = \frac{3}{2}\epsilon_2 + \left(\epsilon_1 - \frac{3}{2}\epsilon_2\right)(1 - \emptyset)^{3/2} \qquad [2.29]$$

and $\sigma_S = \sigma_1(1 - \emptyset)^{3/2}$ $\qquad [2.30]$

(b) $\sigma_2 \gg \sigma_1$ which is termed a water in oil (W/O)

dispersion.

Equation $[2.25]$ is again unchanged but $[2.26]$ to $[2.28]$

reduce to:

$$\frac{\sigma_\infty}{\sigma_2} = \frac{3\epsilon_\infty(\epsilon_\infty - \epsilon_1)}{(\epsilon_2 + 2\epsilon_\infty)(\epsilon_2 - \epsilon_1)} \qquad [2.30a]$$

$$\epsilon_S = \epsilon_1 \frac{\sigma_S(\sigma_2 - \sigma_S)}{\sigma_1(\sigma_2 + 2\sigma_S)} \qquad [2.30b]$$

and

$$\frac{\sigma_2 - \sigma_S}{\sigma_2}\left(\frac{\sigma_1}{\sigma_S}\right)^{1/3} = 1 - \emptyset \qquad [2.30c]$$

when $\sigma_2 \gg \sigma_S$ the equations further reduce to

$$\epsilon_S = \frac{\epsilon_1}{(1 - \emptyset)^3} \qquad [2.31]$$

and

$$\sigma_S = \frac{\sigma_1}{(1 - \emptyset)^3} \qquad [2.32]$$

Hanai pointed out that for an O/W dispersion $\varepsilon_2 << \varepsilon_1$ reducing the Wagner equations to $\varepsilon_\infty \simeq \varepsilon_1 \frac{2(1 - \emptyset)}{2 + \emptyset}$ which is approximately equal to ε_s and the Hanai equations similarly give $\varepsilon_\infty \simeq \varepsilon_s$. Thus for O/W emulsions, the dielectric increment ($\varepsilon_s - \varepsilon_\infty$) predicted by both the Wagner and the Hanai theories will be very small. In contrast, Hanai showed that W/O emulsions should exhibit significant dispersion. An expression from which a relaxation time may be determined has not yet been derived but a numerical estimation by Hanai et al (155) has revealed that the Hanai model gives a Cole-Cole arc type dispersion, with a relaxation time slightly longer than that predicted by the Wagner equations for τ.

As already noted, the Hanai equations have been shown to be applicable for $\emptyset$ values of up to 0.8 (120).

2.2.3 <u>Dielectric theory of spheroidal dispersions</u>

Since the average field inside a dispersed globule will depend on its shape, the permittivity of the mixture will be similarly dependent. Sillars (156) extended the Wagner equations to spheroidal particles using equations applicable to the case of $\emptyset << 1$. For the special case of $\sigma_1 << \sigma_2$:

$$\varepsilon_\infty = \varepsilon_1 \left[1 + 3\emptyset \frac{(\varepsilon_2 - \varepsilon_1)}{2\varepsilon_1 + \varepsilon_2} \right] \qquad [2.33]$$

For spheroidal particles, Sillars derived the expression

$$\varepsilon_\infty = \varepsilon_1 \left[1 + \frac{\emptyset n (\varepsilon_2 - \varepsilon_1)}{(n - 1)\varepsilon_1 + \varepsilon_2} \right] \qquad [2.34]$$

where $n = \left[\frac{1}{e^2} - \left(\frac{(1 - e^2)^{\frac{1}{2}} \text{ arc sin } e}{e^3} \right) \right]^{-1}$

and e is the eccentricity.

Van Beek (140) reported that the equations of Sillars were applicable for $\emptyset < 0.1$ but that the equations were "easily extended" to the more general case and quoted the following equations which he considered should be applicable for values of $\emptyset$ up to 0.2.

$$\tau = \varepsilon_0 \frac{\varepsilon_1 + A_a(1 - \emptyset)(\varepsilon_2 - \varepsilon_1)}{\sigma_1 + A_a(1 - \emptyset)(\sigma_2 - \sigma_1)} \qquad [2.35]$$

$$\varepsilon_\infty = \varepsilon_1 \frac{\varepsilon_1 + \left[A_a(1 - \emptyset) + \emptyset \right](\varepsilon_2 - \varepsilon_1)}{\varepsilon_1 + A_a(1 - \emptyset)(\varepsilon_2 - \varepsilon_1)} \qquad [2.36]$$

and

$$\varepsilon_s = \varepsilon_1 \cdot \frac{\sigma_1 + \left[A_a(1 - \emptyset) + \emptyset \right](\sigma_2 - \sigma_1)}{\sigma_1 + A_a(1 - \emptyset(\sigma_2 - \sigma_1)}$$

$$+ \emptyset \sigma_1 \frac{\left[\sigma_1 + A_a(\sigma_2 - \sigma_1) \right](\varepsilon_2 - \varepsilon_1) - \left[\varepsilon_1 + A_a(\varepsilon_2 - \varepsilon_1) \right](\sigma_2 - \sigma_1)}{\left[\sigma_1 + A_a(1 - \emptyset)(\sigma_2 - \sigma_1) \right]^2}$$

$$[2.37]$$

where A_a is termed the depolarising factor along the a axis which is given by the elliptic integral:

$$A_a = \frac{abc}{2} \int_0^\infty \frac{ds}{(s + a^2)\left[(s + a^2)(s + b^2)(s + c^2) \right]^{\frac{1}{2}}} \qquad [2.38]$$

where a, b and c are the semi-axes of the ellipsoid (157). Van Beek stated, without giving derivations, the following expressions for spheroids of axial ratio (b/a):

when a > b (prolate spheroids)

$$A_a = \frac{-1}{\left(a/b\right)^2 - 1} + \frac{a/b}{\left[\left(a/b\right)^2 - 1\right]^{3/2}} \ln \left\{ \left(a/b\right) + \left[\left(a/b\right)^2 - 1\right]^{\frac{1}{2}} \right\}$$

[2.39]

when a < b (oblate spheroids)

$$A_a = \frac{1}{1 - \left(a/b\right)^2} - \frac{\left(a/b\right)}{\left[1 - \left(a/b\right)^2\right]^{3/2}} \arccos \left(\frac{a}{b}\right)$$

[2.40]

when a = b (spheres)

$$A_a = \frac{1}{3}$$

The author added that for practical calculations, the following approximations are often useful:

when a > b

$$A_a = \left[\ln\left(2a/b\right) - 1\right] \left(b/a\right)^2$$

[2.41]

when a < b

$$A_a \rightarrow 1$$

[2.42]

Van Beek also reported that for small $\emptyset$ and $\sigma_1 \ll A_a \sigma_2$ equations [2.35] [2.36] and [2.37] reduce to

$$\tau = \frac{\varepsilon_0 \left[\varepsilon_1 + A_a(\varepsilon_2 - \varepsilon_1)\right]}{A_a \sigma_2}$$

[2.43]

$$\varepsilon_\infty = \varepsilon_1 \left[1 + \frac{\emptyset(\varepsilon_2 - \varepsilon_1)}{\varepsilon_1 + A_a(\varepsilon_2 - \varepsilon_1)}\right]$$

[2.44]

and $\varepsilon_s = \varepsilon_1 \left[1 + \emptyset/A_a\right]$

[2.45]

Grosse and Greffe (158) have proposed formulae for the

effect of ellipsoidal micelles on the permittivity of a mixture by writing the Rayleigh equation in the form:

$$\varepsilon = \varepsilon_1 \frac{2\varepsilon_1 + \varepsilon_2 + 2\emptyset(\varepsilon_2 - \varepsilon_1)Q(\varepsilon_2,\varepsilon_1)}{2\varepsilon_1 + \varepsilon_2 - \emptyset(\varepsilon_2 - \varepsilon_1)Q(\varepsilon_2,\varepsilon_1)} \qquad [2.46]$$

where the shape factor $Q(\varepsilon_2,\varepsilon_1)$ is defined by

$$Q(\varepsilon_2,\varepsilon_1) = \frac{1}{3}\sum_s \frac{1}{1 + 3\zeta_s(\varepsilon_2 - \varepsilon_1)/\varepsilon_2 + \varepsilon_1} \qquad [2.47]$$

with the ζ_s components given by

$$\zeta_1 = -\frac{2}{15}\left(1 - \frac{b^2}{a^2}\right), \quad \zeta_2 = \zeta_3 = -\frac{\zeta_1}{2} \qquad [2.48]$$

Since these equations are based on the Rayleigh equation [2.14], they should be similarly applicable to $\emptyset < 0.2$.

This theory was not applied to experimental data nor were the types of micelles identified.

A generalised form of the Böttcher equation was given by Polder and Van Santen (159) who obtained an expression of similar form to the equation of Sillars but by using the approximation that the medium surrounding the dispersed particle was one of permittivity ε, the following expression was obtained:

$$\varepsilon = \varepsilon_1 + \frac{\emptyset(\varepsilon_2 - \varepsilon_1)\varepsilon}{\varepsilon + A_a(\varepsilon_2 - \varepsilon)} \qquad [2.49]$$

which reduces to the Böttcher equation when the substitution $A_a = \frac{1}{3}$ for spheres is applied. The equation is often written in the form applicable to a random distribution of orientations namely:

$$\varepsilon = \varepsilon_1 + \frac{\emptyset}{3} \frac{(\varepsilon_2 - \varepsilon_1)\varepsilon}{\sum\limits_{a,b,c} \varepsilon + A_j(\varepsilon_2 - \varepsilon)} \qquad [2.50]$$

For spheres $A_a = A_b = A_c = \frac{1}{3}$ giving the Böttcher equation as required.

The authors considered $[2.49]$ to be applicable to "low" values of $\emptyset$ and Mandel (152) suggested it should be applicable to systems where $\emptyset$ does not exceed "10 to 20%".

de Loor (160) proposed a more general expression for $[2.50]$

$$\varepsilon = \varepsilon_1 + \frac{\emptyset}{3} \frac{(\varepsilon_2 - \varepsilon_1)\overline{\varepsilon}_1}{\sum\limits_{a,b,c} \overline{\varepsilon}_1 + A_j(\varepsilon_2 - \overline{\varepsilon}_1)} \qquad [2.51]$$

where $\overline{\varepsilon}_1$ is the permittivity of the immediate surroundings of the dispersed particle. The author added the statement that "thorough investigation has shown that $\overline{\varepsilon}_1$ always has values between ε and ε_1" (161).

In the case of $\overline{\varepsilon}_1 = \varepsilon$, the Polder and van Santen equation is obtained which reduces to the Böttcher equation when $A_j(j = a, b, c) = \frac{1}{3}$, as already discussed. On the other hand, when $\overline{\varepsilon}_1 = \varepsilon_1$, the Sillar's equation is obtained, since as discussed later $n = \frac{1}{A_a}$. For spheres, the equation reduces to

$$\varepsilon = \varepsilon_1 + \frac{3\emptyset\varepsilon_1(\varepsilon_2 - \varepsilon_1)}{2\varepsilon_1 + \varepsilon_2} \qquad [2.52]$$

which is the Wagner equation for $\emptyset \ll 1$ $[2.33]$.

Kaatze et al (109) proposed the mixture formula:

$$\varepsilon = \varepsilon_1 + \frac{3\phi\varepsilon_1(\varepsilon_2 - \varepsilon_1)}{2\varepsilon_1 + \varepsilon_2 - \phi(\varepsilon_2 - \varepsilon_1)} \qquad [2.53]$$

These authors claimed that $[2.53]$ was a "refined version of the formula of Polder and van Santen". However, simple re-arrangement of their equation gives

$$\varepsilon = \varepsilon_1 \left[\frac{2\varepsilon_1 + \varepsilon_2 - 2\phi(\varepsilon_1 - \varepsilon_2)}{2\varepsilon_1 + \varepsilon_2 + \phi(\varepsilon_1 - \varepsilon_2)}\right] \qquad [2.54]$$

which is identical with the Rayleigh equation $[2.14]$ and should be thus only applicable for $\phi < 0.2$.

These authors also introduced a modification to $[2.54]$ in which ϕ in the denominator was replaced by a factor $[1 - \delta (1 - \phi)]$ where δ is an empirically adjustable parameter. The physical significance of the δ-value was not discussed.

2.2.4 <u>Dielectric theory of spherical dispersions surrounded by shells</u>

Due primarily to relevance to biological cell specimens, the dielectric properties of a dispersed particle surrounded by a shell of different dielectric properties to those of either the particle or the continuous medium, have received considerable attention. Since ternary mixtures of surfactants with water and a hydrocarbon can be regarded as "particle with shell" type structures, the dielectric theory of such systems could well be relevant. The earliest attempt to give a mathematical analysis of a

dispersion of spheres surrounded with shells was by

Maxwell (153). For a globule of radius R with a

permittivity ε_2 surrounded by a shell of thickness d

with a permittivity ε_{sh} in a continuous medium of

permittivity ε_1, Maxwell showed that the permittivity

ε_I of the homogeneous sphere which is equivalent to the

shell-covered sphere is given by

$$\varepsilon_I = \varepsilon_{sh} \frac{2\varepsilon_{sh} + \varepsilon_2 - 2(\varepsilon_{sh} - \varepsilon_2)v}{2\varepsilon_{sh} + \varepsilon_2 + (\varepsilon_{sh} - \varepsilon_2)v} \qquad [2.55]$$

where $v = \left(\frac{R}{R + d}\right)^3$.

(It can be seen that $[2.55]$ is identical with the

Rayleigh equation $[2.14]$ for a volume fraction v of

dispersed phase of permittivity ε_2 in a continuous phase

ε_{sh}.)

Maxwell then showed that the permittivity of the mixture,

for a dispersion of permittivity ε_I in a continuous phase

ε_1 is given by:

$$\varepsilon = \varepsilon_1 \frac{2\varepsilon_1 + \varepsilon_I - 2(\varepsilon_1 - \varepsilon_I)p}{2\varepsilon_1 + \varepsilon_I + (\varepsilon_1 - \varepsilon_I)p} \qquad [2.56]$$

where p is the volume fraction of the dispersed globules

with shells.

Combining equations $[2.55]$ and $[2.56]$ enables ε to be

calculated.

Pauly and Schwan (162) extended these equations to include

conductivity effects by expressing all the permittivity

components in their complex form. Dielectric dispersion

was predicted which was characterised by two relaxation times.

O'Konski (108) considered the case of $\sigma_{sh} \gg \sigma_1$ and showed that, since freely movable ionic charges in the shell can be displaced by an applied field, a surface conductivity occurs which can give rise to dielectric dispersion.

The O'Konski approach was further developed by Schwarz (113) in order to account for very large permittivities and very low dispersion frequencies observed in biological cells and colloidal suspensions which could not be accounted for by O'Konski's theory. Schwarz considered the effect of an external field on the counterion distribution in the interface between the particle and its surrounding continuous medium and showed that the asymmetry in the distribution caused by the field causes dielectric dispersion with a relaxation time related to the particle radius and the surface diffusion coefficient of the counterions.

Although the permittivity values predicted by equations [2.55] and [2.56] may well be applicable to ternary mixtures of non-ionic surfactants with water and a hydro-carbon, the absence of counterion effects can be expected to preclude the dielectric dispersion behaviour discussed by O'Konski (108) and Schwarz (113).

2.2.5 Comparison of heterogeneous mixture equation values with experimental data

Since there are a large number of mixture equations available, it is considered important that comparison with experimental data be included in order to identify the equations most likely to be applicable to the surfactant studies in this work.

Extensive comparisons have been given in the reviews by van Beek (140) Hanai (120) and Kraszewski (163). Their results are summarised briefly in this section.

The review by van Beek reveals that in a number of investigations covering a range of heterogeneous systems, for a non-conducting dispersed phase, the equations of Bruggeman [2.16], Looyenga [2.17] and Böttcher [2.19] give closest agreement with experimental values for $\emptyset$ up to typically 0.5.

The survey by Hanai reveals that in emulsions, the Hanai-Bruggeman equations for both O/W and W/O dispersions generally give closest agreement with experimental values for dispersions with $\emptyset$ up to about 0.8. Marked deviations were revealed when the full Rayleigh equation [2.13] and the Böttcher equation [2.19] were used at volume fractions of dispersed phase higher than 0.2. Similarly, where dielectric dispersion has been observed, it has been shown to be more accurately described by the Hanai equations than the Wagner equations. One notable exception is the data of

Dryden and Meakins (164) for water droplets in wool wax with $\emptyset$ up to 0.381 where the Wagner equations give slightly better agreement. Hanai suggested that the deviation between the experimental values and values calculated from the Hanai equations could be due to an aggregation effect, but justification of this proposal was not given.

Good agreement between experimental values for emulsions and the Hanai equations has been reported for W/O dispersions by Chapman (165), Clausse et al (124, 125) and Le Petit et al (166) and for O/W dispersions by Clausse (127). Similarly Clausse et al (131) reported good agreement between experimental values and the Hanai equations for O/W microemulsions, as discussed in Chapter 1 of this work, and it is thus concluded that for concentrated dispersions, the equations of Hanai (which include the Bruggeman equation) and Looyenga are likely to be most suitable.

Comparison of experimental data with theoretical equations for dispersions surrounded by shells has already been given in Chapter 1.

For non-sperical dispersions in other types of system, comparison between experimental and theoretical values is more sparse. The results of Reynolds (167) and Pradham and Gupta (168) for such dispersions have been considered by van Beek (140) and Kraszewski (163).

Although Reynolds was able to obtain good agreement between theory and experiment for glass lamellae and rods in carbon tetrachloride for $\emptyset$ up to the highest reported value of 0.4 using $\overline{\varepsilon}_1 = \varepsilon_1$ for lamellae and $\overline{\varepsilon}_1 = \varepsilon$ for rods in the de Loor equation [2.51], and also obtained close agreement for glass lamellae in nitrobenzene using $\overline{\varepsilon}_1 = \varepsilon$ for $\emptyset$ up to 0.2, the calculated values by Kraszewski (163) reveal that even closer agreement is obtained using both the Looyenga and Kraszewski equations with the latter being marginally better.

The data of Pradham and Gupta (168) for MgO lamellae dispersed in rosin for $\emptyset$ up to 0.5 revealed close agreement between theory and experiment using the de Loor equation [2.51] with $\overline{\varepsilon}_1 = \varepsilon$ but the agreement was only marginally better than that given by the Kraszewski equation. Further, for cylindrical air-holes in plexiglass for $\emptyset$ up to 0.55, Kraszewski has pointed out that both the Looyenga and Kraszewski equations give better agreement with experiment than equation [2.51] using either $\overline{\varepsilon}_1 = \varepsilon_1$ or $\overline{\varepsilon}_1 = \varepsilon$.

It is concluded that the equation of de Loor which was derived specifically for non-spherical dispersions is not demonstrably better than the Looyenga or the Kraszewski equations, even though these latter two equations are restricted to spherical and multi-layer suspensions respectively. The results support the view that equations for concentrated dispersions of non-spherical particles

are required with equations based on those of Hanai and Looyenga being considered the most suitable.

2.2.6 Derivation of new equations for concentrated dispersions of spheroidal particles

In this work, the studies of micellar mixtures containing non-ionic surfactants have involved concentrated O/W and W/O dispersions and equations enabling a distinction between O/W and W/O dispersions to be made would be of value. Further, following the suggestion of Tanford et al (74) that micellar solutions of some of the polyethylene glycol alkyl ether surfactants studied in this work are oblate ellipsoidal rather than spherical in shape, it was clear that mixture equations for concentrated dispersions of a spheroidal nature were required.

The equations of Bruggeman $[2.17]$, Looyenga $[2.18]$ and Hanai $[2.27]$ to $[2.32]$ which were derived for concentrated spherical dispersions were the obvious ones from which attempts to generalise to spheroidal dispersions should be directed. In particular, the equations of Hanai, which include the Bruggeman equation, were of particular interest since they enable a distinction between O/W and W/O dispersions to be made and have, as already discussed, been shown to give good agreement with experimental data for emulsions.

It was therefore decided to apply the Bruggeman integral method to the generalised Wagner equation for spheroidal dispersions quoted by van Beek (equation [2.36]) in order to derive a generalised form of the Bruggeman equation. Using the method of Sillars (156) as a basis, it has been shown how [2.36] can be considered as an extension of the Sillars equation to higher concentrations of dispersed phase.

Following the approach of Hanai (120) a solution of the generalised Bruggeman equation in complex form has been derived, giving generalised forms of the Hanai equations for both O/W and W/O spheroidal dispersions.

Since the equation derived by Looyenga has proved to be of value in dielectric studies of concentrated dispersions (140, 163), a generalised form of the Looyenga equation has been derived, based on the Bruggeman equation instead of the Böttcher equation as used in the original derivation by Looyenga. It should be noted that, although Looyenga claimed that the equation he derived is not restricted to spherical dispersions, this statement must be disputed since both the Bruggeman and the Böttcher equations were derived on the basis of spherical dispersions and thus any extension of them will still be only applicable to such dispersions.

It is worthy of note that since the shape factors A_a used in the derivations in this work can be determined for both

prolate and oblate ellipsoids, the derived equations will
be applicable to both types of ellipsoidal shape.

The approach adopted has therefore been as follows:

    (i)   use of the method of Sillars to obtain the
           generalised Wagner equation quoted by van Beek,

   (ii)   application of the Bruggeman integral method to
           the equation quoted by van Beek to derive a
           generalised Bruggeman equation,

  (iii)   application of the method of Hanai to the
           generalised Bruggeman equation in complex form
           to derive generalised Hanai equations for both
           O/W and W/O dispersions and

   (iv)   application of the method of Looyenga to the
           generalised Bruggeman equation to derive a
           generalised Looyenga equation.

2.2.6.1. Extension of Sillars equation to obtain equation quoted

by van Beek

Sillars (156) used the equation given by Wagner applicable
to $\emptyset \ll 1$.

$$\varepsilon^* = \varepsilon_1^* \left(1 + 3\emptyset \cdot \frac{\varepsilon_2^* - \varepsilon_1^*}{2\varepsilon_1^* + \varepsilon_2^*} \right) \qquad\qquad [2.56\,\mathrm{a}]$$

which gives

$$\varepsilon_\infty = \varepsilon_1 \left[1 + \frac{3\emptyset(\varepsilon_2 - \varepsilon_1)}{2\varepsilon_1 + \varepsilon_2} \right] \qquad\qquad (\text{see } [2.33])$$

$$= \varepsilon_1 \left[\frac{2\varepsilon_1 + \varepsilon_2 + 3\emptyset(\varepsilon_2 - \varepsilon_1)}{2\varepsilon_1 + \varepsilon_2} \right] \qquad [2.57]$$

For spheroids of axial ratio b/a, Sillars derived the equation

$$\varepsilon_\infty = \varepsilon_1 \left[1 + \frac{\emptyset n(\varepsilon_2 - \varepsilon_1)}{\varepsilon_1(n-1) + \varepsilon_2} \right]$$

$$= \varepsilon_1 \left[\frac{\varepsilon_1(n-1) + \varepsilon_2 + \emptyset n(\varepsilon_2 - \varepsilon_1)}{\varepsilon_1(n-1) + \varepsilon_2} \right] \qquad [2.58]$$

where $n = \left[\frac{1}{e^2} - \frac{(1 - e^2)^{\frac{1}{2}} \text{ arc sin } e}{e^3} \right]^{-1} \qquad [2.59]$

[2.58] reduces to [2.57] when n = 3.

e was termed the eccentricity which for oblate spheroids (b > a) is given by

$$e = \left[1 - \left(\frac{a}{b} \right)^2 \right]^{\frac{1}{2}} \qquad [2.59a]$$

Now let arc sin e = θ

ie sin θ = e

$1 - \sin^2\theta = e^2 = \cos^2\theta$

ie cos $\theta = (1 - e^2)^{\frac{1}{2}}$

$$= \left\{ 1 - \left[1 - \left(\frac{a}{b} \right)^2 \right] \right\}^{\frac{1}{2}} = \frac{a}{b}$$

hence $\theta = \text{arc cos} \left(\frac{a}{b} \right)$

thus for oblate spheroids [2.59] can be re-written as

$$\frac{1}{n} = \frac{1}{1 - (a/b)^2} - \frac{(a/b) \text{ arc cos } (a/b)}{\left[1 - (a/b)^2 \right]^{3/2}} \qquad [2.60]$$

which is equation [2.40] given by van Beek where $\frac{1}{n} = A_a$.

For prolate spheroids, Sillars obtained the relation

$$\frac{1}{n} = \left(\frac{1}{e^2} - 1\right)\left[\frac{1}{2e} \ln \left(\frac{1+e}{1-e}\right) - 1\right] \qquad [2.60\,a]$$

where $e = \left[1 - (b/a)^2\right]^{\frac{1}{2}}$ $\qquad$ $(a > b)$

Re-arranging $[2.60\,a]$ gives

$$\frac{1}{n} = \frac{1-e^2}{e^2}\left[\frac{1}{2e} \ln \left\{\frac{(1+e)^2}{1-e^2}\right\} - 1\right]$$

$$= \frac{(b/a)^2}{e^2}\left[\frac{1}{e} \ln \left((1+e)\frac{a}{b}\right) - 1\right]$$

$$= \frac{(b/a)^2}{\left[1-(b/a)^2\right]^{3/2}} \ln \left\{\frac{a}{b} + \left[1-(b/a)^2\right]^{\frac{1}{2}}\frac{a}{b}\right\} - \frac{(b/a)^2}{1-(b/a)^2}$$

$$= \frac{-1}{(a/b)^2 - 1} + \frac{(a/b)}{\left[(a/b)^2 - 1\right]^{3/2}} \ln \left\{\frac{a}{b} + \left[(a/b)^2 - 1\right]^{\frac{1}{2}}\right\}$$

which is equation $[2.39]$ quoted by van Beek where $n = \frac{1}{A_a}$.

Now the complete equation for ε_∞ given by Wagner is:

$$\varepsilon_\infty = \varepsilon_1 \frac{2\varepsilon_1 + \varepsilon_2 + 2\emptyset(\varepsilon_2 - \varepsilon_1)}{2\varepsilon_1 + \varepsilon_2 - \emptyset(\varepsilon_2 - \varepsilon_1)} \qquad \text{(see } [2.22]\text{)}$$

Following the procedure of Sillars but here retaining the volume fraction term in the denominator to enable application to higher volume fraction of dispersed phase and, in addition, noting that the volume fraction term in the numerator contains the factor two instead of three, we can write:

$$\varepsilon_\infty = \varepsilon_1 \frac{(n-1)\varepsilon_1 + \varepsilon_2 + (n-1)\emptyset(\varepsilon_2 - \varepsilon_1)}{(n-1)\varepsilon_1 + \varepsilon_2 - \emptyset(\varepsilon_2 - \varepsilon_1)} \qquad [2.61]$$

In the case of $n = 3$ $[2.61]$ reduces to $[2.22]$ as required.

Writing $n = \frac{1}{A_a}$ gives

$$\varepsilon_\infty = \varepsilon_1 \left[\frac{\left(\frac{1}{A_a} - 1\right)\varepsilon_1 + \varepsilon_2 + \left(\frac{1}{A_a} - 1\right)\emptyset(\varepsilon_2 - \varepsilon_1)}{\left(\frac{1}{A_a} - 1\right)\varepsilon_1 + \varepsilon_2 - \emptyset(\varepsilon_2 - \varepsilon_1)} \right]$$

$$= \varepsilon_1 \left[\frac{(1 - A_a)\varepsilon_1 + A_a\varepsilon_2 + (1 - A_a)\emptyset(\varepsilon_2 - \varepsilon_1)}{(1 - A_a)\varepsilon_1 + A_a\varepsilon_2 - A_a\emptyset(\varepsilon_2 - \varepsilon_1)} \right]$$

$$= \varepsilon_1 \cdot \frac{A_a(\varepsilon_2 - \varepsilon_1) + \varepsilon_1 + (1 - A_a)\emptyset(\varepsilon_2 - \varepsilon_1)}{A_a(\varepsilon_2 - \varepsilon_1) + \varepsilon_1 - A_a\emptyset(\varepsilon_2 - \varepsilon_1)}$$

$$= \varepsilon_1 \frac{\varepsilon_1 + \{A_a(1 - \emptyset) + \emptyset\}(\varepsilon_2 - \varepsilon_1)}{\varepsilon_1 + A_a(1 - \emptyset)(\varepsilon_2 - \varepsilon_1)} \qquad [2.62]$$

which is equation $[2.36]$ quoted by van Beek. Substitution of $A_a = \frac{1}{3}$ into the equation gives the Wagner equation for ε_∞ $[2.22]$ as required.

2.2.6.2 Derivation of generalised Bruggeman equation

We have, from above,

$$\varepsilon_\infty = \varepsilon = \varepsilon_1 \cdot \frac{\varepsilon_1 + \{A_a(1 - \emptyset) + \emptyset\}(\varepsilon_2 - \varepsilon_1)}{\varepsilon_1 + A_a(1 - \emptyset)(\varepsilon_2 - \varepsilon_1)}$$

or $\varepsilon\varepsilon_1 + A_a\varepsilon(1 - \emptyset)(\varepsilon_2 - \varepsilon_1) = \varepsilon_1^2 + \varepsilon_1\{A_a(1 - \emptyset) + \emptyset\}(\varepsilon_2 - \varepsilon_1)$

$\varepsilon\varepsilon_1 - \varepsilon_1^2 = A_a(1 - \emptyset)(\varepsilon_2 - \varepsilon_1)(\varepsilon_1 - \varepsilon) + \varepsilon_1\emptyset(\varepsilon_2 - \varepsilon_1)$

$$\varepsilon_1(\varepsilon - \varepsilon_1) = (\varepsilon_2 - \varepsilon_1)(A_a\varepsilon_1 - A_a\varepsilon - A_a\phi\varepsilon_1 + A_a\phi\varepsilon + \varepsilon_1\phi)$$

$$= (\varepsilon_2 - \varepsilon_1)\{A_a(\varepsilon_1 - \varepsilon) + \phi(\varepsilon_1 + A_a\varepsilon - A_a\varepsilon_1)\}$$

$$= (\varepsilon_2 - \varepsilon_1)\left[A_a(\varepsilon_1 - \varepsilon) + \phi\{\varepsilon_1 + A_a(\varepsilon - \varepsilon_1)\}\right]$$

Using the Bruggeman method as discussed earlier $\varepsilon_1 \to \varepsilon$ and $\varepsilon \to \varepsilon + \Delta\varepsilon$, also $\phi \to \dfrac{\Delta\phi`}{1 - \phi`}$

then

$$\varepsilon\Delta\varepsilon = (\varepsilon_2 - \varepsilon)\left[-A_a\Delta\varepsilon + \frac{\Delta\phi`}{1 - \phi`}(\varepsilon + A_a\Delta\varepsilon)\right]$$

$$= (\varepsilon_2 - \varepsilon)\left(-A_a\Delta\varepsilon + \frac{\Delta\phi`}{1 - \phi`}\varepsilon\right) \quad \text{(neglecting } \Delta\phi`\Delta\varepsilon)$$

$$= -\varepsilon_2 A_a\Delta\varepsilon + \varepsilon A_a\Delta\varepsilon + \frac{\Delta\phi`}{1 - \phi`}\varepsilon(\varepsilon_2 - \varepsilon)$$

$$\Delta\varepsilon(-\varepsilon + \varepsilon A_a - \varepsilon_2 A_a) = \frac{-\Delta\phi`}{1 - \phi`}\varepsilon(\varepsilon_2 - \varepsilon)$$

$$\Delta\varepsilon\frac{\left[\varepsilon(-1 + A_a) - \varepsilon_2 A_a\right]}{\varepsilon(\varepsilon_2 - \varepsilon)} = \frac{-\Delta\phi`}{1 - \phi`} \qquad\qquad [2.63]$$

Express LHS in form $\dfrac{ax - b}{x(c - x)} = \dfrac{M}{x} + \dfrac{N}{c - x}$

or $M(c - x) + Nx = ax - b$

Equating coefficients: $\quad Mc = -b \quad$ ie $M = -b/c$

$\qquad\qquad$ and $\quad -M + N = a \quad$ ie $N = a + M = a - b/c$

thus in equation for ε:

$$M = -\varepsilon_2 A_a/\varepsilon_2 = -A_a$$

$$N = (-1 + A_a) - A_a = -1$$

Rewriting equation $[2.63]$ and inserting limits that ε is integrated between ε_1 and ε, $\phi`$ between 0 and ϕ

$$- \int_{\varepsilon_1}^{\varepsilon} \frac{d\varepsilon}{\varepsilon} A_a - \int_{\varepsilon_1}^{\varepsilon} \frac{d\varepsilon}{\varepsilon_2 - \varepsilon} = - \int_0^{\emptyset} \frac{d\emptyset}{1 - \emptyset}$$

$$- A_a \ln\left(\frac{\varepsilon}{\varepsilon_1}\right) + \ln\left(\frac{\varepsilon_2 - \varepsilon}{\varepsilon_2 - \varepsilon_1}\right) = \ln(1 - \emptyset)$$

$$\text{or } A_a \ln\left(\frac{\varepsilon_1}{\varepsilon}\right) + \ln\left(\frac{\varepsilon_2 - \varepsilon}{\varepsilon_2 - \varepsilon_1}\right) = \ln(1 - \emptyset)$$

$$\therefore \quad \frac{\varepsilon_2 - \varepsilon}{\varepsilon_2 - \varepsilon_1} \left(\frac{\varepsilon_1}{\varepsilon}\right)^{A_a} = 1 - \emptyset \qquad\qquad [2.64]$$

For spheres $A_a = \frac{1}{3}$ giving the Bruggeman equation, thus equation [2.64] can be regarded as the Bruggeman equation extended to spheroidal dispersions and can be used for $0 \leqslant A_a \leqslant 1$.

2.2.6.3 <u>Derivation of generalised Hanai equations</u>

Using the approach of Hanai (120), the generalised Bruggeman equation [2.64] can be similarly expressed in complex form, and solution is obtained simply by replacing the $\frac{1}{3}$ in [2.24a] by A_a and the 3 in [2.24b] by $\frac{1}{A_a}$.

In the high frequency limiting case $\varepsilon_1 \gg \gamma_1$, $\varepsilon_2 \gg \gamma_2$ and $\varepsilon \gg \gamma$ $\left(\gamma = \frac{\sigma}{j\omega\varepsilon_0}\right)$ giving

$$\frac{\varepsilon_\infty - \varepsilon_2}{\varepsilon_1 - \varepsilon_2} \left(\frac{\varepsilon_1}{\varepsilon_\infty}\right)^{A_a} = 1 - \emptyset \qquad\qquad [2.65]$$

and

$$\sigma_\infty \left[\frac{1}{A_a(\epsilon_\infty - \epsilon_2)} - \frac{1}{\epsilon_\infty} \right] = \left(A_a\right)^{-1}\left[\frac{\sigma_1 - \sigma_2}{\epsilon_1 - \epsilon_2} + \frac{\sigma_2}{\epsilon_\infty - \epsilon_2} \right] - \frac{\sigma_1}{\epsilon_1} \quad [2.66]$$

In the low frequency limiting case $\gamma_1 \gg \epsilon_1$,

$\gamma_2 \gg \epsilon_2$ and $\gamma \gg \epsilon$ giving

$$\epsilon_s \left[\frac{1}{A_a(\sigma_s - \sigma_2)} - \frac{1}{\sigma_s} \right] = \frac{1}{A_a}\left[\frac{\epsilon_1 - \epsilon_2}{\sigma_1 - \sigma_2} + \frac{\epsilon_2}{\sigma_s - \sigma_2} \right] - \frac{\epsilon_1}{\sigma_1} \quad [2.67]$$

and

$$\frac{\sigma_s - \sigma_2}{\sigma_1 - \sigma_2} \left(\frac{\sigma_1}{\sigma_s} \right)^{A_a} = 1 - \emptyset \quad [2.68]$$

.2.6.3.1 <u>O/W Dispersion</u>

Writing $\sigma_1 \gg \sigma_2$ and $\sigma \gg \sigma_2$, $[2.65]$ is unchanged, $[2.66]$ reduces to:

$$\sigma_\infty \left[\frac{1}{A_a(\epsilon_\infty - \epsilon_2)} - \frac{1}{\epsilon_\infty} \right] = \left(A_a\right)^{-1}\left[\frac{\sigma_1}{\epsilon_1 - \epsilon_2} \right] - \frac{\sigma_1}{\epsilon_1}$$

$$= \left(A_a\right)^{-1}\sigma_1 \left[\frac{1}{\epsilon_1 - \epsilon_2} - \frac{1}{\epsilon_1} \right] \quad [2.69]$$

$[2.67]$ reduces to

$$\epsilon_s \left[\frac{1}{A_a \sigma_s} - \frac{1}{\sigma_s} \right] = \frac{1}{A_a}\left[\frac{\epsilon_1 - \epsilon_2}{\sigma_1} + \frac{\epsilon_2}{\sigma_s} \right] - \frac{\epsilon_1}{\sigma_1}$$

$$\epsilon_s \left[\frac{\sigma_s(1 - A_a)}{A_a \, \sigma_s^2} \right] = \frac{1}{A_a}\left[\frac{(\epsilon_1 - \epsilon_2)\sigma_s + \epsilon_2\sigma_1 - A_a\epsilon_1\sigma_s}{\sigma_1\sigma_s} \right]$$

$$\varepsilon_s \sigma_s (1 - A_a) = \frac{\sigma_s}{\sigma_1} \left[\{\varepsilon_1 (1 - A_a) - \varepsilon_2\} \sigma_s + \varepsilon_2 \sigma_1 \right] \quad \boxed{2.70}$$

Also $\boxed{2.68}$ reduces to

$$\frac{\sigma_s}{\sigma_1} \left[\frac{\sigma_1}{\sigma_s} \right]^{A_a} = 1 - \emptyset$$

ie

$$\left[\frac{\sigma_1}{\sigma_s} \right]^{A_a - 1} = 1 - \emptyset$$

$$\sigma_1 = \sigma_s (1 - \emptyset)^{\frac{1}{A_a - 1}}$$

or

$$\sigma_s = \sigma_1 (1 - \emptyset)^{\frac{1}{1 - A_a}} \quad \boxed{2.71}$$

Substitution into $\boxed{2.70}$ gives

$$\varepsilon_s (1 - A_a) \sigma_s = (1 - \emptyset)^{\frac{1}{1 - A_a}} \left[\{\varepsilon_1 (1 - A_a) - \varepsilon_2\} \sigma_s + \frac{\varepsilon_2 \sigma_s}{(1 - \emptyset)^{\frac{1}{1 - A_a}}} \right]$$

ie

$$\varepsilon_s = \frac{1}{1 - A_a} \left[\{\varepsilon_1 (1 - A_a) - \varepsilon_2\} (1 - \emptyset)^{\frac{1}{1 - A_a}} + \varepsilon_2 \right] \quad \boxed{2.72}$$

For spheres $A_a = \frac{1}{3}$ giving the Hanai equations for an O/W dispersion, thus $\boxed{2.65}$, $\boxed{2.69}$, $\boxed{2.71}$ and $\boxed{2.72}$ can be regarded as the Hanai equations extended to spheroidal dispersions and can be used for $0 \leq A_a < 1$.

2.2.6.3.2 W/O Dispersion

Writing $\sigma_2 \gg \sigma_1$ and $\sigma_2 \gg \sigma_s$ [2.65] is unchanged.
[2.66] reduces to

$$\sigma_\infty \left[\frac{1}{A_a(\varepsilon_\infty - \varepsilon_2)} - \frac{1}{\varepsilon_\infty} \right] = \left(A_a\right)^{-1} \left[\frac{-\sigma_2}{\varepsilon_1 - \varepsilon_2} + \frac{\sigma_2}{\varepsilon_\infty - \varepsilon_2} \right]$$

$$= \left(A_a\right)^{-1} \sigma_2 \left[\frac{1}{\varepsilon_\infty - \varepsilon_2} - \frac{1}{\varepsilon_1 - \varepsilon_2} \right] \qquad [2.73]$$

[2.67] reduces to:

$$-\frac{\varepsilon_s}{\sigma_s} = -\frac{\varepsilon_1}{\sigma_1}$$

ie

$$\varepsilon_s = \varepsilon_1 \frac{\sigma_s}{\sigma_1} \qquad\qquad\qquad [2.74]$$

Also [2.68] reduces to

$$\left(\frac{\sigma_1}{\sigma_s} \right)^{A_a} = 1 - \emptyset$$

or

$$\sigma_s = \frac{\sigma_1}{(1-\emptyset)^{\frac{1}{A_a}}} \qquad\qquad\qquad [2.75]$$

Substitution of [2.74] into [2.75] gives

$$\varepsilon_s = \frac{\varepsilon_1}{(1-\emptyset)^{\frac{1}{A_a}}} \qquad\qquad\qquad [2.76]$$

For spheres $A_a = \frac{1}{3}$ giving the Hanai equations for a W/O dispersion, thus [2.65], [2.73], [2.75] and [2.76]

can be regarded as the Hanai equations extended to spheroidal dispersions and can be used for $0 < A_a \leqslant 1$.

2.2.6.4 Derivation of generalised Looyenga equation

Using the generalised Bruggeman equation [2.64] and assuming the infinitesimal changes $\varepsilon_1 \rightarrow \varepsilon - \Delta\varepsilon$ and $\varepsilon_2 \rightarrow \varepsilon + \Delta\varepsilon$ and replacing $\emptyset$ by the variable volume fraction $\emptyset^{\backprime}$ as in the derivation of the Looyenga equation [2.17] gives:

$$\frac{(\varepsilon + \Delta\varepsilon) - \Delta\varepsilon}{(\varepsilon + \Delta\varepsilon) - (\varepsilon - \Delta\varepsilon)} \left(\frac{\varepsilon - \Delta\varepsilon}{\varepsilon}\right)^{A_a} = 1 - \emptyset^{\backprime}$$

or

$$\frac{\Delta\varepsilon}{2\Delta\varepsilon} \left(\frac{\varepsilon - \Delta\varepsilon}{\varepsilon}\right)^{A_a} = 1 - \emptyset^{\backprime}$$

$$\frac{1}{2} \left(1 - \frac{\Delta\varepsilon}{\varepsilon}\right)^{A_a} = 1 - \emptyset^{\backprime}$$

Applying binomial expansion and neglecting $(\Delta\varepsilon)^2$ terms

$$\frac{1}{2} - \frac{A_a}{2} \frac{\Delta\varepsilon}{\varepsilon} = 1 - \emptyset^{\backprime}$$

ie

$$\emptyset^{\backprime} = 1 - \left(\frac{1}{2} - \frac{A_a}{2} \frac{\Delta\varepsilon}{\varepsilon}\right)$$

$$= \frac{1}{2} + \frac{A_a}{2} \frac{\Delta\varepsilon}{\varepsilon} \qquad\qquad [2.77]$$

Combining [2.77] with [2.16a] gives

$$\frac{1}{2} + \frac{A_a}{2} \frac{\Delta\varepsilon}{\varepsilon} = \frac{1}{2} - \frac{1}{4} \Delta\varepsilon \frac{d^2\emptyset/d\varepsilon^2}{d\emptyset/d\varepsilon}$$

ie

$$\left(\frac{1}{2A_a}\right)\varepsilon\frac{d^2\emptyset}{d\varepsilon^2} + \frac{d\emptyset}{d\varepsilon} = 0$$

This equation is of the form $kx\dfrac{d^2y}{dx^2} + \dfrac{dy}{dx} = 0$ and has a

solution

$$y = \frac{Cx^{1 - 1/k}}{1 - 1/k} + D$$

where C and D are constants.

Hence we can write

$$\emptyset = \frac{C\varepsilon^{1 - 1/k}}{1 - 1/k} + D \quad \text{where } k = \frac{1}{2A_a}$$

$$\therefore \emptyset = \frac{C\varepsilon^{1 - 2A_a}}{1 - 2A_a} + D$$

Applying boundary conditions when $\emptyset = 0$, $\varepsilon = \varepsilon_1$ and when

$\emptyset = 1$, $\varepsilon = \varepsilon_2$ gives:

$$0 = \frac{C\varepsilon_1^{1 - 2A_a}}{1 - 2A_a} + D \qquad \text{ie } \varepsilon_1^{1 - 2A_a} = -\frac{D}{C}(1 - 2A_a)$$

and

$$1 = \frac{C\varepsilon_2^{1 - 2A_a}}{1 - 2A_a} + D \qquad \text{ie } \varepsilon_2^{1 - 2A_a} = \frac{(1 - D)}{C}(1 - 2A_a)$$

$$\therefore \quad \frac{\varepsilon_1^{1 - 2A_a}}{\varepsilon_2^{1 - 2A_a}} = \frac{-D}{1 - D} \quad \text{or} \quad D = \frac{\varepsilon_1^{1 - 2A_a}}{\varepsilon_1^{1 - 2A_a} - \varepsilon_2^{1 - 2A_a}}$$

thus

$$C = \frac{-D(1 - 2A_a)}{\varepsilon_1^{1 - 2A_a}} = \frac{-(1 - 2A_a)}{\varepsilon_1^{1 - 2A_a} - \varepsilon_2^{1 - 2A_a}}$$

$$\therefore \quad \emptyset = \frac{-\varepsilon^{1-2A_a}}{\varepsilon_1^{1-2A_a} - \varepsilon_2^{1-2A_a}} + \frac{\varepsilon_1^{1-2A_a}}{\varepsilon_1^{1-2A_a} - \varepsilon_2^{1-2A_a}}$$

$$= \frac{\varepsilon^{1-2A_a} - \varepsilon_1^{1-2A_a}}{\varepsilon_2^{1-2A_a} - \varepsilon_1^{1-2A_a}}$$

or

$$\varepsilon = \left[\varepsilon_1^{1-2A_a} + \emptyset \left(\varepsilon_2^{1-2A_a} - \varepsilon_1^{1-2A_a} \right) \right]^{\frac{1}{1-2A_a}}$$

$$[2.78]$$

For spheres $A_a = \frac{1}{3}$ giving the Looyenga equation.

In addition, when $A_a = \frac{1}{4}$ [2.78] reduces to the Kraszewski

equation [2.18]. For this extension, the range of A_a

is restricted to $0 \leqslant A_a < 0.5$.

2.2.6.5 Summary of new equations

.2.6.5.1 Permittivity

The following new equations for the permittivity of a

mixture have been derived:

(i) $\dfrac{\varepsilon_2 - \varepsilon}{\varepsilon_2 - \varepsilon_1} \left(\dfrac{\varepsilon_1}{\varepsilon} \right)^{A_a} = 1 - \emptyset$ $\qquad [2.64]$

$0 \leqslant A_a \leqslant 1$

which is the Bruggeman equation extended to spheroidal

dispersions of both prolate and oblate shape.

(ii) $\varepsilon_s = \dfrac{1}{1 - A_a} \left[\{ \varepsilon_1 (1 - A_a) - \varepsilon_2 \} (1 - \emptyset)^{1/1-A_a} + \varepsilon_2 \right]$

$$[2.72]$$

- 109 -

$$0 \leq A_a < 1$$

which is the Hanai equation for the low frequency limiting

value of ε extended to O/W spheroidal dispersions of both

prolate and oblate shape.

The high frequency limiting value of ε $\boxed{2.65}$ is given

by (i) above writing $\varepsilon = \varepsilon_\infty$

(iii) $\quad \varepsilon_s = \dfrac{\varepsilon_1}{(1 - \emptyset)^{1/A_a}}$ $\qquad \boxed{2.76}$

$$0 < A_a \leq 1$$

which is the Hanai equation for the low frequency limiting

value of ε extended to a W/O spheroidal dispersion of

both prolate and oblate shape.

The high frequency limiting value is again given by (i)

$\boxed{2.64}$ writing $\varepsilon = \varepsilon_\infty$.

(iv)
$$\varepsilon = \left[\varepsilon_1^{1 - 2A_a} + \emptyset \left(\varepsilon_2^{1 - 2A_a} - \varepsilon_1^{1 - 2A_a} \right) \right]^{\frac{1}{1 - 2A_a}}$$

$$\boxed{2.78}$$

$$0 \leq A_a < 0.5$$

which is the Looyenga equation extended to spheroidal

dispersions of both prolate and oblate shape.

.2.6.5.2 <u>Conductivity</u>

The following new equations for the high and low

frequency limiting values of the conductivity of a

mixture, σ_∞ and σ_S, have been derived:

(i)
$$\sigma_\infty \left[\frac{1}{A_a(\varepsilon_\infty - \varepsilon_2)} - \frac{1}{\varepsilon_\infty} \right] = (A_a)^{-1} \sigma_1 \left[\frac{1}{\varepsilon_1 - \varepsilon_2} - \frac{1}{\varepsilon_1} \right] \qquad [2.69]$$

$$0 \leqslant A_a < 1$$

(ii)
$$\sigma_S = \sigma_1 (1 - \emptyset)^{\frac{1}{1 - A_a}} \qquad [2.71]$$

$$0 \leqslant A_a < 1$$

(i) and (ii) are the Hanai equations extended to an O/W spheroidal dispersion of both prolate and oblate shape.

(iii)
$$\sigma_\infty \left[\frac{1}{A_a(\varepsilon_\infty - \varepsilon_2)} - \frac{1}{\varepsilon_\infty} \right] = (A_a)^{-1} \sigma_2 \left[\frac{1}{\varepsilon_\infty - \varepsilon_2} - \frac{1}{\varepsilon_1 - \varepsilon_2} \right]$$

$$0 < A_a \leqslant 1 \qquad\qquad\qquad [2.73]$$

(iv)
$$\sigma_S = \frac{\sigma_1}{(1 - \emptyset)^{1/A_a}} \qquad [2.75]$$

$$0 < A_a \leqslant 1$$

(iii) and (iv) are the Hanai equations extended to a W/O spheroidal dispersion of both prolate and oblate shape.

CHAPTER 3   EXPERIMENTAL

3.1   Materials and Preparation of Mixtures

3.1.1   Alcohols

The alcohol t butanol was Analar grade (BDH), the
cyclohexanol and the 1 heptanol were both General
Purpose Reagent grade (BDH) and the 1 butanol was Puriss
grade (Koch Light).   All the alcohols were fractionally
distilled immediately before use from freshly ignited
quick-lime using a Gallenkamp fractional distillation
unit with variable take-off head.   When the alcohols had
to be stored, they were kept in dessicators over phosphorus
pentoxide.

3.1.2   Water

Pure water was obtained by refluxing distilled water over
alkaline permanganate and then distilling through a 61 cm
fractionating column.   Later in the experimental programme
double-distilled water was obtained directly from a Fisons
Fi-Stream unit.

3.1.3   Alcohol-water Mixtures

Alcohol-water mixtures were prepared by weighing the
required amounts of liquid using a precision balance which
was usually a Mettler H10 or Oertling V20.   These balances
enabled masses to be determined to a precision of better
than $\pm$ 0.0005 g, and the mole fractions of the mixtures
could be formulated to a precision of better than $\pm$ 0.01.

3.1.4 Surfactants

The commercial surfactant Brij 30 (Batch 51) was obtained from Honeywill-Atlas Ltd. The pure surfactants $C_{12}E_4$, $C_{12}E_6$ and $C_{12}E_8$ were obtained from Nikkol Chemicals Ltd; Japan. In order to achieve consistency, the Brij 30 was stored for 24 hours at 30° C and then filtered through Whatman 41 ashless paper at the same temperature. The filtering requirement arose because this batch of Brij 30 contained a small amount of insoluble solids. Again to achieve consistency, all measurements were performed using the same batch {51}. The pure surfactants were used as obtained without further purification.

3.1.5 Hydrocarbons

The hydrocarbon heptane was IP normal grade (BDH), the decane was Laboratory Reagent grade (BDH) and the hexadecane was Puriss grade (Koch Light). The hydrocarbons were used as obtained without further purification.

3.1.6 Binary and ternary mixtures of surfactants

The binary and ternary mixtures of surfactant with water, surfactant with hydrocarbon and surfactant with water and a hydrocarbon were prepared by the precision balance method already described, where for the binary aqueous mixtures of $C_{12}E_n$ (n = 4, 6 and 8), a successive dilution method was adopted because of the high cost of the surfactants. The method involved addition of the required amount of water by a pipette so that the mixtures could be

- 113 -

studied over the whole composition range at 10% by mass
intervals. In order to ensure consistency and
reproducibility of results, additional mixtures at both
90% and 80% by mass of water were formulated by the
method of addition of surfactant to water. For these two
mixtures, the values of e` obtained by the two formulation
methods agreed within $\pm$ 0.2%.

3.2 Development of time domain technique and its use

3.2.1 Introduction

At the time that this research programme was commenced,
time domain spectroscopy was in an early stage of
development for use in liquids. Accordingly, the
development of a specific method applicable to the
materials of interest here has formed an essential part
of the work and is presented as such.

Time domain reflectometry (TDR) has been used for some
years in cable testing and makes use of the very fast
switching properties of tunnel diodes and wide band
facilities of sampling oscilloscopes together with the
good VSWR properties of precision coaxial air lines such as
the Amphenol APC7 and General Radio GR 900.

The application of TDR techniques to dielectric measure-
ments was originally suggested by Fellner-Feldegg (169).
The method involves the generation of a fast rise-time
(and thus wideband) pulse and study of the change in pulse

shape after reflection from the surface of a dielectric

medium inside a coaxial air-line. A representative time

dependence of the reflection coefficient for reflection

from a dielectric is given in Figure 7.

Reflection
Coefficient ρ
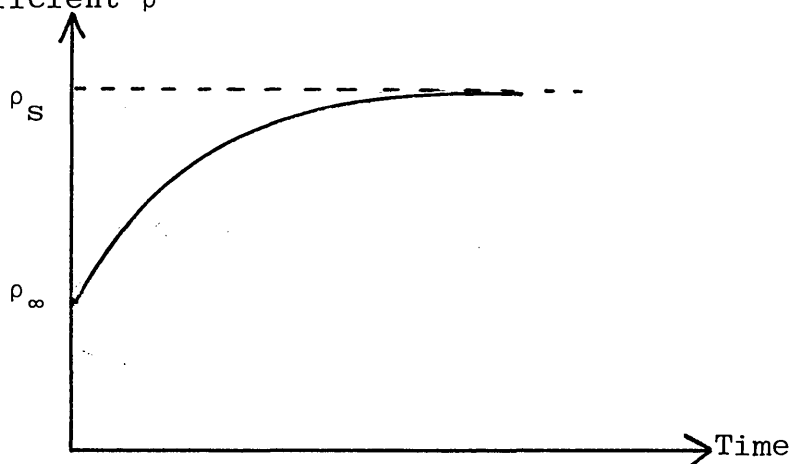
ρ_∞ = high frequency limiting value of reflection coefficient

ρ_S = low frequency limiting value of reflection coefficient

In the paper of Fellner Feldegg (169) rather poor agreement

was obtained between the measured relaxation time of some

alcohols compared with literature values. However,

 Whittingham (170) pointed out that the method of deter-

mining relaxation times used by Fellner-Feldegg was not

mathematically valid and subsequent work by Suggett et al

(171) using the correct forms of the equations gave results

which compared favourably with literature values. Loeb et

al (172) discussed some of the errors associated with the

time domain reflection technique and, in addition, described an alternative measurement method based on transmission instead of reflection. The transmission method is more involved in that a transfer function is required from two cells of different lengths in order to determine $\varepsilon*$. The method has the advantage of improved high frequency precision due to the generation of larger phase shifts which results in substantially less error in time referencing, but it suffers from the disadvantage of more limited frequency range than the reflection methods as well as requiring results from two different measuring cells. Van Gemert et al (173) have reported an accuracy in relaxation times of "about 5%" for the single reflection method.

Following the suggestion of Fellner-Feldegg (174), multiple reflections from a thin dielectric sample can be utilised and a number of multiple response methods have been developed. These demand greater experimental expertise but have advantages in biological applications since little liquid is required.

A number of review articles in which the various time domain methods are evaluated have been published with the work of van Gemert (175), Suggett (176), Clark et al (177), Clarkson et al (178) Giese and Tiemann (179) and Grant et al (42) being particularly worthy of mention.

Clarkson et al (178) suggested that in many medium to

high loss systems, the single reflection method is the
most favourable since (i) the effects of sample termination
do not need to be taken into account and (ii) that extra-
neous reflections can be minimised by appropriate choice
of delay lines linking the components of the system.
This method has formed the basis of the time domain part
of the experimental programme in this work. Relaxation
times can be determined directly from the time domain data
or by use of Fourier transformation. Both of these
techniques are described in the following sections.

3.2.2 Direct time domain methods

3.2.2.1 Fellner-Feldegg method τ_D

In this method, it is assumed that the time-dependence of
the reflection coefficient ρ is such that the time
dependent permittivity ε, which is given by $\varepsilon = \left(\frac{1 + |\rho|}{1 - |\rho|} \right)^2$,
obeys an exponential relationship. This gives a linear
relation between $\ln (\varepsilon_S - \varepsilon)$ against time, t, where ε_S
is the low frequency limiting value of the permittivity and
the reciprocal of the slope of the $\ln (\varepsilon_S - \varepsilon)$ against t
graph is the relaxation time τ_D.

Despite its basic mathematical invalidity in assuming that
the complex component in ρ may be neglected, Loeb et al
(172) have reported that this τ_D method can be of value
when used together with a single low frequency measurement
to estimate relaxation times in liquids where echo
reflections appear before the relaxation process is complete.

Such behaviour occurs in slower relaxation processes.
Although examples were not given, these authors reported
that in Debye-type dispersions, the method gives good
agreement with literature values. They further added that
this direct method is useful in revealing the presence
of overlapping relaxations.

The τ_D method has been applied to the time domain data
obtained in this work with the values of ε_s being
obtained from Dipolmeter values using the procedure
described in 3.2.4.4.

3.2.2.2 <u>Fellner-Feldegg and Barnett method τ_{FF+B}</u>

The basic mathematical invalidity in the τ_D method has
been corrected by Fellner-Feldegg and Barnett but the
method is restricted to single relaxation time (Debye-
type) dispersions.

The Fellner-Feldegg and Barnett (FF+B) paper (180) presents
three sets of curves for values of the time-dependent
reflection coefficient, ρ, given by:

$$\frac{\rho_s - \rho}{\rho_s - \rho_\infty} = 0.2, \frac{1}{e} \text{ and } 0.8 \text{ respectively where } \rho_s \text{ and } \rho_\infty \text{ are}$$

the respective low and high frequency limiting values of
the reflection coefficient.

The curves permit the determination of the relaxation time
τ_{FF+B} from the measured time $\tau^\prime$, at the 0.8, $\frac{1}{e}$ and 0.2
values respectively of the reflection coefficient, by

providing scaling factors whose values depend on (a) which of the reflection coefficient values is selected and (b) the values of ε_S and ε_∞. The $\dfrac{\rho_S - \rho}{\rho_S - \rho_\infty} = 0.2$ curves enable the most precise determination of the required scaling factor and were therefore used whenever possible in this work.

In this work, the values of ε_S and ρ_S $\left| = \dfrac{\varepsilon_S^{\frac{1}{2}} - 1}{\varepsilon_S^{\frac{1}{2}} + 1} \right|$ were obtained from Dipolmeter values. Estimated of the ρ_∞ values posed some difficulty due to the reflection coefficient at times close to t = 0 being very sensitive to error in the time zero reference. The value of ρ_∞ adopted was the one which was the lowest value given by the time domain data. This was attained after typically two data points from the time zero and corresponded to about 30 ps. This figure is considered reasonable as the system rise-time was quoted as 35 ps. The values of τ at the 0.8, $\dfrac{1}{e}$ or 0.2 points of the reflection coefficient curve were obtained directly from the time domain data.

3.2.2.3   <u>Brehm and Stockmayer method</u> τ_{B+S}

The basic mathematical invalidity in the τ_D method has been corrected by Brehm and Stockmayer (181) and their treatment is more general than that of FF+B as the possibility of Cole-Davidson type dispersion (equation [2.9]) with values of the parameter β between 0.3 and 1 is taken into account. However, the curves in this paper

are much less detailed than those in FF+B.

The Brehm and Stockmayer method requires the determination
of two times t_1 and t_2 when the reflection coefficient
has fallen by $\frac{1}{3}$ and $\frac{2}{3}$ respectively from its initial
ρ_∞ value to its final ρ_S value. Two sets of curves
are given, one set enables the β parameter to be
determined from the ratio $t_{\frac{1}{3}}/t_{\frac{2}{3}}$ for values of ε_S and ε_∞
in the ratios $\varepsilon_S/\varepsilon_\infty = 4$, 3, 2 and 1 respectively. The
other set of curves enables the relaxation time τ_{B+S}
to be determined, for values of $\varepsilon_S/\varepsilon_\infty$ as given above,
from the $t_{\frac{1}{3}}$ data.

In this work, the same procedure as used in the FF+B
method was used for the determination of ε_S, ε_∞, ρ_S
and ρ_∞. The $t_{\frac{1}{3}}$ and $t_{\frac{2}{3}}$ values were obtained directly
from the time domain data.

3.2.3 <u>Fourier transform method</u> τ_F

3.2.3.1 <u>Theory</u>

Time domain spectroscopy (TDS) applied to dielectric
studies has been discussed in some detail by a number of
authors; the approach below follows that of Loeb et al
(172).

For a coaxial line filled with a dielectric of
permittivity $\varepsilon^*(\omega)$ the characteristic impedance Z is
given by

$$Z = \frac{Z_O}{\left[\varepsilon^*(\omega)\right]^{\frac{1}{2}}} \qquad\qquad [3.1]$$

where $\varepsilon^* = \varepsilon` - j\varepsilon`` - \dfrac{j\sigma}{\omega\varepsilon} = \varepsilon` - j\varepsilon``$ when conductivity

is negligible. [3.2]

and Z_O is the characteristic impedance of an air-filled

line.

The propagation constant γ is given by

$$\gamma = \gamma_0 \left[\varepsilon^*(\omega)\right]^{\frac{1}{2}} \qquad [3.3]$$

where $\gamma_0 \left(= \dfrac{j\omega}{c}\right)$ is the propagation constant of an air-

filled line.

When the wave encounters a region of characteristic

impedance Z where $Z \neq Z_O$, reflection occurs with

reflection coefficient, $\rho^*(\omega)$ where

$$\rho^*(\omega) = \frac{Z - Z_O}{Z + Z_O} \qquad [3.4]$$

and since Z, Z_O are complex, $\rho^*(\omega)$ will also be complex.

In order to convert the time domain data into the

equivalent frequency domain information, Fourier

transformation is necessary. The Fourier transform

expression states that

$$F(\omega) = \int_{-\infty}^{\infty} f(t) \exp(-j\omega t)\, dt \qquad [3.5]$$

indicating that any time domain response f(t) is equiva-

lent to an infinite number of frequency components.

The frequency domain response of a dielectric sample is

determined by calculating the ratio of the Fourier

transforms of the time domain responses of the incident

and reflected pulses.

For an incident pulse $f_i(t)$ and reflected pulse $f_r(t)$, the frequency response of the system $G(\omega)$ is given by:

$$G(\omega) = \frac{F_r(\omega)}{F_i(\omega)} = \frac{\int_{-\infty}^{\infty} f_r(t) \exp(-j\omega t)\, dt}{\int_{-\infty}^{\infty} f_i(t) \exp(-j\omega t)\, dt} \qquad [3.6]$$

Fourier transformation is achieved using the modification to the Shannon sampling theorem (182) due to Samulon (183) by writing:

$$F(\omega) = \frac{\exp(j\omega\, \Delta t/2)}{2j \sin(\omega\, \Delta t/2)} \sum_{n=-\infty}^{n=\infty} \left[f(n\Delta t) - f(n\Delta t - \Delta t) \right] \exp(-jn\omega\Delta t)$$

$$[3.7]$$

provided $F(\omega) = 0$ for $\omega > \pi/\Delta t$

Combining equations $[3.1]$ and $[3.4]$ yields

$$\varepsilon^*(\omega) = \left[\frac{1 - \rho^*(\omega)}{1 + \rho^*(\omega)} \right]^2 \qquad [3.8]$$

and writing $\rho^*(\omega) = r \exp(j\phi)$ gives after separating real and imaginary parts:

$$\varepsilon' = \frac{(1 - r^2)^2 - 4(r \sin \phi)^2}{(1 + r^2 + 2r \cos \phi)^2} \qquad [3.9]$$

and $$\varepsilon'' = \frac{4(1 - r^2)\, r \sin \phi}{(1 + r^2 + 2r \cos \phi)^2} \qquad [3.10]$$

3.2.3.2   Development of computer program

The experimental procedure for determining $F_r(\omega)$ involves measuring the amplitudes of the reflected pulse a_1, a_2, a_3, ..., a_n from the dielectric at time intervals Δt.

The change in amplitude b_n ($= a_n - a_{n-1}$) is then
determined for $b_1 = a_1$ and substitution into the transform
expression gives for a frequency $\omega = \omega_1$:

$$F_r(\omega_1) = \frac{-\exp(j\omega_1 \Delta t/2)}{2j \sin(\omega_1 \Delta t/2)}\left[b_1\exp(-j\omega_1\Delta t) + b_2\exp(-\exp j2\omega_1\Delta t) + \right.$$

$$\left. \ldots + b_n\exp(-jn\omega_1\Delta t)\right]$$

$$= \frac{-1}{2j \sin(\omega_1 \Delta t/2)}\left[b_1\cos\left(\frac{\omega_1\Delta t}{2}\right) - jb_1\sin\left(\frac{\omega_1\Delta t}{2}\right) + \right.$$

$$b_2\cos\left(\frac{3\omega_1\Delta t}{2}\right) - jb_2\sin\left(\frac{3\omega_1\Delta t}{2}\right) +$$

$$\left. \ldots + b_n\cos\{(n - \tfrac{1}{2})\omega_1\Delta t\} - jb_n\sin\{(n - \tfrac{1}{2})\omega_1\Delta t\}\right]$$

$$= \frac{\sum\limits_{n=0}^{n} b_n\sin\{(n - \tfrac{1}{2})\omega_1\Delta t\} + j \sum\limits_{n=0}^{n} b_n\cos\{(n - \tfrac{1}{2})\omega_1\Delta t\}}{2 \sin\left(\frac{\omega_1\Delta t}{2}\right)}$$

$$= B_s + jB_c$$

putting $B_s + jB_c = R \exp^{j\Theta}$

then $R = (B_s^2 + B_c^2)^{\frac{1}{2}}$

and $\Theta = \arctan(B_c/B_s)$

The transform for the incident pulse is determined by
measuring the amplitude of the pulse obtained when a short
circuit termination replaces the dielectric. In this case
amplitudes c_1, c_2, ... c_n are measured at intervals of
Δt and

$d_n = c_n - c_{n-1}$ for $d_1 = c_1$ is found.

An expression similar to that for $F_r(\omega)$ is obtained except that the negative sign is not required. We thus obtain:

$$F_i(\omega_1) = -\left[\frac{\sum\limits_{n=0}^{n} d_n \sin\{(n - \tfrac{1}{2})\omega_1 \Delta t\} + j\sum\limits_{n=0}^{n} d_n \cos\{(n - \tfrac{1}{2})\omega_1 \Delta t\}}{2 \sin\left[\frac{\omega_1 \Delta t}{2}\right]}\right]$$

$$= -\left[D_s + jD_c\right]$$

and putting $D_s + jD_c = S \exp^{j\alpha}$

$$S = -\left[D_s^2 + D_c^2\right]^{\tfrac{1}{2}} \quad \text{and} \quad \alpha = \text{arc tan}\left(\frac{D_c}{D_s}\right)$$

Now $G(\omega_1) = \dfrac{F_r(\omega_1)}{F_i(\omega_1)}$

putting $G(\omega_1) = T \exp^{j\phi}$

then $T = -\dfrac{R}{S}$ and $\phi = \theta - \alpha$

Hence by application of equations $[3.9]$ and $[3.10]$ $\varepsilon^{\grave{}}$ and $\varepsilon^{\grave{}\grave{}}$ can be found.

A computer program for the determination of ε^* from a_n and c_n values has been written in Fortran IV MUSIC.

The computer program for the transform has been extended in order to give improved performance in data-handling. This has been done to permit

  (i) evaluation of the effect of error in the time zero reference points,

(ii) optimisation of the number of data points to minimise both short time and long time truncation errors in

the Fourier transform.

Truncation effects can be studied because the computer program enables the Fourier transform to be obtained for a specified varying number of data points. Also the transform for each number of data points can be found for a number of time zero reference points by repeating the transform for the zero data point shifted by a specified integral number of data points. This latter procedure can be applied to both the dielectric and the short circuit data and enables the time zero reference to be effectively both advanced and retarded by one or more data points as instructed in the program input data.

An addition that has been included is an instruction to the short circuit transform program ensuring that the transform has the correct sign. This is required due to the non-ideal shapes of the time domain waveforms which occasionally reverse the transform sign for the short circuit data at certain frequencies, resulting in ε^* being unobtainable at those frequencies. The program instruction removes this possibility. A copy of the computer program is given in the Appendix.

3.2.4   TDR measurement system

3.2.4.1   Basic system

The measurement system incorporated a Hewlett Packard HP 180A mainframe oscilloscope, HP 1815A TDR/sampler, HP 1817A sampling-gate and HP 1106A tunnel diode mount.

The coaxial air lines incorporated Amphenol APC 7 type
connectors and two brands were used, namely HP 11567A
20 cm lines and Amphenol APC7 30 cm lines. Since the
Amphenol lines were the only ones which could be
dismantled, these were used as the measurement cell.
The time domain data was recorded on an HP 7035B X-Y
recorder which was replaced in later measurements by a
Farnell PR1 chart recorder. The X-Y recorder was
directly connected to the system via the output connections
on the rear of the 180A main frame. The "Main Sweep
Output" provided the X input and the "Delayed Gate
Output" provided the Y input. An appropriately large
sized X-Y plot was obtained simply by adjusting the
vernier controls on the recorder. In later measurements
the HP recorder exhibited poor stability and was replaced
by a Farnell PR1 chart recorder. With this instrument
it was necessary to 'back off' some of the recorder input
in order to obtain a suitable sized trace. This was
achieved by placing a stabilised voltage supply (Farnell
E30) in conjunction with a Beckman Helipot potentiometer
in series with the input. The PR1 chart recorder was
found to give comparable performance to the HP 7035B
X-Y recorder.

A variety of air line configurations were studied in order
to gain information on the relative effects of the various
impedance mismatches in the system and thus ultimately
obtain the optimum response. A configuration as given in

Figure 8 was found to be the most suitable with the air line components available, and is similar, but not identical, to that described by Loeb et al (172).

Figure 8
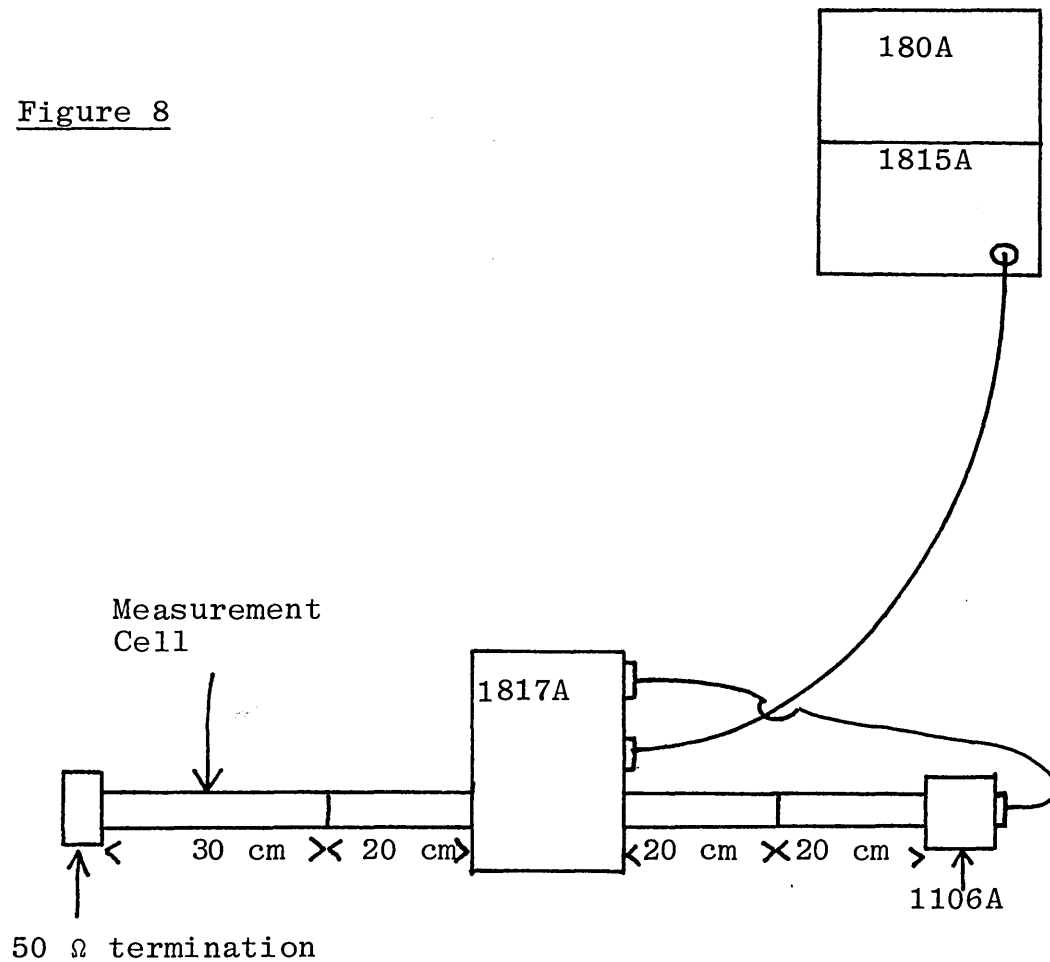
The 1815A was used in the Signal Averaging mode as the operating manual quoted an improvement of 2:1 in noise and "jitter" when compared with the Normal mode. This clearly cannot offer the precision obtainable with the Signal Averagers used by many workers in this field, but it is suitable for studies up to a maximum frequency of approximately 3 GHz (171, 172, 175).

The Amphenol APC7 30 cm line measurement cell could be
dismantled without difficulty. The translucent nature of
the bead which terminated the line used in the earlier
part of the experimental programme enabled any air
bubbles present in the sample to be seen and thus minimal
problems due to air bubbles were encountered. In the
latter part of the programme, a later design Amphenol
line was used. This had an opaque bead and thus made air
bubble elimination more difficult, but because the
presence of a significant air bubble content is revealed
in the time domain trace, minimisation of such effects
was achieved without difficulty.

Most of the measurements were made at temperatures close
to 25° C with temperature control being achieved by
enclosing the coaxial line measurement cell in a glass
jacket which was circulated with water driven by a Grant
SU controller which maintained the temperature constant to
better than $\pm$ 0.2° C. In order to facilitate measurements
at lower temperatures, a refrigeration unit was also
incorporated and used when required. After allowing
sufficient time for the dielectric liquid to attain the
required temperature, a minimum of five traces on the X-Y
recorder were taken to ensure stability was maintained.
Similarly, when the dielectric was replaced with an APC 7
precision short circuit, a minimum of five X-Y plots were
again taken.

3.2.4.2 <u>Voltage base line and time zero reference determination</u>

The base line for the voltage transient on the X-Y plot was determined using a method similar to that of Clarkson and Williams (184). The base line chosen was obtained from an average of typically 30 values of the voltage level before the reference step signal. This procedure was used for both a dielectric and short-circuit terminated line. The time zero reference point was obtained using a method described by Loeb et al (172) in which linear extrapolation from the steepest part of the voltage step to intersect with the voltage base line was drawn. This intersection was used as the time zero reference.

3.2.4.3 <u>Errors in time domain data</u>

Giese and Tiemann (179) have shown that the impedance mismatch between the sampler and air line causes erroneous values at lower frequencies. This problem was also discussed by Campbell et al (34) in studies of dilute alcohols in non-polar solvents. These authors used liquid benzene, which is known not to exhibit dielectric dispersion in this time range, to obtain a frequency dependent apparent reflection coefficient for the benzene this was then used to correct the data obtained for the alcohol solutions. The method used for this correction, which effectively incorporates a data smoothing procedure, was not described but the authors reported that the mismatch between the sampler and air line was corrected by

adjusting the measured reflection coefficient for the
benzene until the low frequency permittivity of the pure
alcohol, as extrapolated from the time domain data,
attained its experimentally correct value. It is presumed
that the 'correct' value was obtained from literature data.

The approach of Campbell et al is open to criticism
because some of the effects of the impedance mismatch in
the system are dependent on the magnitude of the reflection
coefficient of the dielectric. This aspect has been
discussed in detail by Loeb et al (172) and the outcome
is that the approach is only strictly valid for liquids
with the same permittivity as that of the reference liquid.

3.2.4.4 Correction Procedure : WTW Dipolmeter

In this work, correction for the sampler and air line
mismatch together with voltage drift and time "jitter"
was achieved by adjusting the measured steady state
reflection coefficient of the liquid until the low
frequency permittivity obtained from the time domain data
agreed with the value given by a WTW Dipolmeter type DM01
which operated at the constant frequency of 2MHz.

The measurement cell used with the Dipolmeter was the cell
type MFL 2 which enabled relative permittivities within a
range of 3.6 to 22 to be measured. The MFL 2 cell was
calibrated using the following purified liquids at 25° C
as standards : chlorobenzene ($\varepsilon^{`}$ = 5.602), 1,2 - dichloro-
ethane ($\varepsilon^{`}$ = 10.387) and acetone ($\varepsilon^{`}$ = 20.820). The

Dipolmeter readings were used to determine the constants a, b and c in a polynomial expression relating $\varepsilon^\backprime$ to the Dipolmeter reading D of the form $\varepsilon^\backprime = a + bD + cD^2$. This method gave higher precision in determining $\varepsilon^\backprime$ than the calibration procedure of Stevens (185) which involved determination of the best straight line for an assumed linear relation between $\varepsilon^\backprime$ and D. An uncertainty of less than 0.01 in $\varepsilon^\backprime$ was achieved here.

Application of this correction procedure involved scaling the dielectric data by a constant factor which was always within the range 0.98 to 1.02. It was found that the results obtained by the method used in this work gave Cole-Cole plots and a relaxation time value for the pure alcohol 1-butanol very similar to those obtained by Campbell et al (34), thus validating this correction procedure.

Correction could not be applied to the cyclohexanol-water mixtures at less than 0.2 mf of water nor to the pure alcohol 1-heptanol. This was because the steady state reflection coefficient was not attained at the completion of the time domain scan due to the long relaxation times of these liquids. Thus scaling was not applied to the time domain data for these liquids.

3.3 Other measurement techniques : RF bridge studies of surfactant mixtures

3.3.1 Calibration of RF bridge

The surfactant mixtures were studied primarily in the
RF range. Measurements were performed within the
frequency range 30 kHz to 15 MHz using a Hatfield
transformer ratio arm bridge type 300 A with an Airmec
video oscillator type 399 as source and an Eddystone
communication receiver type 830 as detector in the range
300 kHz to 15 MHz. At the lower frequencies, a Telequip-
ment oscilloscope type D53 was used as detector. The
oscilloscope was much less sensitive than the receiver
as a detector but was able to reveal large amplitude
dispersion effects. The Hatfield bridge was found to
give a progressively poorer performance during the latter
part of the experimental programme and was replaced in
subsequent measurements by a Wayne Kerr bridge type B601.
This operated in the frequency range 30 kHz to 5 MHz.

On both the Hatfield and Wayne Kerr bridges, the balance
conditions for both the conductance and capacitance
components were established by use of standard resistors
and standard capacitors. It was found necessary to set
the balance conditions for both bridges at each
measurement frequency used, with this requirement being
particularly important with the B601.

The WTW cell type MFL 2 was used as the measurement cell
for the RF bridges. The cell was connected to the bridge
by a short length of coaxial cable. The cell constants
for the RF bridge were established by measuring a number

of liquids on both the RF bridge at 2 MHz and the Dipolmeter. In addition, double distilled water at 20° C was used as a standard since the upper limit of permittivity, $\varepsilon^\backprime$, of the MFL2 cell on the Dipolmeter was 22.

With the cell constants obtained, permittivity values could be determined with the Hatfield bridge, to a precision of $\pm$ 0.2 for $\varepsilon^\backprime$ values in the range 1.8 to 78.0.

In order to achieve the highest precision in determining $\varepsilon^\backprime$ values with the Wayne Kerr bridge, it was found necessary to use slightly different values for the cable capacitance component depending on the value of the measured capacitance on the bridge. This effect was attributed to the relatively poor ($\pm$ 1%) precision quoted for the bridge. By using the cable capacitance values obtained, the precision of the results was increased and enabled permittivity values to be determined to the same precision as that for the Hatfield bridge for the same permittivity range.

3.4 Specimen conditions

3.4.1 Measurement temperatures

For nearly all of the investigations of the surfactant behaviour, measurements were performed only when the mixtures were optically transparent. The required temperatures for the $C_{12}E_4$- and Brij 30- water mixtures were obtained from phase diagram data of Bostock (83). These

diagrams are reproduced by kind permission of the author
in chapter 5 of this work. The phase diagram for $C_{12}E_6$-
water mixtures was obtained from literature data (186) and
that for $C_{12}E_8$- water mixtures from Unilever Ltd (187).
These phase diagrams are also given in chapter 5.

An important feature of some of the surfactant-water and
surfactant-water-hydrocarbon compositions was that optical
transparency was attained only over a very narrow temper-
ature range, being typically about 1° C. In order to
ensure that the mixtures were measured in the transparent
state, the cap of the MFL2 cell was briefly removed to
inspect the mixture in the cell and secondly, it was also
checked that the mixture was transparent when drained from
the cell immediately on completion of the measurements.

3.4.2 Surfactant-water and surfactant-hydrocarbon binary mixtures

Binary mixtures of the surfactants $C_{12}E_n$ (n = 4, 6 and 8)
and Brij 30 with water were studied over the whole
composition range at 10% by mass intervals. Their
temperatures were adjusted as required in order to main-
tain the transparency condition.

For all of the surfactants and, in addition for mixtures
which were transparent over a wide temperature range, the
temperature dependence of the permittivity was studied.

Some studies were performed on binary mixtures of Brij 30
with the hydrocarbon heptane. In contrast to the Brij 30

water mixtures, the binary mixtures with heptane were miscible at all compositions at temperatures above 45° C. The mixtures were all studied at 56° C at 20% by mass intervals using the Dipolmeter with the DFL2 cell on the D1 range. Cell calibration was performed with heptane $(\epsilon^{\backprime} = 1.92)$ and Brij 30 as the reference liquids with a presumed linear relationship between the Dipolmeter reading (D1) and permittivity $\epsilon^{\backprime}$ being considered of adequate precision. The permittivity of Brij 30 was obtained from data given by the calibrated MFL2 cell. A precision of better than $\pm$ 0.03 in $\epsilon^{\backprime}$ values was obtained.

3.4.3 Surfactant, water and hydrocarbon ternary mixtures

The ternary mixture investigations were restricted to the surfactants $C_{12}E_4$ and Brij 30. The compositions studied were selected in order to cover the major transparent regions of the ternary phase diagrams of the two surfactants and, in addition, to check dielectrically proposals of micellar inversion suggested by Bostock (83) on the basis of phase diagram and conductivity investigations.

In addition, some ternary mixtures of Brij 30 were studied at temperatures just outside the upper and lower limits for transparency in order to detect possible structural changes which occur in the transition from transparent solution to a two phase or liquid crystalline structure.

3.4.4 Time domain studies of surfactant mixtures

In order to check for the occurrence or otherwise of

dielectric relaxation effects, the surfactant Brij 30 and some of the binary and ternary mixtures of the surfactants $C_{12}E_4$ and Brij 30 were studied using the time domain measuring system. For mixtures having a relatively wide temperature range of transparency, performing these measurements proved straightforward but for mixtures where the temperature range was narrow and significantly different from room temperature, serious measurement difficulties were encountered. In particular, it was deemed impossible to obtain reliable data on such systems. The difficulty was attributed to the high thermal conductivity of the air-line system causing the liquid at the ends of the coaxial line measuring cell to be at some temperature intermediate between the cell and room temperature. This view was strengthened by the observation of the liquid being cloudy when drained from the cell even though the cell was at the required temperature. It was considered that for this problem to be overcome, it would be necessary to completely re-design the temperature control system so that the whole air-line system between the sampler gate and the measuring cell, together with the 50 Ω line termination, could be held at the required temperature by an appropriate cooling or heating method. Since such a design modification was not feasible, the data on such mixtures is not open to unequivocal interpretation and the results have not been included.

CHAPTER 4 : RESULTS

4.1 Calibration of the WTW Dipolmeter

4.1.1 MFL2 Cell

Table 1

Measurement temperature = 25.0° C

Calibration Liquid	Permittivity $\varepsilon`$	Dipolmeter scale reading D
Chlorobenzene	5.602	364.3
1,2 dichloroethane	10.387	1224.0
Acetone	20.820	3031.0

Writing $\varepsilon` = a + bD + cD^2$

the constants are

a = 3.609

b = 5.442 x 10^{-3}

c = 7.790 x 10^{-8}

Using these values for a, b and c, the permittivity value

for each of the three calibration liquids is obtained

correct to the third decimal place with the above values

for D. It is therefore considered appropriate to assign

a maximum uncertainty of $\pm$ 0.01 for the permittivity

values for the range over which the cell can be used

namely $\varepsilon` = 3.60$ to 21.00.

4.1.2 DFL2 Cell

Table 2

Calibration Liquid	Temperature ($^{\circ}$C)	Permittivity $\varepsilon^{\backprime}$	Dipolmeter scale reading (D1)
Heptane	24.8	1.92	380.0
Brij 30	56.5	5.61	2739.0

Writing $\varepsilon^{\backprime} = a^{\backprime} + b^{\backprime}(D1)$

the constants obtained are

$a^{\backprime} = 1.326$

$b^{\backprime} = 1.564 \times 10^{-3}$

Use of these values gives a maximum uncertainty of $\pm$ 0.03

for $\varepsilon^{\backprime}$ values between 1.90 and 6.00.

4.2 Calibration of the RF bridges

4.2.1 Hatfield 300A

Measurement temperature = 24.9° C

Table 3

Calibration Liquid	Capacitance on bridge (pF)	Permittivity $\varepsilon^{\backprime}$
Heptane	36.9	1.92
1 butanol	77.1	17.60
Acetone	85.2	20.82
Water	231.7	78.3

Applying the relation:

Capacitance on bridge = capacitance of cell + capacitance

of cable

with the known $\varepsilon^\vee$ values gives:

Capacitance cell when empty, C_O = 2.55 pF and

Capacitance of cable = 32.0 pF.

With these values for the bridge constants, relative

permittivity $\varepsilon^\vee$ values could be determined with a

maximum uncertainty in $\varepsilon^\vee$ of $\pm$ 0.2 for $\varepsilon^\vee$ between 1.9 and

79.0.

4.2.2 Wayne Kerr B601

Measurement temperature = 25.0° C

Table 4

Calibration Liquid	Capacitance on bridge (pF)	Permittivity $\varepsilon^\vee$
Heptane	24.0	1.92
1 butanol	64.2	17.60
Acetone	71.8	20.82
Water	218.2	78.3

Using the same procedure as for 4.2.1, the capacitance of

cell when empty, C_O = 2.55 pF. In order to correct for a

dial reading error which increased with increased

capacitance values, as discussed in the experimental

section, a value of cable capacitance, C_C, which varied

with the capacitance reading on the bridge, C_B, was adopted.

Using the values of C_C as a function of C_B given in Table 5

the calibration graph (Figure 9) was drawn.

Table 5

Capacitance on bridge C_B/pF	Capacitance of cable C_c/pF
20	19.3
60	19.1
100	18.9
140	18.7
220	18.4

With values of C_c obtained from the calibration graph together with the value of 2.55 pF for C_o, the maximum uncertainty in $\varepsilon^{\check{}}$ was $\pm$ 0.2 for $\varepsilon^{\check{}}$ values between 1.9 and 79.0.

4.3 <u>Dipolmeter values for the static permittivity of alcohol water mixtures</u>

The values in Tables 6 to 9 were obtained from results with the MFL2 using the constants given in 4.1.1.

<u>Table 6</u>

t butanol-water mixtures

Mole fraction of water	Temperature $/°C$	Static Permittivity ε_s
0.000	27.3	11.93
0.052	27.3	11.53
0.101	27.3	11.44
0.153	27.3	11.59
0.197	27.3	11.90
0.250	27.3	12.38
0.299	27.3	12.96
0.350	27.3	13.76
0.400	27.3	14.72

These values agree within ± 0.02 with the values obtained

by Brown and Ives (7).

Table 7

Cyclohexanol-water mixtures

Mole fraction of water	Temperature /°C	Static Permittivity ε_s
0.000	25.0	16.49
0.098	25.0	15.60
0.148	24.0	15.39
0.198	24.2	15.30
0.251	24.2	15.34
0.298	24.1	15.53
0.353	24.1	15.92
0.399	24.5	16.35

These values are between 0.05 and 0.09 lower than the

values obtained by Stevens (185). Small differences are

to be expected due to the different calibration procedure

used in this work.

Table 8

1 butanol-water mixtures

Mole fraction of water	Temperature /°C	Static Permittivity ε_s
0.000	24.9	17.31
0.150	24.8	17.56
0.248	24.8	17.79
0.351	24.9	18.04

The value for the pure alcohol compares very satisfactorily

with the value of 17.3 obtained by both Suggett et al (171)

and van den Berg et al (37). Published values for 1 butanol water mixtures are not available.

Table 9

1 heptanol-water mixtures

Mole fraction of water	Temperature / °C	Static Permittivity ε_s
0.000	24.9	11.48
0.153	24.9	10.52
0.252	24.8	10.41

These values are 0.05 lower than the values obtained by Stevens (185). This will be again due to the different calibration procedure used.

4.4 Dielectric relaxation of alcohol-water mixtures

4.4.1 Fourier transform values

Optimisation of the number of data points to minimise errors due to anomalous truncation was performed by inspection of the results for a varying number of data cards, N, and then noting the minimum value N_{min} for which the Fourier transform interpolated static permittivity ε_s attained the Dipolmeter value to within 3%. This 3% figure was adopted to take account of uncertainties arising in amplitude measurements of the reflection from both the dielectric and short-circuit terminated line.

The relaxation time $\overline{\tau}_F$ was determined from the mean value of τ_F corresponding to all values of N where $N \geq N_{min}$. The standard deviation of the τ_F values was adopted as a measure of the uncertainty arising from truncation errors.

This procedure was not applied to the cyclohexanol-water mixture results for x < 0.250 as the slower relaxation in these mixtures precluded complete truncation of the transform within the time window of the time domain scan. ($\simeq$ 2 ns).

The relaxation frequencies $\nu_c = \left(\dfrac{1}{2\pi\tau_F}\right)$ together with the interpolated ε_s values for $N \geqslant N_{min}$ are given in Tables 10 to 13.

Mean values of ν_c, τ_F and ε_s together with the standard deviation values are also given with the tables.

It should be noted that the largest range of N-values was used in the higher water content t butanol mixtures due to the relaxation being particularly rapid and therefore most susceptible to error. In addition, the very similar $\overline{\tau_F}$ values for two of the t butanol mixtures reinforced the requirement to give more attention to these mixtures. In order to be economical in time usage in the Central Processor Unit of the computer, other mixtures were studied over a more limited range of $N > N_{min}$ values.

4.4.2 Determination of relaxation time $\overline{\tau_F}$

Table 10
t butanol-water mixtures

t butanol

N	ν_c/MHz	ε_s	(Dipolmeter value = 11.93)
111	330	11.63	
106	306	11.70	
96	350	11.51	

$$\overline{\varepsilon}_S = 11.60 \pm 0.10$$

$$\overline{\nu}_c = (329 \pm 22) \text{ MHz}$$

$$\overline{\tau}_F = (486 \pm 32) \text{ ps}$$

t butanol with 0.052 mf of water

N	ν_c/MHz	ε_S	(Dipolmeter value = 11.53)
111	408	11.61	
106	408	11.53	
101	412	11.56	
96	410	11.73	
91	418	11.63	
86	437	11.67	
81	394	11.70	

$$\overline{\varepsilon}_S = 11.63 \pm 0.07$$

$$\overline{\nu}_c = (412 \pm 12) \text{ MHz}$$

$$\overline{\tau}_F = (386 \pm 12) \text{ ps}$$

t butanol with 0.101 mf of water

N	ν_c/MHz	ε_S	(Dipolmeter value = 11.44)
81	500	11.74	
76	616	11.78	
71	530	11.56	
66	548	11.45	
61	548	11.42	
56	575	11.29	
51	565	11.36	

$\bar{\epsilon}_S = 11.51 \pm 0.19$

$\bar{\nu}_c = (555 \pm 36)$ MHz

$\bar{\tau}_F = (288 \pm 19)$ ps

t butanol with 0.153 mf water

N	ν_c/MHz	ϵ_S	
71	770	11.70	(Dipolmeter value = 11.59)
66	683	11.46	
61	690	11.63	
56	705	11.49	
51	692	11.57	
46	710	11.51	

$\bar{\epsilon}_S = 11.56 \pm 0.09$

$\bar{\nu}_c = (708 \pm 32)$ MHz

$\bar{\tau}_F = (225 \pm 10)$ ps

t butanol with 0.197 mf of water

N	ν_c/MHz	ϵ_S	
61	780	11.90	(Dipolmeter value = 11.90)
56	752	11.76	
51	750	11.90	
46	790	11.83	
41	790	11.80	
36	740	12.00	

$\bar{\epsilon}_S = 11.92 \pm 0.13$

$\bar{\nu}_c = (805 \pm 73)$ MHz

$\bar{\tau}_F = (208 \pm 6)$ ps

t butanol with 0.250 mf of water

N	ν_c/MHz	ε_S	(Dipolmeter value = 12.38)
81	916	12.40	
76	930	12.43	
71	972	12.50	
66	890	12.30	
61	812	12.18	
56	848	12.25	
51	852	12.26	
46	850	12.26	
41	880	12.16	
36	822	12.36	
31	863	12.22	

$\overline{\varepsilon}_S = 12.30 \pm 0.11$

$\overline{\nu}_c = (876 \pm 48)$ MHz

$\overline{\tau}_F = (182 \pm 10)$ ps

t butanol with 0.299 mf of water

N	ν_c/MHz	ε_S	(Dipolmeter value = 12.96)
71	1,145	13.16	
66	1,190	13.02	
61	1,200	12.91	
56	1,105	12.75	
51	1,110	12.76	
46	1,155	12.84	
41	1,140	12.80	
36	1,150	12.95	
31	1,145	12.95	

$\overline{\varepsilon}_S = 12.90 \pm 0.13$

$\overline{\nu}_c = (1,149 \pm 31)$ MHz

$\overline{\tau}_F = (139 \pm 4)$ ps

t butanol with 0.350 mf of water

N	ν_c/MHz	ε_s	(Dipolmeter value = 13.76)
51	1,140	13.75	
46	1,130	13.75	
41	1,145	13.80	
36	1,248	14.04	
31	1,160	14.04	
26	1,225	13.80	
21	1,335	13.40	

$\overline{\varepsilon}_s = 13.80 \pm 0.22$

$\overline{\nu}_c = (1,198 \pm 76)$ MHz

$\overline{\tau}_F = (133 \pm 9)$ ps

t butanol with 0.400 mf of water

N	ν_c/MHz	ε_s	(Dipolmeter value = 14.72)
56	1,220	14.70	
51	1,215	14.72	
46	1,175	14.63	
41	1,240	14.86	
36	1,645	15.24	
31	1,450	14.94	
26	1,455	14.99	
21	1,400	14.95	

$\overline{\varepsilon}_s = 14.88 \pm 0.20$

$\overline{\nu}_c = (1,350 \pm 164)$ MHz

$\overline{\tau}_F = (119 \pm 15)$ ps

Table 11

Cyclohexanol-water mixtures

Cyclohexanol

N	ν_c/MHz	ε_s	(Dipolmeter value = 16.49
71	116	9.86	

τ_F = 1,372 ps

Cyclohexanol with 0.098 mf of water

N	ν_c/MHz	ε_s	(Dipolmeter value = 15.60)
61	145	12.44	

τ_F = 1,098 ps

Cyclohexanol with 0.148 mf of water

N	ν_c/MHz	ε_s	(Dipolmeter value = 15.39)
61	176	10.99	

τ_F = 904 ps

Cyclohexanol with 0.198 mf of water

N	ν_c/MHz	ε_s	(Dipolmeter value = 15.30)
111	225	13.12	

τ_F = 707 ps

Cyclohexanol with 0.251 mf of water

N	ν_c/MHz	ε_s	(Dipolmeter value = 15.34)
96	255	14.30	
91	263	14.25	
86	250	14.35	
76	272	14.06	

$\overline{\varepsilon}_s = 14.24 \pm 0.13$

$\overline{\nu}_c = (260 \pm 10)$ MHz

$\overline{\tau}_F = (612 \pm 24)$ ps

Cyclohexanol with 0.298 mf of water

N	ν_c/MHz	ε_s	(Dipolmeter value = 15.53)
81	308	15.65	
76	329	15.50	

$\overline{\varepsilon}_s = 15.57 \pm 0.11$

$\overline{\nu}_c = (318 \pm 15)$ MHz

$\overline{\tau}_F = (500 \pm 24)$ ps

Cyclohexanol with 0.353 mf of water

N	ν_c/MHz	ε_s	(Dipolmeter value = 15.92)
66	375	15.89	
61	398	15.63	

$\overline{\varepsilon}_s = 15.76 \pm 0.18$

$\overline{\nu}_c = (386 \pm 16)$ MHz

$\overline{\tau}_F = (412 \pm 18)$ ps

Cyclohexanol with 0.399 mf of water

N	ν_c/MHz	ε_s	(Dipolmeter value = 16.35
50	416	16.65	
45	454	16.37	
40	478	16.13	

$\overline{\varepsilon}_s = 16.38 \pm 0.26$

$\overline{\nu}_c = (449 \pm 31)$ MHz

$\overline{\tau}_F = (356 \pm 25)$ ps

Table 12

1 butanol-water mixtures

1 butanol

N	ν_c/MHz	ε_s	(Dipolmeter value = 17.31)
106	285	17.61	
96	292	17.23	
86	273	17.26	
76	320	16.95	

$\overline{\varepsilon}_s = 17.26 \pm 0.27$

$\overline{\nu}_c = (295 \pm 24)$ MHz

$\overline{\tau}_F = (543 \pm 40)$ ps

1 butanol with 0.150 mf of water

N	ν_c/MHz	ε_s	(Dipolmeter value = 17.56
82	438	17.27	
72	442	17.42	
62	438	17.58	
52	396	18.08	
42	448	17.53	

$$\overline{\varepsilon}_S = 17.58 \pm 0.31$$

$$\overline{\nu}_c = (432 \pm 21) \text{ MHz}$$

$$\overline{\tau}_F = (387 \pm 18) \text{ ps}$$

1 butanol with 0.248 mf of water

N	ν_c/MHz	ε_S	(Dipolmeter value = 17.79)
82	648	17.53	
72	602	17.34	
62	575	16.90	
52	552	17.82	
42	552	17.73	

$$\overline{\varepsilon}_S = 17.46 \pm 0.36$$

$$\overline{\nu}_c = (586 \pm 40) \text{ MHz}$$

$$\overline{\tau}_F = (272 \pm 19) \text{ ps}$$

1 butanol with 0.351 mf of water

N	ν_c/MHz	ε_S	(Dipolmeter value = 18.04)
56	690	18.03	
51	692	18.01	
46	688	18.09	
41	690	18.11	
36	720	18.01	

$$\overline{\varepsilon}_S = 18.05 \pm 0.05$$

$$\overline{\nu}_c = (696 \pm 13) \text{ MHz}$$

$$\overline{\tau}_F = (230 \pm 6) \text{ ps}$$

Table 13

1 heptanol-water mixtures

1 heptanol

N	ν_c/MHz	ε_s	(Dipolmeter value = 11.48)
50	167	10.50	
47	159	10.68	
44	173	10.36	

$\overline{\varepsilon}_s = 10.51 \pm 0.16$

$\overline{\nu}_c = (166 \pm 7)$ MHz

$\overline{\tau}_F = (960 \pm 40)$ ps

1 heptanol with 0.153 mf of water

N	ν_c/MHz	ε_s	(Dipolmeter value = 10.52)
50	204	10.63	
47	188	10.82	
44	220	10.40	

$\overline{\varepsilon}_s = 10.62 \pm 0.21$

$\overline{\nu}_c = (204 \pm 16)$ MHz

$\overline{\tau}_F = (785 \pm 62)$ ps

1 heptanol with 0.252 mf of water

N	ν_c/MHz	ε_s	(Dipolmeter value = 10.41)
50	258	10.25	
47	244	10.39	
44	256	10.33	

$$\overline{\varepsilon}_S = 10.32 \pm 0.07$$

$$\overline{\nu}_c = (253 \pm 8)\text{MHz}$$

$$\overline{\tau}_F = (630 \pm 20)\text{ps}$$

4.4.3 <u>Dielectric relaxation parameters</u>

The dielectric dispersion curves of $\varepsilon^{\backprime\backprime}$ against $\varepsilon^{\backprime}$ for each mixture have been drawn for the value of N which gave a τ_F value closest to $\overline{\tau}_F$ (Figures 10 to 22).

For all alcohol-water mixtures studied, a semi-circle can be drawn through the data points corresponding to the principal dispersion and it is therefore concluded that this dispersion is Debye-type. Deviation from the semi-circle is evident at the higher frequencies.
This will be due primarily to impedance mismatch effects causing anomalous truncation (184). In addition, there are possibly contributions from higher frequency relaxation processes. The less satisfactory semi-circles for the cyclohexanol-water mixtures at low water content will be due to impedance mismatch effects in these long relaxation time dispersions.

The Fourier transform values for the dielectric relaxation parameters of the alcohol-water mixtures are given in Tables 14 to 17.

Table 14

t butanol-water mixtures

Mole Fraction of water	Temperature / °C	Relaxation Time τ_F/ps	Static Permittivity ε_S	High frequency limiting value of permittivity ε_∞
0.000	27.3	486	11.4	3.9
0.052	27.3	386	11.4	3.4
0.101	27.3	288	11.4	3.9
0.153	27.3	215	11.3	4.2
0.197	27.3	208	11.8	4.2
0.250	27.3	182	12.2	4.7
0.299	27.3	137	13.0	4.9
0.350	27.3	135	13.8	4.1
0.400	27.3	136	14.0	4.6

The value of $\bar{\tau}_F$ = 486 ps for the pure alcohol is in fair

agreement with the value of approximately 520 ps obtained

by Sato et al (188) at 25° C.   The 520 ps figure is

approximate as it was obtained from graphical data.   It

should be noted that the frequency domain value of Sato et

al was obtained from a Cole-Cole plot which contained only

five data points, all of which were at frequencies above

the relaxation frequency ν_c.

The value of ε_∞ for the pure alcohol is rather higher

than the value of approximately 3.2 obtained by Sato et al.

Literature values for τ and ε_∞ of t butanol-water mixtures

is not available.

Table 15

Cyclohexanol-water mixtures

Mole Fraction of water	Temperature /$^\circ$C	Relaxation Time τ_F/ps	ε_S	ε_∞
0.000	25.0	1,372	10.1	3.6
0.098	25.0	1,098	12.6	4.9
0.148	24.0	904	12.3	4.7
0.198	24.2	707	13.2	5.5
0.251	24.2	622	14.4	4.9
0.298	24.1	500	15.6	4.9
0.353	24.1	412	15.9	4.2
0.399	24.5	356	16.3	3.5

The value of τ_F = 1,372 ps for the pure alcohol is substantially lower than the values of 2,290 ps obtained by Garg and Smyth (20) and 2,430 ps obtained by Arnoult et al (189). Both values were obtained at 25° C. This discrepancy is to be expected, since for slower relaxations, truncation of the Fourier transform will occur before the relaxation has been completed, giving too low a value for τ_F. This effect will also give ε_S values which are too low, which was the case for the pure alcohol and for mixtures with mole fractions of water of 0.25 and below. The value of ε_∞ = 3.6 for the pure alcohol is somewhat higher than the value of 2.9 obtained by Garg and Smyth (20) and 3.4 obtained by Arnoult et al (189).

Literature data for τ and ε_∞ for cyclohexanol-water mixtures are not available.

Table 16

1 butanol-water mixtures

Mole Fraction of water	Temperature / $^\circ$C	Relaxation Time $\overline{\tau}_F$/ps	ε_s	ε_∞
0.000	25.1	543	17.3	3.3
0.150	25.0	387	17.3	2.8
0.245	25.1	272	17.8	4.1
0.351	24.9	230	18.1	5.5

The value of $\overline{\tau}_F$ = 543 ps for the pure alcohol is in satisfactory agreement with values of 561 ps obtained by Campbell et al (34) at 20° C, 575 ps obtained by Garg and Smyth (20) at 25° C and 488 ps obtained by Sagal (35) at 25° C. The value of ε_∞ = 3.3 is in good agreement with the values of approximately 3.6 obtained by Campbell et al (34) and 3.3 obtained by Sagal (35).

The fall in $\overline{\tau}_F$ for 1 butanol-water mixtures on addition of water is in disagreement with the results of Sarojini (67) who reported a monotonous increase in τ as water was added to 1 butanol.

Table 17

1 heptanol-water mixtures

Mole Fraction of water	Temperature / $^\circ$C	Relaxation Time $\overline{\tau}_F$/ps	ε_s	ε_∞
0.000	25.0	960	10.8	1.9
0.153	24.8	785	10.5	3.7
0.252	24.8	630	10.2	3.2

The value of $\bar{\tau}_F$ = 960 ps for the pure alcohol is
substantially lower than the value of 1,660 ps obtained by
Lebrun (190) at 20° C. The value of ε_∞ = 1.9 is also
substantially lower than the value of 3.2 obtained by
Lebrun. The discrepancy in the τ values is to be
expected since the slower relaxation of the pure alcohol
will lead to truncation errors as observed in the pure
alcohol cyclohexanol. The low ε_S value confirms this view.
The value of ε_∞ = 1.9 is clearly too low since n^2 (where
n is the refractive index) would be expected to be slightly
higher than this.

The observed reduction of $\bar{\tau}_F$ on addition of water to
1 heptanol is in agreement with the results of Tjia (59)
on 1 heptanol-water mixtures up to 0.115 mf of water over
the lower temperature range of - 35 to - 10° C. The value
of ε_∞ = 3.7 for the 0.153 mf mixture is rather higher than
the almost temperature independent value of 2.9 obtained
by Tjia for the 0.115 mf water content mixture over the
- 35 to - 10° C temperature range.

For all four alcohols studied, the results reveal that
addition of water causes a progressive reduction in the
relaxation time $\bar{\tau}_F$ with the very close τ values for the
0.299 and 0.300 mf of water t butanol mixtures being a
possible exception to this trend.

The results for ε_∞ show considerable scatter with no trend
being revealed. However, the results for the t butanol

mixture with 0.400 mf of water with the time zero
reference both retarded and advanced by 3.9 ps (Figure 14b)
reveal that the value of ε_∞ is critically dependent on
precision in the time zero reference. For this reason,
the variation in ε_∞ exhibited by the alcohol-water mixtures
is attributed to experimental error.

It should be noted that the value of $\overline{\tau}_F$ is, in contrast,
relatively insensitive to small errors in the time zero
reference since the results for the 0.400 mf mixture
both (i) retarded and (ii) advanced by 3.9 ps together
with (iii) the actual time zero adopted give τ_F values of
(i) 111 ps, (ii) 104 ps and (iii) 105 ps respectively,
giving a mean value of 107 ps with a standard deviation
of 4 ps.

4.5 Direct time domain methods

4.5.1 Fellner-Feldegg method, τ_D

The WTW Dipolmeter data for ε_S has been used. The graphs
of ln ($\varepsilon_S - \varepsilon$) against time are given in Figures 23 to
25. The relaxation times τ_D are given by the reciprocal
of the slopes of graphs.

The τ_D values are given in Tables 18 to 21.

Table 18 Alcohol	Mole Fraction of Water	Temperature /°C	Relaxation Time τ_D/ps
t butanol	0.000	27.3	355
	0.052	27.3	241
	0.101	27.3	220
	0.153	27.3	203
	0.197	27.3	153
	0.250	27.3	142
	0.299	27.3	99
	0.350	27.3	97
	0.400	27.3	73

Table 19

Cyclohexanol	0.000	25.0	4,321
	0.098	25.0	2,664
	0.148	24.0	1,751
	0.198	24.2	748
	0.251	24.2	512
	0.298	24.1	291
	0.353	24.1	253
	0.399	24.5	219

- 159 -

Table 20

Alcohol	Mole Fraction of Water	Temperature /$^\circ$C	Relaxation Time τ_D/ps
1 butanol	0.000	25.1	355
	0.150	25.0	191
	0.245	25.1	163
	0.351	24.9	146

Table 21

Alcohol	Mole Fraction of Water	Temperature /$^\circ$C	Relaxation Time τ_D/ps
1 heptanol	0.000	25.0	1,017
	0.153	24.8	538
	0.252	24.8	450

4.5.2 Fellner Feldegg and Barnett method, τ_{FF+B}

As discussed in the experimental chapter, the curves
appropriate to $\dfrac{\rho_s - \rho(t)}{\rho_s - \rho_\infty} = 0.2$ ($\rho_{0.2}$) were used wherever

possible. In order to use these curves, it is necessary

for the reflection coefficient to be within 20% of its

low frequency value at the end of the time domain scan.

This condition was fulfilled in all cases except for the

cyclohexanol-water mixtures below 0.250 mole fraction of

water and for the pure alcohol 1 heptanol. Use of the

curves was straightforward except for two related major

difficulties, namely selection of the appropriate values

of ρ_∞ and ε_∞. Since the values of these two quantities are critically dependent on the accuracy of time zero referencing and, as revealed in the study of the 0.400 mf t butanol-water mixture with a 3.9 ps sampling interval, these values are subject to a high degree of uncertainty.

The problem has two aspects because in addition to affecting the value of $\rho(t)$, the value of ρ_∞ (and hence ε_∞) selected also determines which set of curves in the FF+B paper are to be used. The values of ρ_∞ and ε_∞ selected were obtained using the procedure described in the experimental chapter. The ρ_S values were obtained from the Dipolmeter values of ε_S.

The values of ρ_S, ρ_∞, $\rho(t)$, the scaling factor obtained from the FF+B paper and τ_{FF+B} are given in Tables 22 to 25.

Table 22

t butanol-water mixtures

Mole Fraction of water	Temperature °C	ρ_S	ρ_∞	ε_∞	$\rho_{0.2}$	$t_{0.2}$ /ps	Scaling factor	τ_{FF+B} /ps
0.000	27.3	0.552	0.33	4.0	0.508	419	1.2	503
0.052	27.3	0.545	0.31	3.6	0.498	300	1.3	390
0.101	27.3	0.544	0.32	3.8	0.499	264	1.2	317
0.153	27.3	0.546	0.37	4.7	0.511	284	1.1	312
0.197	27.3	0.550	0.37	4.7	0.514	229	1.1	252
0.250	27.3	0.557	0.38	5.0	0.522	216	1.1	238
0.299	27.3	0.565	0.42	6.0	0.537	158	1.0	158
0.350	27.3	0.575	0.39	5.2	0.538	142	1.1	156
0.400	27.3	0.587	0.46	7.3	0.562	139	1.0	139

Table 23

Cyclohexanol-water mixtures

Mole Fraction of water	Temperature /°C	ρ_s	ρ_∞	ε_∞	$\rho_{1/e}$	$t_{1/e}$ /ps	Scaling Factor	τ_{FF+B} /ps
0.000	25.0	0.605	0.36	4.5	0.515	2560	2.7	6910
0.098	25.0	0.596	0.40	5.4	0.524	1143	2.0	2286
0.148	24.0	0.594	0.33	3.9	0.495	749	2.2	1648
0.198	24.2	0.593	0.40	5.4	0.522	553	2.0	1106
					$\rho_{0.2}$	$t_{0.2}$		
0.251	24.2	0.593	0.37	4.7	0.548	640	1.2	768
0.298	24.1	0.595	0.33	3.9	0.542	348	1.3	452
0.353	24.1	0.599	0.29	3.3	0.537	269	1.6	430
0.399	24.5	0.603	0.33	4.0	0.548	235	1.5	353

Table 24

1 butanol-water mixtures

Mole Fraction of water	Temperature /°C	ρ_s	ρ_∞	ε_∞	$\rho_{0.2}$	$t_{0.2}$ /ps	Scaling Factor	τ_{FF+B} /ps
0.000	24.9	0.612	0.29	3.3	0.548	375	1.7	638
0.150	24.8	0.615	0.30	3.4	0.553	242	1.6	387
0.248	24.8	0.617	0.32	3.7	0.557	192	1.6	308
0.351	24.9	0.619	0.33	3.9	0.561	170	1.5	255

Table 25

1 heptanol-water mixtures

Mole Fraction of water	Temperature /°C	ρ_s	ρ_∞	ε_∞	$\rho_{0.2}$	$t_{0.2}$ /ps	Scaling Factor	τ_{FF+B} /ps
0.000	24.9	0.545	0.27	3.0	0.491	977	1.35	1319
0.153	24.9	0.530	0.27	3.0	0.478	579	1.25	724
0.252	24.8	0.527	0.33	3.9	0.488	558	1.1	614

4.5.3 Brehm and Stockmayer method (B+S) τ_{B+S}

Application of this method posed some difficulty since, in addition to the requirement of knowledge of the values of ρ_∞ and ε_∞, the faster relaxation in the higher water-content mixtures resulted in the $t_{\frac{1}{3}}$ condition being attained very rapidly. This made the value of $t_{\frac{1}{3}}$ subject to rather high uncertainty, and possibly due to this effect, the ratio $t_{\frac{1}{3}}/t_{\frac{2}{3}}$ gave Cole-Davidson β-values greater than unity in many mixtures. Because of this difficulty with the β-values, it was decided to assume Debye-type dispersion as in the FF+B paper giving $\beta=1$. Relaxation time values were then determined by two different methods. In the first (τ_{B+S_1}), the values of ε_S and ε_∞ of the FF+B method were used to determine the most appropriate curve for $(\varepsilon_S/\varepsilon_\infty)$ in the B+S paper from which the required scaling factor for $t_{\frac{1}{3}}$ was obtained. In the second method (τ_{B+S_2}), the value of $t_{\frac{1}{3}}$ was obtained from the more precisely measureable $t_{\frac{2}{3}}$ value by assuming that $t_{\frac{1}{3}} = 0.31\ t_{\frac{2}{3}}$ which corresponds to $\beta = 1$ and $\varepsilon_S/\varepsilon_\infty = 4$ in the B+S paper. The ratio $\varepsilon_S/\varepsilon_\infty = 4$ was considered to be the optimum choice based on literature data for the four pure alcohols and 1 heptanol-water mixtures (185, 19, 20, 59).

The values of $t_{\frac{1}{3}}$, $t_{\frac{2}{3}}$, β, the scaling factor, τ_{B+S_1}, and τ_{B+S_2} are given in Tables 26 to 29.

Table 26

t butanol-water mixtures

Mole Fraction of water, x	$\dfrac{\varepsilon_s}{\varepsilon_\infty}$	t_1 /ps³	t_2 /ps³	β	Scaling Factor	$^\tau B{+}S_1$ /ps	$^\tau B{+}S_2$ /ps
0.000	3.0	134	300	≃ 1.5	5.7	764	514
0.052	3.2	86.9	237	≃ 1.2	6.25	543	444
0.101	3.0	79	180	≃ 0.8	5.7	450	309
0.153	2.5	94.8	193	≃ 1.6	4.0	379	232
0.197	2.5	79	153	≃ 2.0	4.0	316	184
0.250	2.6	71.1	145	≃ 1.6	4.3	306	189
0.299	2.2	75.8	123	≃ 2	3.4	258	127
0.350	2.6	63.2	99.5	≃ 2	4.5	284	136
0.400	2.0	66.3	102	≃ 2	3.1	206	96

Cyclohexanol-water mixtures

Mole Fraction of water, x	$\dfrac{\varepsilon_s}{\varepsilon_\infty}$	t_1 /ps³	t_2 /ps³	β	Scaling Factor	$^\tau B{+}S_1$ /ps	$^\tau B{+}S_2$ /ps
0.000	3.7	827	*	–	7.1	5871	–
0.098	2.9	394	1280	0.95	5.3	2088	2021
0.148	2.9	433	1615	0.8	5.3	2294	1796
0.198	2.8	205	616	0.94	4.8	984	881
0.251	3.3	134	382	≃ 1.1	6.25	837	719
0.298	4.0	83.7	218	≃ 1.3	7.9	661	515
0.353	4.8	69.5	166	≃ 1.6	10.0	695	498
0.399	4.1	45.8	111	≃ 1.4	8.3	380	277

1 butanol-water mixtures

Mole Fraction of water, x	$\dfrac{\varepsilon_s}{\varepsilon_\infty}$	t_1 /ps³	t_2 /ps³	β	Scaling Factor	$^\tau B{+}S_1$ /ps	$^\tau B{+}S_2$ /ps
0.000	5.2	91	235	≃ 1.2	10.0	910	705
0.150	5.1	69.8	161	≃ 1.3	10.0	698	483
0.245	4.8	60.9	123	≃ 1.8	9.1	554	337
0.351	4.5	28.6	93.1	≃ 1.1	7.7	220	215

1 heptanol-water mixtures

Mole Fraction of water, x	$\varepsilon_s/\varepsilon_\infty$	$t_{1/3}$ /ps	$t_{2/3}$ /ps	β	Scaling Factor	τ_{B+S_1} /ps	τ_{B+S_2} /ps
0.000	3.7	279	639	$\simeq$ 1.5	7.1	1980	1,371
0.153	3.5	139.6	384	$\simeq$ 1.1	6.7	935	767
0.252	2.6	174.5	387	$\simeq$ 1.4	4.3	750	504

NB All values for $\beta > 1.0$ are approximate since extrapolation of the B+S curves had to be applied.

4.6 Estimation of experimental error in relaxation time values

4.6.1 Fourier transform method

The experimental technique has errors arising from the following:

(a) non-linearity in the X-Y plotter,

(b) amplitude uncertainty for both the dielectric and short circuit terminated coaxial line,

(c) truncation errors due to impedance mismatches,

(d) time zero reference uncertainty,

(e) sampling interval uncertainty due to uncertainty in the calibration of (i) the 180 CRO "mainframe" and (ii) the time-base for the X-Y plots,

and

(f) errors due to too early truncation of the Fourier transform when the relaxation time is long.

The operating manuals quote a figure of $\pm$ 0.1% for X-Y plotter non-linearity, $\pm$ 0.2% for full-scale Y deflection

and $\pm$ 3% for the CRO "mainframe" calibration.

The $\pm$ 0.1% quoted for (a) is considered negligible. Since the effect of amplitude uncertainties in (b) have been included in the procedure adopted to account for truncation effects, the value $\overline{\tau}_F$ is considered to include the contributions from both (b) and (c). The effect of time zero reference uncertainty is indicated in the results for the t butanol water mixture at 0.400 mf of water for which a $\pm$ 4% spread in τ was revealed for the time zero reference shift of $\pm$ 3.9 ps. Since an uncertainty of $\pm$ 2 ps is considered appropriate, a figure of $\pm$ 2% has been adopted for the effect of (d).

For the t butanol-, 1 butanol- and 1 heptanol-water mixtures both the CRO mainframe setting (0.2 ns/cm for t and 1 butanol-water mixtures, 0.5 ns/cm for 1 heptanol-water mixtures) and the X sensitivity of the recorder were maintained constant for each set of alcohol-water mixtures. Thus for each of these sets of mixtures, errors in the sampling interval will not affect the relative values of τ_F. In addition, since the experimental values for the pure alcohols t butanol and 1 butanol agree with literature data within uncertainty limits set by addition of the truncation and time zero reference error contributions, it will be presumed that the sampling interval error (e) is negligible.

For the cyclohexanol-water mixtures, the CRO "mainframe" setting was 0.5 ns/cm at up to and including 0.148 mf of water and 0.2 ns/cm for the higher water content mixtures. This change of setting will introduce additional error but study of the relative precision of these two mainframe settings has shown that they agree within 1%. This 1% figure has been added to the contributions from (b) and (c) for the cyclohexanol-water mixtures.

The longest relaxation time, τ_{max}, above which errors arise due to too early truncation of the transform (f) can be estimated by determining the maximum value of τ for which the transform interpolated static permittivity ε_s, truncates to the Dipolmeter value. Inspection of the $\bar{\tau}_F$ and ε_s values for the cyclohexanol-water mixtures reveals that the transform truncates to the published value of ε_s when the mole fraction of water is 0.298 for which $\bar{\tau}_F$ is 500 ps, whereas the 0.251 mixture which has a $\bar{\tau}_F$ value of 622 ps exhibits truncation limitations. Satisfactory truncation was also obtained for the pure alcohol 1 butanol with a $\bar{\tau}_F$ value of 551 ps. It is therefore suggested that with the experimental procedure adopted in this work, the Fourier transform values should be free of too-early-trunction limitations for relaxation times $\tau \lesssim 600$ ps.

In order to correct the transform values for relaxation times longer than 600 ps, a scaling procedure has been

adopted since the Fourier transform values will give an increasing difference between measured and 'correct' values as the τ value increases above the 600 ps figure. A simple method has been adopted in which a graph of corrected τ value against measured τ value has been plotted (Figure 26) based on the assumption that for $\tau_F \lesssim 600$ ps the scaling factor is unity. Two other points have been used to set the position of this calibration line. The first is based on a mean of the two literature values for cyclohexanol at 25° C (20,189) which was taken as 2,360 ps. The second is based on literature data for 1 heptanol at 20° C (190) where adjustment to the τ value at 25° C has been obtained using an activation enthalpy value of 33.2 kJ mol^{-1} (35). Applying this figure gives a value 1,320 ps for 1 heptanol at 25° C.

The above figures thus give values as in Table 30.

Table 30

Measured Relaxation Time/ps	Corrected Relaxation Time/ps	
600	600	
960	1320	(1 heptanol)
1372	2360	(cyclohexanol)

Applying linear regression analysis to the above relation between measured and corrected values for $\tau_F > 600$ ps gives corrected values for the cyclohexanol-water mixtures as in Table 31.

Table 31

Mole Fraction of water	Temperature /°C	Corrected Relaxation Time τ_F/ps
0.000	25.0	2,329
0.098	25.0	1,702
0.148	24.0	1,259
0.198	24.2	809

(The higher water content mixtures containing this alcohol will not be significantly affected.)

The corrected values for the 1 heptanol-water mixtures are given in Table 32.

Table 32

Mole Fraction of water	Temperature /°C	Corrected Relaxation time τ_F/ps
0.000	25.0	1,387
0.153	24.8	987
0.252	24.8	633

The relaxation times of the alcohol-water mixtures together with the uncertainty limits are given in Table 33.

Table 33

Alcohol	Mole fraction of water	Relaxation Time τ_F/ps
t butanol	0.000	486 ± 42
	0.052	386 ± 20
	0.101	288 ± 25
	0.153	215 ± 14
	0.197	208 ± 10

Alcohol	Mole fraction of water	Relaxation time $\overline{\tau}_F$/ps
	0.250	182 $\pm$ 14
	0.299	137 $\pm$ 12
	0.350	135 $\pm$ 12
	0.400	136 $\pm$ 20
Cyclohexanol	0.000	2329 $\pm$ 279
	0.098	1702 $\pm$ 204
	0.148	1259 $\pm$ 151
	0.198	809 $\pm$ 97
	0.251	622 $\pm$ 43
	0.298	500 $\pm$ 39
	0.353	412 $\pm$ 30
	0.399	366 $\pm$ 37
1 butanol	0.000	543 $\pm$ 51
	0.150	387 $\pm$ 26
	0.245	272 $\pm$ 24
	0.351	230 $\pm$ 11
1 heptanol	0.000	1387 $\pm$ 153
	0.153	987 $\pm$ 109
	0.252	633 $\pm$ 51

It can be seen that the highest error occurs for the longest relaxation time mixtures; this is due to the scatter in the graph for conversion from measured to corrected values.

Rather higher error would also be expected in the faster relaxations of the higher water content t butanol mixtures. This is observed to occur in the relatively high uncertainty in the 0.400 mf t butanol mixture. The quoted uncertainty for the 0.299 and 0.350 mf mixtures is possibly too low. The variation of relaxation time determined by the Fourier transform method for the alcohol-water mixtures is given in Figures 27 and 28.

4.6.2 Fellner-Feldegg method

Experimental errors have not been estimated here but the relatively high scatter in the $\ln(\varepsilon_s - \varepsilon)$ against time graphs reveals that the uncertainty in τ_D will be significantly higher than for the Fourier transform value $\overline{\tau}_F$.

4.6.3 Fellner-Feldegg and Barnett method

The relatively high uncertainty of about 25% in the value of ρ_∞ contributes significant uncertainty in the appropriate value of $\rho_{0.2}$. Determination of the required $t_{0.2}$ value and the scaling factor introduces additional error. The error in $t_{0.2}$ will be typically about $\pm$ 10% and that in the scaling factor about $\pm$ 5%. The error in $\rho_{0.2}$ is not easy to estimate since the value selected for $\rho_{0.2}$ also affects both $t_{0.2}$ and the scaling factor, but investigation has shown that a figure of $\pm$ 5% is realistic giving a net uncertainty of $\pm$ 20% which is again substantially higher than that for the Fourier transform value.

4.6.4 Brehm and Stockmayer method

The uncertainty in τ_{B+S} will be even higher than that for τ_{FF+B} due to the requirement of knowledge of two times $t_{1/3}$ and $t_{2/3}$ instead of the single value (eg $t_{0.2}$) for the FF+B method. The scaling factor will also have a higher uncertainty giving a net uncertainty significantly larger than the $\pm$ 20% assigned to the FF+B method.

4.7 Comparison of the methods used for determination of τ

Both the FF+B and B+S$_1$ methods give τ values for the pure alcohol cyclohexanol which are about a factor of 2.5 higher than literature values, which suggests that, in practice, these two methods are not suitable for studying slow relaxations where the Fourier transform data will be unreliable due to truncation effects. Similarly the direct time domain method τ_D gives a value of τ for cyclohexanol which is about a factor of 2 too high, revealing that this method is also unsuitable in the study of slow relaxations.

For $\tau \leqslant 600$ ps, comparison with literature values for the pure alcohols t butanol and 1 butanol, both of which have τ values lower than 600 ps reveals that, of the various methods of calculation used in this work, the Fourier transform values $\overline{\tau}_F$ give closest agreement with literature values. For both t butanol and 1 butanol, the τ_D method gives τ values which are too low. The FF+B method gives good agreeement with literature values for t butanol but the value for 1 butanol is about 25% too high.

The B+S$_1$ method gives τ values which are too high for both t and 1 butanol whereas the B+S$_2$ method proposed in this work gives much closer agreement with literature values than the B+S$_1$ method but the τ value for 1 butanol is still too high. In addition, the B+S$_1$ method gives in many cases $\beta > 1$ which is physically meaningless.

Of the direct methods studied, FF+B appears most suitable in terms of correlation with $\bar{\tau}_F$, although the B+S_2 method is only marginally poorer. In contrast, B+S_1 gives such highly inaccurate values that it is considered to be of no use.

Since the Fourier transform method is considered to give the most accurate relaxation time values, the discussion in Chapter 5 will be restricted to the $\bar{\tau}_F$ values.

4.8 Dielectric properties of surfactants

Dielectric dispersion was not observed in the frequency range 30 kHz to 15 MHz. The static permittivity values were obtained from Dipolmeter data using the MFL 2 cell.

4.8.1 Static Permittivity

Static permittivity values as a function of temperature for all the surfactants are given in Tables 34 to 37 and Figure 29.

Table 34

Brij 30	Temperature/^{o}C	Static Permittivity ε_s
	25.0	6.28
	29.8	6.18
	34.9	6.07
	40.2	5.96
	45.2	5.86
	49.8	5.78
	54.4	5.69
	60.3	5.58
	65.7	5.48

Temperature coefficient $d\varepsilon_S/dT = -1.96 \times 10^{-2}$ $^{\circ}C^{-1}$

Table 35

$C_{12}E_4$ (Lot 80928)	Temperature/ $^{\circ}C$	Static Permittivity ε_S
	24.5	6.00
	30.2	5.88
	35.1	5.78
	40.2	5.68
	45.2	5.58
	50.0	5.49
	54.6	5.40
	60.5	5.30
	66.1	5.20

Temperature coefficient $d\varepsilon_S/dT = -1.92 \times 10^{-2}$ $^{\circ}C^{-1}$

Table 36

$C_{12}E_6$ (Lot 81002)	Temperature/ $^{\circ}C$	Static Permittivity ε_S
	30.0	6.21
	35.0	6.11
	40.2	6.01
	45.4	5.91
	50.1	5.82
	55.1	5.74
	60.8	5.64
	66.6	5.54

Temperature coefficient $d\varepsilon_S/dT = -1.83 \times 10^{-2}$ $^{\circ}C^{-1}$

Table 37

$C_{12}E_8$ (Lot 81024)	Temperature/$^{\circ}$C	Static Permittivity ε_s
	35.4	6.36
	40.2	6.27
	45.2	6.17
	50.2	6.07
	55.0	5.98
	60.8	5.87
	66.4	5.78

Temperature coefficient $d\varepsilon_s/dT = -1.89 \times 10^{-2}\ ^{\circ}C^{-1}$

These results reveal an increase of ε_s at any given temperature as the oxyethylene chain length is increased. The commercial product Brij 30 has a slightly higher permittivity than its pure counterpart $C_{12}E_4$. All surfactants exhibit an almost linear temperature dependence for ε_s with almost identical values for the temperature coefficient.

4.8.2 Time domain data for surfactant Brij 30

The TDR system revealed that a rapid but measurable dielectric relaxation occurred in Brij 30. The relaxation was studied at the two temperatures 44 and 70° C and the relaxation time was determined using both the τ_D and FF+B methods. In both methods, the static permittivity ε_s was obtained from Dipolmeter values. The graphs of $\ln(\varepsilon_s - \varepsilon)$ against time are given in Figure 30. Linear regression analysis of the values of $\ln(\varepsilon_s - \varepsilon)$

against time gave τ_D values of 46 ps at 44°C and 39 ps at 70°C.

The FF+B method gave the values appearing in Table 38.

Table 38

Temperature °C	ρ_S	ρ_∞	$\rho_{0.2}$	$t_{0.2}$ /ps	Scaling Factor	τ_{FF+B} /ps
44	0.415	0.29	0.390	97	0.9	87
70	0.396	0.29	0.375	92	0.9	83

As in the alcohol-water mixtures, τ_D is lower than τ_{FF+B}. The relaxation time determinations reveal a slightly lower τ at the higher temperature. However, there will be a high uncertainty in both the τ_D and τ_{FF+B} values due to the relaxation being very rapid and therefore being very sensitive to both time zero reference and impedance mismatch errors.

In view of the high uncertainty in these results, it is considered that the difference in τ_D values at 44 and 70°C may be wholly accounted for by experimental error.

4.9 Densities of surfactants

In order to compare the dielectric properties of the binary and ternary mixtures of the surfactants with values predicted by the various dielectric mixture equations, the density values of each of the surfactants were required as the mixture equations involve the use of volume fraction ϕ rather than mass fraction p.

The density values were determined with a standard 10 ml
SG bottle, and are given in Table 39.

Table 39

Surfactant	Temperature $/^oC$	Density $/10^3$ kgm^{-3}
Brij 30	23	0.947
$C_{12}E_4$	23	0.942
	63	0.912
$C_{12}E_6$	29	0.971
$C_{12}E_8$	32	0.990

An uncertainty of $\pm$ 0.003 in these density values is
considered appropriate. The density data for $C_{12}E_4$
at two temperatures gives a temperature dependence value
of -7.5 $.10^{-4}$ kgm^{-3} $^oC^{-1}$. The results reveal an increase
in density as the oxyethylene chain length is increased
which is in agreement with the trend revealed in the
literature values reported by Mulley (191) for $C_{12}E_1$
to $C_{12}E_5$. The value of 0.942 compares fairly satisfactorily
with the value of 0.9502 at the same temperature reported
by Mulley. Brij 30 has a density similar to that of its
pure counterpart $C_{12}E_4$.

4.10 Static Permittivity of tetraethylene glycol (E_4)

As with the surfactants, the static permittivity of E_4
as a function of temperature was studied using the
Dipolmeter with the MFL2 cell. The results are given in
Table 40 and Figure 31.

Table 40

Temperature /°C	Static Permittivity ε_S
25.0	20.12
35.3	19.09
44.8	18.18
54.6	17.32
65.4	16.44

Temperature coefficient of ε_S, $d\varepsilon_S/dT = -9.12 \times 10^{-2}$ °C^{-1}

The ε_S values compare very favourably with the value of 21.1 at 21.4° C obtained by Davies et al (192).

This exhibits higher values of both ε_S and $d\varepsilon_S/dT$ than any of the surfactants studied. The lower values in the surfactants will be due to the depolarising effect of the non-polar alkyl ether chain.

4.11 <u>Dielectric properties of surfactant-water binary mixtures</u>

Dielectric dispersion was not observed in the frequency range of 30 kHz to 15 MHz. Dipolmeter values could not be obtained due to the dc conductivity being too high and the static permittivity values were thus obtained from the RF bridge. The measurement frequency adopted was 2 MHz. The temperature was adjusted so that all measurements were performed on transparent solutions and, with the exception of the $C_{12}E_8$-water mixtures, it was not possible to study all compositions at the same temperature.

4.11.1 Static Permittivity

The static permittivity values as a function of mass fraction p of surfactant together with the measurement temperatures are given in Tables 41 to 44 and Figures 32 to 35.

Table 41

Brij 30-water mixtures

Mass fraction of surfactant, p	Temperature/$^{\circ}$C	Static Permittivity ε_s
0.101	56.8	54.7
0.202	61.3	44.7
0.300	63.2	37.5
0.400	68.8	32.0
0.500	68.8	27.1
0.600	69.7	22.1
0.700	69.7	17.4
0.802	69.7	12.5
0.897	69.7	9.0

Table 42

$C_{12}E_4$ -water mixtures

Mass fraction of surfactant, p	Temperature/$^{\circ}$C	Static Permittivity ε_s
0.099	60.0	51.0
	5.6	72.7
0.198	64.2	41.2
	8.4	61.9
0.301	67.3	34.1
	13.3	51.2
0.400	70.5	28.4
	11.9	43.7
0.500	72.6	24.5
(0.600)	(72.6)	(20.1)

0.700	69.6	16.3
0.802	43.7	12.4
0.904	68.0	8.9

For mass fractions up to and including p = 0.4, two permittivity values are given due to the existence of two separate clear regions. The p = 0.6 data is given in brackets as the transparency could not be attained for this composition. At the temperature quoted the translucent mixture was as close to transparency as could be achieved.

Table 43

C$_{12}$E$_6$-water mixtures

Mass fraction of surfactant, p	Temperature/^{o}C	Static Permittivity ε_s
0.097	25.4	69.0
0.201	24.8	60.5
0.300	35.2	49.3
0.400	43.1	39.5
0.500	44.7	32.7
0.600	66.5	23.5
0.699	66.5	18.7
0.798	51.1	15.4
0.880	51.1	12.5

Table 44

C$_{12}$E$_8$-water mixtures

Mass fraction of surfactant, p	Temperature/^{o}C	Static Permittivity ε_s
0.100	66.1	57.6
0.200	66.1	50.6

0.300	66.1	44.2
0.400	66.1	38.1
0.500	66.1	32.3
0.600	66.1	26.5
0.699	66.1	21.1
0.801	66.1	15.5
0.801	66.1	9.4

A general trend of decrease in ε_s as the mass fraction of surfactant is increased is revealed. The necessity of changing the temperature for the Brij 30, $C_{12}E_4$ and $C_{12}E_6$ mixtures precludes conclusions based simply on the graphs. One notable feature however, is that there is a significant difference between $C_{12}E_4$ and Brij 30 in that at low surfactant concentration $C_{12}E_4$ forms transparent solutions in two separate temperature ranges whereas Brij 30 only exhibits transparency in one temperature range.

4.11.2 Temperature dependence of ε_s for binary mixtures

The temperature dependence of ε_s for some of the aqueous mixtures which were transparent over a wide range of temperature are given in Tables 45 to 48 and Figure 36. The $C_{12}E_n$-water mixtures with $p = 0.900$ were measured with the Dipolmeter. The other mixtures were measured with the RF bridge operating at 2 MHz.

Table 45

C$_{12}$E$_4$-water with p = 0.900

Temperature /°C	Static Permittivity ϵ_S
25.0	10.88
46.0	10.05
64.0	9.29

Temperature coefficient dϵ_S/dT = 4.08.10^{-2} °C^{-1}

Table 46

C$_{12}$E$_6$-water with p = 0.097

Temperature /°C	Static Permittivity ϵ_S
14.9	72.4
20.2	71.1
25.4	69.0
29.6	67.7
34.8	66.1
40.0	64.5

Temperature coefficient dϵ_S/dT = -0.32 °C^{-1}

Table 47

C$_{12}$E$_8$-water with p = 0.100

Temperature /°C	Static Permittivity ϵ_S
25.0	69.6
35.3	66.2
45.4	63.3
55.0	60.55
66.1	57.6

Temperature coefficient $d\varepsilon_s/dT = -0.29$ $^\circ C^{-1}$

Table 48

C$_{12}$E$_8$-water with p = 0.901

Temperature / $^\circ$C	Static Permittivity ε_s
30.4	11.85
46.8	10.95
66.2	9.35

Temperature coefficient $d\varepsilon_s/dT = -7.02.10^{-2}$ $^\circ C^{-1}$

The variation of ε_s with temperature for both C$_{12}$E$_4$- and C$_{12}$E$_8$-water mixtures for mass fraction of surfactant p = 0.9 is almost linear but the C$_{12}$E$_8$ mixture has a temperature coefficient almost twice that of the C$_{12}$E$_4$ mixture.

The variation of ε_s with temperature for both C$_{12}$E$_6$- and C$_{12}$E$_8$-water mixtures for mass fraction of surfactant p = 0.10 is again almost linear with the temperature coefficient of ε_s for both surfactants being notably very similar.

4.11.3 Time domain data for Brij 30-water binary mixtures

Mixtures of Brij 30 with water at mass fractions of surfactant p = 0.90 and 0.70 were studied. As with the surfactant Brij 30 alone, the dielectric relaxation was again rapid and, in addition, the high dc conductivity of both mixtures was manifested in the TDR system as a

superimposed apparent slow relaxation causing the reflection coefficient to exhibit a monotonous increase for the whole duration of the time domain scan.

The high conductivity precluded use of the Dipolmeter for ε_s determination, and instead the less precise RF bridge method was used. The relaxation time was determined by the τ_D and FF+B methods. The graphs of $\ln(\varepsilon_s - \varepsilon)$ against time are given in Figure 37. Linear regression analysis of the values of $\ln(\varepsilon_s - \varepsilon)$ against time gave a value of $\tau_D = 64$ ps for $p = 0.90$ at 44° C and 50 ps for $p = 0.70$ at 70° C.

The FF+B method gave values as tabulated:

Table 49

Mass fraction of surfactant, p	Temperature /$^{\circ}$C	ρ_S	ρ_∞	$\rho_{0.2}$	$t_{0.2}$ /ps	Scaling Factor	τ_{FF+B} /ps
0.9	44	0.525	0.358	0.492	107	1.0	107
0.7	70	0.613	0.400	0.570	82	1.3	107

Although the FF+B method is considered to give relaxation time values which are closer in magnitude to the correct values, the significant dc conductivity will cause the FF+B values to be more susceptible to error. These results reveal a similarly rapid relaxation to that observed for Brij 30.

4.12 Static permittivity of tetra ethylene glycol (E_4)-water mixtures

The results are given in Table 50 and Figure 38.

Table 50

Mass fraction of E_4	Temperature /$^\circ$C	Static Permittivity ε_s
0.100	25.0	74.2
0.200	25.0	69.6
0.300	25.0	65.3
0.400	25.0	60.3
0.500	25.0	55.3
0.600	25.0	49.5
0.700	25.0	43.4
0.800	25.0	36.7
0.900	25.0	28.8

As with the surfactants, a general trend of decrease in ε_s as the mass fraction of E_4 is increased is revealed.

4.13 <u>Static permittivity of Brij 30-heptane binary mixtures</u>

Static permittivity values for mixtures of Brij 30 with heptane were determined from Dipolmeter data using the DFL2 cell. The results are given in Table 51 and Figure 39.

<u>Table 51</u>

Measurement temperature = 56.3° C

Mass fraction of Brij 30	Static Permittivity ε_s
0.20	2.29
0.40	2.82
0.60	3.62
0.80	4.55

The results reveal a monotonous increase in ε_s as the proportion of the non-polar solvent heptane is decreased.

- 185 -

4.14 Dielectric properties of surfactant, water and a hydrocarbon ternary mixtures

In ternary mixtures which were transparent, dielectric dispersion was not observed in the frequency range 30 kHz to 15 MHz. In addition, dielectric dispersion was not in general observed in the higher frequency range of the TDR system and the static permittivity values given by the TDR system agreed with the RF range values within experimental error limits of $\pm$ 3%. It is thus concluded that dielectric dispersion does not occur within the frequency range of 30 kHz to approximately 3 GHz.

The exceptions to this general trend were surfactant rich ternary mixtures of Brij 30 which exhibited dielectric dispersion in the TDR range.

4.14.1 Static permittivity

Static permittivity values of Brij 30 mixtures were obtained from RF bridge data at a measurement frequency of 2 MHz. The static permittivity values of $C_{12}E_4$ mixtures were obtained using the Dipolmeter when the permittivity was within the range of the MFL2 cell (3.60 to 22.0), and for permittivity values outside this range the RF bridge operating at 2 MHz was again used.

The values of ε_s for a range of ternary mixtures of both $C_{12}E_4$ and Brij 30, together with the measurement temperatures are given in Tables 52 and 53.

Table 52

$C_{12}E_4$-water-n-alkane systems

Mass fraction of water	Mass fraction of heptane	Temperature /°C	Static Permittivity ε_s
0.10	0.70	17.2	3.7
0.10	0.60	17.7	4.3
0.10	0.40	17.4	5.7
0.10	0.20	17.4	7.8
0.30	0.50	16.9	7.0
0.40	0.50	4.2	20.3
		13.0	7.3
0.70	0.10	20.2	32.3

	Mass fraction of decane		
0.51	0.34	7.5	32.0
		19.0	15.6

	Mass fraction of hexadecane		
0.49	0.33	24.3	28.1
		33.3	19.2
0.52	0.35	28.4	26.3
		31.4	23.1

Table 53

Brij 30-water-n-heptane systems

Mass fraction of water	Mass fraction of heptane	Temperature /$^\circ$C	Static Permittivity ε_s
0.10	0.60	27.5	3.0
	0.50	27.5	4.4
	0.40	30.0	5.0
	0.30	27.0	5.7
	0.20	23.2	7.3
	0.10	40.0	9.1
0.20	0.60	33.5	4.8
	0.50	34.5	5.6
	0.40	32.4	6.8
	0.30	30.0	7.3
	0.20	29.0	8.8
	0.10	40.0	11.3
0.30	0.50	27.5	5.5
	0.40	23.0	8.2
	0.30	26.4	9.6
0.35	0.50	27.5	6.0
0.40	0.40	21.2	7.9
	0.30	21.2	8.8

A general trend of an increase in ε_s as either the proportion of water is increased or the proportion of heptane is decreased is revealed.

Comparison of the $C_{12}E_4$ with the Brij 30 ternary mixture results reveals in a number of cases, similarity in ε_s

values, but there are important differences between the
two surfactants. In certain $C_{12}E_4$ mixtures, two separate
clear regions with a relatively small temperature
difference between these two regions were observed,
whereas in Brij 30 only one clear region appeared.
Inspection of the ε_s values for these $C_{12}E_4$ mixtures
reveals a large reduction in ε_s for a relatively small
temperature change. The effect is possibly most marked
for the $C_{12}E_4$ mixture with mass fraction of water = 0.40
and mass fraction of heptane = 0.50 where for a
temperature change from 4.2 to 13° C the static
permittivity falls from 20.3 to 7.3.

4.14.2 <u>Temperature dependence of ε_s for ternary mixtures
of $C_{12}E_4$ with mass fraction of water = 0.10</u>

With the exception of the mass fraction of heptane = 0.70
mixture above 18° C, all measurements were performed with
the Dipolmeter with MFL2 cell. The results are given
in Tables 54 to 57 and Figure 40.

<u>Table 54</u>

Mass fraction of heptane = 0.70

Temperature / $^\circ$C	Static Permittivity ε_s
17.2	3.70
20.0	3.41
21.8	3.22
25.0	2.93

Temperature coefficient $d\varepsilon_s/dT = -9.9 \cdot 10^{-2}$ $^\circ C^{-1}$

Table 55

Mass fraction of heptane = 0.60

Temperature /$^{\circ}$C	Static Permittivity ε_s
10.9	4.82
13.5	4.61
17.7	4.29
22.0	3.99
26.4	3.66

Temperature coefficient $d\varepsilon_s/dT = -7.43 \cdot 10^{-2}$ $^{\circ}C^{-1}$

Comparison of these four sets of results for mass fraction of water = 0.10 reveals that as the proportion of the non-polar heptane is decreased, the static permittivity ε_s increases but its temperature coefficient decreases from -9.9×10^{-2} $^{\circ}C^{-1}$ at 70% by mass of heptane to -3.2×10^{-2} $^{\circ}C^{-1}$ at 40% and then remaining unchanged at 20% of heptane.

Table 56

Mass fraction of heptane = 0.40

Temperature /$^{\circ}$C	Static Permittivity ε_s
9.6	6.01
13.2	5.87
17.4	5.71
21.0	5.58
25.6	5.44
31.8	5.24

36.2	5.11
40.7	4.98
45.8	4.85

Temperature coefficient $d\varepsilon_s/dT = -3.20 \times 10^{-2}$ $^{\circ}C^{-1}$

Table 57

Mass fraction of heptane = 0.20

Temperature /$^{\circ}$C	Static Permittivity ε_s
8.1	8.33
12.5	8.16
17.4	7.97
23.8	7.75
31.5	7.49
39.2	7.26
45.7	7.06
52.8	6.86
61.3	6.64

Temperature coefficient $d\varepsilon_s/dT = -3.18.10^{-2}$ $^{\circ}C^{-1}$

4.14.3 Time domain data for surfactant, water and heptane ternary mixtures

For nearly all mixtures studied, the TDR system did not reveal dielectric relaxation. Exceptions to this trend were surfactant-rich ternary mixtures, which revealed a rapid but measurable relaxation. The slowest relaxation observed was in the ternary mixture 0.70 Brij 30, 0.10 heptane and 0.20 water. This was given detailed attention and the relaxation time values were determined by the

Fourier transform, τ_D and FF+B methods, at three different temperatures.

The dielectric dispersion curves given by the Fourier transform value data given in Figure 41 reveal Debye-type relaxation. The τ_D values were obtained from a linear regression analysis of the $\ln(\varepsilon_S - \varepsilon)$ against time graphs given in Figure 41.

The relaxation data obtained by the three methods is given in Table 58.

Table 58 Temperature /°C	τ_F /ps	τ_D /ps	ρ_S	ρ_∞	$\rho_{0.2}$	$t_{0.2}$ /ps	Scaling Factor	τ_{FF+B} /ps
31.7	93	64	0.54	0.36	0.505	107	1.10	118
37.3	95	49	0.54	0.32	0.496	99	1.10	109
46.0	76	49	0.54	0.40	0.510	102	1.05	107

Comparison of the τ values obtained by the three methods reveals a slight fall in relaxation time with increasing temperature. As in the studies detailed earlier in this chapter, the τ_D values are somewhat lower than those of both τ_F and τ_{FF+B}. The apparent difference in the temperature dependence of τ_F compared with that of τ_D and τ_{FF+B} is attributed to the high experimental uncertainty which occurs in the TDR method for fast relaxations, and the principal conclusion drawn here is simply that the dielectric relaxation is very rapid with τ values comparable to the surfactant only and surfactant-water

binary mixtures.

4.14.4 <u>Dielectric properties of ternary mixtures at temperatures outside the limits for transparent solutions</u>

When the temperature was raised to just above the cloud point, dielectric dispersion in the frequency range 30 kHz to 10 MHz was not observed. In contrast, when the temperature was lowered to just below the lower limit for transparency, dielectric dispersion in the above frequency range was a general feature. A representative selection of the results for four compositions is given in Tables 59 to 62 and Figure 42. The lower temperature limit for transparent solutions is given in brackets.

<u>Table 59</u>

0.20 Brij 30 : 0.60 hexane : 0.20 water

Temperature = 29.2° C (lower limit for transparency = 32°C)

Frequency /MHz	$\varepsilon^{\grave{}}$	$\varepsilon^{\grave{}\grave{}}$
0.07	9.7	0.81
0.10	8.9	1.7
0.30	7.6	2.0
1.00	6.2	1.4
2.00	5.6	1.0
5.00	5.2	0.63
15.00	5.1	0.25

The dispersion curve is Cole-Cole arc type with α = 0.24 and τ = 5.3.10^{-7} s

Table 60

0.20 Brij 30 : 0.40 hexane : 0.40 water

Temperature = 19.0° C (lower limit for transparency = 20°C)

Frequency /MHz	$\varepsilon^{`}$	$\varepsilon^{``}$
0.10	14.1	1.02
0.15	13.8	1.7
0.30	12.5	2.5
0.50	11.6	2.7
0.70	10.9	2.6
1.00	10.6	2.55
1.50	9.9	2.4
2.00	9.4	2.1
7.00	8.25	1.3
15.00	8.1	0.9

The dispersion curve is Cole-Cole arc type with $\alpha = 0.20$ and $\tau = 2.7 . 10^{-7}$ s.

Table 61

0.60 Brij 30 : 0.20 hexane : 0.20 water

Temperature = 29.5° C (lower limit for transparency = 30°C)

dc conductance = 6.0 μS

Frequency /MHz	$\varepsilon^{`}$	$\varepsilon^{``}$
0.10	11.6	0.85
0.15	10.9	1.3
0.30	10.2	1.5
0.50	9.6	1.44
0.70	9.1	1.3
1.50	8.8	0.9
3.00	8.7	0.64
7.00	8.5	0.4
15.00	8.5	0.12

The dispersion curve is Cole-Cole ar type with $\alpha = 0.11$
and $\tau = 4.5.10^{-7}$ s.

Table 62

0.30 Brij 30 : 0.30 hexane : 0.40 water

Temperature = 21.0° C (lower limit for transparency = 22°C)

Frequency /MHz	$\varepsilon^{\backprime}$	$\varepsilon^{\backprime\backprime}$
0.30	12.2	0.95
0.50	11.9	1.3
0.70	11.7	1.4
1.00	11.2	1.5
1.50	10.9	1.5
3.00	10.2	1.3
7.00	9.7	0.9
15.00	9.5	0.7

The dispersion curve is Cole-Cole arc type with $\alpha = 0.18$
and $\tau = 1.2.10^{-7}$ s.

For all four compositions the relaxation times are of a
similar order. The dispersion parameter values are similar
with $\alpha = 0.21 \pm 0.03$ for three of the mixtures but a
lower value of 0.11 ± 0.06 is obtained for the mixture
with high surfactant content. This difference could be
associated with the liquid crystalline structure which forms
at lower temperatures in this composition, in contrast with
the other three which behave as two phase emulsions at
lower temperatures. However the uncertainty in the α value
is higher in the high surfactant content mixture due to
the presence of a relatively high dc conductivity. In view

of this uncertainty, it is considered that conclusions
based on distinction between liquid crystalline and two
phase emulsion formation are precluded.

FIGURE 9

Calibration curve for cell constant of
B601 RF bridge

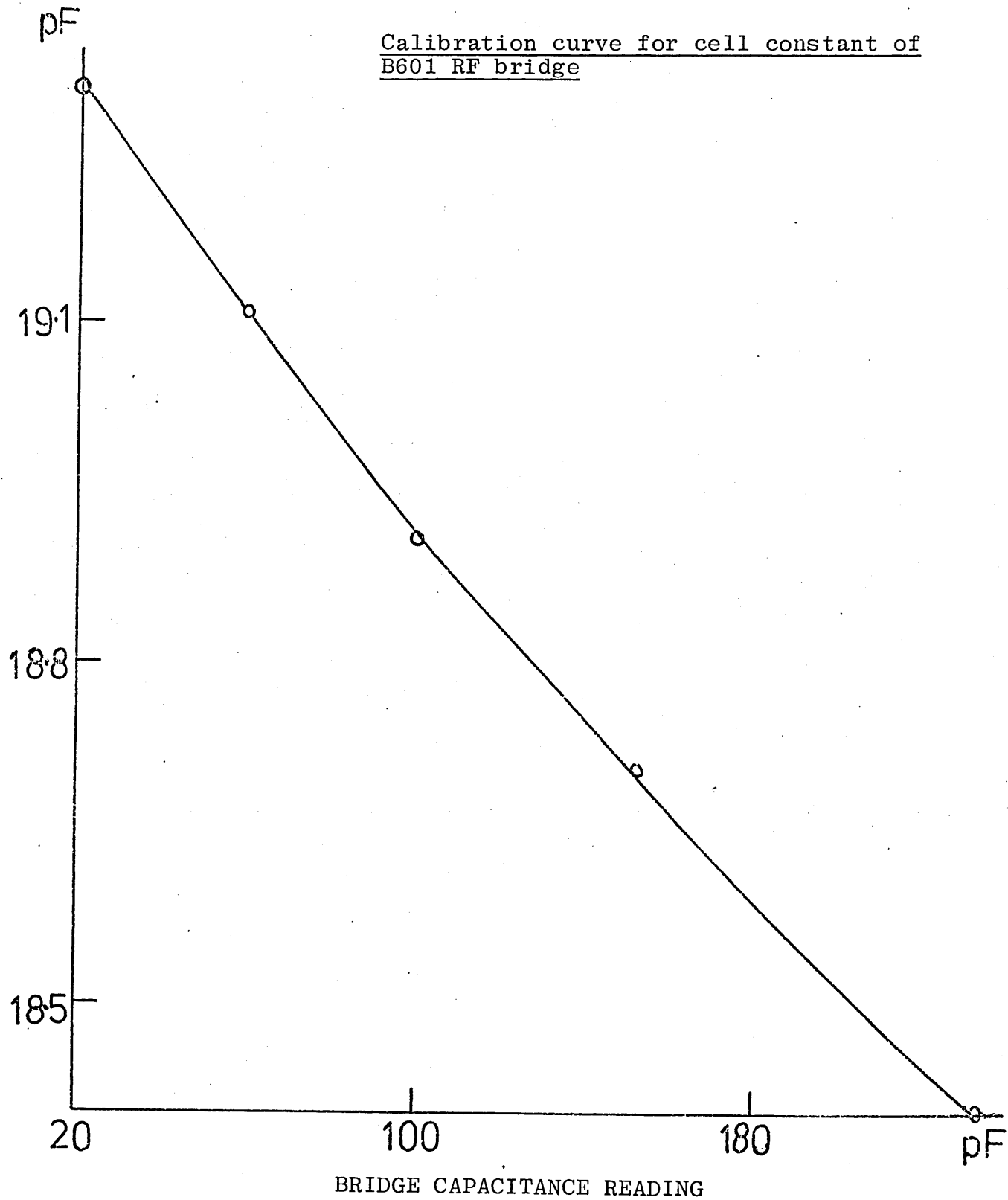FIGURE 10

Cole-Cole plots (Indicated frequencies are in GHz)
a) t butanol
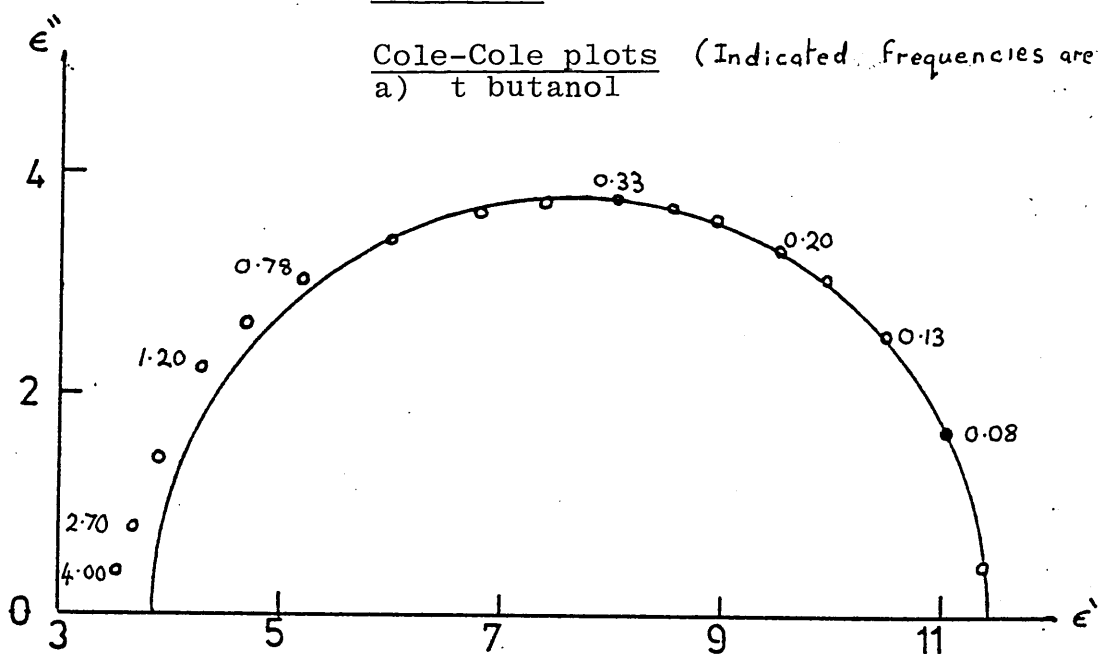
b) t butanol with 0.052 mf of water

FIGURE 11

Cole–Cole Plots (Indicated frequencies are in GHz)

a)   t butanol with 0.101 mf of water

b)   t butanol with 0.153 mf of water

FIGURE 12

Cole-Cole plots (Indicated frequencies are in GHz)

a) t butanol with 0.197 mf of water

b) t butanol with 0.250 mf of water

FIGURE 13

Cole-Cole plots (Indicated frequencies are in GHz)

a) t butanol with 0.299 mf of water

b) t butanol with 0.350 mf of water

FIGURE 14

Cole-Cole plots (Indicated frequencies are in GHz)
a) t butanol with 0.400 mf of water
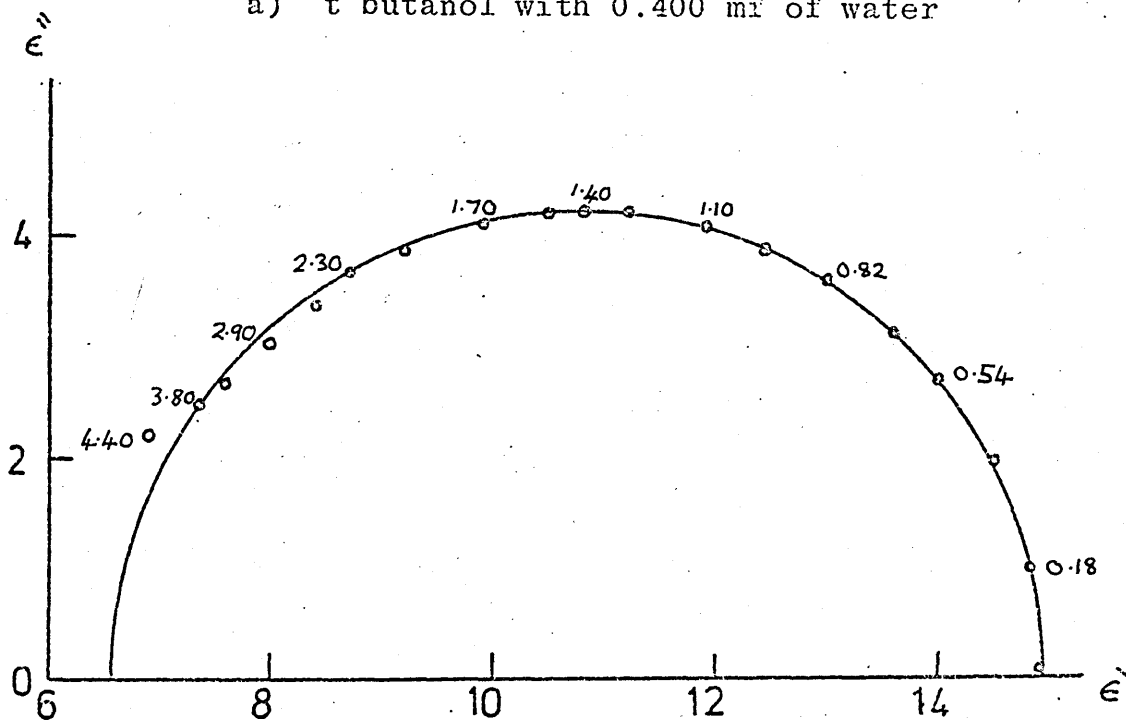
b) t butanol with 0.400 mf of water
effect of time zero reference change

◻ ≡ Zero advanced by 3.9 ps

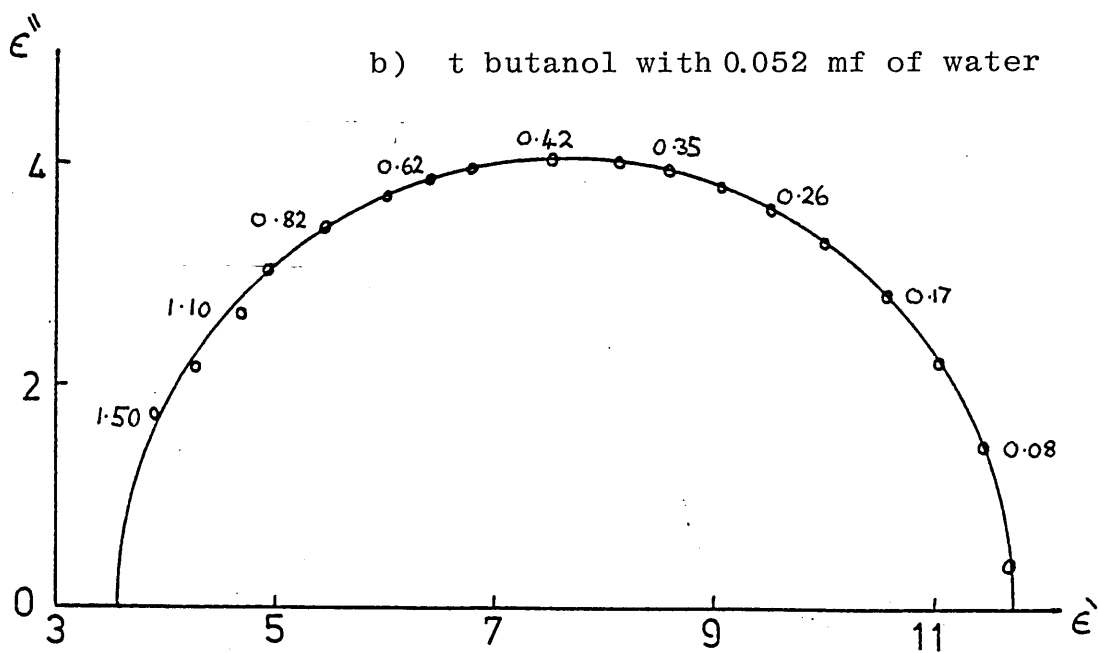▽ ≡ Actual zero used   ○ ≡ Zero retarded by 3.9 p
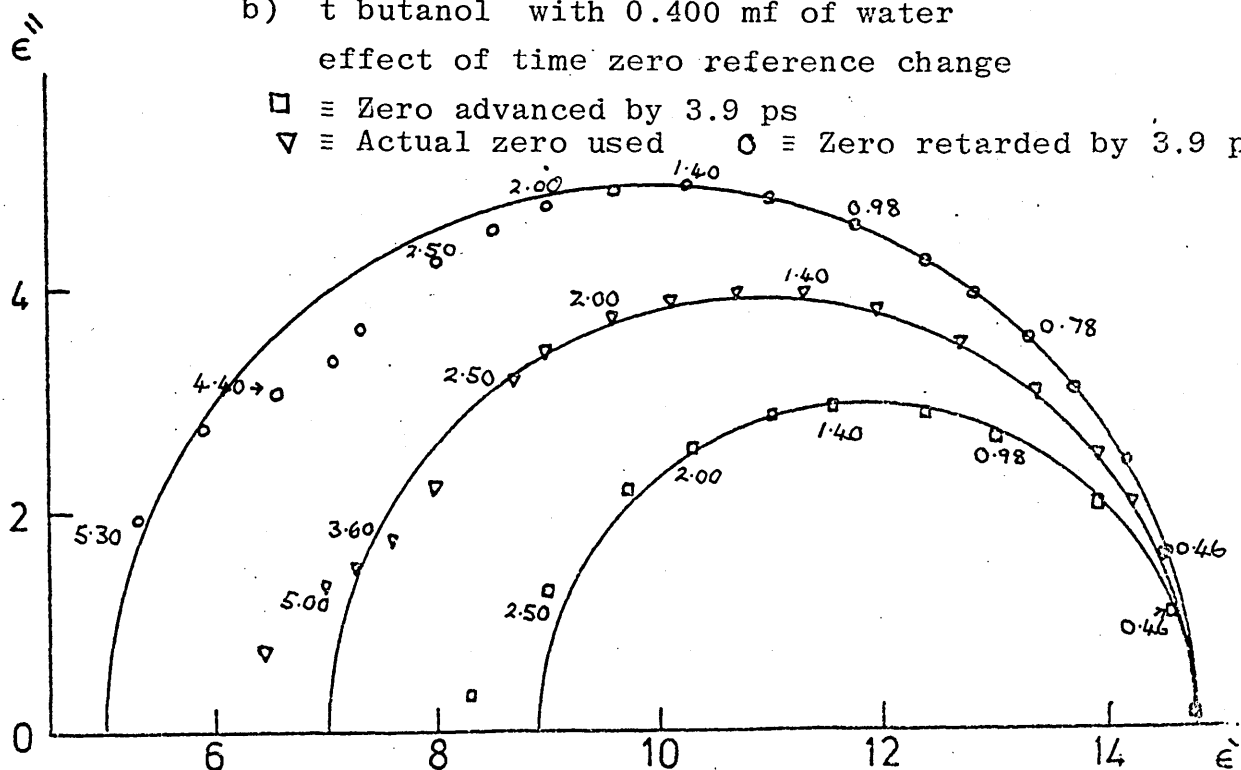
FIGURE 15

Cole-Cole plots (Indicated frequencies are in GHz)
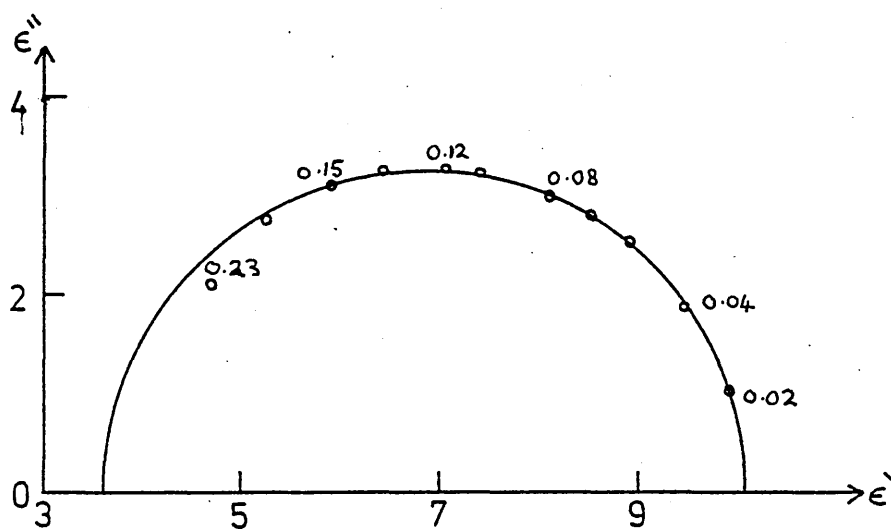
a) cyclohexanol

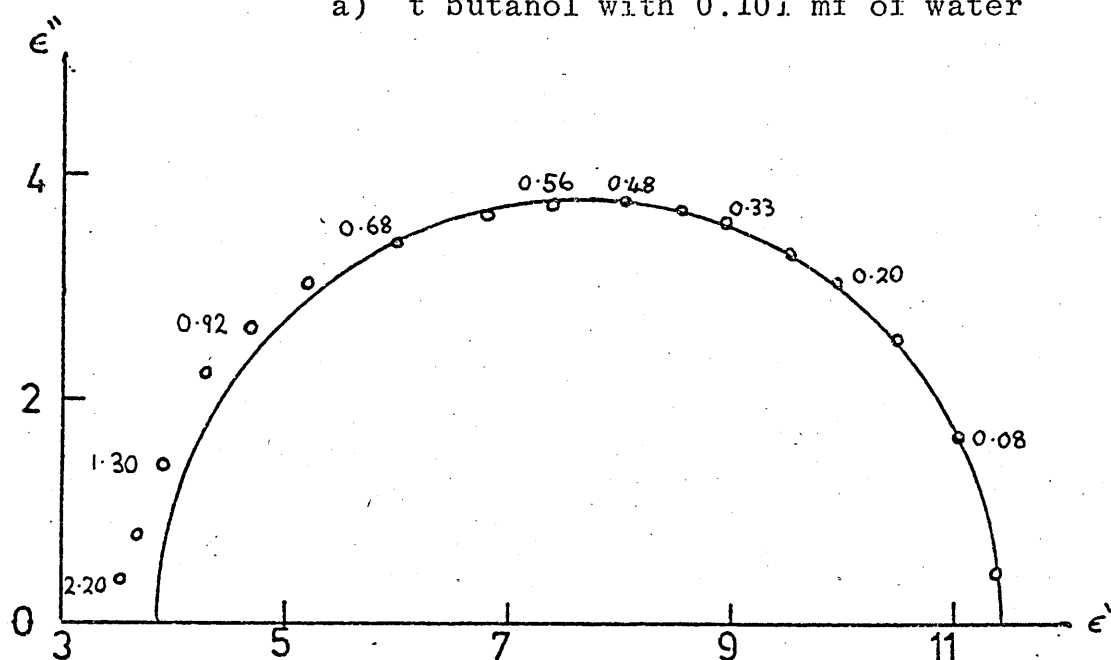b) cyclohexanol with 0.098 mf of water
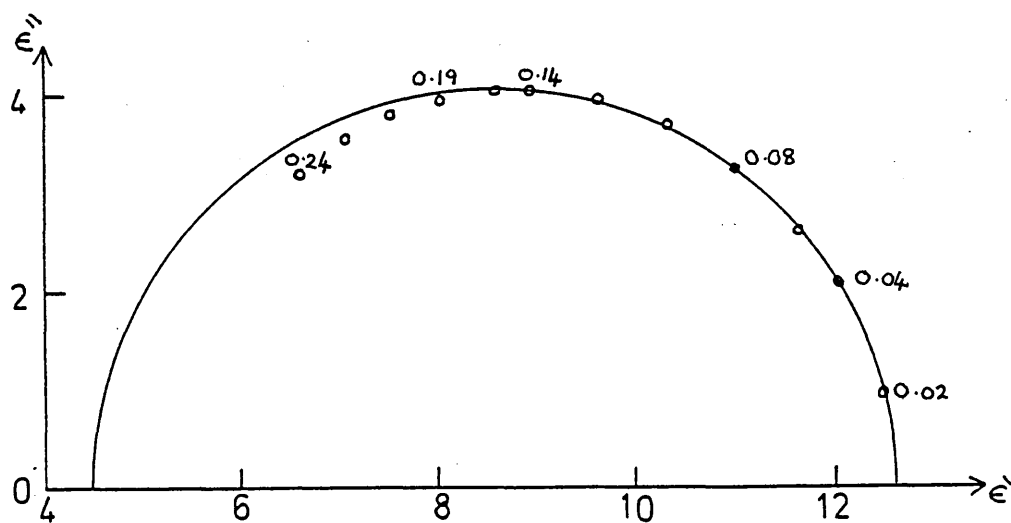
FIGURE 16

Cole-Cole plots (Indicated frequencies are in GHz)

a) cyclohexanol with 0.148 mf of water
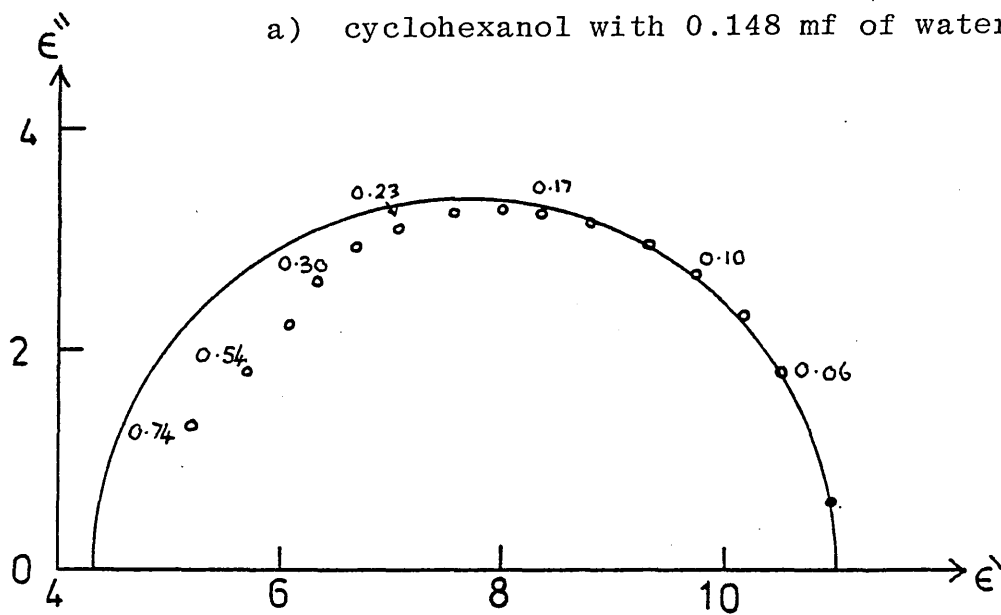
b) cyclohexanol with 0.198 mf of water
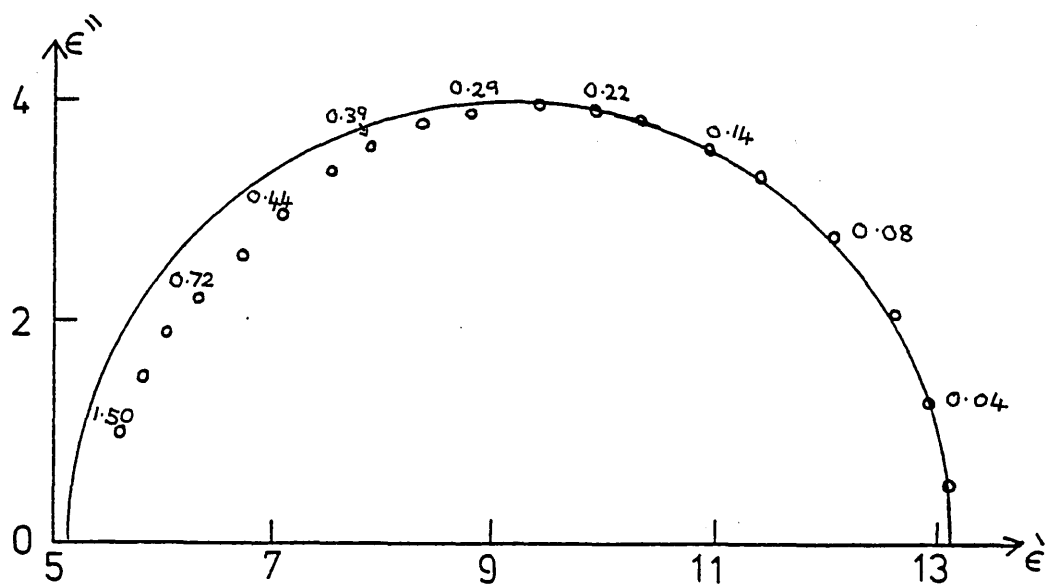
FIGURE 17

Cole-Cole plots (Indicated frequencies are in GHz)

a) cyclohexanol with 0.251 mf of water
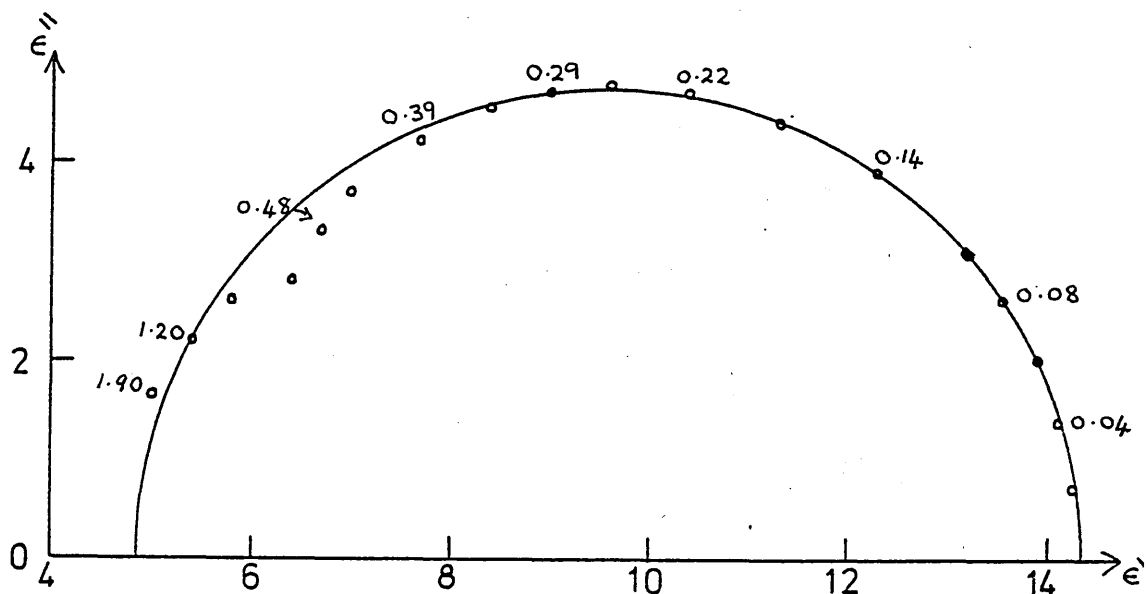
b) cyclohexanol with 0.298 mf of water
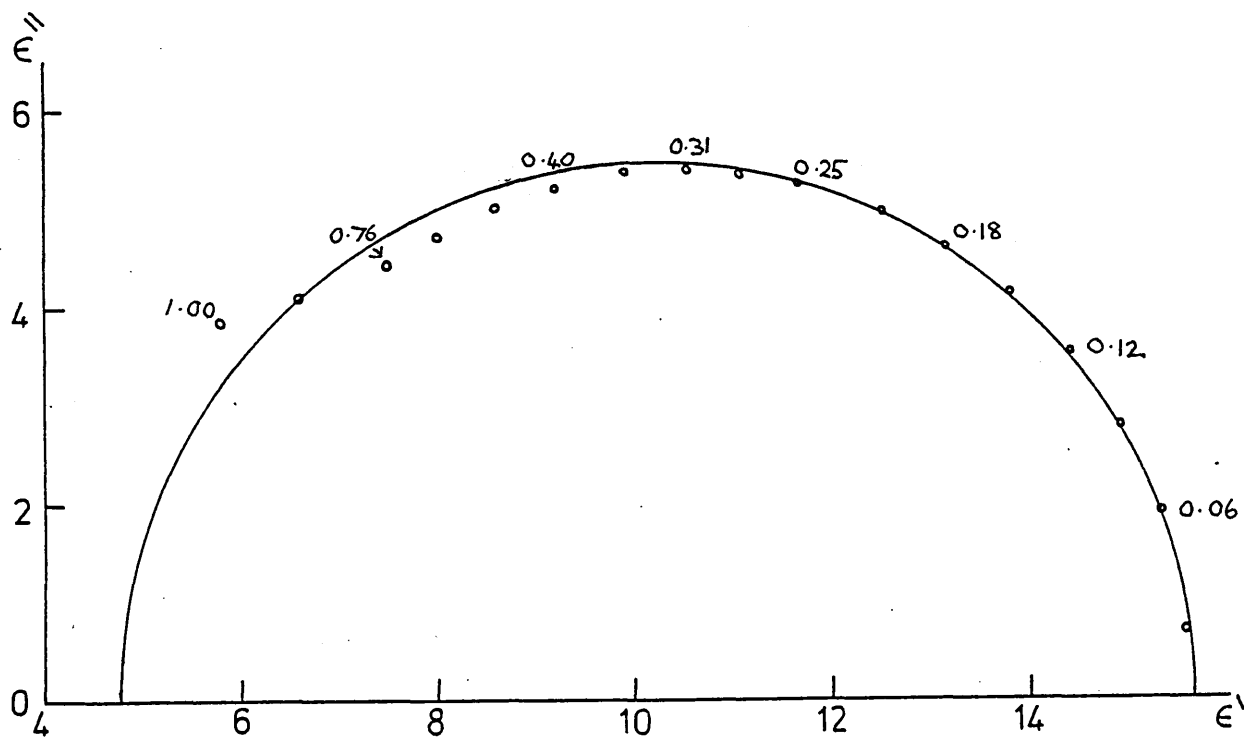
FIGURE 18

Cole-Cole plots (Indicated frequencies are in GHz)

a)   cyclohexanol with 0.353 mf of water
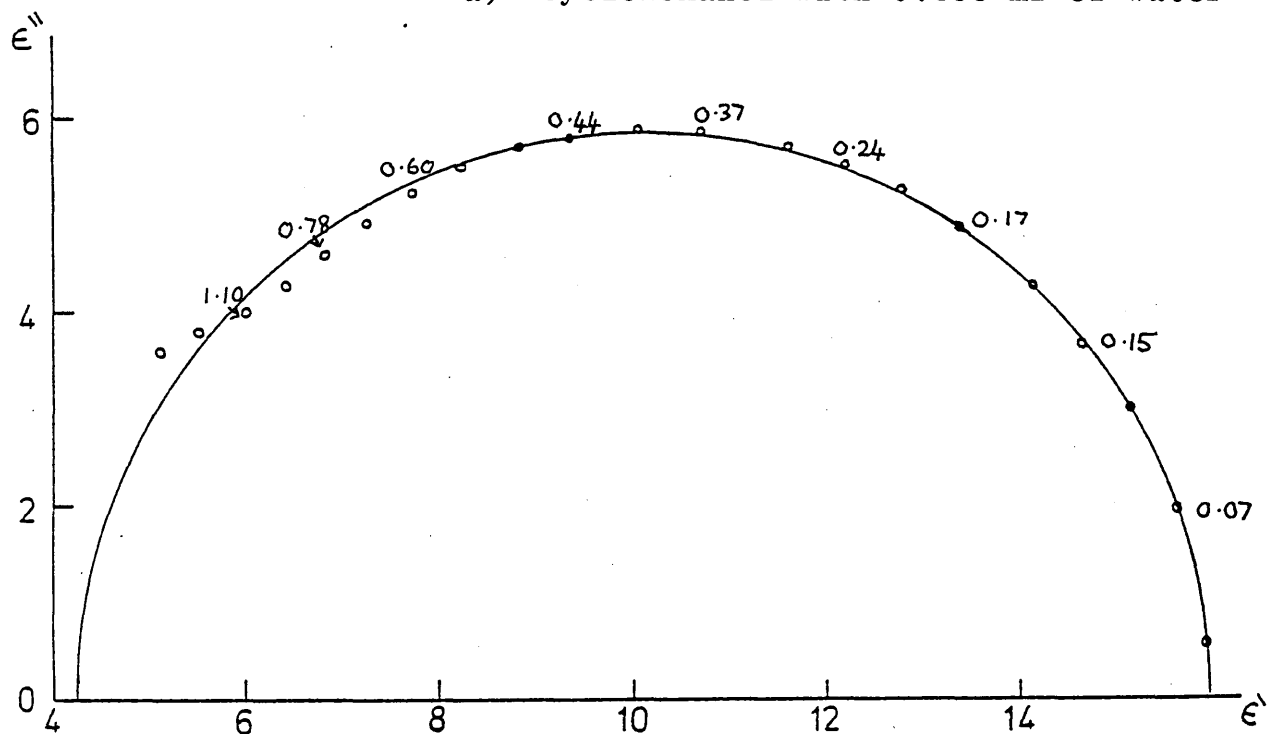
b)   cyclohexanol with 0.399 mf of water
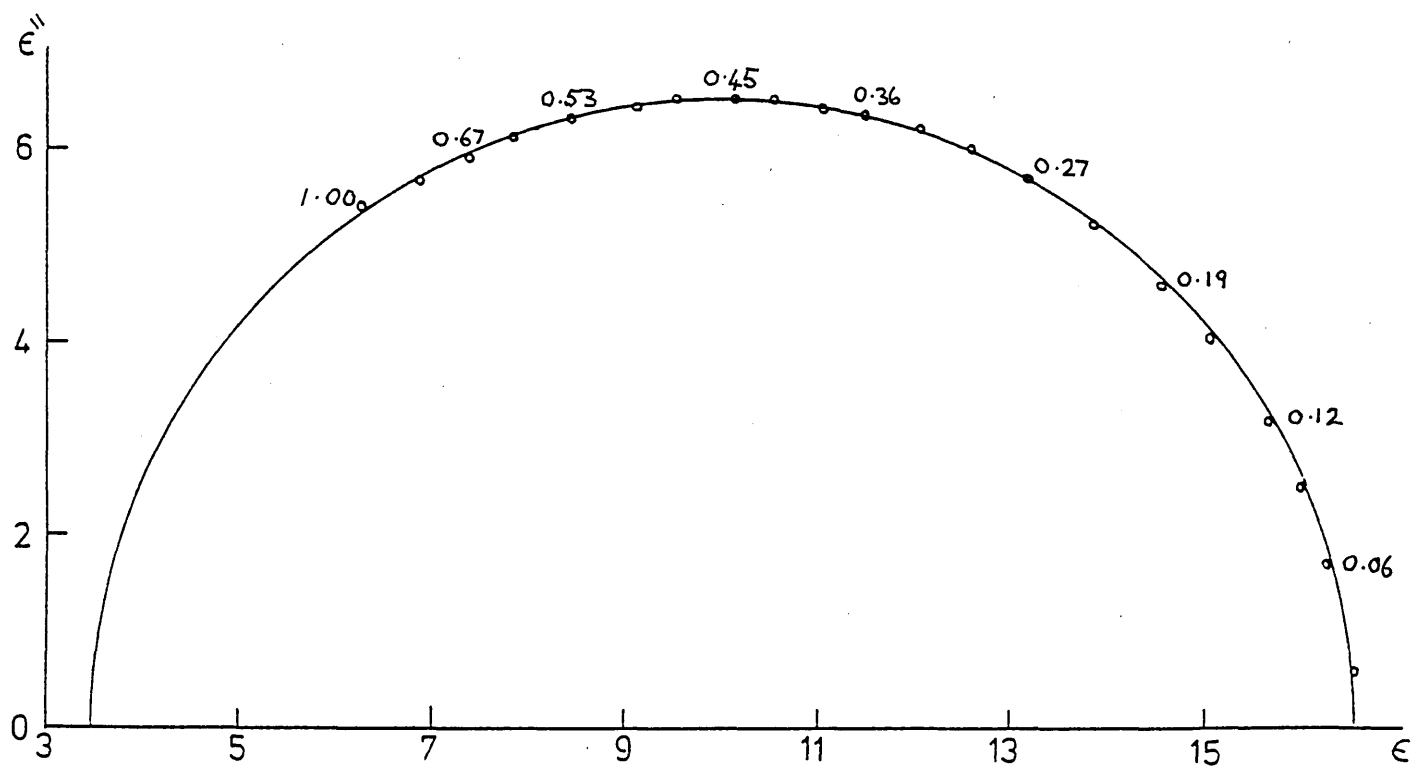
FIGURE 19

Cole-Cole plots (Indicated frequencies are in GHz)
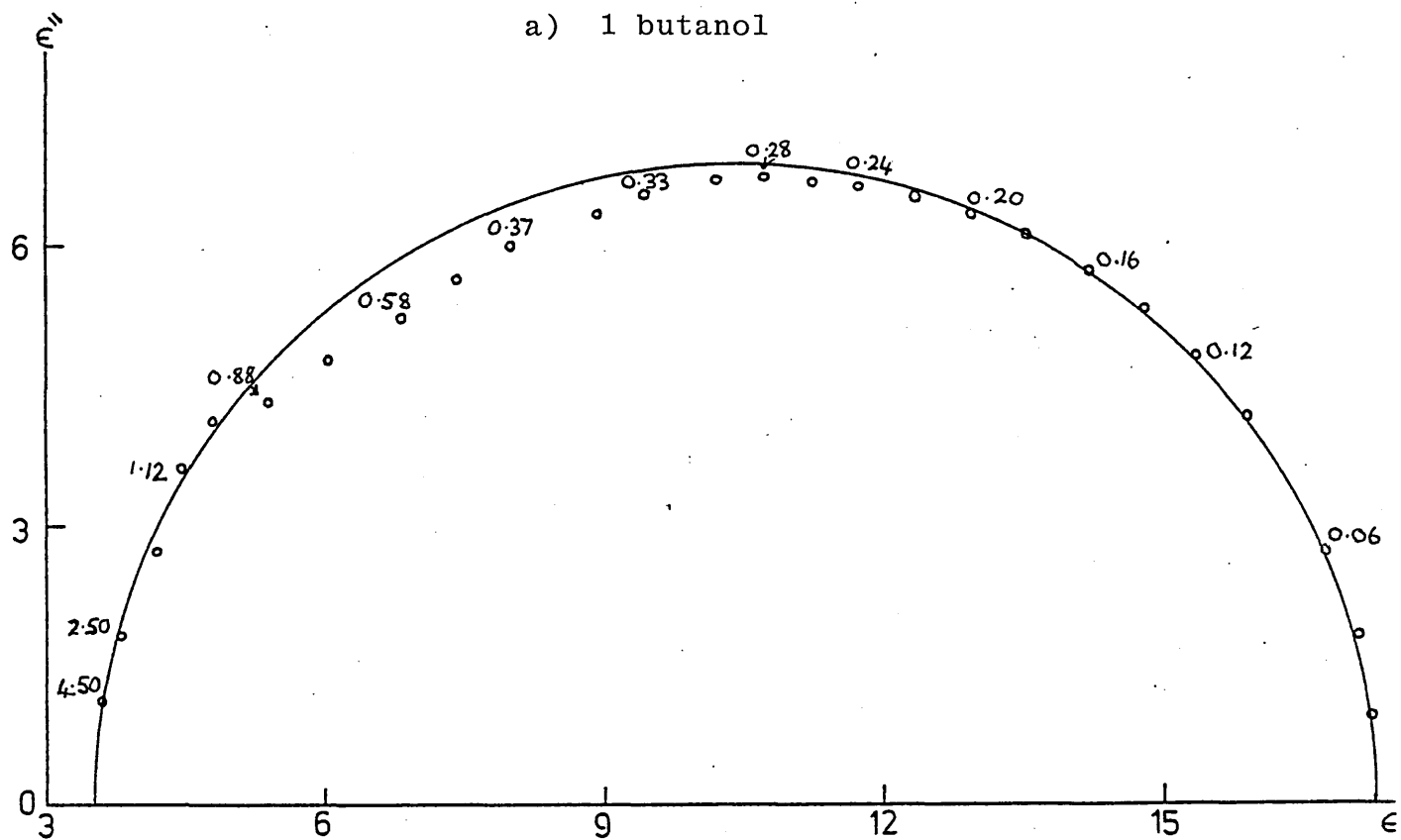
a) 1 butanol

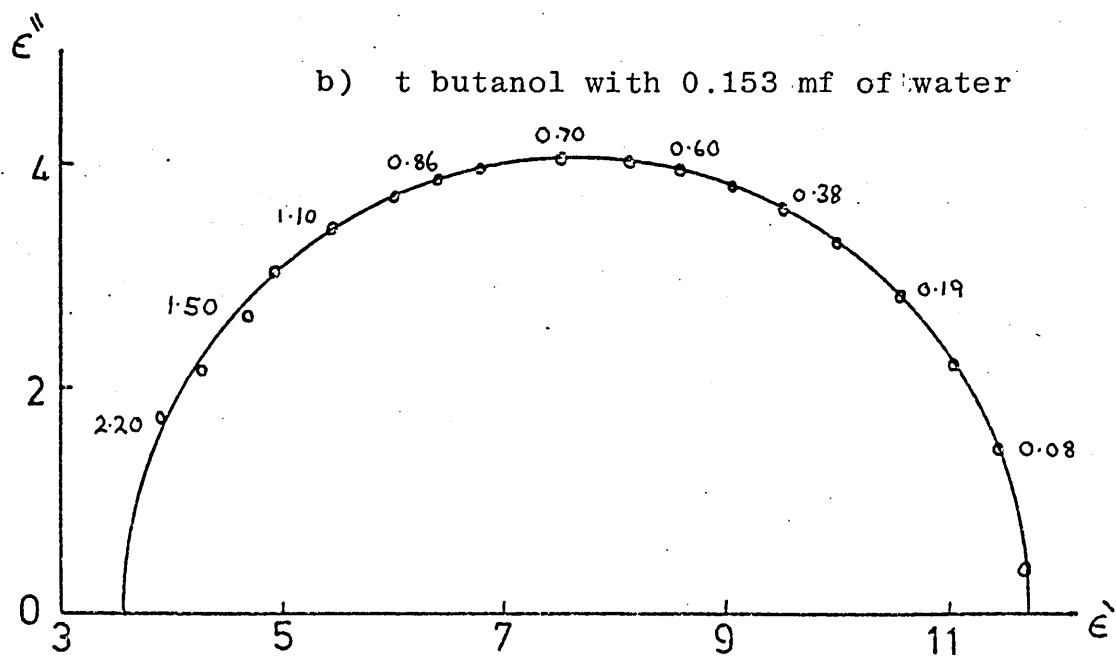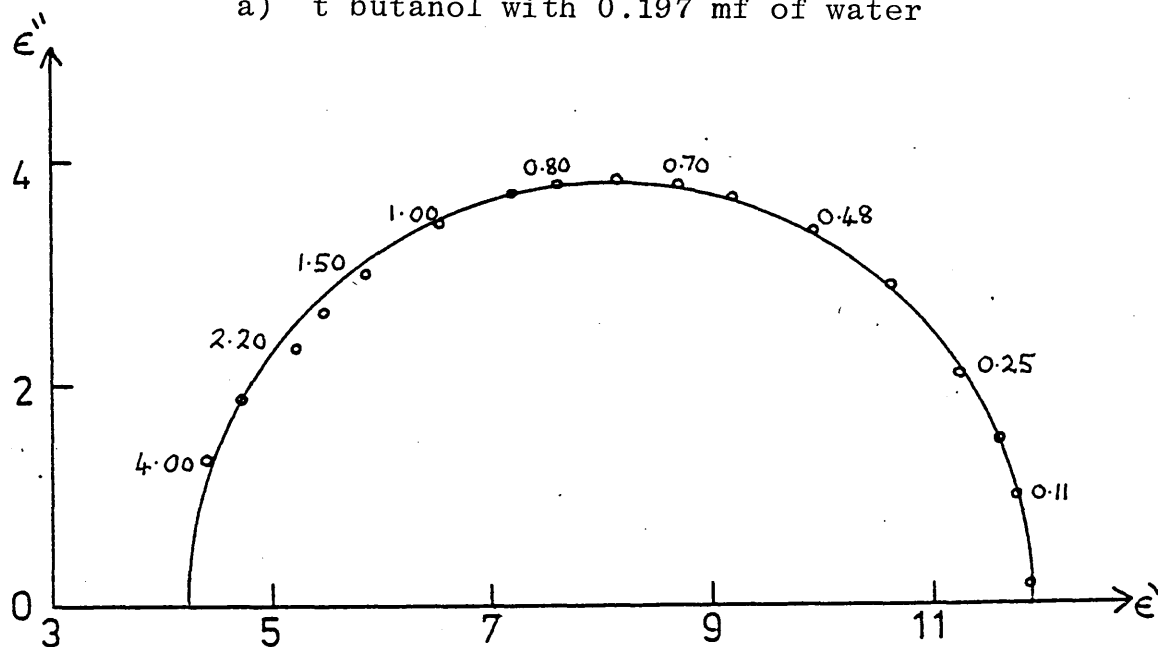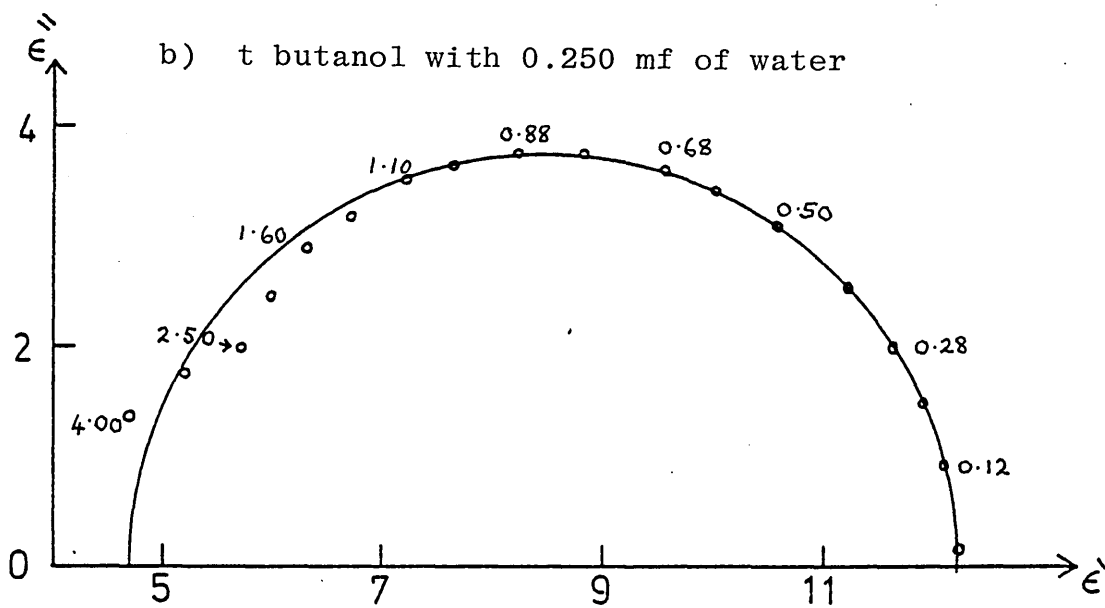b) 1 butanol with 0.150 mf of water
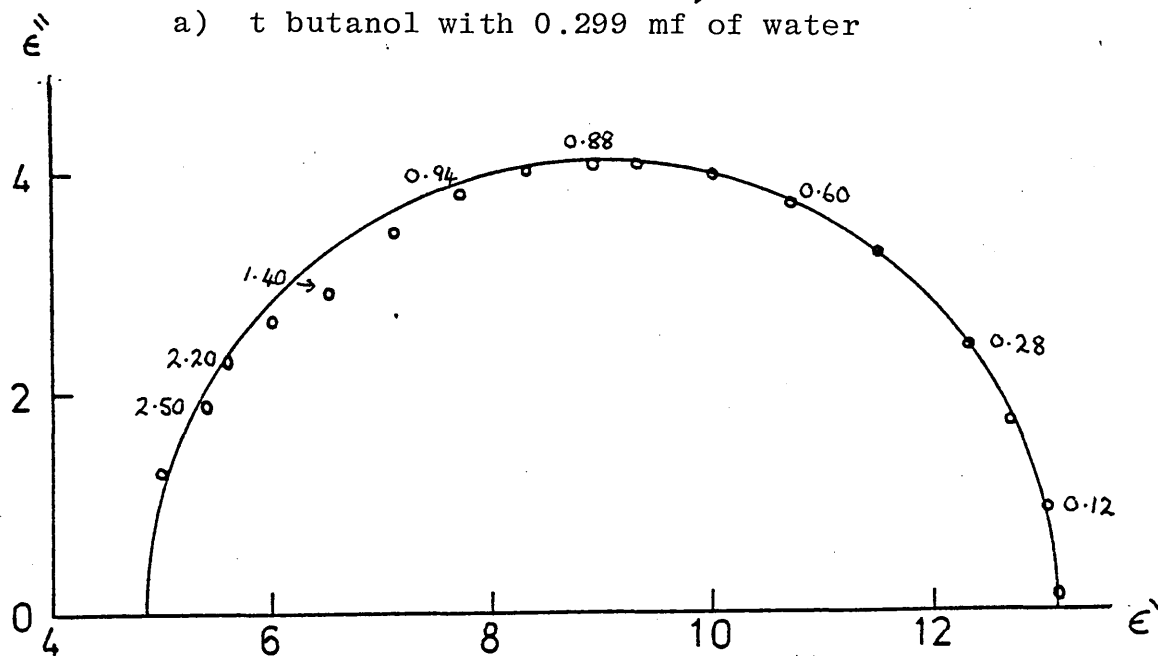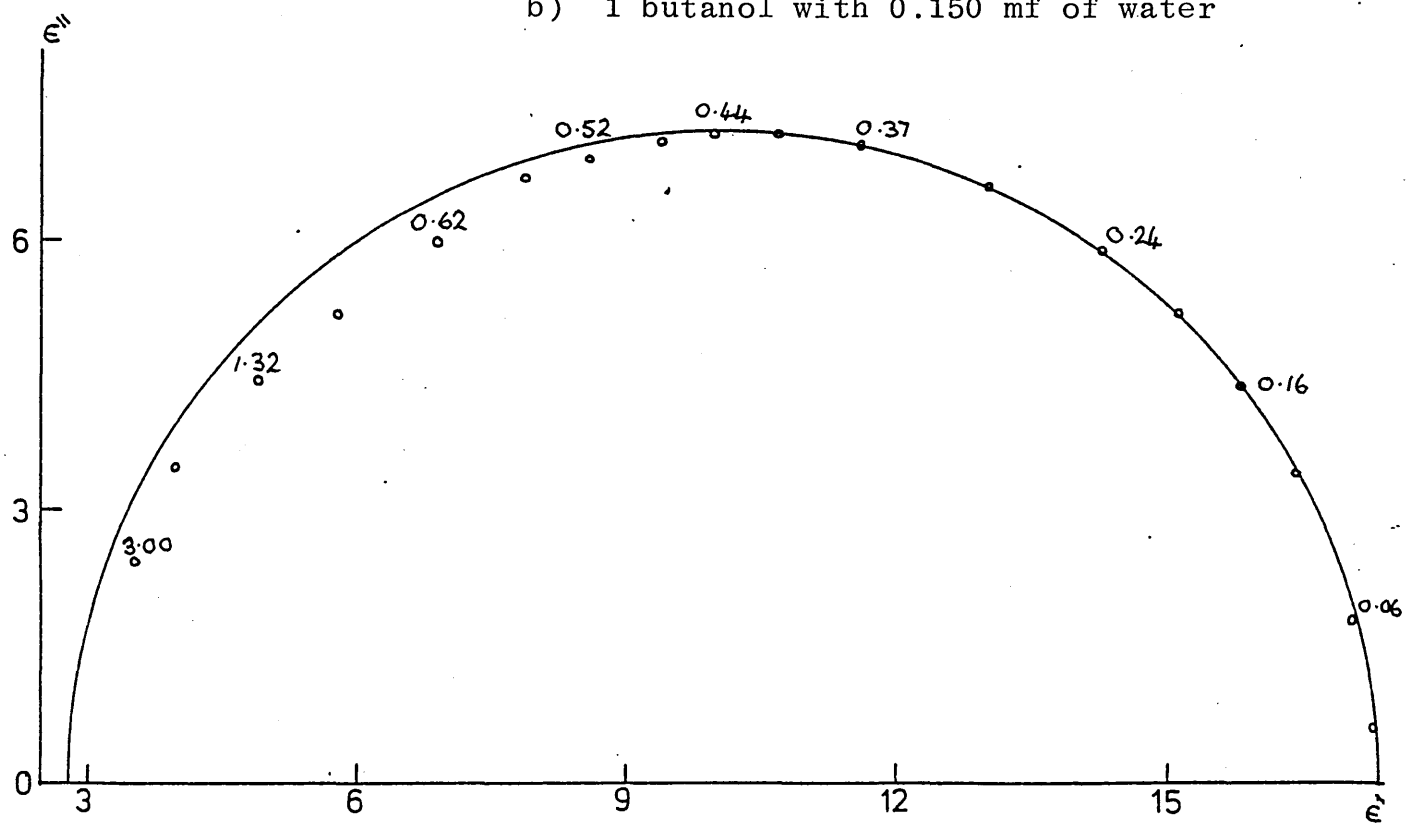
FIGURE 20

Cole-Cole plots (Indicated frequencies are in GHz)

a) 1 butanol with 0.245 mf of water
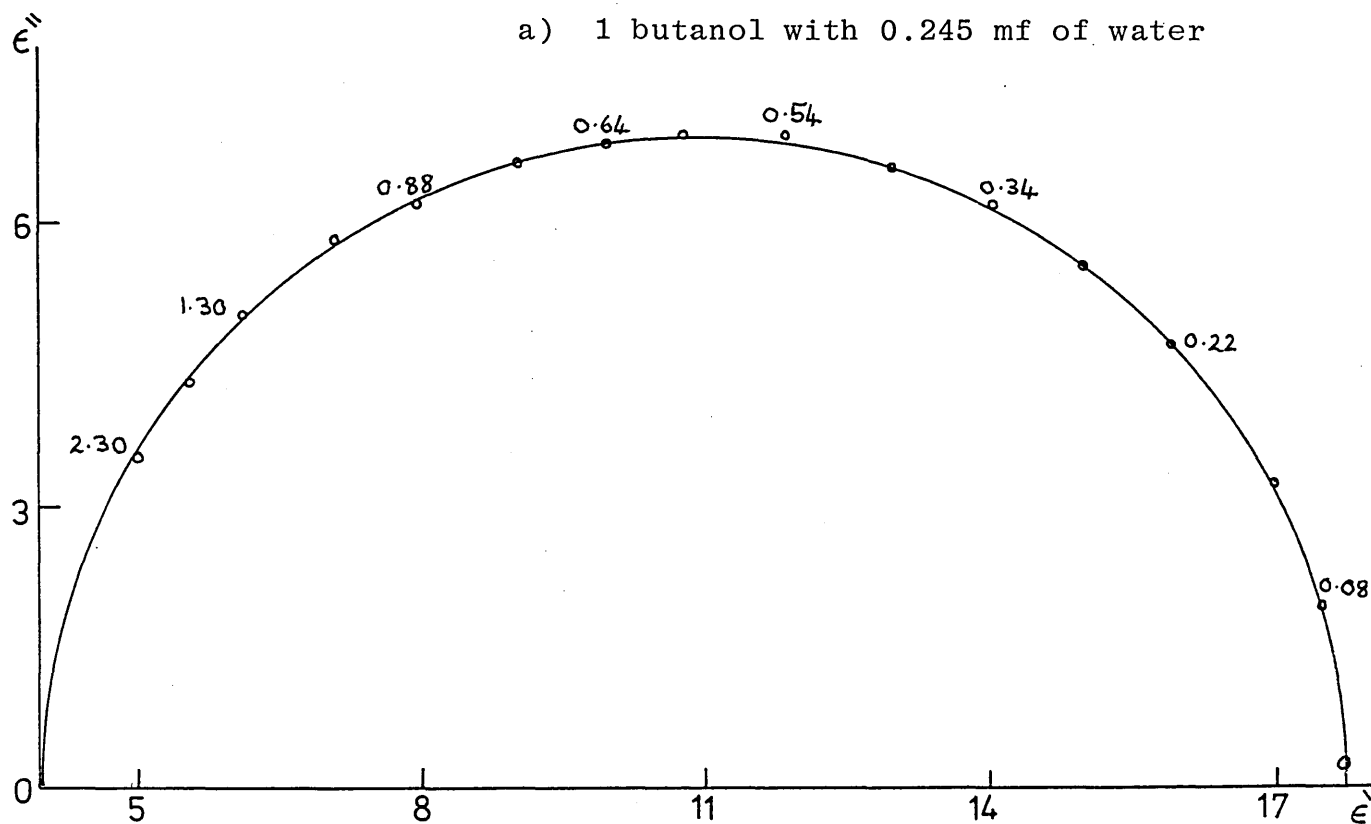
b) 1 butanol with 0.351 mf of water
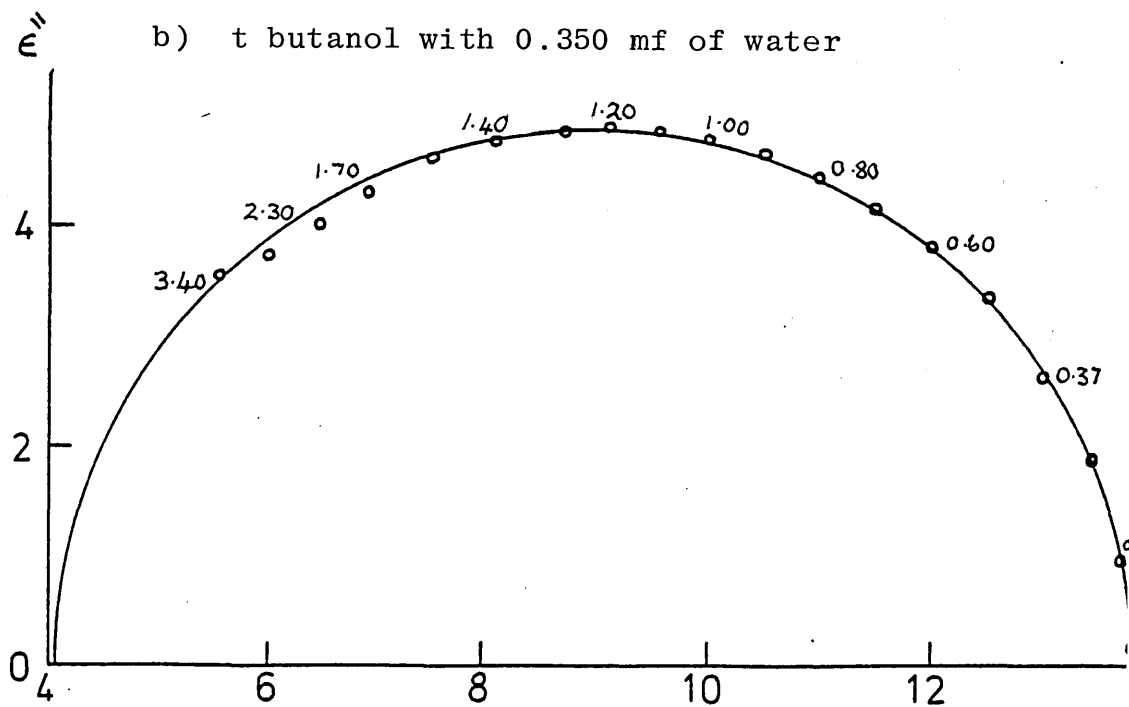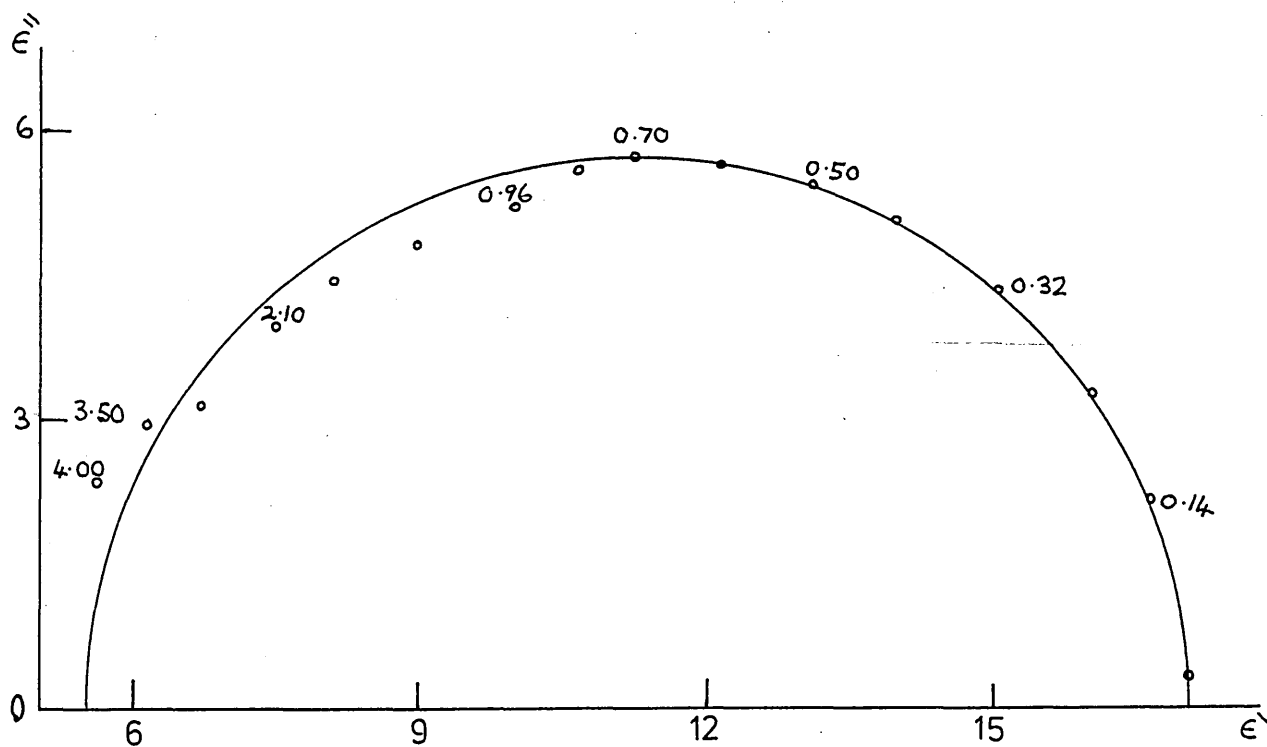
FIGURE 21

Cole-Cole plots (Indicated frequencies are in GHz)
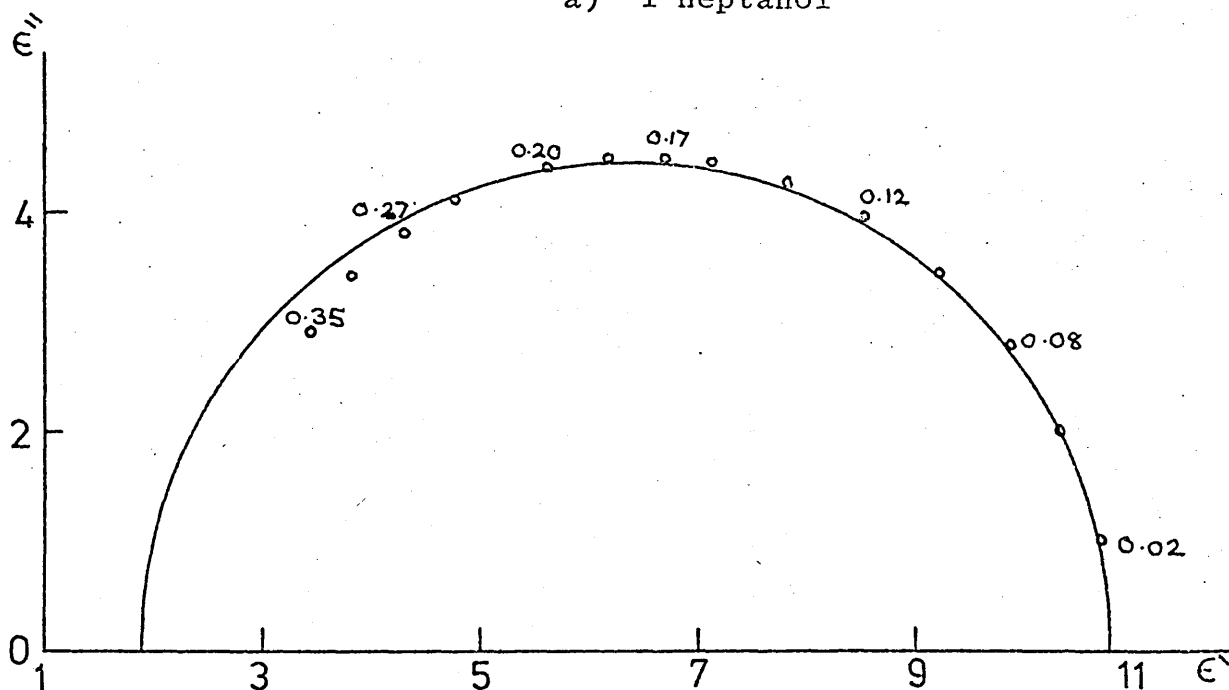
a) 1 heptanol

b) 1 heptanol with 0.153 mf of water
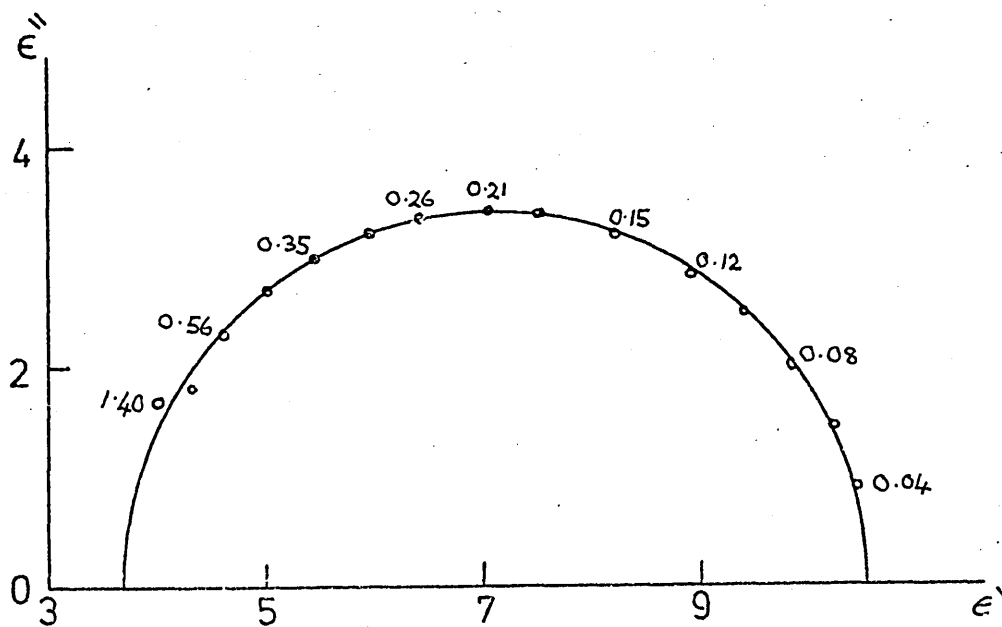
FIGURE 22

Cole-Cole plots (Indicated frequencies are in GHz)

a) 1 heptanol with 0.252 mf of water

(a)
- △ ≡ 0.000 mf
- ○ ≡ 0.052 mf
- □ ≡ 0.101 mf
- × ≡ 0.153 mf

$\ln(\epsilon_s - \epsilon)$

0·8

1·2

0·6

0

63·2 ps

(b)
- ○ ≡ 0.197 mf
- ◁ ≡ 0.250 mf
- × ≡ 0.299 mf
- □ ≡ 0.350 mf
- ▽ ≡ 0.400 mf

$\ln(\epsilon_s - \epsilon)$

1·8

1

1·2

0·6

0

31·6 ps
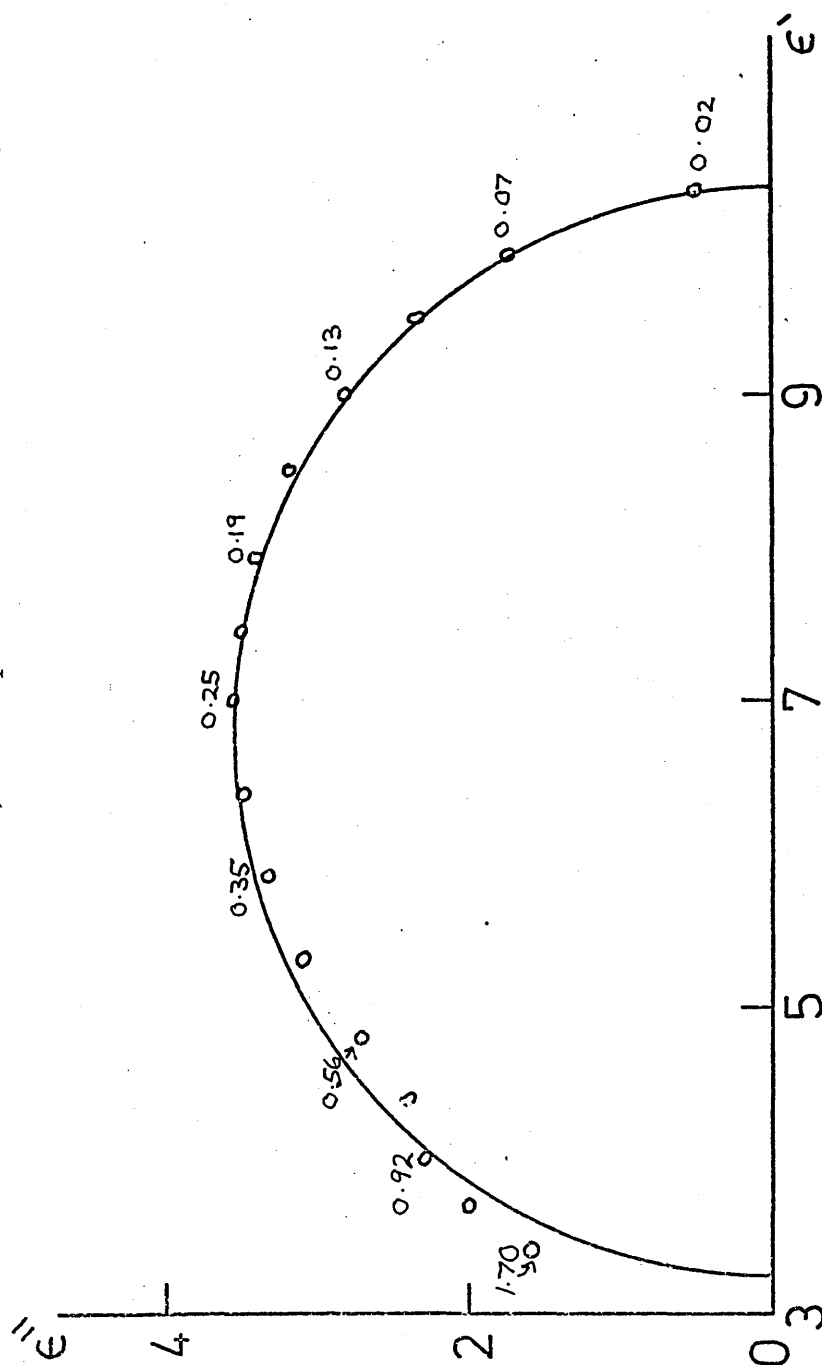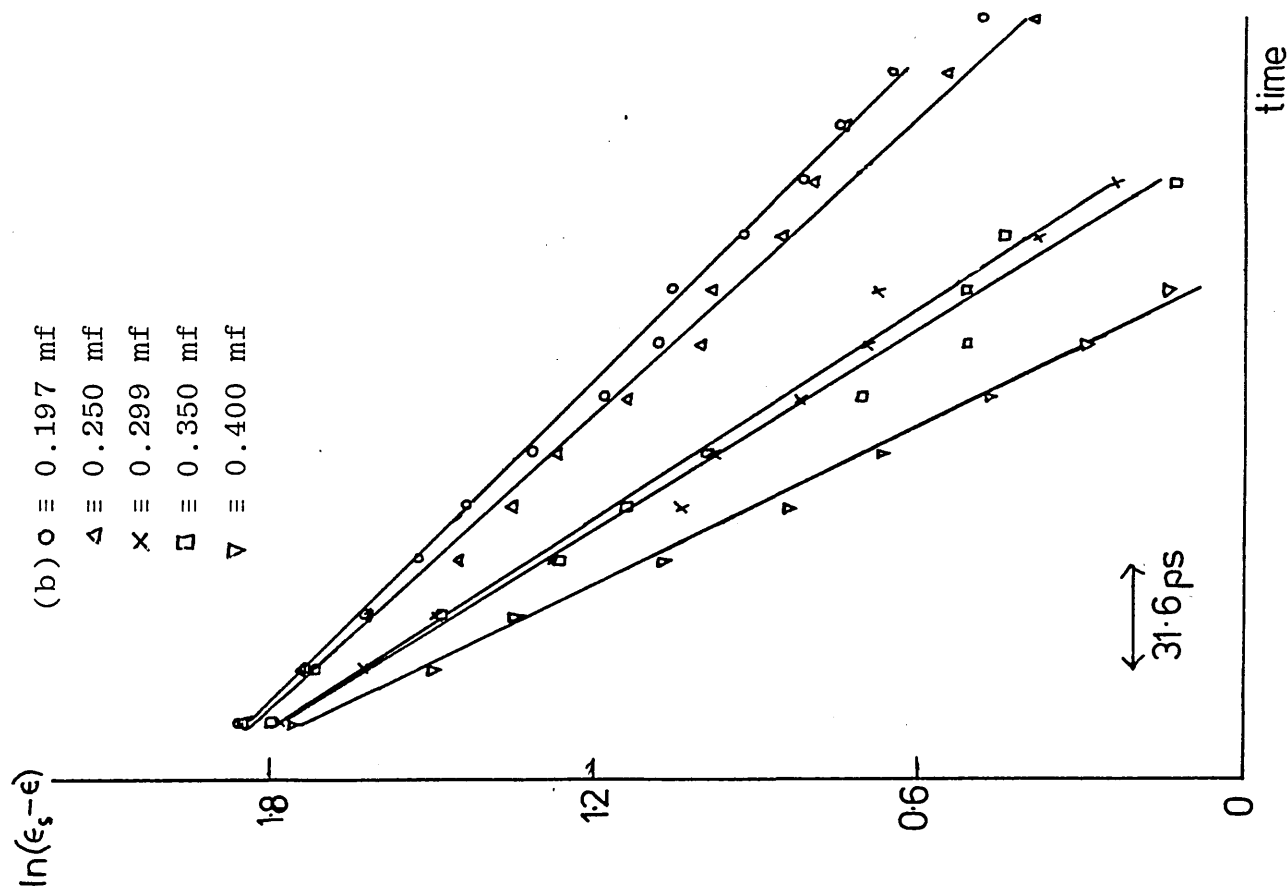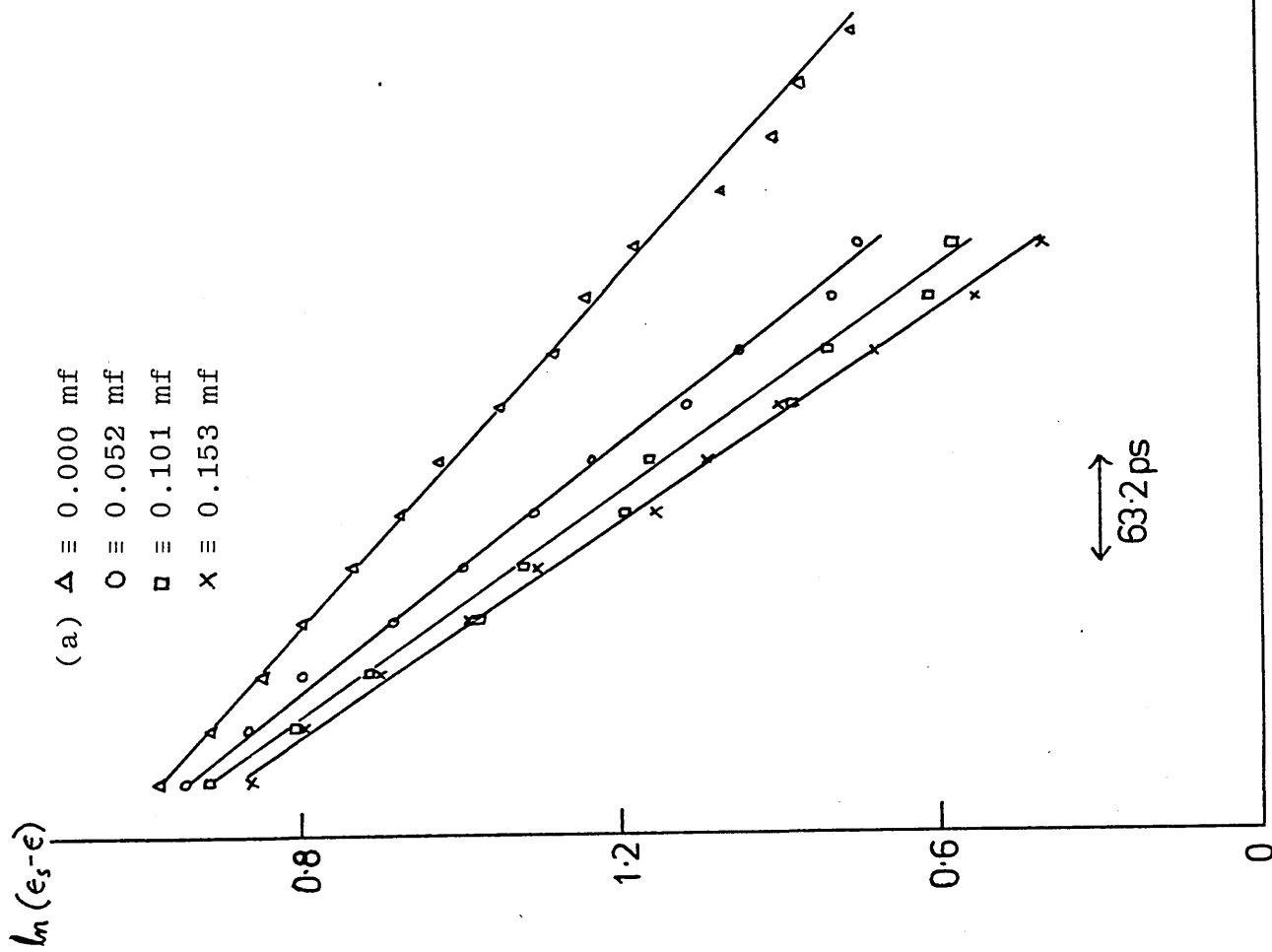
time

The time marker defines the time scale used on the time axis

FIGURE 24

Direct time domain plots for cyclohexanol-water mixtures

(a) o ≡ 0.000 mf
    □ ≡ 0.098 mf
    ◁ ≡ 0.148 mf

(b) o ≡ 0.198 mf
    ◁ ≡ 0.251 mf
    □ ≡ 0.298 mf
    × ≡ 0.353 mf
    ▽ ≡ 0.399 mf

The time marker defines the time scale on the time axis

- 212 -

Direct time domain plots

(a) 1 butanol-water mixtures

o ≡ 0.000 mf
△ ≡ 0.150 mf
□ ≡ 0.245 mf
× ≡ 0.351 mf

$\ln(\varepsilon_s - \varepsilon)$

2·5

1·5

0·5

time

588 ps

(b) 1 heptanol-water mixtures

o ≡ 0.000 mf
△ ≡ 0.153 mf
□ ≡ 0.252 mf

$\ln(\varepsilon_s - \varepsilon)$

1·8

1·2

0·6
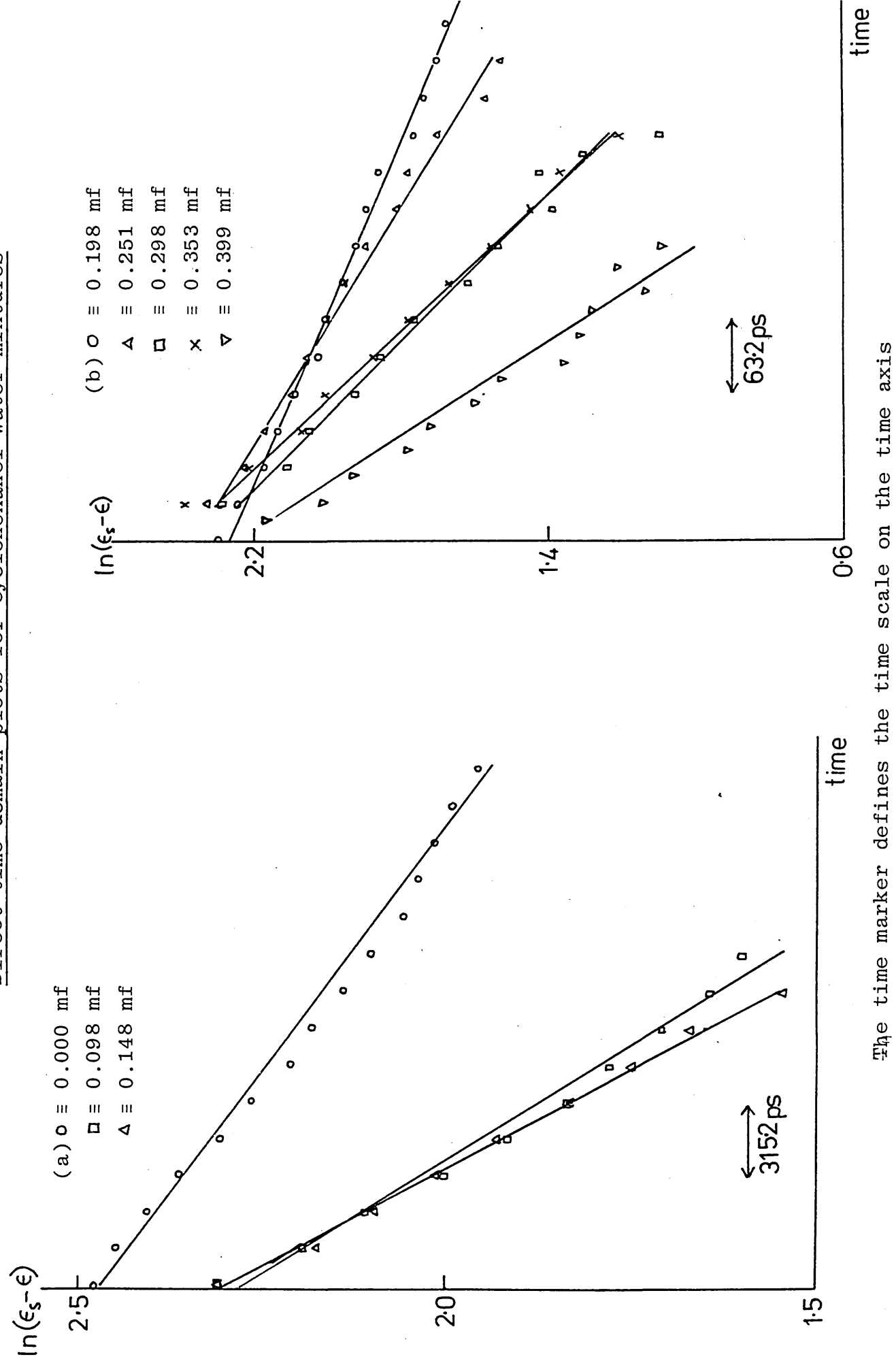
time

1396 ps
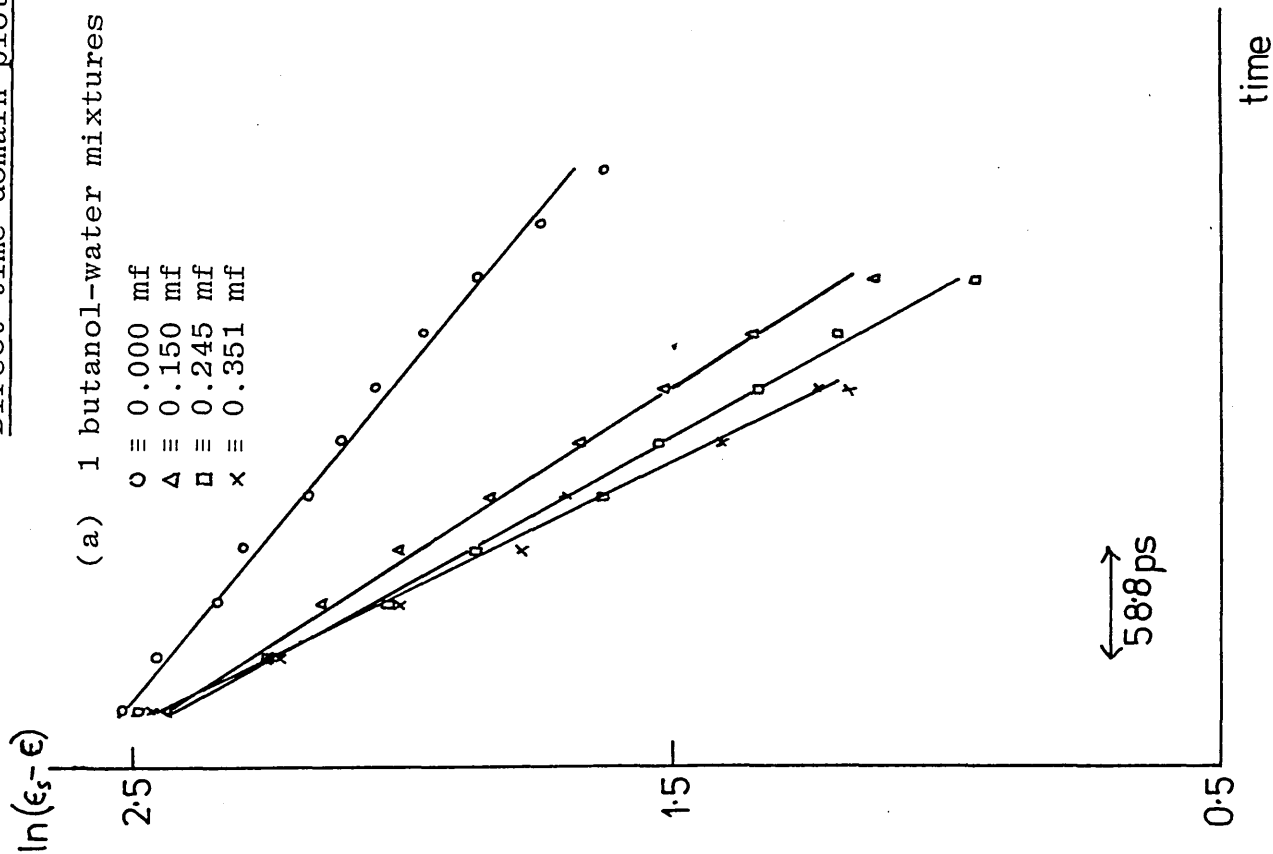
The time marker defines the time scale on the time axis
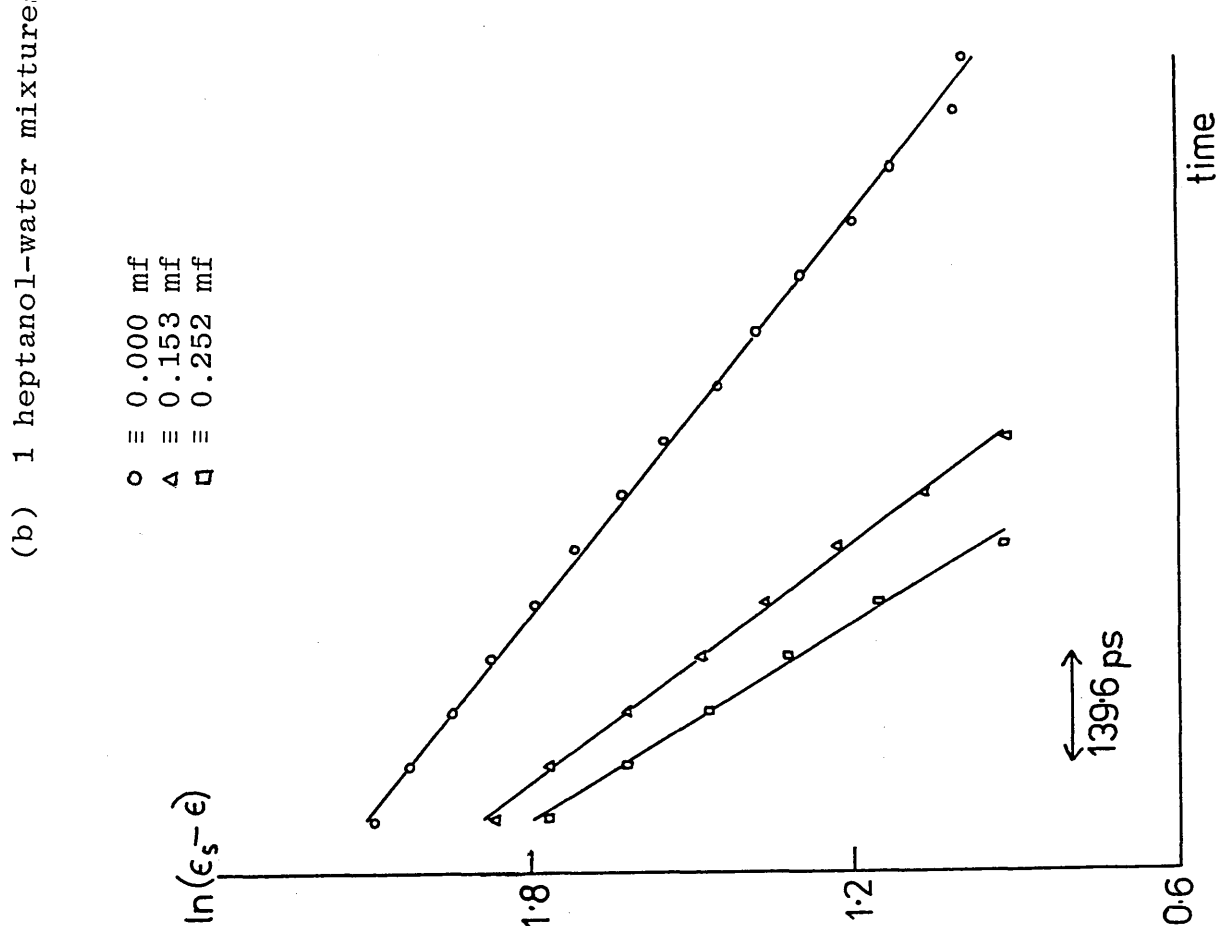
FIGURE 26

Correction curve for τ_F values in slower relaxations

Corrected value s/10^{-9}

Measured value s/10^{-9}
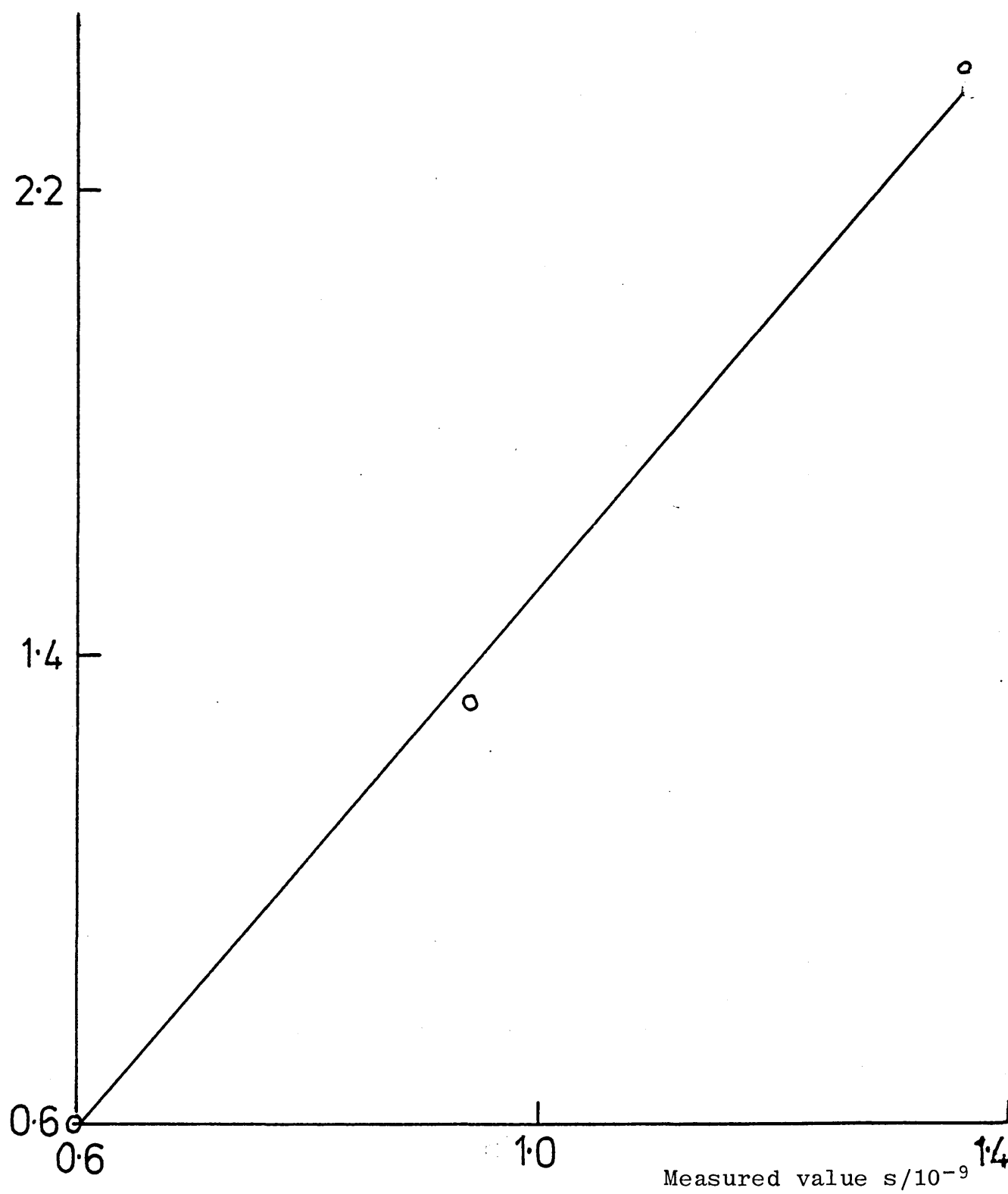
FIGURE 27

Relaxation time τ against mole fraction of water x
for alcohol-water mixtures

△ ≡ t butanol-water mixtures
○ ≡ 1 butanol-water mixtures

FIGURE 28

Relaxation time τ against mole fraction of water x for alcohol–water mixtures

○ ≡ cyclohexanol–water mixtures
△ ≡ 1 heptanol–water mixtures

- 216 -
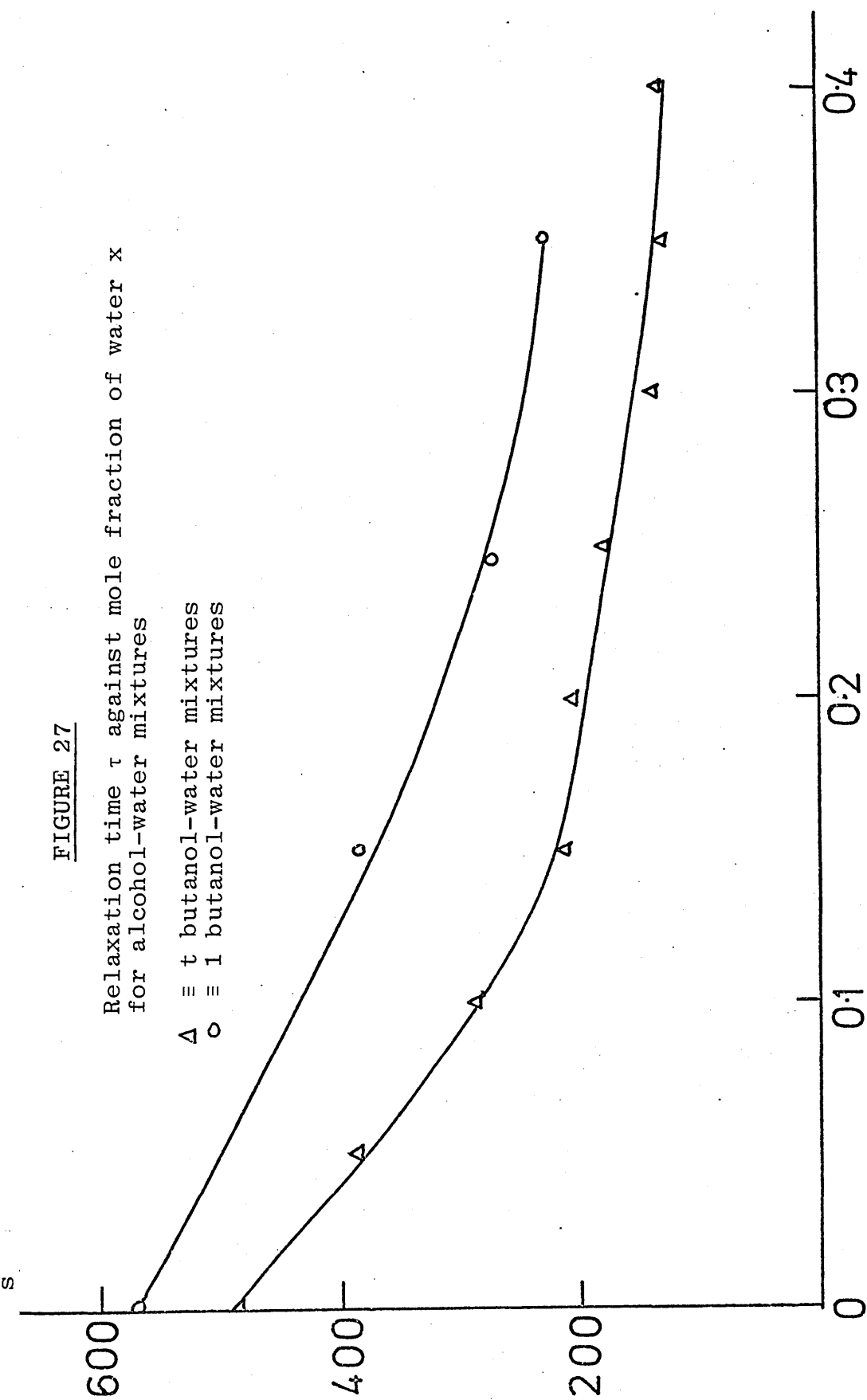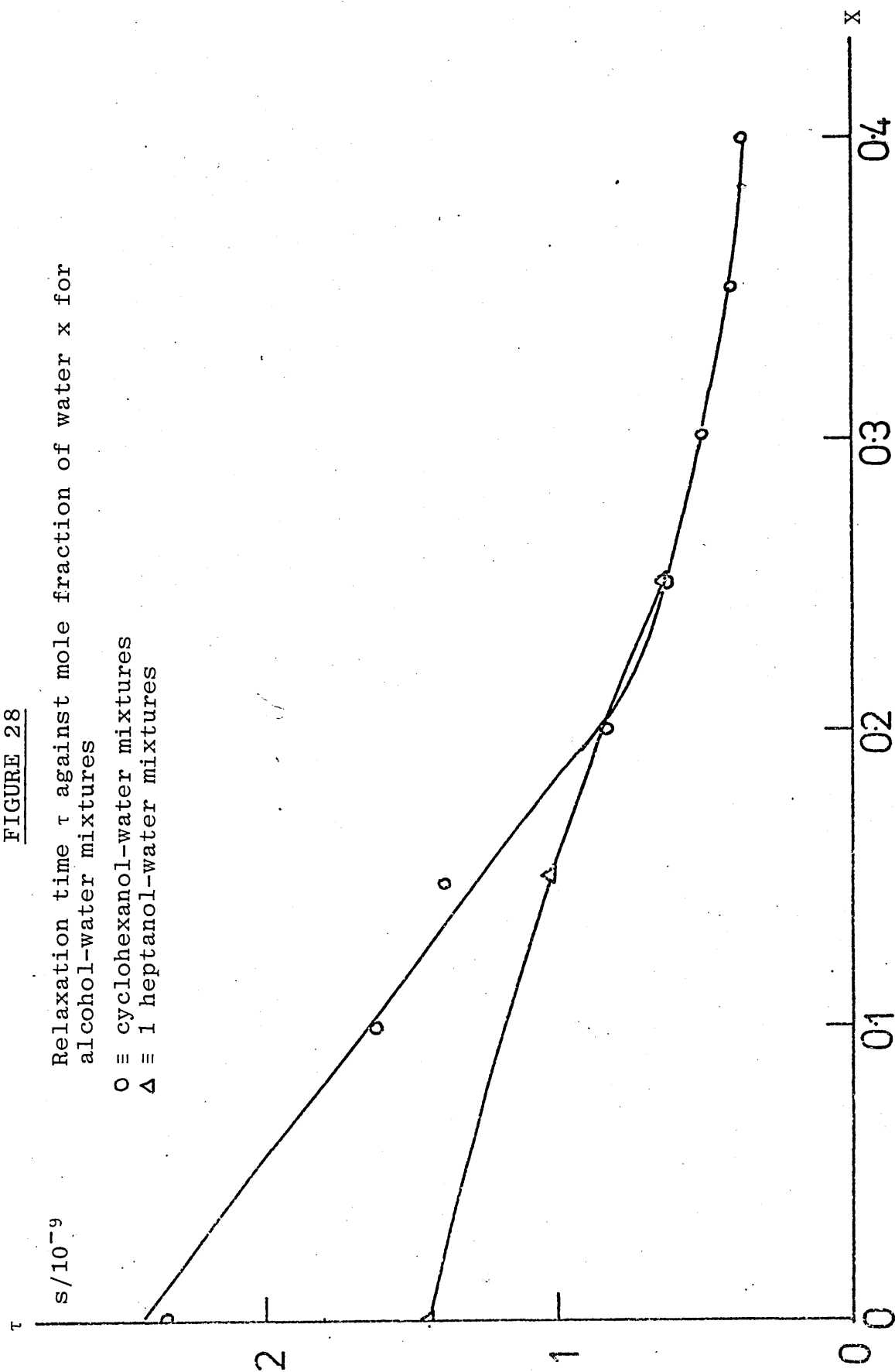
FIGURE 29

Temperature dependence of static permittivity for $C_{12}E_n$ and Brij 30 surfactants

$\times \equiv C_{12}E_4$
$\equiv C_{12}E_6$
$\square \equiv C_{12}E_8$ 30
$\triangledown \equiv$ Brij 30
$\circ \equiv$

Temperature dependence
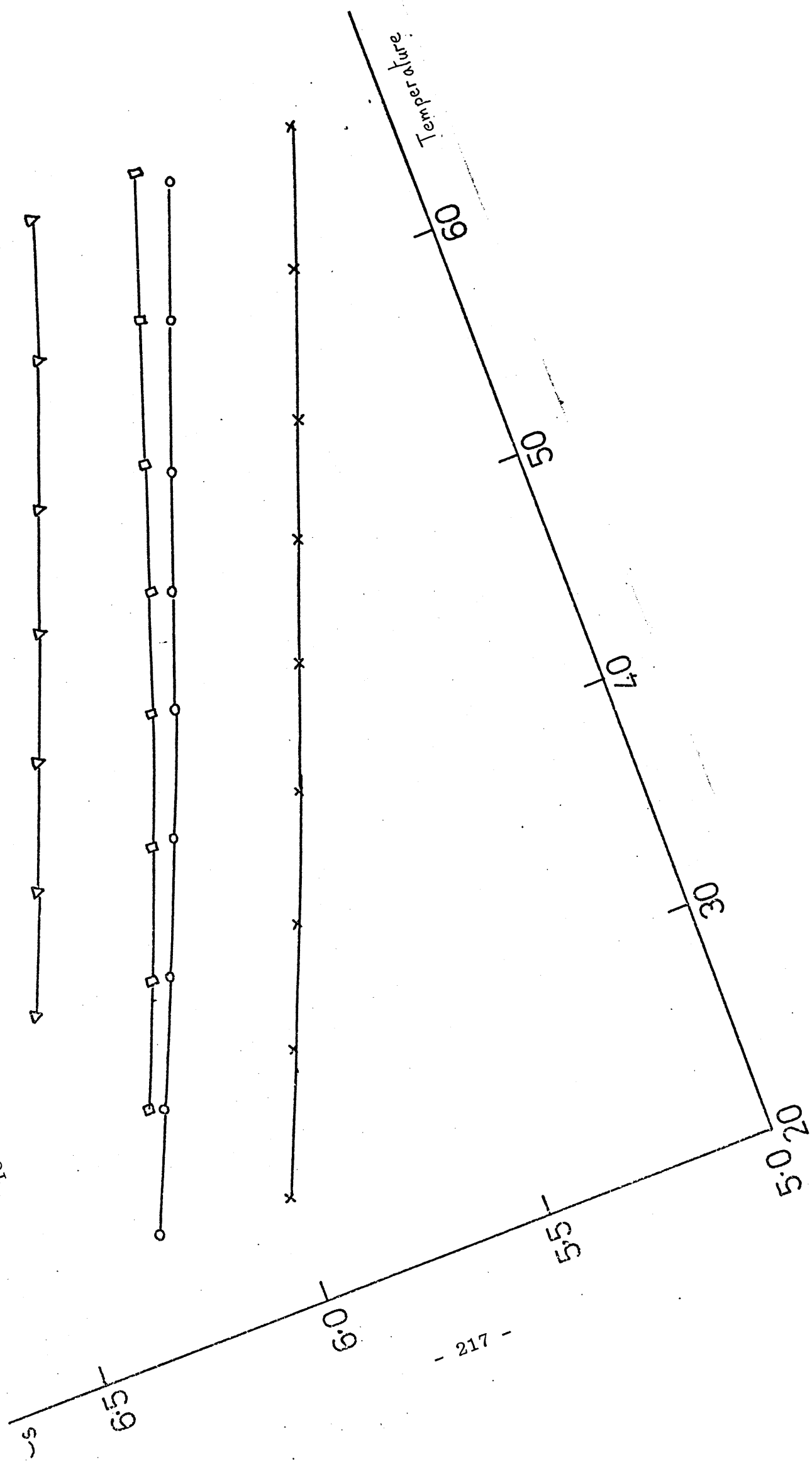
Temperature

FIGURE 30

Direct time domain plots for Brij 30

$O \equiv 44^{\circ} C$
$\triangle \equiv 70^{\circ} C$

$\ln(\epsilon_s - \epsilon)$

0·5

0

-0·5

$\overleftrightarrow{10\cdot2\,ps}$
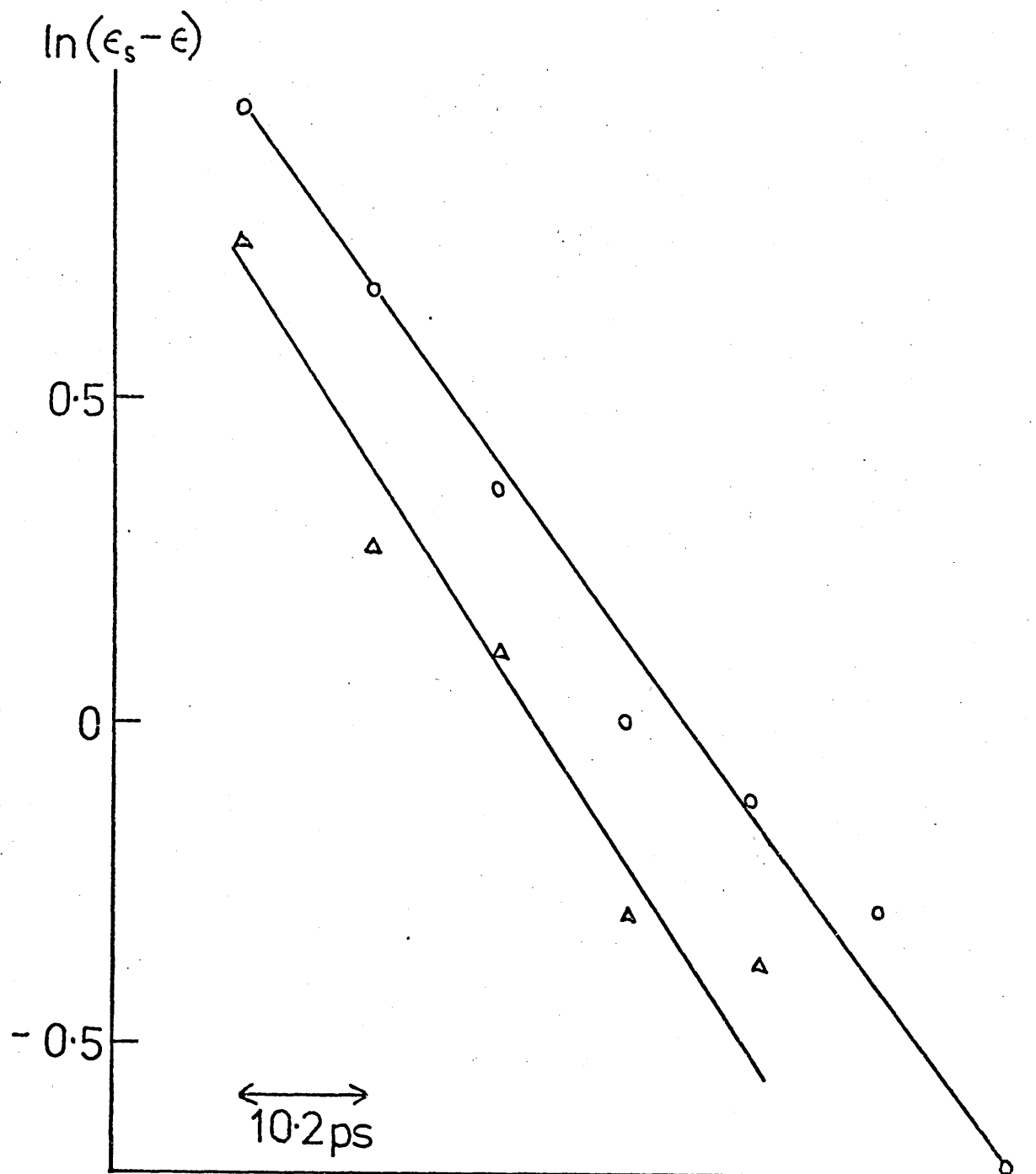
time

The time marker defines the time scale used on the time axis.

FIGURE 31

Temperature dependence of static permittivity
for tetra ethylene glycol

FIGURE 32

Static permittivity of $C_{12}E_4$ mixtures (predicted and measured values)

(The values on any curve do not necessarily refer to the same temperature.)

o ≡ measured values
— ≡ Hanai O/W equation
----- ≡ Rayleigh O/W equation

Mass fraction of $C_{12}E_4$
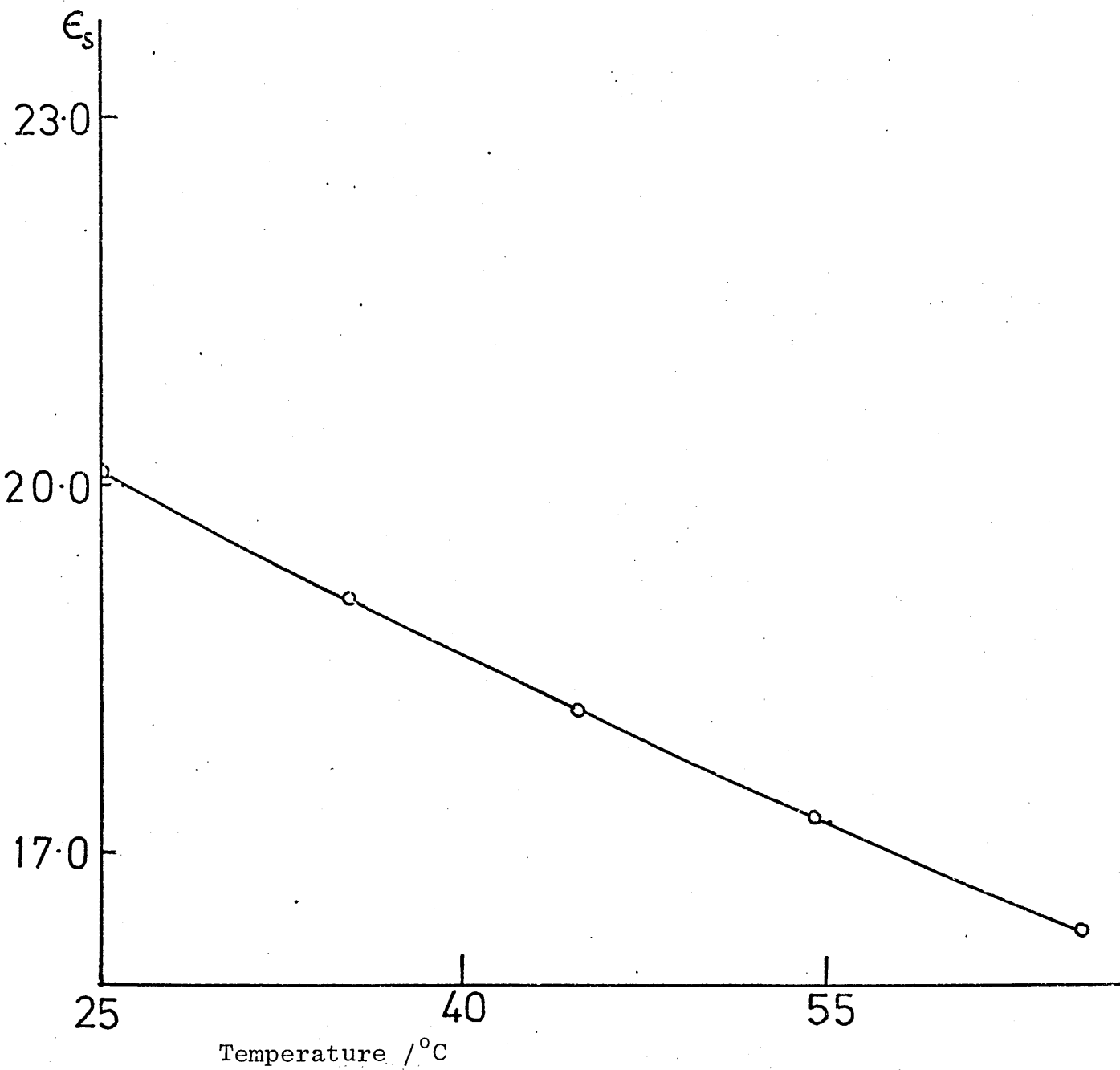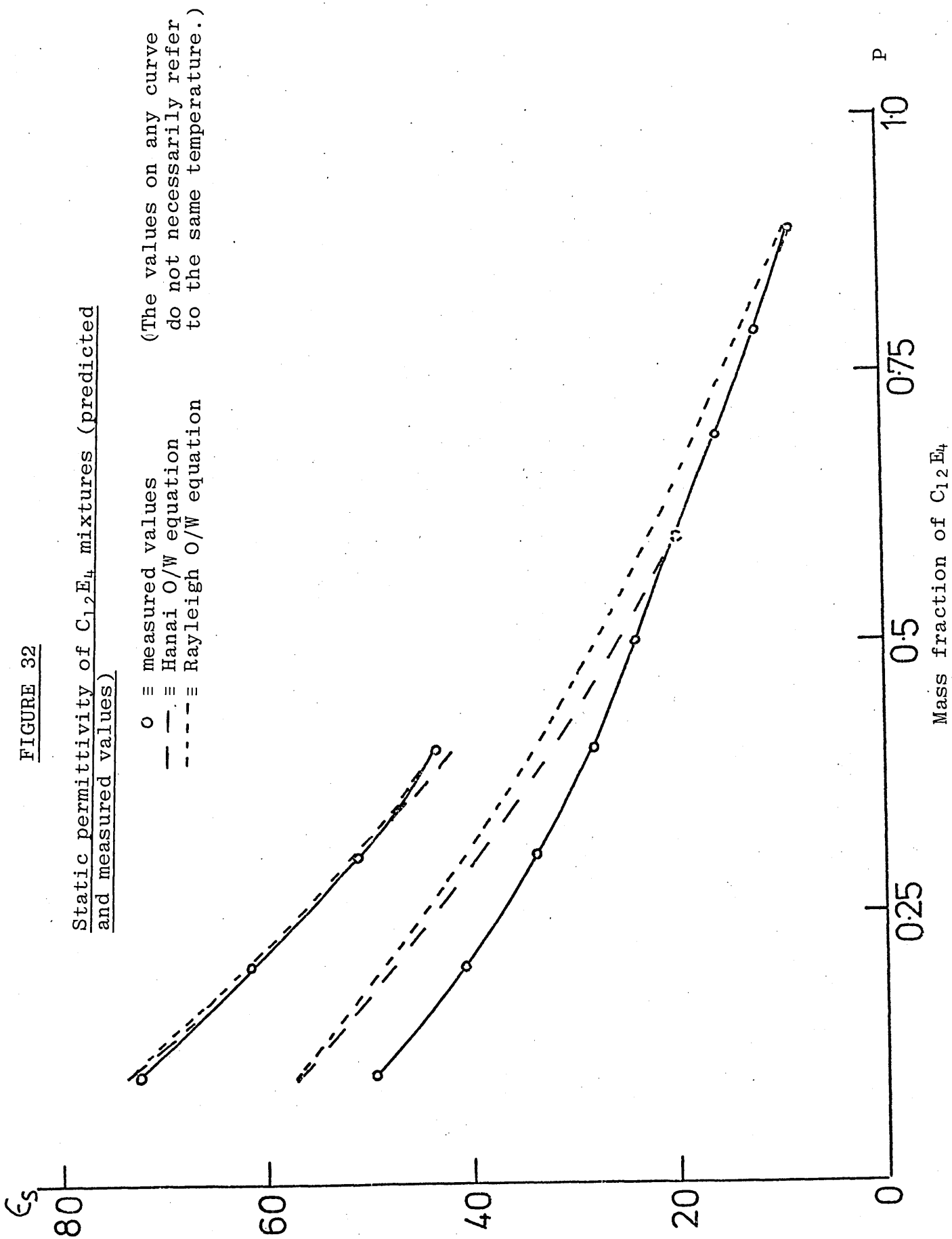
FIGURE 33

Static permittivity of Brij 30-water mixtures
(predicted and measured values)

o ≡ measured values
— ≡ Hanai O/W equation
·—···· ≡ Rayleigh O/W equation
·—·—· ≡ Böttcher equation
— — ≡ Looyenga equation

(The values on any curve
do not necessarily refe
to the same temperature

ϵ_s

Mass fraction of Brij 30
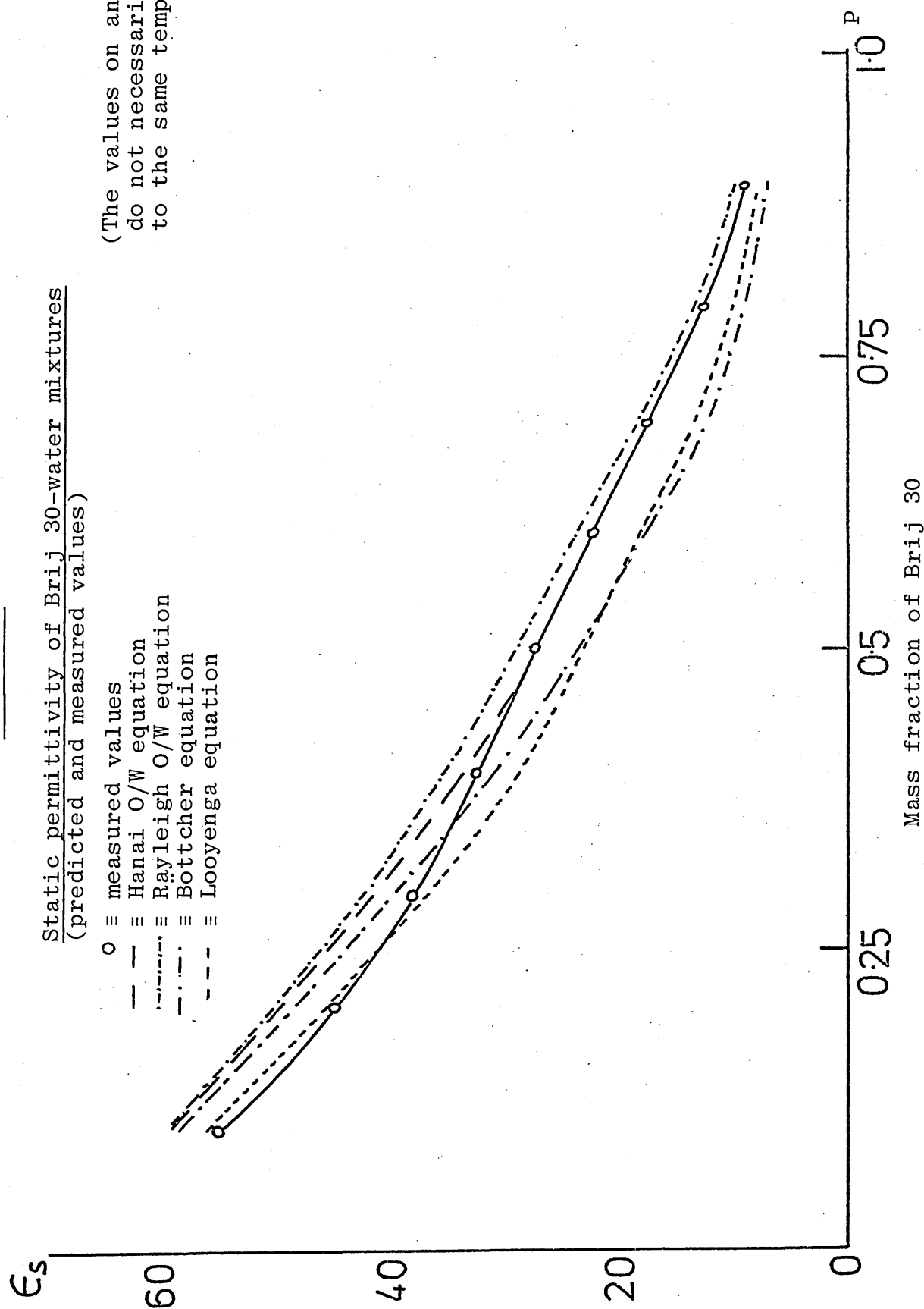
FIGURE 34

Static permittivity of $C_{12}E_6$-water mixtures
(predicted and measured values)

o ≡ measured values
— ≡ Hanai O/W equation
– – ≡ Rayleigh O/W equation

(The values on any curve
do not necessarily refer
to the same temperature.)

Mass fraction of $C_{12}E_6$
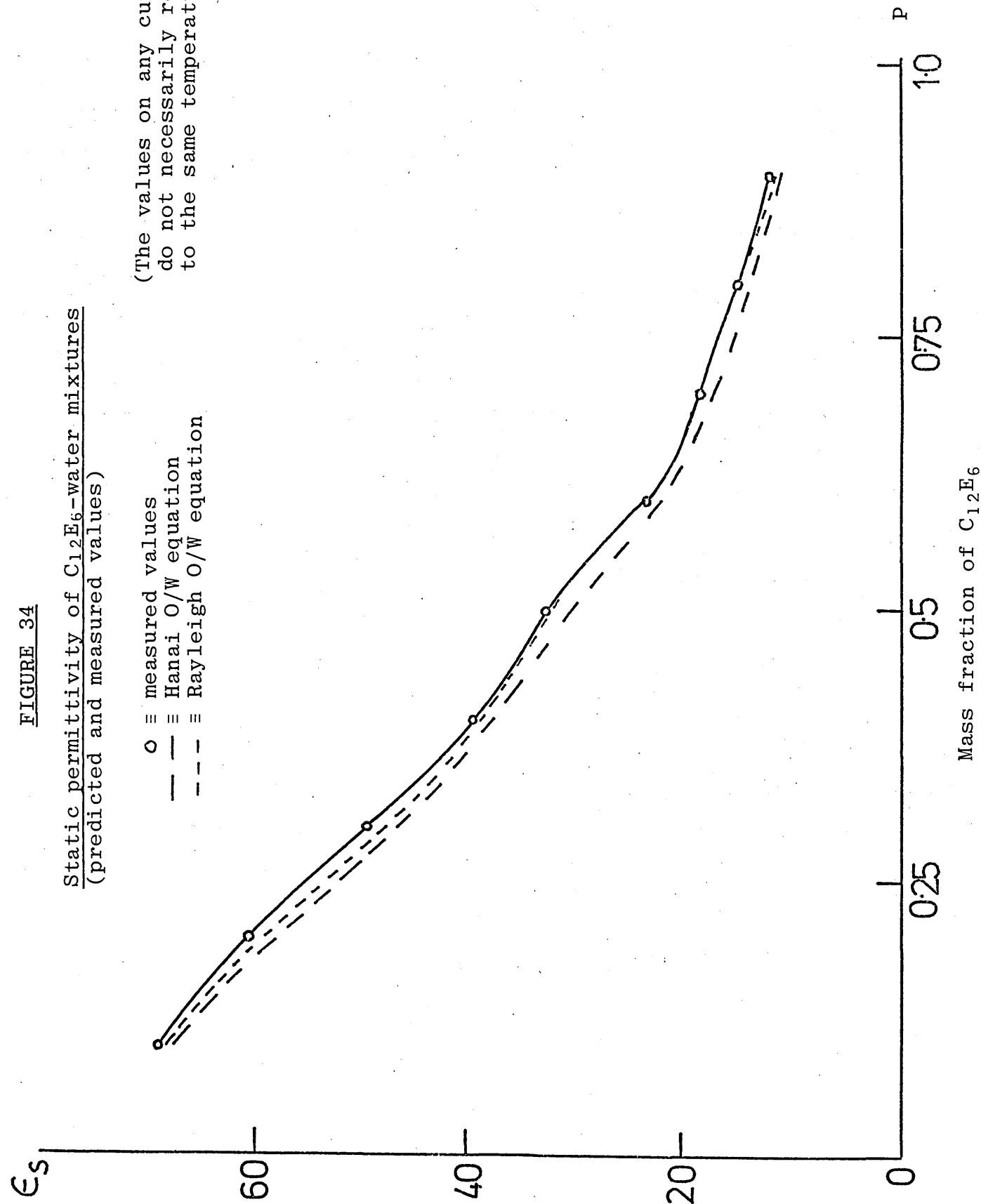
FIGURE 35

Static permittivity of $C_{12}E_8$-water mixtures
(predicted and measured values)

o ≡ Measured values
— ≡ Hanai O/W equation
---- ≡ Rayleigh O/W equation
—·—·— ≡ Ideal mixing equation

Mass fraction of $C_{12}E_8$

ϵ_s
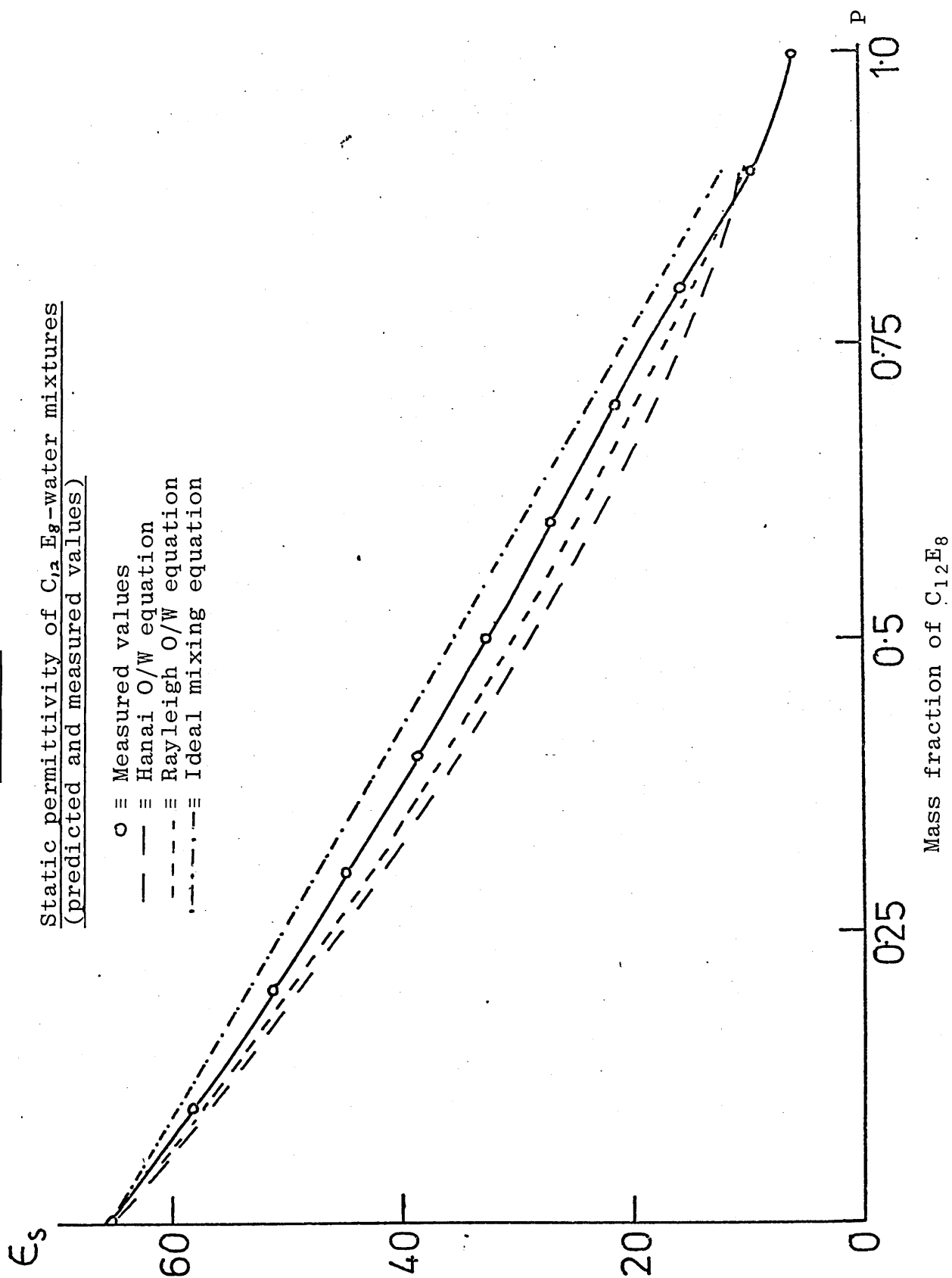
FIGURE 36

Temperature dependence of static permittivity for surfactant-water binary mixtures

(a) Mass fraction of surfactant, p = 0.9

$\triangle \equiv C_{12}E_4$

$\circ \equiv C_{12}E_8$

Temperature /$^\circ$C

(b) Mass fraction of surfactant, p = 0.1

$\circ \equiv C_{12}E_6$

$\triangle \equiv C_{12}E_8$

Temperature /$^\circ$C
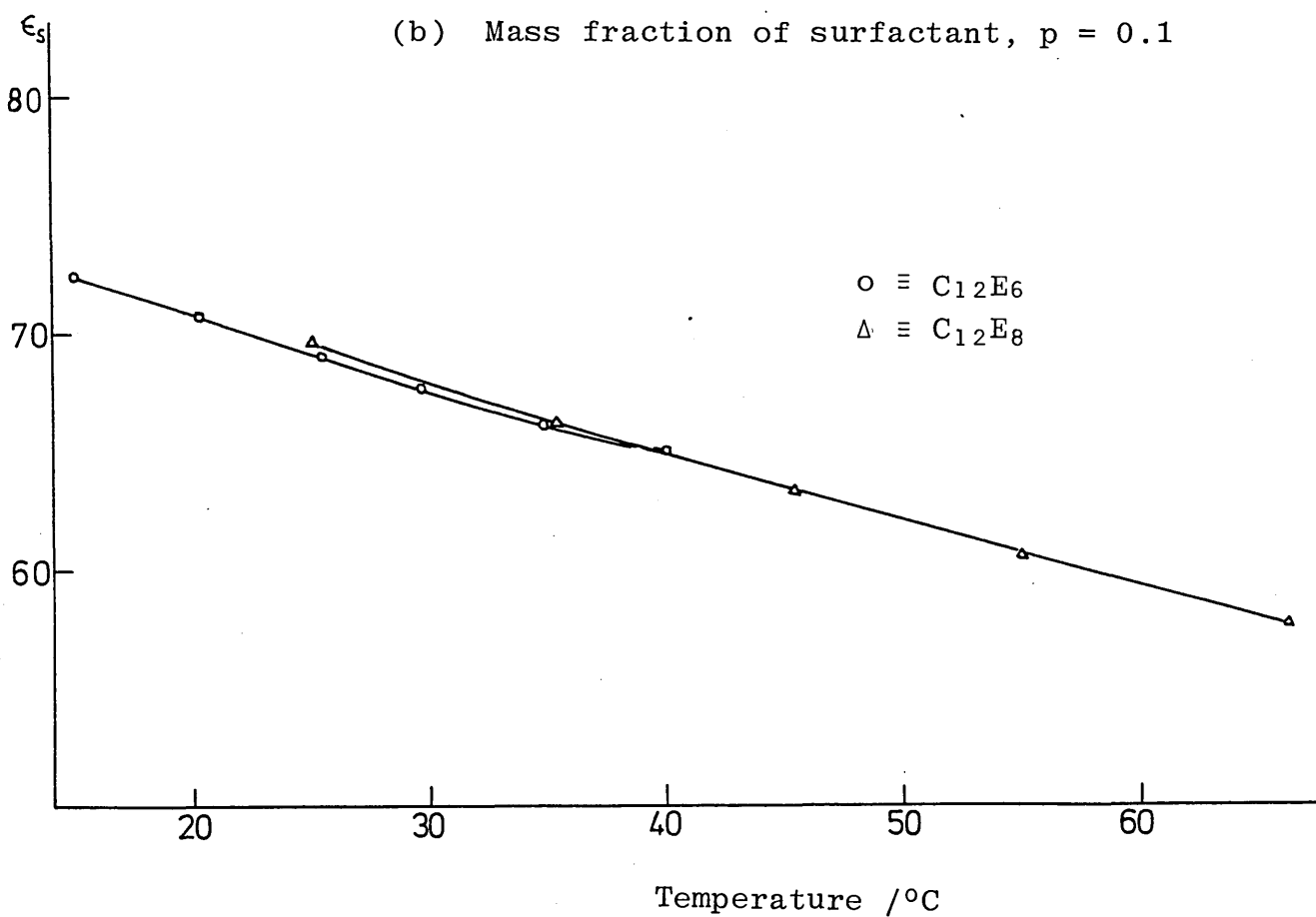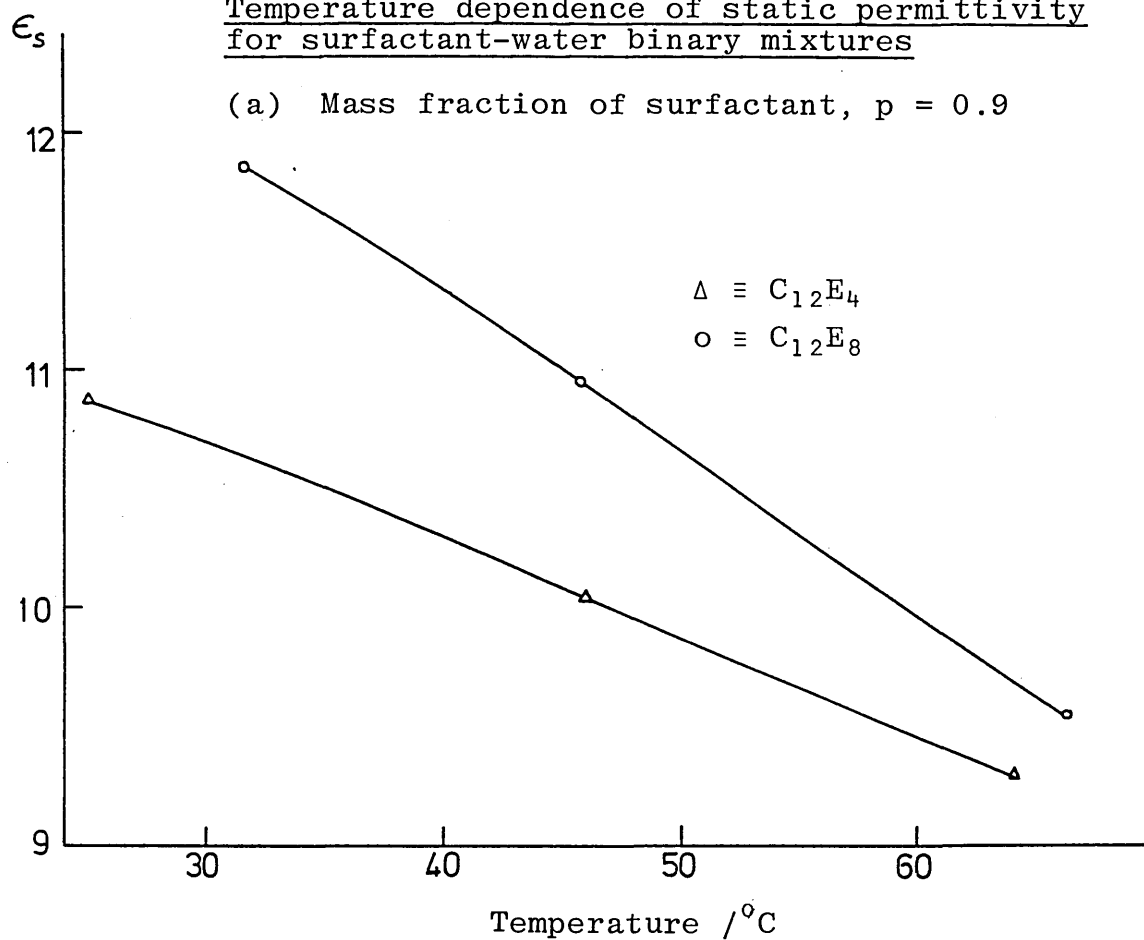
FIGURE 37

Direct time domain plots for Brij 30-water mixtures

(a) Mass fraction of surfactant p = 0.9

(b) Mass fraction of surfactant p = 0.7
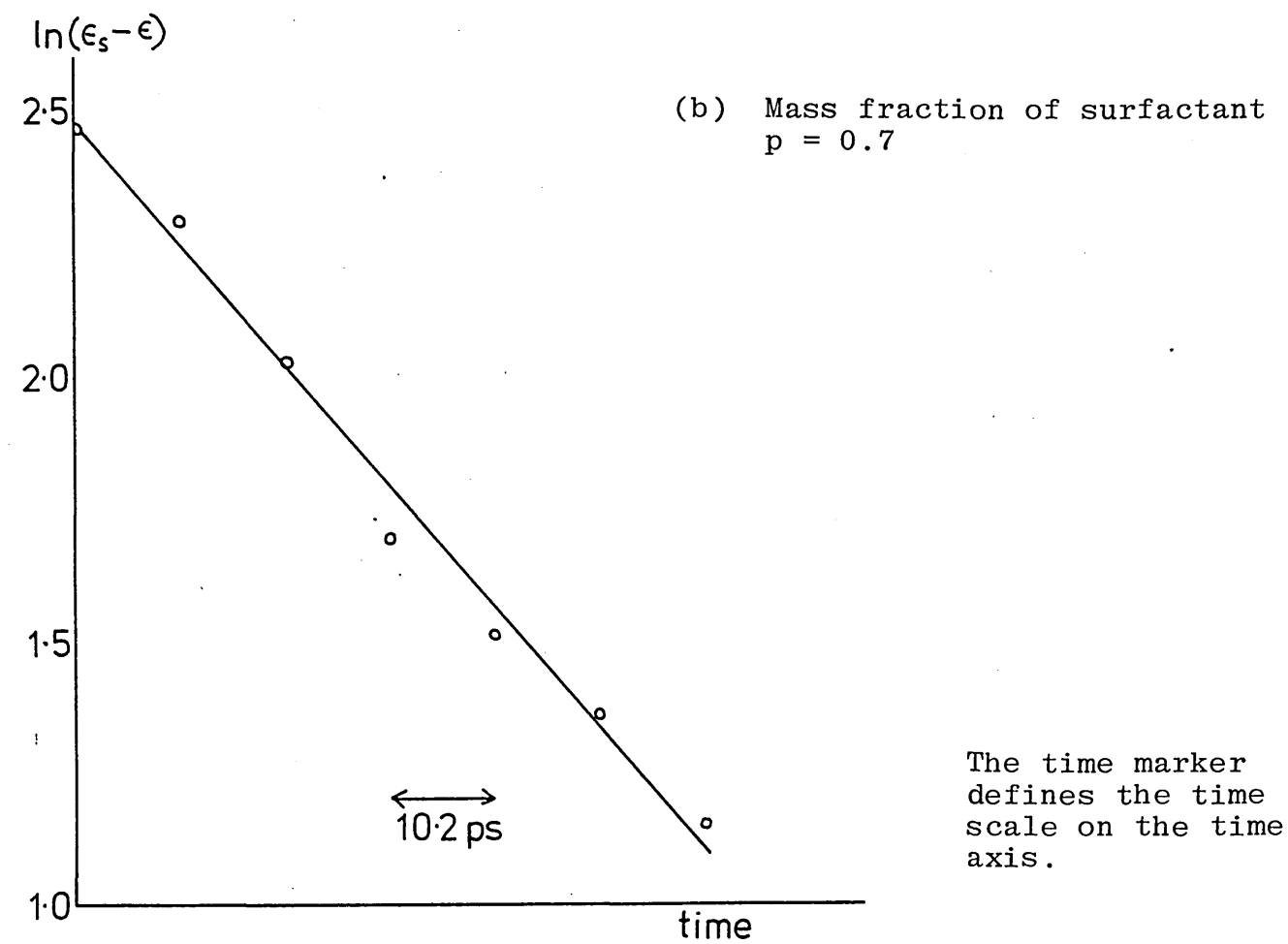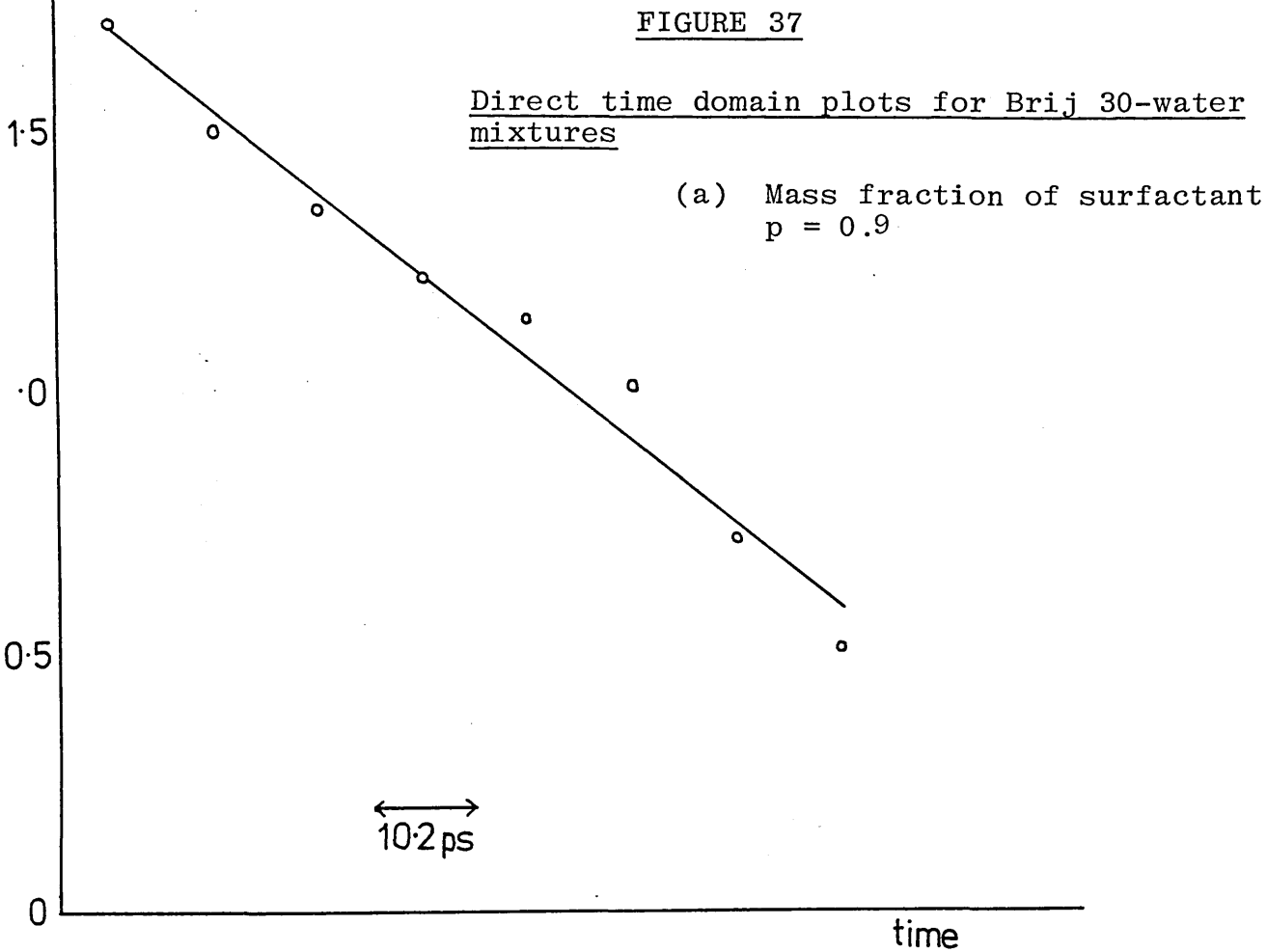
The time marker defines the time scale on the time axis.

FIGURE 38

Static permittivity of tetra ethylene glycol (E_4)-water mixtures

o ≡ Measured values

△ ≡ Ideal mixing equation

Mass fraction of E_4
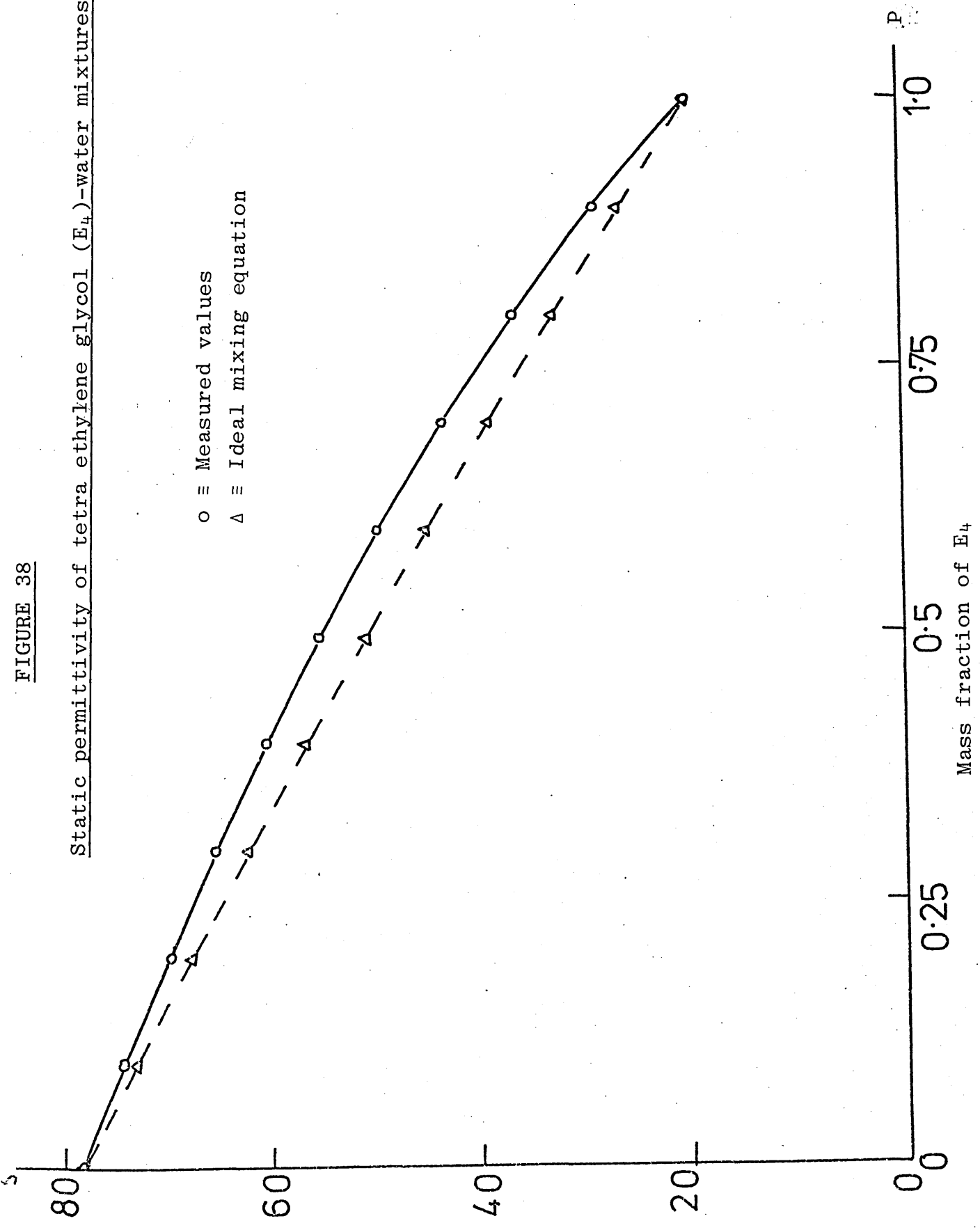
FIGURE 39

Static permittivity of Brij-30 heptane mixtures
(predicted and measured values)

— · — ≡ Rayleigh O/W

— — ≡ Rayleigh W/O

Mass fraction of surfactant
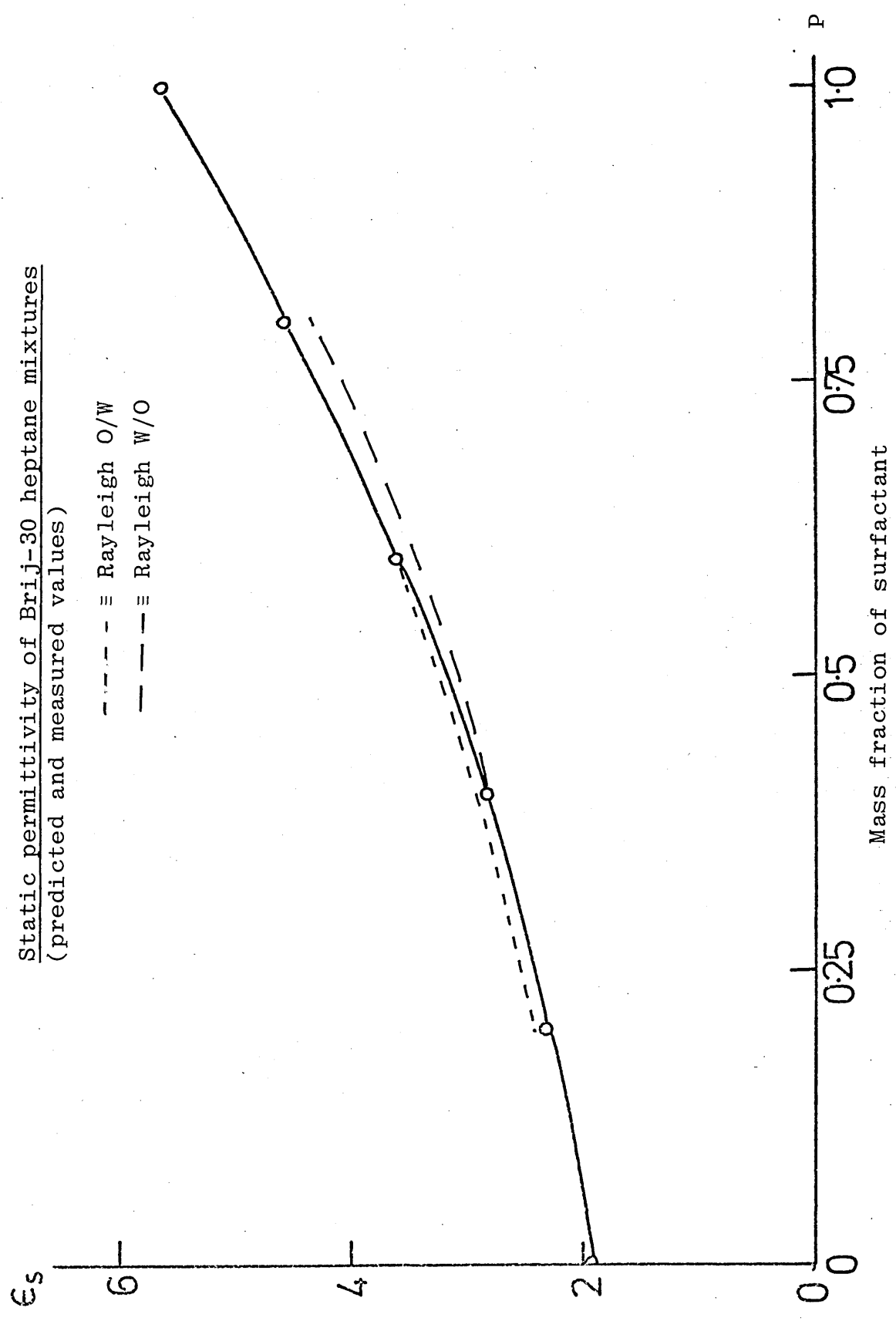
Temperature dependence of the static permittivity of
ternary mixtures containing 10% by mass of water

(a) △ ≡ 60% by mass of heptane
     □ ≡ 70% by mass of heptane

(b) o ≡ 20% by mass of heptane
     x ≡ 40% by mass of heptane
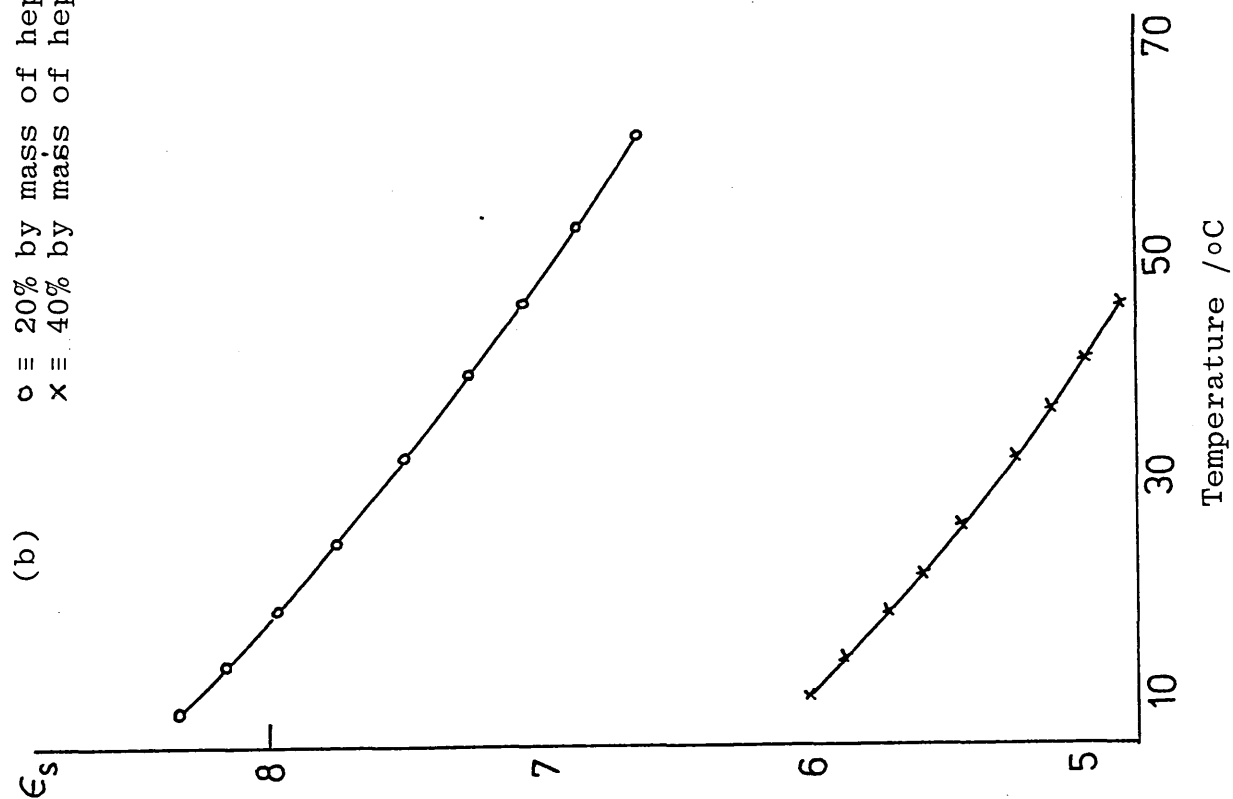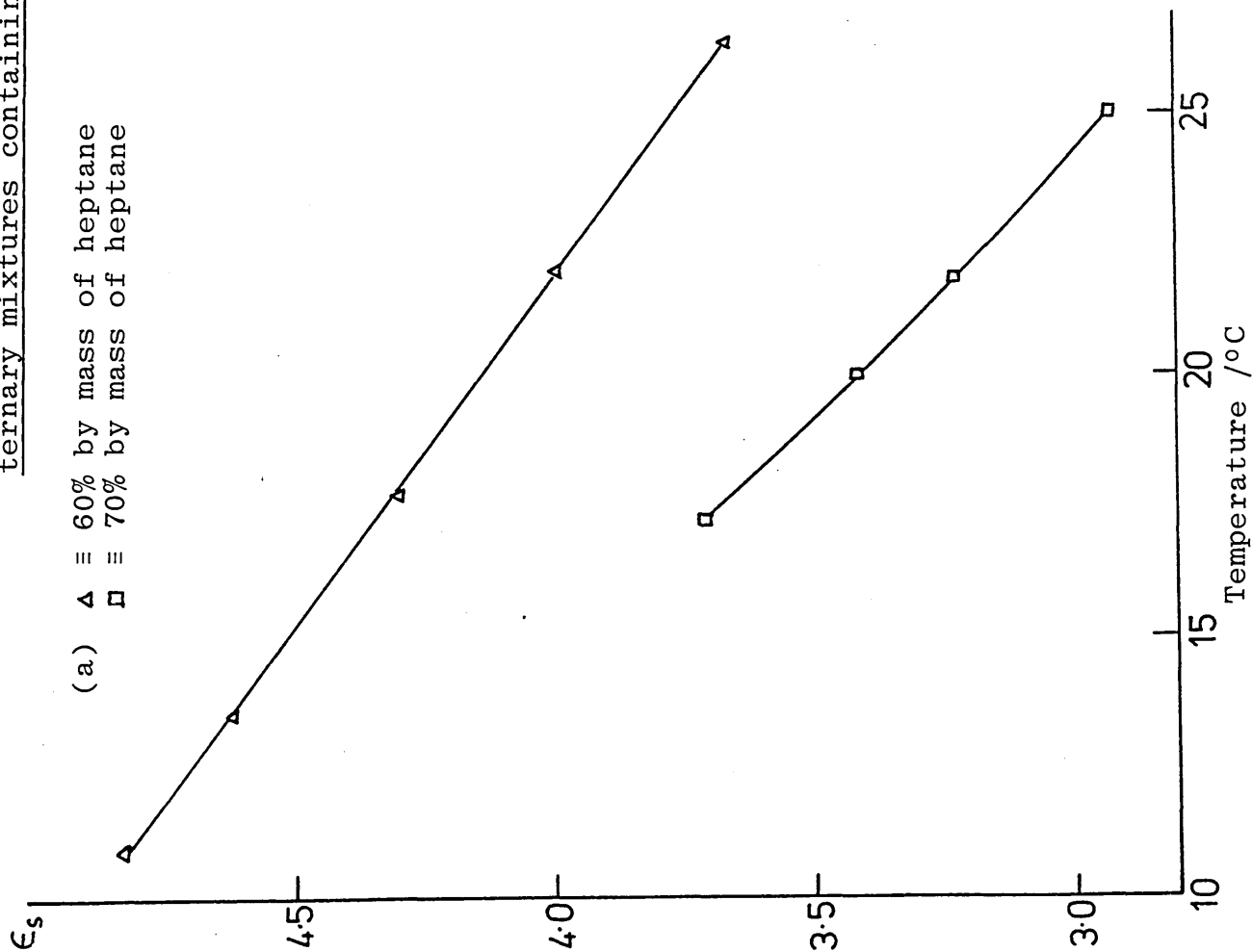
FIGURE 41

Ternary mixture 70% Brij 30, 20% water
and 10% heptane

(a) Cole-Cole plots (Indicated frequencies are in GHz)

  $\circ \equiv 31.7^\circ$ C
  $\triangle \equiv 37.3^\circ$ C
  $\square \equiv 46.0^\circ$ C

(b) Direct time domain plots

  $\circ \equiv 31.7^\circ$ C
  $\triangle \equiv 37.3^\circ$ C
  $\square \equiv 46.0^\circ$ C

The time marke
defines the
time scale on
the time axis

$\overleftrightarrow{10.2\,ps}$
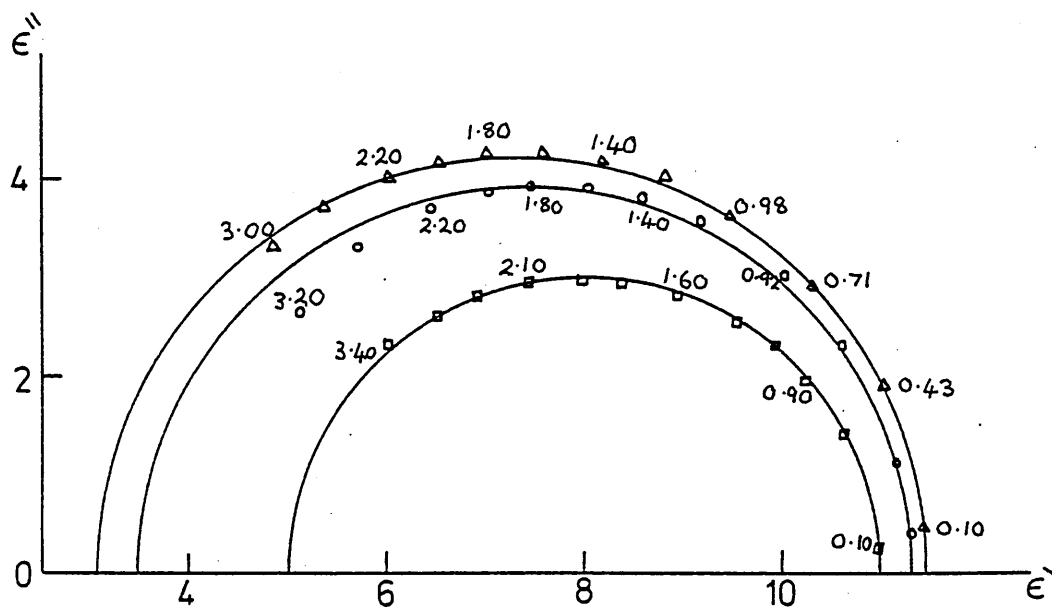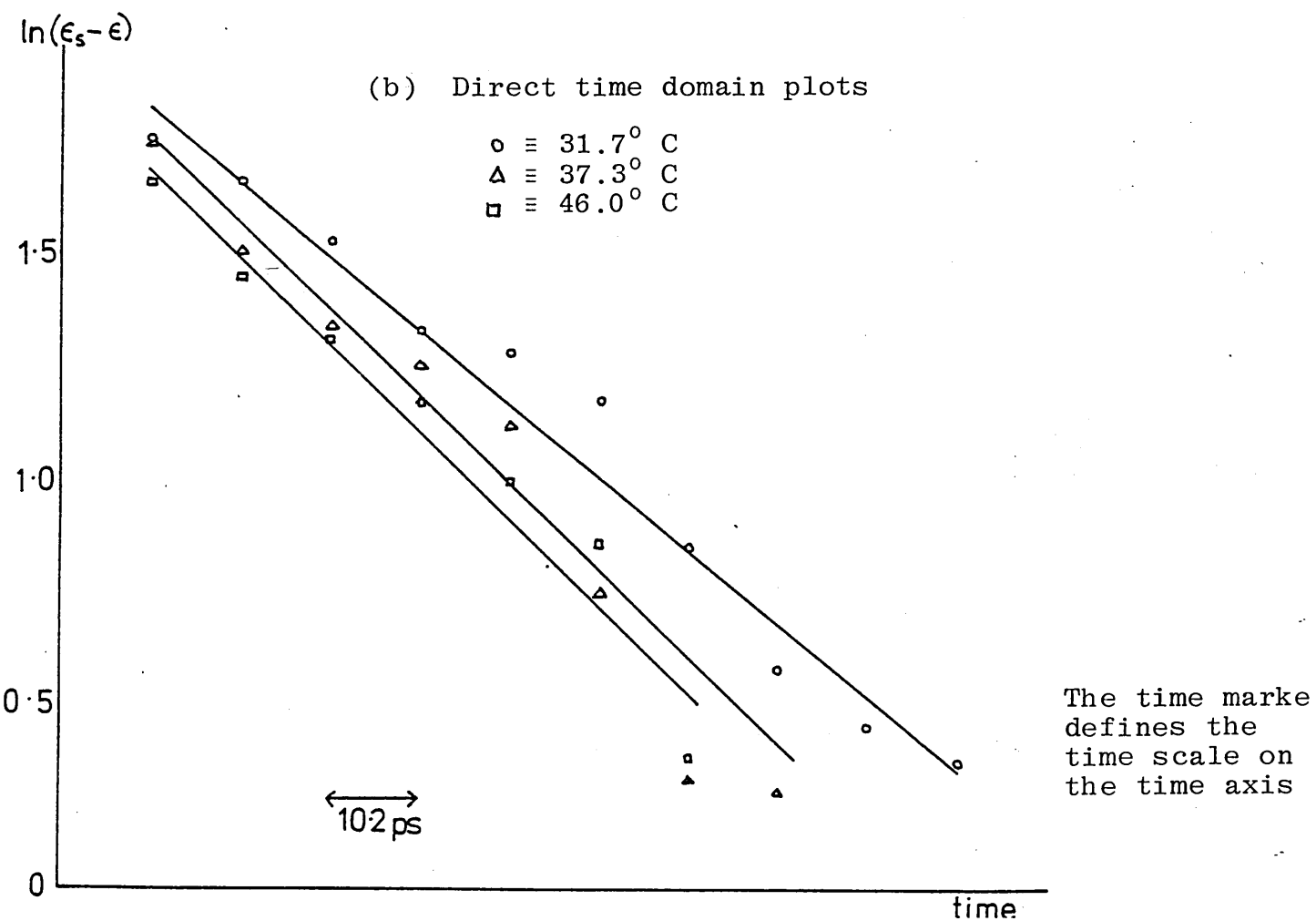
FIGURE 42

Cole-Cole plots for Brij 30 ternary mixtures at temperatures below lower limit for transparency (Indicated frequencies are in MHz)

(a) o ≡ 20% Brij 30, 60% heptane and 20% water at 29.2° C
(b) △ ≡ 20% Brij 30, 40% heptane and 40% water at 19.0° C
(c) □ ≡ 30% Brij 30, 30% heptane and 40% water at 21.0° C
(d) × ≡ 60% Brij 30, 20% heptane and 20% water at 29.5° C
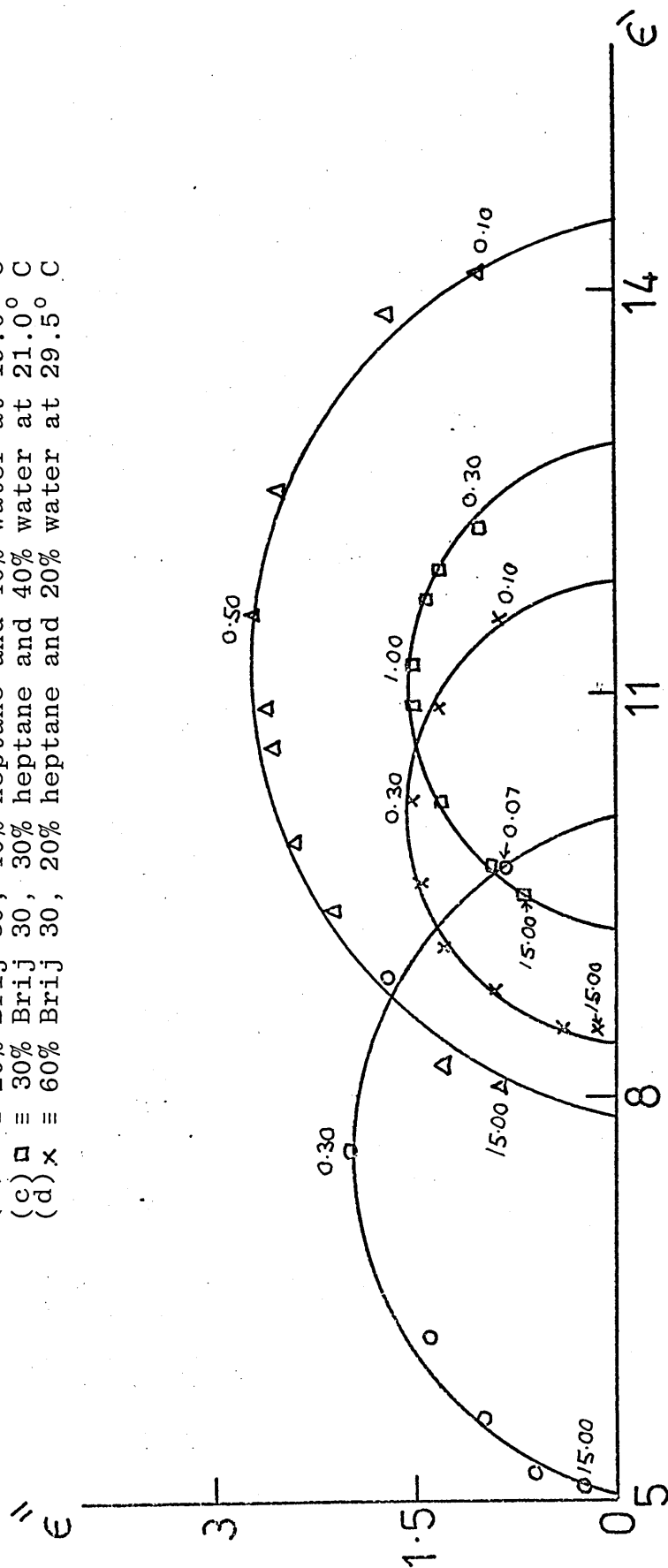
CHAPTER 5 : DISCUSSION

5.1   Alcohol-water mixtures

5.1.1   Summary of Results

The results for t butanol-, cyclohexanol-, 1 butanol- and
1 heptanol-water mixtures reveal that addition of water to
all four alcohols causes a reduction in the relaxation
time, τ, of the principal dispersion and that the
relaxation is Debye-type for all mixtures, as shown in
Figures 10 to 22. These observations follow the trend
revealed in the results of Chekalin and Shakhparonov (65)
for methanol- and 1 propanol-water mixtures, Buck (68)
for ethanol-water mixtures and Tjia (59) for 1, 2, 3 and
4 heptanol-water mixtures; 3 heptanol-water mixtures at
- 70° C being the only exception. They confirm the
present proposal given in Chapter 1 that addition of
water to an alcohol generally causes a reduction of
relaxation time irrespective of the sign of the variation
of static permittivity, ε_{s}, with water content. The
results of Sarojini (67) for 1 butanol-water mixtures,
in which an increase in τ on addition of water was reported,
are therefore considered to be erroneous.

The observation of Debye-type dispersion for all mixtures
is in accord with the comment of Davies (60) that
"compatible pairs of liquids appear to merge molecularly
giving a single relaxation time". It should be noted
that the only reported exception to Debye-type dispersion
in alcohol-water mixtures is the data of Peyrelasse (66)

for methanol-water mixtures for which Cole-Cole arc behaviour was suggested with parameter α increasing from 0.046 at 44% by mass of alcohol to an approximately constant value of 0.08 at and above 60% by mass of alcohol. However, this interpretation of Peyrelasse is based on Cole-Cole plots containing a similarly small number of four or five data points to those of Chekalin and Shakhparonov for methanol-water mixtures (65) and both sets of results lie on the Cole-Cole arc plot drawn by Peyrelasse for this mixture. Since the latter authors favoured an interpretation based on two Debye-type relaxations rather than a distribution of relaxation times, it is considered that for all alcohol-water mixtures studied, there is not yet sufficient justification for considering the principal dispersion to be other than Debye-type.

5.1.2 Interpretation of the relaxation time variation

When small quantities of water are added to an alcohol, the specific structure of water can be regarded as entirely lost and the presumed chain-like structure of the pure alcohol will be modified. Although a chain-like structure involving mixed water-alcohol molecules has been suggested by Chekalin and Shakhparonov (64, 65) for methanol-water mixtures, this model is not favoured since such a structure involves an alcohol oxygen atom being H-bonded to two other molecules, which is not supported by any other data.

In this work, a mechanism based on alcohol chain
breakage by water molecules is considered more appropriate
and addition of water to a pure alcohol with its presumed
chains of indefinite length is assumed to cause a
progressive reduction in average chain length.

The fall of relaxation time with increasing water content
can be explained using the 'switch' model of Campbell et
al (34) which was based on the proposals of Sagal (35). In
this model dielectric relaxation is attributed to H-bond
rupture and dipole orientation, which occurs when a
hydroxyl group approaches the associated alcohol chain
with its oxygen atom favourably oriented for a switch
(Fig 2, p 12). The oxygen may be present in a monomer
or at the end of another alcohol chain. With this model,
the increase in relaxation time of the principal dispersion
in pure alcohols as the length of the hydrocarbon chain is
increased occurs because the total concentration of
hydroxyl groups decreases with increasing hydrocarbon
chain length, thus decreasing the probability that an
oxygen atom will be favourably oriented for a switch.

When water is added to an alcohol, as the alcohol chains
are shortened, there will be more chain ends and thus
more oxygen atoms available for a switch. In addition,
the presence of water molecules causes an increased
density of hydroxyl groups which will further enhance
the probability of an oxygen atom being favourably

oriented for a switch. This combination of increased chain ends and increased density of hydroxyl groups would be expected to lead to a progressive reduction in relaxation time when water is added to an alcohol.

Although it has been suggested that steric factors limit the association in t butanol to small size complexes (69), in contrast with the chain-association model proposed for cyclohexanol (17), the relaxation data for these two alcohols does not support this proposal. The variation of τ with water content for both cyclohexanol and t butanol is similar except for the substantially higher τ value of cyclohexanol, which on the basis of the Sagal model, will be due to the lower concentration of hydroxyl groups in this alcohol. Both of these alcohols also have similar values for both ε_s and the Kirkwood g factor for which g values of 2.12 for t butanol (18) and 2.50 for cyclohexanol (17) have been reported. When account is taken of the uncertainty in the value of ε_∞ and thus of g for both of these alcohols, the correct g-values for these two alcohols could be very similar. Since chain association has been proposed for the pure alcohol cyclohexanol, it is suggested that a similar mode of association occurs in t butanol.

5.1.3 <u>Comparison with other data</u>

The rather limited literature data on the relaxation times of alcohol-water mixtures reveal an almost linear variation of τ with mole fraction of water, x, in

FIGURE 43A

Relaxation time τ, against mole fraction of water, x, for methanol and 1 propanol-water mixtures

Δ ≡ methanol-water mixtures
o ≡ 1 propanol-water mixtures

$\tau/10^{-12}$ s
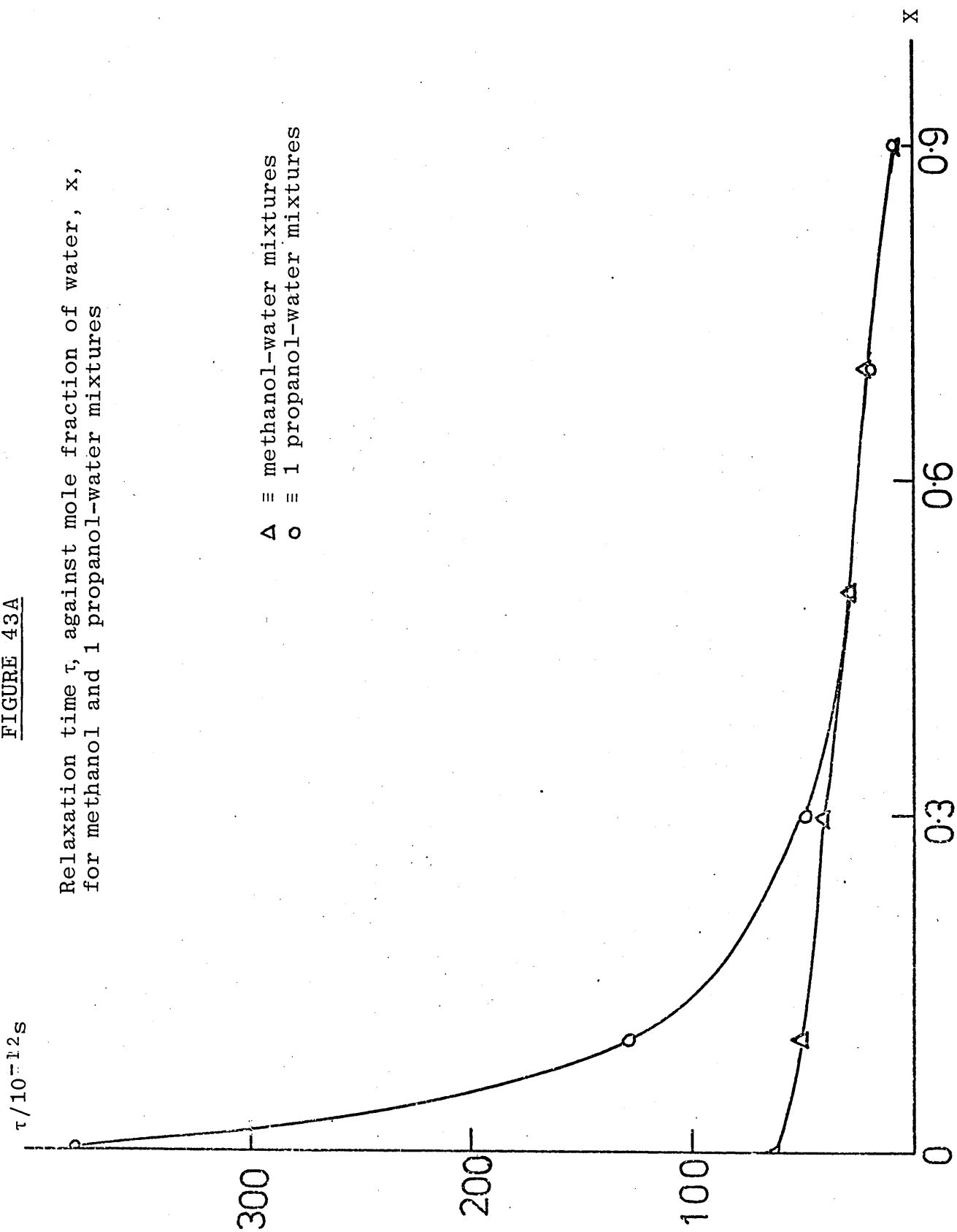
methanol-water mixtures at 20° C (65). In contrast,

1 propanol-water mixtures at 20° C show a rapid fall in

τ with x up to about 0.3 mf above which $d\tau/dx$ is much

lower (65, 171). The graphs of τ against x for methanol-

and 1 propanol-water mixtures given in Figure 43A reveal

that, although the dependence of τ on x in 1 propanol-

water mixtures is significantly different from that in

methanol-water mixtures, there is no evidence of

deviation from a single function relationship. The data of Tjia (59)

on 1 heptanol-water mixtures at up to 0.115 mf of water

at $- 10^\circ$ C reveal a very small change in τ for x between

zero and 0.05 mf above which $d\tau/dx$ is rather higher up to

the highest water content studied. There is no evidence

of deviation from a single function relationship in Tjia's 1 heptanol-

water data.

The graphs of relaxation time τ against mole fraction of

water x for the alcohol-water mixtures studied in this

work (Figures 27 and 28) reveal that the relaxation

behaviour of cyclohexanol-water mixtures may be described

by two separate functions which meet at about 0.20 mf of

water. It is also possible that there is similar

behaviour in the t butanol-water mixtures at about 0.15 mf

of water.

5.1.4 Evidence for associated species

It is worthy of note that aqueous mixtures of both

t butanol and cyclohexanol exhibit a minimum in the

static permittivity, ε_s, which at the measurement

FIGURE 43B

The 4A/W Species
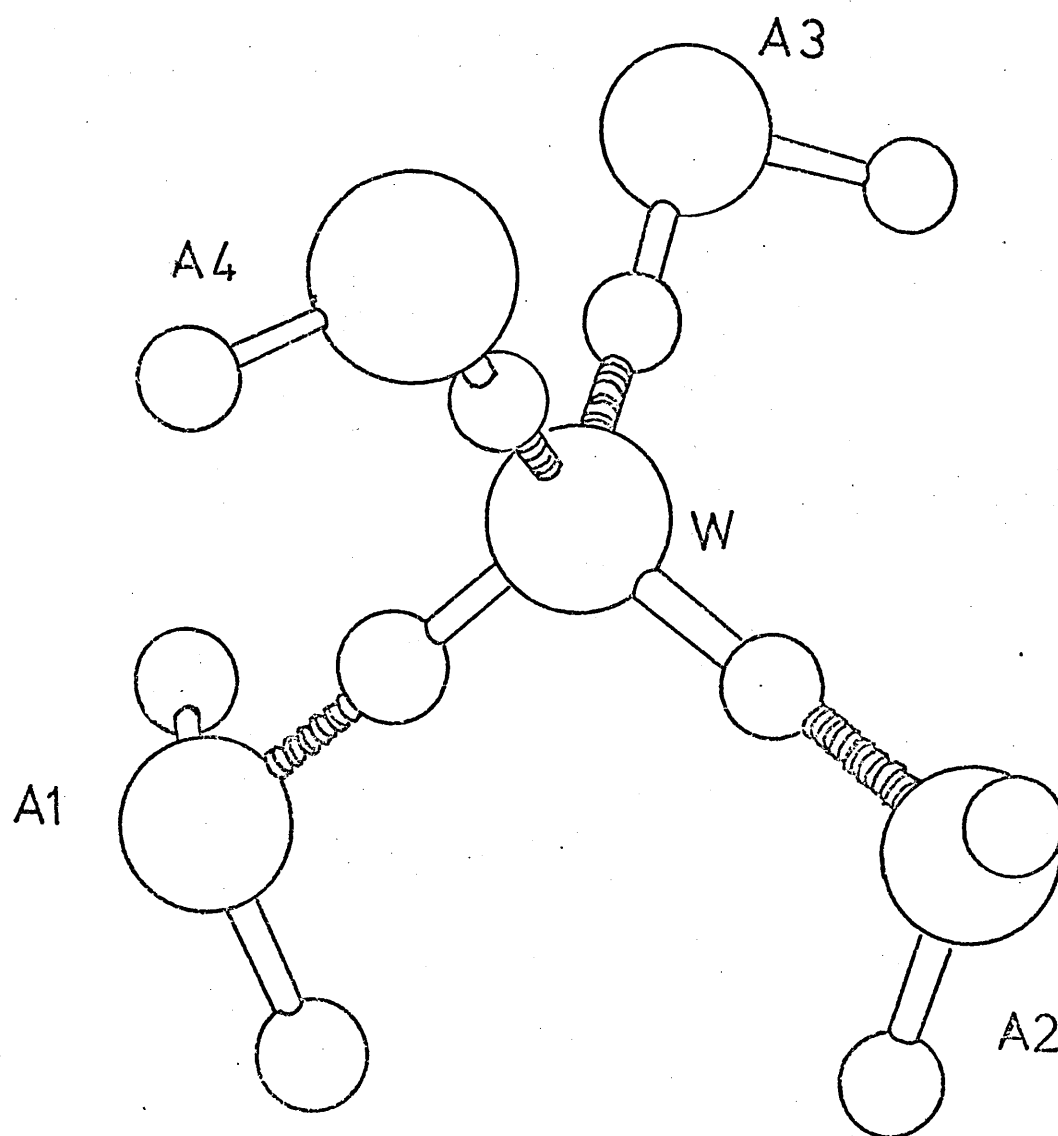
temperature of 25° C used in these relaxation studies, is at 0.14 mf of water for t butanol (7) and 0.20 mf for cyclohexanol (8). It is thus evident that the possible change in relaxation behaviour for both t butanol- and cyclohexanol-water mixtures occurs at a similar composition to that at which ε_S is a minimum.

The occurrence of a minimum in ε_S in both t butanol- and cyclohexanol-water mixtures has been attributed to the formation of an associated species in which four alcohol molecules are H-bonded to one water molecule (7,8), and additional support for this 4A/W species interpretation has been obtained from nmr and viscosity data (8). In view of the correlation between the possible change in relaxation behaviour and the ε_S minimum, it is suggested that the relaxation behaviour could similarly be due to the formation of a 4A/W species.

5.1.5 Effect of associated species on relaxation time

The $d\tau/dx$ value in alcohol-water mixtures should be affected if specific associated species are formed. Since the 4A/W model of Brown and Ives (7) for the t butanol-water system was also favoured by Lawrence et al (8) for the cyclohexanol-water system, an effect on the relaxation behaviour by this species would be expected here. The model favoured by these authors is given in Figure 43B.

In this associated species, there will be more shielding of the two alcohol hydrogen atoms which are H-bonded to theoxygen atom of the water molecule (A_3 and A_4) than for the other two H-bonded alcohol atoms. This shielding effect would be expected to reduce the likelihood of a switch and thus for alcohols in which such an associated species is present, a change in the variation of relaxation with water content would be expected in that $d\tau/dx$ will be lower at mole fractions of water above that required for formation of the 4A/W complex. The observed lower value of $d\tau/dx$ at values above that corresponding to the minimum in ε_s is thus consistent with such a 4A/W model proposed for both t butanol- and cyclohexanol-water mixtures. It should be added that since a variety of species are likely to be formed on addition of water to an alcohol, it is not surprising that the $d\tau/dx$ change is not well defined.

The more limited relaxation data for the 1 butanol- and 1 heptanol-water mixtures studied in this work show a monotonous fall in relaxation time on addition of water and thus the presence of specific complexes such as the 4A/W associated species is not revealed, although there is possibly slight evidence for complex formation in the 0.35 mf 1 butanol mixture. Specific association complexes in 1 butanol-water mixtures have not been proposed but the presence of a 4A/W complex in 1 heptanol-water mixtures was proposed by Lawrence et al (8), even

though at temperatures below 35° C a continuing decrease in ε_s was observed at mole fractions of water higher than 0.2 mf. This effect was attributed to reduction of the average dipole moment of the species by additional H-bonding of the peripheral alcohol molecules of the 4A/W complex causing the water to effectively cross-link alcohol molecule chains. With this model, even more shielding than that exhibited by the single 4A/W complex would be expected causing a further reduction in the likelihood of a switch and thus giving a possibly almost constant value of $d\tau/dx$ at compositions above 0.2 mf of water. Since such behaviour is not exhibited in the results in this work, these proposals of Lawrence et al concerning 4A/W complex formation in 1 heptanol must be considered to be open to doubt. However, it is difficult to be unequivocal in describing complex formation in alcohols because in addition to linear species, it is agreed that cyclic species are also present in pure alcohols (2). It should be added that for 1 heptanol in particular, Bordewijk et al (3) considered effects due to cyclic species to be important. If indeed in addition to linear species, cyclic species are also present in the pure alcohol 1 heptanol it is not surprising that rather different relaxation behaviour is observed.

Since the longer alkyl chain n alcohols generally exhibit a fall in permittivity on addition of water, the association between the water and alcohol molecules in

these alcohols could be related to the formation of a low dipole moment species rather than to the high dipole moment 4A/W type proposed by Brown and Ives (7) and Lawrence et al (8). Tjia (59) suggested that in describing the behaviour of alcohol-water mixtures allowance should be made for the existence of at least two kinds of complexes where one has a relatively high dipole moment and the other a relatively low dipole moment. If the association between 1 heptanol and water does involve more than one type of associated species, then on the basis of the 'switch' model, there is likely to be a contribution to the dielectric relaxation due to shielding arising from the structure of the various species. Since there is no information available on the structure of any other species in 1 heptanol-water mixtures, it is impossible to assess the effect of such species on the relaxation behaviour. However, if there are contributions by other species, then the 4A/W contribution to the relaxation might well be masked by these other species and thus the apparent discrepancy between the relaxation data in this work and the results of Lawrence et al (8) could be resolved.

The results of Tjia for 3 heptanol-water mixtures at -70° C in which τ remained constant for mole fractions of water between 0.020 and 0.086 also exhibit a minimum in ε_s at about 0.04 mf of water. It is tempting to

suggest that the relaxation time variation with water content, $d\tau/dx$, is linked with the occurrence of an ϵ_s minimum. In this case, it is hardly likely to be due to the formation of a 4A/W associated species, but it is possible that a complex involving association of water with a rather larger number of alcohol molecules has been formed and since the behaviour of $d\tau/dx$ and ϵ_s resembles that of the t butanol- and cyclohexanol-water mixtures studied in this work, it is suggested that these low temperature results of Tjia are more likely to be due to the formation of an associated species than to inhomogeneity in the liquid as Tjia proposed. If this behaviour is due to the formation of an associated species, it further reinforces proposals that alcohol-water mixtures can contain a number of associated species of different types.

Although, as already noted, it is considered that the variation of τ with mole fraction of water x in 1 propanol-water mixtures at 20° C does not exhibit any deviation from a single function, there is some similarity in the $d\tau/dx$ variation with the data in this work for t butanol- and cyclohexanol-water mixtures. It might therefore be considered possible that there is evidence for the 4A/W species in 1 propanol-water mixtures. However, since there is no minimum in ϵ_s in these mixtures at 20° C, it must be presumed that either there is no 4A/W associated species present or that there are

a number of different species occurring which effectively mask the contribution by the 4A/W type.

Since 1 propanol has a short alkyl chain, a greater number of associated species in aqueous mixtures can be expected. Assuming the pure alcohol contains chains of indefinite length, addition of water is considered to cause chain breakage and thus, whether or not a 4A/W species is formed, an initial rapid fall of τ with increasing water content is expected. If it is supposed that a 4A/W species is formed, then because the alcohol is miscible with water, it must also be presumed that further addition of water above that required for the 4A/W species leads to the formation of small sized species such as 3A/W and 2A/W types. A possible 3A/W species is one which is similar to the 4A/W already discussed but without one of the peripheral alcohol molecules (A_1 or A_2 in Fig 43B). A 2A/W species would then be one in which both peripheral alcohol molecules are absent. Comparing this 2A/W species with the 4A/W type and noting that, in a given volume, a mixture containing only the 4A/W type (0.2 mf of water) will contain a smaller number of such species than one which contains only the 2A/W type (0.33 mf of water), it can be argued that the number of oxygen atoms favourably oriented for a switch is significantly higher in the 2A/W mixture. It would thus be expected that the 0.33 mf mixture will have a significantly lower

relaxation time than the 0.2 mf one which is not in agreement with the experimental data which shows a relatively small change in τ over this concentration range. It is thus concluded that the presence of specific species such as the 4A/W type in 1 propanol-water mixtures is difficult to maintain even if $d\tau/dx$ is not describable by a single function.

5.1.6 Conclusions on alcohol-water mixtures

It is concluded that if the variation of relaxation time with water content for both t butanol- and cyclohexanol-water mixtures is describable by two separate functions and that, in addition, the data for 1 propanol-water mixtures is describable by a single function, then there is evidence that the relaxation behaviour is modified by the formation of the 4A/W complex proposed by other workers for the t butanol- and cyclohexanol-water systems. This is because the change in behaviour of $d\tau/dx$ occurs at a similar composition to that at which the ε_s minimum occurs. The results for 1 butanol- and 1 heptanol-water mixtures do not reveal the presence of the 4A/W aggregate.

The fall of relaxation time when water is added to an alcohol is considered to be satisfactorily accounted for by a switch model based on the proposals of Sagal (35).

5.1.7 Further work

In order to gain more information on the contribution or otherwise of the proposed 4A/W aggregate to the dielectric

relaxation, it is highly desirable that studies be made using frequency domain measuring equipment which is capable of giving more precise values for relaxation times. In addition, further investigation is required to determine the correct values of ε_∞ for both pure alcohols and alcohol-water mixtures. If this is done, it will open the higher frequency behaviour of the dielectric dispersion of these systems to more certain interpretation. This will also enable a more precise value for the g factor to be obtained, and thus perhaps give more information on association behaviour. Further information on this behaviour may possibly be obtained from activation enthalpy data.

5.2 Surfactants

5.2.1 Static permittivity ε_s

The results for $C_{12}E_4$, $C_{12}E_6$ and $C_{12}E_8$ given in Figure 29 reveal a progressive increase in ε_s as the length of the polar ethylene oxide chain is increased. However, the change in ε_s between $C_{12}E_4$ and $C_{12}E_8$ at a given temperature is small, indicating the substantial depolarising effect of the dodecyl ether chain. On the basis of permittivity values, Brij 30 is much closer to $C_{12}E_6$ than to $C_{12}E_4$. This effect is doubtless due to contributions from longer ethylene oxide chain components present in the surfactant. Since polarisation is related to the square of the dipole moment, it is to be expected that, although the average ethylene oxide chain length $\overline{E}_n$

is 4, the measured permittivity will be slightly higher than that of $C_{12}E_4$ as was observed.

The almost identical temperature dependences of the static permittivity $d\varepsilon_s/dT$ indicate that for all the surfactants studied, very similar structural changes occur when the temperature is varied. The negative temperature dependence of ε_s for all the surfactants is in accord with predictions given by the homogeneous mixture equations $\boxed{2.1}$ and $\boxed{2.3}$ if it is assumed that the $g\mu^2$ term is constant over the temperature range studied.

5.2.2 <u>Relaxation behaviour of Brij 30</u>

Although the observed time domain relaxation was considered to be too rapid for precise determination of a relaxation time, the value of τ is within the range 50 to 100 ps which is much longer than that of pure water and is approximately a factor of 2.5 faster than the value of 197 ps obtained by Davies et al (192) for tetra ethylene glycol (E_4) at 20° C. These authors suggested that the dielectric relaxation was due to movement of the whole molecule during reorientation.

Viscosities (η) of Brij 30 and E_4 compared using an Ostwald viscometer at the temperature of 34.0° C, show Brij 30 to be a factor of 19.7 higher than that of E_4. Using the Debye expression for the molecular relaxation time $\tau \left(= \dfrac{4\pi\eta a^3}{kT} \quad \text{where a is the radius of the molecule} \right)$

with the assumption that $\tau` \simeq \tau$, putting $\tau_{E_4} = 2.5 \; \tau_{Brij \; 30}$ gives the result $a_{Brij \; 30} \simeq 0.3 \; a_{E_4}$. The lower value of 'a' correlates with the shorter relaxation time of Brij 30. It is therefore considered that the relaxation of Brij 30 is also due to movement of the whole molecule. The higher τ value for E_4 would also be expected due to the more extensive H-bonding in polyethylene glycols. This is indicated in the high g-value of 2.7 at 20° C for ethylene glycol (40). The presence of the alkyl ether chains in Brij 30 will result in reduced association analagous to the behaviour of H-bonded molecules diluted in non-polar solvents, and thus give a lower value for τ.

5.3   Tetra ethylene glycol (E_4)-water mixtures

The experimental values together with those given by the ideal mixing equation $\boxed{2.5}$ are given in Table 63 and Figure 38. In order to obtain the appropriate volume fraction, the density was measured in this laboratory using a standard 25 ml SG bottle. A value of $1.129 \cdot 10^3$ kg m^{-3} at the measurement temperature was obtained.

Table 63

Static permittivity of tetra ethylene glycol-water mixtures.

Mass fraction of E_4	Temperature / $^\circ$C	Experimental Value	Ideal Mixing
0.100	25.0	74.2	73.1
0.200	25.0	69.6	67.7
0.300	25.0	65.3	62.2
0.400	25.0	60.3	56.7
0.500	25.0	55.3	50.9
0.600	25.0	49.5	45.1
0.700	25.0	43.4	39.0
0.800	25.0	36.7	32.9
0.900	25.0	28.8	26.6

In these mixtures, the permittivity values are higher than those given by the ideal mixing equation. This behaviour is attributed to co-operative molecular association between the E_4 and water causing an enhanced dipole moment as occurs in alcohols. Deviations from the ideal mixing equation have been observed for many mixtures of associated liquids, the extensive studies of Decroocq (56) being worthy of note. In aqueous

solutions, permittivity values higher than those given
by the ideal mixing equation are exhibited by methanol
(56), ethylene glycol (55) and polyethylene glycol E_n
{n = 91} (192). Davies et al (192) made the comment
that the observed permittivity behaviour in E_n {n = 91}
"is surprising and is not understood".

5.4   Surfactant-water binary mixtures

The regions in which isotropic solutions occur in aqueous
mixtures of $C_{12}E_4$ and Brij 30 are indicated on the phase
diagrams given in Figure 44 (page 250). Comparison of
the two diagrams reveals similarity in the surfactant-
rich section but in the water-rich section, there is the
important difference that $C_{12}E_4$ has two separate clear
regions whereas Brij 30 has only one.

The phase diagram for aqueous mixtures of $C_{12}E_6$ given in
Figure 45 reveals that isotropic solutions are formed (p 263)
in water-rich mixtures over a much larger temperature
range than in the $C_{12}E_4$ case. This is due to the longer
oxyethylene chain giving greater solubility. This
aspect is emphasised in the phase diagram for aqueous

Phase diagrams for binary mixtures of
surfactant with water

a) $C_{12}E_4$

Temperature/°C

WATER + L_2

LIQUID (L_2)

WATER + L_3

LIQUID L_3

L_3 + LAM

LAMELLAR

WATER +
LAMELLAR

WATER +
L_1

LIQUID
(L_1)

%$C_{12}E_4$ (by mass)

(b) Brij 30

Temperature
/°C

WATER + L_2

LIQUID (L_2)

WATER
+ LAM.

LAMELLAR

%Brij 30 (by mass)
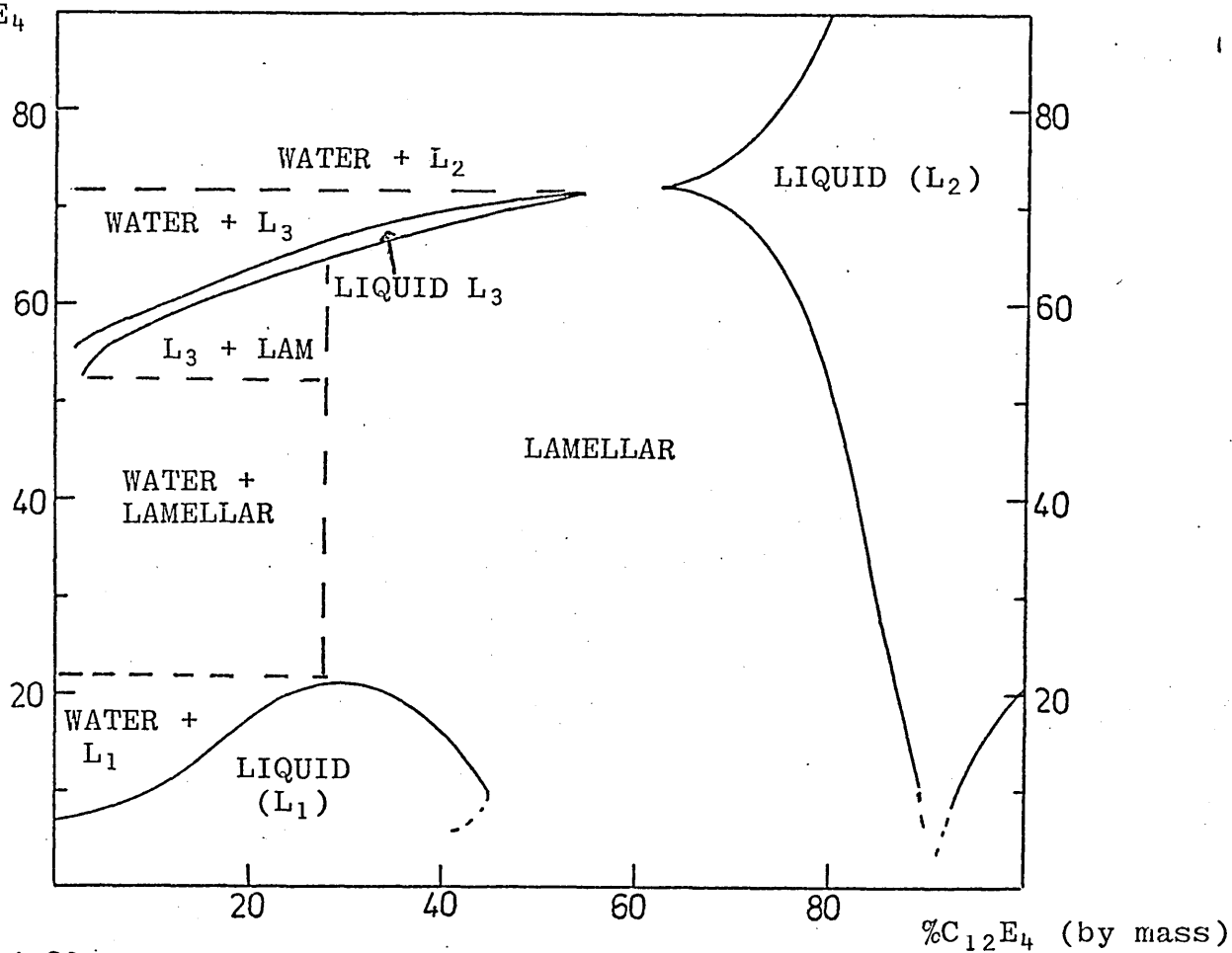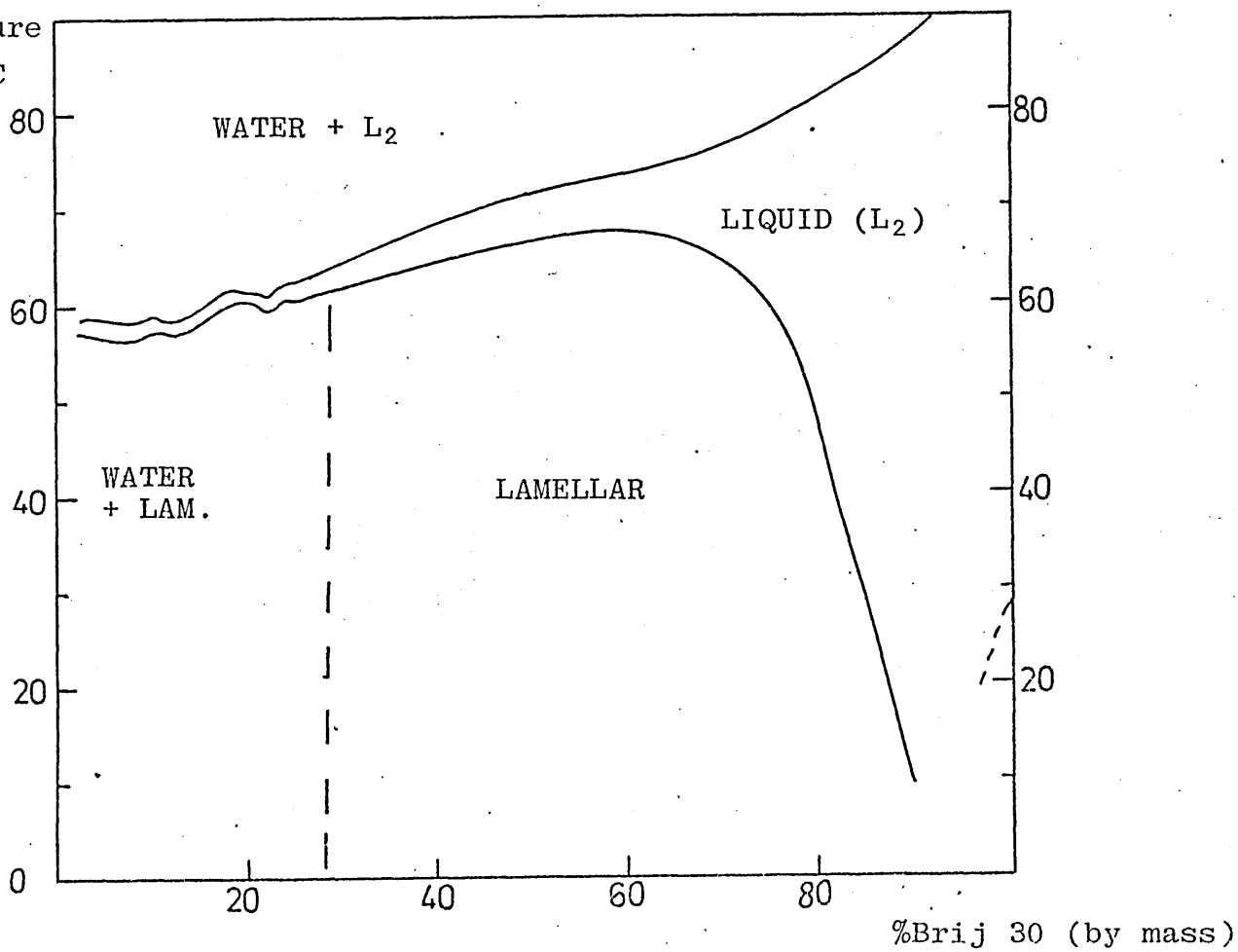
mixtures of $C_{12}E_8$ (Figure 45) which reveal the presence
of isotropic solutions over a wide temperature range for
an even wider range of compositions than in the $C_{12}E_6$
case. In order to explain the observed dielectric
behaviour of the binary mixtures, a number of mixture
equations have been tested. In the first instance,
spherical micelles have been assumed and the ideal
mixing [2.5], Rayleigh [2.14], Bruggeman [2.16],
Looyenga [2.17], Böttcher [2.19], Hanai O/W [2.29] and
Hanai W/O [2.31] equations have been applied. The
permittivity of water at the measurement temperature was
obtained using the precise relation given by Malmberg
and Maryott (43) and that of the surfactants from the
data obtained in this work. The volume fraction of the
component liquids was obtained from the known mass
fraction values together with the appropriate density
values at the measurement temperature. The temperature
dependence of the density was assumed to be the same for
all the surfactants and the value of $7.5 \ 10^{-4}$ kgm^{-3} $^{\circ}$C^{-1}
obtained for $C_{12}E_4$ was used. The densities of water were
obtained from Kaye and Laby (193).

5.4.1 <u>$C_{12}E_4$- and Brij 30-water mixtures</u>

The permittivity values given by the mixture equations
together with the experimental values for (i) the $C_{12}E_4$-
water mixtures are given in Table 64 and Figure 32 and
(ii) the Brij 30-water mixtures are given in Table 65 and

Figure 33. (NB Since the Bruggeman equation gives almost identical values to the Hanai equation when the dispersion is O/W, only the Hanai equation has been used for such dispersions).

Table 64

$C_{12}E_4$-water mixtures

Comparison of experimental static permittivity values with values given by mixture equations.

Mass Fraction of Surfactant p	Temperature /°C	Experimental Value	Ideal Mixing	Rayleigh O/W	Rayleigh W/O	Bruggeman W/O	Looyenga	Böttcher O/W	Hanai O/W	Hanai W/O
0.099)	5.4	72.7	77.0	73.8	55.4	67.0	67.9	73.3	73.7	5,323.0
)	60.6	51.0	60.1	57.6	44.1	52.8	55.3	57.3	57.5	4,408.0
0.198)	8.6	61.9	67.8	62.5	39.2	51.3	57.0	61.3	61.9	678.1
)	64.4	41.2	52.8	48.8	31.4	40.4	44.7	47.5	48.3	559.3
0.301)	13.2	51.2	58.5	52.1	29.1	38.5	45.2	48.8	50.0	201.9
)	67.5	34.1	46.0	41.0	23.6	30.8	36.8	38.4	40.1	167.0
0.400)	11.8	43.7	51.2	44.1	22.8	29.5	36.5	39.1	42.3	87.7
)	70.7	28.5	39.4	34.1	18.2	23.3	28.4	30.0	32.8	70.7
0.500	72.8	24.4	33.2	28.0	14.4	17.6	22.3	22.6	26.3	36.6
0.600*	72.8	20.1	27.4	22.7	11.6	13.4	17.4	16.5	20.9	21.5
0.700	69.8	16.3	22.0	18.0	9.6	10.5	13.5	12.0	16.4	14.0
0.802	69.4	12.4	16.5	13.5	7.8	8.2	10.1	8.7	12.5	9.6
0.904	68.2	8.9	10.8	9.2	6.3	6.4	7.4	6.5	9.4	6.9

* The mixture for p = 0.600 would not turn fully transparent as noted in Chapter 4.

Table 65

Brij 30-water mixtures

Comparison of experimental static permittivity values

with values given by mixture equations

Mass fraction of Surfactant p	Temperature /°C	Experimental Value	Ideal Mixing	Rayleigh O/W	Rayleigh W/O	Bruggeman W/O	Looyenga O/W	Böttcher O/W	Hanai O/W	Hanai W/O
0.101	57.1	54.5	61.1	58.6	45.9	53.7	56.3	58.3	58.6	5,014.0
0.202	61.4	44.6	53.6	49.5	32.9	41.4	45.5	48.3	49.1	609.0
0.300	63.5	37.6	46.9	41.9	25.5	31.6	36.8	39.3	41.0	178.4
0.400	69.1	32.1	39.7	34.4	19.4	24.0	28.9	30.5	33.1	75.0
0.500	69.1	27.2	33.8	28.6	15.4	18.4	22.9	23.4	27.0	39.1
0.600	70.0	22.1	27.9	23.2	12.4	14.1	17.9	17.2	21.4	23.0
0.700	70.0	17.4	22.2	18.1	10.3	10.9	13.7	12.4	16.6	14.7
0.802	70.0	12.5	16.5	13.5	8.2	8.5	10.3	9.0	12.6	10.1
0.897	70.0	9.0	10.9	9.3	6.7	6.7	7.5	6.8	9.6	7.2

Comparison of the permittivity values given by the various mixture equations with the experimental values reveals that at the measurement temperatures, none of the equations gives ε values close to the experimental ones over the whole composition range. However, for both the $C_{12}E_4$- and Brij 30-water mixtures, a number of conclusions can be drawn.

(a) the ideal mixture equation is clearly unsuitable over the whole composition range in giving much too high values for the permittivity.

(b) substantially better agreement with the experimental data is given by both the Rayleigh O/W and Hanai O/W equations than with either the Böttcher O/W or the Looyenga equations.

(c) for $p > 0.3$, the Rayleigh and Hanai equations for O/W dispersions give much better agreement with experimental values than for W/O dispersions; the Hanai O/W equation gives closest agreement.

(d) for $p \leqslant 0.4$, the experimental values for the low temperature mixtures of $C_{12}E_4$ are in good agreement with values given by the Hanai O/W equation but both the high temperature experimental values for $C_{12}E_4$ and those for the Brij 30 mixtures are significantly lower than the values given by the Hanai O/W equation.

Since the permittivity values given by the Hanai O/W equation give the closest agreement with experimental values over the range $p = 0.6$ to 0.9, it is considered

that at the measurement temperatures, these micellar mixtures of the surfactants $C_{12}E_4$ and Brij 30 are water continuous over the $p = 0.6$ to 0.9 range of surfactant concentration and that the dielectric behaviour is best described by a heterogeneous mixture model. Since the low surfactant concentration mixtures give good agreement with the Hanai O/W equations at low temperatures, it is considered that the low surfactant concentration mixtures are also water continuous.

In the low surfactant concentration mixtures of both Brij 30 and $C_{12}E_4$ at the higher temperature, the temperature range for transparency was typically only about 1° C. Thus these studies were of necessity performed at a temperature only just below the cloud point. Since it is well established that very rapid micellar growth occurs at the cloud point (80), it was considered that the anomalous dielectric behaviour of these mixtures could be related to the presence of large micelles. This is supported by the appearance of a marked blue opalescence in these mixtures which was particularly evident at the lowest concentrations. In order to account for the marked deviations between the experimental data and the Hanai O/W values in these high temperature solutions, two approaches have been considered, these are (i) deviation from spherical shape causing a reduction in the measured permittivity value and (ii) secondary aggregation effects causing an increase in the effective volume of the dispersed oil phase.

(i)   It has been shown by Tanford et al (74) that non-
ionic surfactants form oblate spheroidal rather than
spherical micelles at low surfactant concentrations.   In
order to determine the effect of such a spheroidal shape
on the permittivity, the extended form of the Bruggeman
equation derived in this work (equation $[2.64]$) has been
used to calculate the shape factor A_a required to attain
agreement between calculated values and the higher
temperature experimental data.   The required A_a values
together with the axial ratios b/a given by equation
$[2.40]$ to obtain agreement with the experimental values
for the $C_{12}E_4$-water mixtures at low concentration are
given in Table 66.

Table 66

Micelle shape factors for $C_{12}E_4$-water mixtures

Mass Fraction of Surfactant, p	Shape Factor A_a	Axial Ratio b/a
0.099	0.68	3.6
0.198	0.60	2.6
0.301	0.54	2.1
0.400	0.48	1.7
0.500	0.39	1.2

For all compositions A_a is $> \frac{1}{3}$, indicating an oblate
rather than prolate spheroidal shape which agrees with
the proposals of Tanford et al (74).   The results also
indicate a steadily decreasing eccentricity towards

spherical shape as the proportion of surfactant is

increased.   The values of A_a required to obtain

agreement with the experimental values for Brij ·30-water

mixtures at low concentration are given in Table 67.

Table 67

Micelle shape factors for Brij 30-water mixtures

Mass fraction of Surfactant, p	Shape Factor A_a
0.101	0.60
0.202	0.53
0.300	0.48
0.400	0.38

Comparison of these A_a values with those for the $C_{12}E_4$

mixtures given in Table 66 reveals a slightly lower

value of A_a at the lowest concentration of surfactant

corresponding to an axial ratio (b/a) of 2.6:1.

The (b/a) values for both surfactants are similar to

those reported by Tanford et al (74) for micelles in

aqueous solutions of $C_{12}E_8$ where values in the range

2.5:1 to 1.9:1 were reported.   The rather higher figure

of 3.5:1 for the $C_{12}E_4$ mixtures at the lowest concentration

is to be expected because, as reported by Tanford et al

(74, 194), reduction in the length of the oxyethylene

chain produces a reduction in the repulsive forces

between the surfactant headgroups which leads to an

increase in the aggregation number and thus micelle size.
These authors pointed out that large size can only be
achieved by a change from spherical to spheroidal
shape due to a limitation that one dimension of the
hydrocarbon core of the micelle cannot exceed the length
of two fully extended alkyl chains. Thus increased
aggregation number must be accompanied by a more
spheroidal shape which is in agreement with the higher
(b/a) values obtained in this work.

The lower (b/a) value obtained for the Brij 30 mixtures
at any given surfactant concentration is probably due to
contributions by the lower aggregation number E_n (n > 4)
components present in this surfactant.

It is considered that neither the Böttcher [2.19] nor
the Looyenga [2.17] equations are suitable for describing
the above dielectric behaviour even when they are used
in the generalised forms of Polder and van Santen [2.49]
for the Böttcher equation and equation [2.78] derived in
this work for the Looyenga equation. Both equations
[2.49] and [2.78] give similar results to those of the
generalised Hanai-Bruggeman equations derived in this
work, in that for oblate spheroids the permittivity is
reduced and for prolates it is increased. However
application of [2.49] and [2.78] to this data would
required postulation of a much wider range of the shape
factor A_a to account for the fact that at some

compositions, the spheroids are oblate and at others prolate in shape.

Another point that should be noted is that the equations of Grosse and Greffe ([2.46] to [2.48]) are considered to be unsuitable for application to the experimental data in this work because, although their equations give an increased permittivity for the prolate spheroidal shape, for an oblate shape the permittivity change is negligibly small.

(ii) Interpretation of the higher temperature dielectric behaviour of these surfactant water mixtures based on secondary aggregation poses difficulties because there is uncertainty as to whether or not such aggregation involves association of the oxyethylene chains between different micelles. If the proposed secondary aggregation does involve such association, as suggested by Tanford et al (74), it is quite possible that the dielectric properties will be affected. However Staples and Tiddy (80) have suggested that this association is unlikely because, calculations using cloud point data showed the average distance between micelles to be too large. If it is assumed that this association does not occur, but that the primary micelles form clusters and act as rigid spheres, for a close-packed structure they will only be able to occupy a maximum of 74% of the total volume of the aggregated micellar clusters. The

26% interstitial volume between the micelles can be considered as effectively increasing the total volume of the dispersed oil phase and would thus give a reduction in the measured permittivity. However inspection of the results given in Figure 32 reveals that for the p = 0.099 mixture, the required mass fraction to achieve agreement between the Hanai O/W value and the experimental value is approximately 0.2. This doubling of the effective mass fraction of the dispersed phase cannot be justified on the basis of the increase in volume arising from close-packing considerations. However, such an increase could be accounted for by a more loosely-packed structure.

An alternative suggestion based on secondary aggregation is that the 26% interstitial volume between the aggregated micelles is filled with unassociated water. This would similarly produce a reduction in permittivity because the volume fraction of the continuous aqueous phase would have been reduced due to some of the water being used to fill the interstitial volume. However the required volume fraction correction is still too large and a more loosely-packed structure would again be required.

It is concluded that the $C_{12}E_4$- and Brij 30-water mixtures contain normal micelles over the whole composition range. For mass fractions of surfactant above 0.5, the static permittivity values are in good agreement with those given by the Hanai-Bruggeman mixture equation for

spherical dispersions. At lower surfactant concentrations, the permittivity values of the $C_{12}E_4$ mixtures at the lower temperature give similarly good agreement with the predictions of the above equation but deviations occur in both the $C_{12}E_4$ mixtures at the higher temperature and the Brij 30 mixtures.

The deviations can be accounted for by proposing oblate spheroidal micelle shape with an axial ratio of 3.6:1 in $C_{12}E_4$ and 2.6:1 in Brij 30 at the lowest concentration studied, which with increase of surfactant concentration, progressively changes towards spherical shape.

An alternative interpretation to account for the deviations between theory and experiment at low surfactant concentration is based on secondary aggregation involving loose-packing of the primary micelles.

5.4.2   <u>$C_{12}E_6$-water mixtures</u>

Since the Looyenga [2.17] and Böttcher [2.19] equations have already been found to be unsuitable for the $C_{12}E_4$ and Brij 30 mixtures, only the ideal mixing [2.5], Rayleigh O/W [2.14] and Hanai O/W [2.29] equations have been applied here. The permittivity values given by these equations together with the experimental values are given in Table 68 and in Figure 34.

Table 68

$C_{12}E_6$-water mixtures

Comparison of experimental static permittivity values with values given by mixture equations.

Mass fraction of Surfactant,p	Temperature /°C	Experimental Value	Ideal Mixing	Rayleigh O/W	Hanai O/W
0.097	25.4	69.1	71.0	68.2	68.1
0.201	24.8	60.8	63.5	58.7	58.1
0.300	35.2	49.5	53.7	48.0	47.0
0.400	43.3	39.7	45.2	39.2	37.8
0.500	44.7	32.8	38.3	32.4	30.6
0.600	66.6	23.5	28.8	23.9	22.3
0.699	66.6	18.7	23.0	18.9	17.4
0.798	51.2	15.3	18.4	15.1	14.0
0.880	51.2	12.4	13.3	11.2	11.1

Even though the micellar mixtures are again considered to be water continuous, they exhibit significantly different behaviour from that of the $C_{12}E_4$ and Brij 30 mixtures. Of the equations used, the Rayleigh O/W gives in general closest agreement with the experimental data, the agreement for p between 0.4 and 0.8 being very good. However for p $\leq$ 0.3 and p = 0.9, significant deviations are evident and for both low and high values of p, the ideal mixing equation is almost as good as the Rayleigh O/W.

Phase diagrams for binary mixtures of surfactant
and water

(a) $C_{12}E_8$

Temperature $/^\circ C$

WATER + L_1

LIQUID (L_1)

HEXAGONAL

CUBIC

SOLID

D

% C_{12} % $C_{12}E_8$ (by mass)

20   40   60   80

(b) $C_{12}E_6$

Temperature $/^\circ C$

WATER + L_1

LIQUID (L_1)

LAM.

HEX.

80

40

0

ICE + SOLID

0   30   60   90 % $C_{12}E_6$ (by mass)

If a prolate spheroidal shape is proposed, the Hanai O/W values can be made to agree with the experimental values by using the appropriate A_a value in equations [2.64] or [2.72]. There is some justification for proposing micelles of this shape because the phase diagrams for aqueous mixtures of $C_{12}E_6$ and $C_{12}E_8$ (Figure 45) reveal the presence of a hexagonal liquid crystalline phase containing cylindrical micelles at surfactant concentrations within the range 40 to 60% whereas in $C_{12}E_4$ and Brij 30 (Figure 44) only a lamellar phase occurs. It is quite possible that over the concentration range at which the hexagonal phase occurs, when the temperature is raised so that an isotropic solution is formed, this solution contains prolate spheroidal micelles. However such a propsal cannot be maintained at concentrations of 60% and above because a lamellar liquid crystalline phase forms at lower temperatures at these concentrations. Since the agreement with the Rayleigh equation is good over the range p = 0.4 to 0.8, it is considered that a prolate spheroidal shape interpretation is inadequate.

As the aggregation number in these mixtures is lower than that in both the $C_{12}E_4$ and Brij 30 solutions (74), the micelle sizes will be smaller and thus effects due to deviation from spherical shape and secondary aggregation are less likely. It is suggested that the better agreement with the Rayleigh rather than the Hanai equation is related to the micelles in these mixtures being of

smaller size. The deviation at high surfactant concentration could be due to limitations of the Rayleigh equation at these concentrations but this will not be the case for the $p \leqslant 0.3$ mixtures which have unexpectedly high permittivity values These higher values could be due to deviation from spherical to prolate spheroidal shape at very low surfactant concentrations, because deviation from spherical shape is most likely at these concentrations.

5.4.3 $C_{12}E_8$-water mixtures

As in the $C_{12}E_6$-water mixtures, only the ideal mixing [2.5], Rayleigh O/W [2.14] and Hanai O/W [2.29] equations have been applied here.

The permittivity values given by these equations together with the experimental values are given in Table 69 and Figure 35.
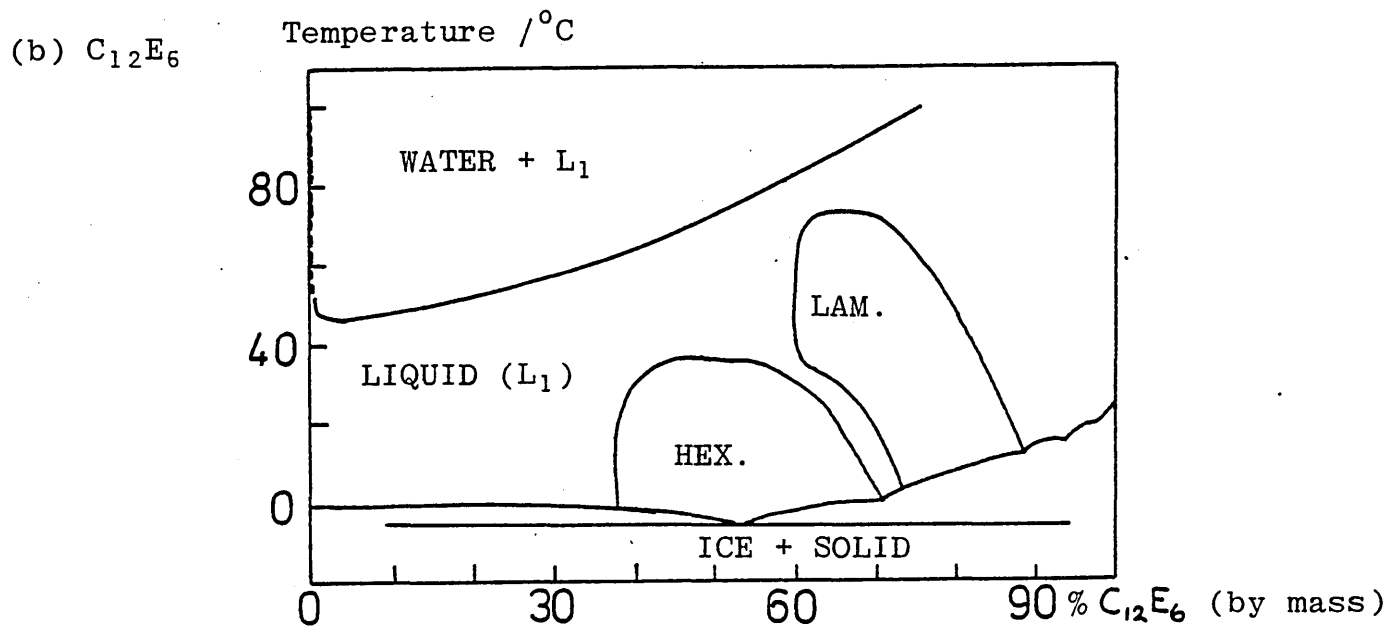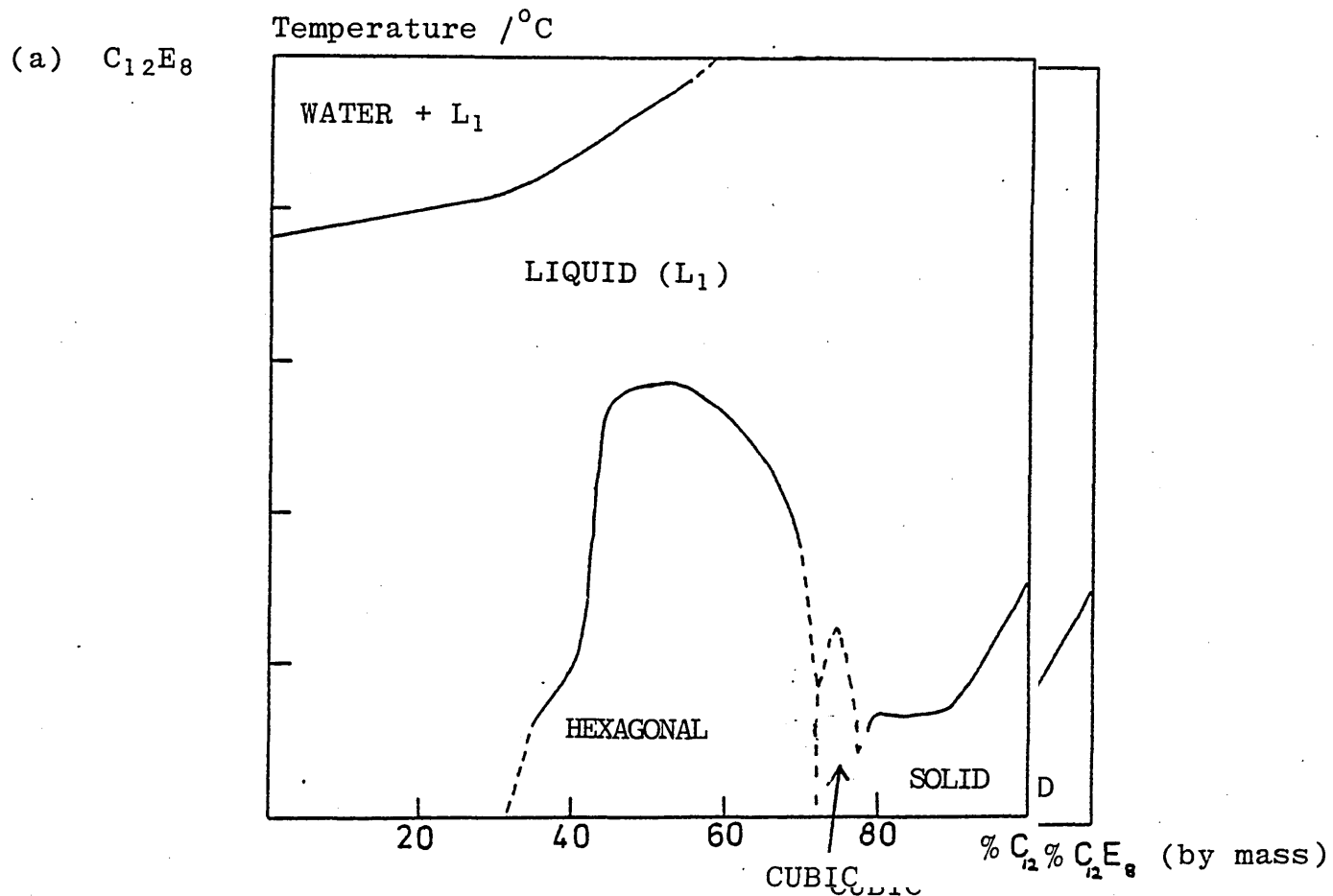
Table 69

$C_{12}E_8$-water mixtures

Comparison of experimental static permittivities with values given by mixture equations.

Mass fraction of Surfactant, p	Temperature /°C	Experimental Value	Ideal Mixing	Rayleigh O/W	Hanai O/W
0.100	25.0	57.6	59.0	56.8	56.7
0.200	25.0	50.6	53.0	49.2	48.8
0.300	25.0	44.2	47.1	42.3	41.5
0.400	25.0	38.1	41.2	35.9	34.7
0.500	25.0	32.3	35.2	29.9	28.4

Table 69 (Continued)

Mass fraction of Surfactant	Temperature /°C	Experimental Values	Ideal Mixing	Rayleigh O/W	Hanai O/W
0.600	25.0	26.5	29.2	24.5	22.8
0.699	25.0	21.1	23.5	19.3	17.9
0.801	25.0	15.5	17.5	14.4	13.6
0.901	25.0	9.5	11.6	10.0	10.5

Again as in the $C_{12}E_6$-water mixtures, the Rayleigh O/W gives closest agreement with the experimental values but in this case, the agreement is only marginally better than that given by the ideal mixing equation. These results confirm the trend of increasing permittivity at any given concentration of surfactant with increase in oxyethylene chain length, and in these mixtures there is almost equal justification for using the ideal mixing equation as for using the heterogeneous mixture equation of Rayleigh.

On the basis of an interpretation in which deviation from the ideal mixing equation is related to micelle size, it would appear that the micelles in $C_{12}E_8$-water mixtures are even smaller than those in the $C_{12}E_6$ mixtures. This conclusion gives further support to the proposal of Tanford et al (74) that for a given length of alkyl ether chain (C_{12} in this case), increasing oxyethylene chain length leads to a progressive reduction in micelle aggregation number and thus micelle size. In addition

to smaller size, prolate spheroidal shape is also more
probable in these mixtures because the $C_{12}E_8$ phase
diagram reveals a hexagonal phase over a larger concen-
tration range than in $C_{12}E_6$ and the lamellar phase is
absent. As the prolate spheroidal shape gives a higher
permittivity than a sphere, there could be a contribution
by this shape to the permittivity.

Interpretation of the dielectric behaviour is made more
complicated by the contribution due to association between
the surfactant headgroups and water, which as observed
in the tetra ethylene glycol-water mixture studies
leads to an enhanced permittivity value. As the length
of the surfactant oxyethylene chain increases, the
contribution by this effect will become progressively
more significant.

5.4.4   Temperature dependence of permittivity of surfactant-
         water binary mixtures

5.4.4.1 Mass fraction of surfactant, p = 0.9

The results for the $C_{12}E_4$ and $C_{12}E_8$ surfactants given in
Figure 36a display a montonous fall in permittivity with
increasing temperature for this concentration. Such
behaviour is to be expected on the basis of both
homogeneous and heterogeneous models. In the homogeneous
case, increase of temperature leads to a reduction in
permittivity provided that the $g\mu^2$ term , is
unchanged (see eg equation $[2.3]$). For the heterogeneous

mixture model, a fall in permittivity is expected because of the negative temperature dependence of the permittivity of both components of the mixture.

The rather smaller temperature dependence for the $C_{12}E_4$ mixture compared with that obtained for the $C_{12}E_8$ is probably due to H-bonding differences. It is possible that the behaviour is due to more pronounced micellar growth with increasing temperature in the $C_{12}E_8$ mixture. Since increase of micelle size has already been suggested as giving a lower permittivity value, the higher temperature dependence in the $C_{12}E_8$ mixture could be related to more rapid micellar growth. Alternatively if the micelles are non-spherical, the behaviour could be due to more pronounced shape changes in the $C_{12}E_8$.

5.4.4.2 Mass fraction of surfactant, p = 0.1

The temperature dependences of ε_s for the $C_{12}E_6$- and $C_{12}E_8$- water mixtures at $p \simeq 0.1$ given in Figure 36b are identical indicating similar structural changes as the temperature is increased. It is worthy of note that there is no deviation from linearity even at the highest temperatures where more pronounced micellar growth effects might have been expected. Since in both mixtures the highest temperature was at least 10° C below the cloud point, the results are consistent with the proposal that effects such as rapid micelle growth and secondary aggregation only occur at temperatures close to the cloud point (80).

5.5 Surfactant-n-alkane binary mixtures

In order to explain the observed dielectric behaviour of the binary mixtures of Brij 30 with n-heptane, the ideal mixing [2.5], Rayleigh [2.14] for both W/O and O/W, Hanai W/O [2.31] and O/W [2.29] and Bruggeman W/O [2.16] equations have been applied taking Brij 30 as the 'water' component. The permittivity of heptane was obtained from literature data (195) and that of Brij 30, at the measurement temperature, from this work. The density of heptane at the measurement temperature was obtained from literature data (193,196).

The permittivity values given by the mixture equations together with the experimental values are given in Table 70 and Figure 39.

Table 70

Brij 30-n-heptane mixtures

Comparison of experimental static permittivity values with values given by mixture equations.

Mass fraction of Surfactant p	Temperature /°C	Experimental Value	Ideal Mixing	Rayleigh W/O	Rayleigh O/W	Hanai W/O	Hanai O/W	Bruggeman W/O
0.20	56.3	2.32	2.48	2.28	2.38	3.16	3.04	2.29
0.40	56.3	2.80	3.13	2.77	2.94	6.33	3.39	2.80
0.60	56.3	3.65	3.84	3.39	3.61	17.36	3.90	3.45
0.80	56.3	4.53	4.66	4.27	4.48	113.1	4.63	4.38

(NB   Hanai O/W = Bruggeman O/W)

The agreement given by both the Rayleigh W/O and
Bruggeman W/O values with the experimental data for
p = 0.20 and 0.40 is very close and significantly
better than that given by the ideal mixing equation.
Similarly the agreement between the Rayleigh O/W and
the Bruggeman O/W equations and the experimental data for
high p values is also very close, with the ideal mixing
equation being again less satisfactory. The Hanai W/O
equation is unsatisfactory at all compositions.

The agreement of the experimental data with a W/O value
at low p and an O/W value at higher p values is consistent
with an interpretation in which the micellar structure
is inverted (W/O) at low surfactant concentration and
normal (O/W) at high concentration. It would thus
appear that in the limit of p = 1 corresponding to the
surfactant alone, the micelle structure is likely to
be O/W. This is in agreement with the proposals of
Bostock et al (81) that the surfactant is aggregated into
normal micelles.

On the basis of proposals given earlier in which
permittivity is dependent on micelle size, the
better agreement given with the Rayleigh rather than
the Hanai equations could be due to smaller sized
micelles in these mixtures when compared with the binary
mixtures of this surfactant with water.

FIGURE 46

Isotropic liquid regions in ternary mixtures
of $C_{12}E_4$ with water and n-heptane

n-heptane

Temperature

4° C $I\phi \equiv$ Isotropic liquid

$I\phi$

$I\phi$

$I\phi$

Water $C_{12}E_4$

n-heptane

Temperature

0° C

$I\phi$

$I\phi$

Water $C_{12}E_4$
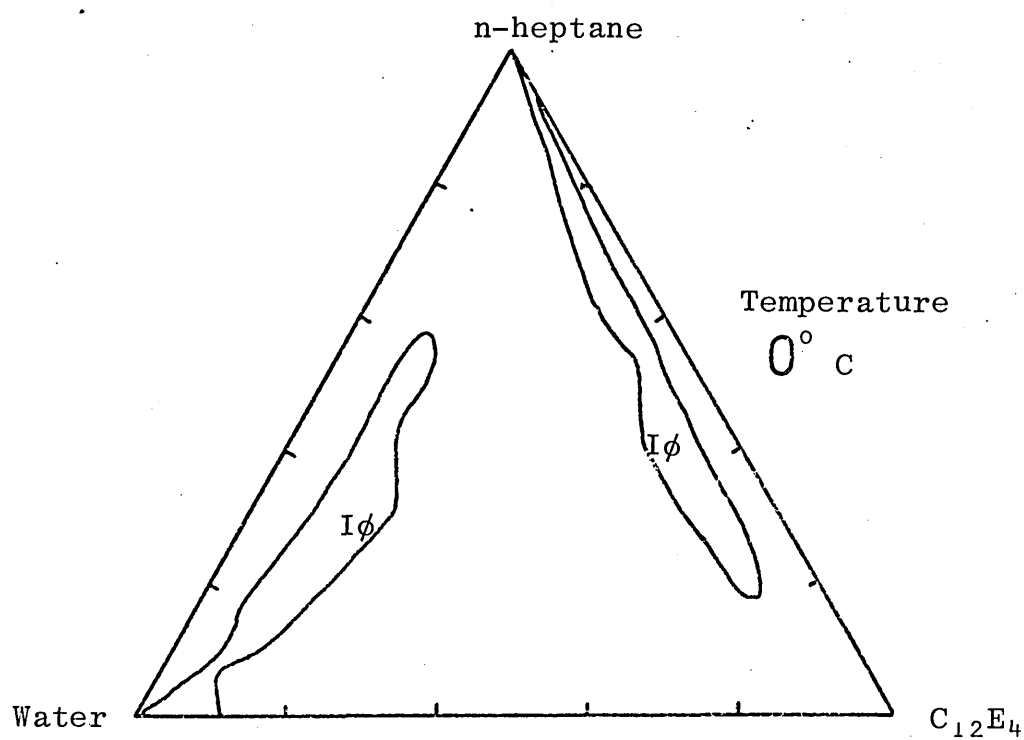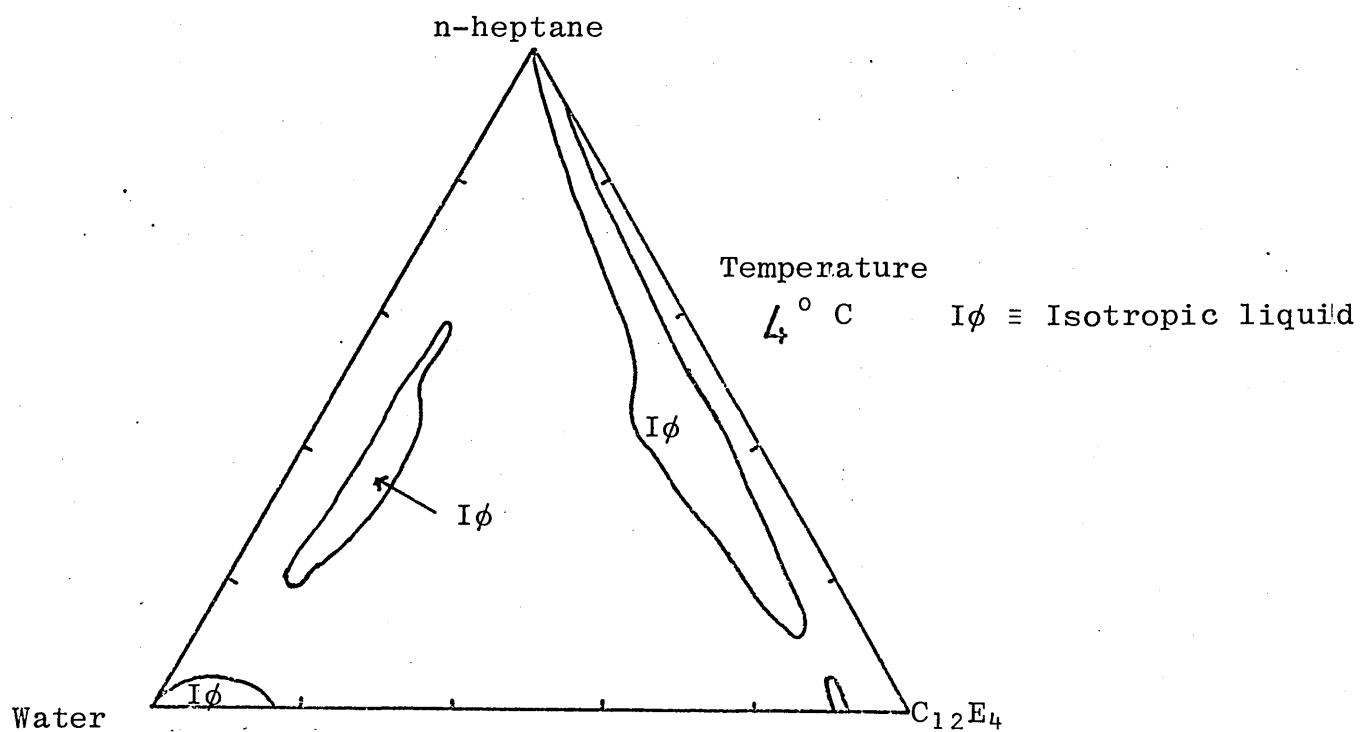
FIGURE 47

Isotropic liquid regions in ternary mixtures of
$C_{12}E_4$ with water and n-heptane

n-heptane

Temperature

17° C $I\phi \equiv$ Isotropic
                              liquid

$I\phi$

Water $C_{12}E_4$

$I\phi$

n-heptane

$I\phi$

$I\phi$

Temperature

13° C

Water $C_{12}E_4$

$I\phi$
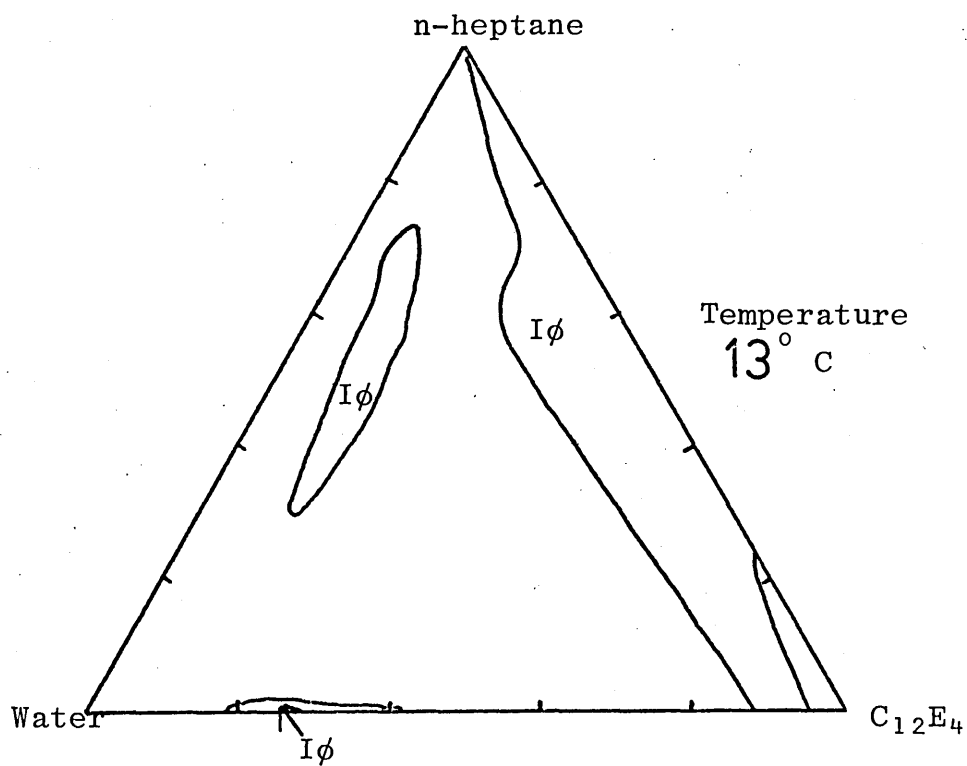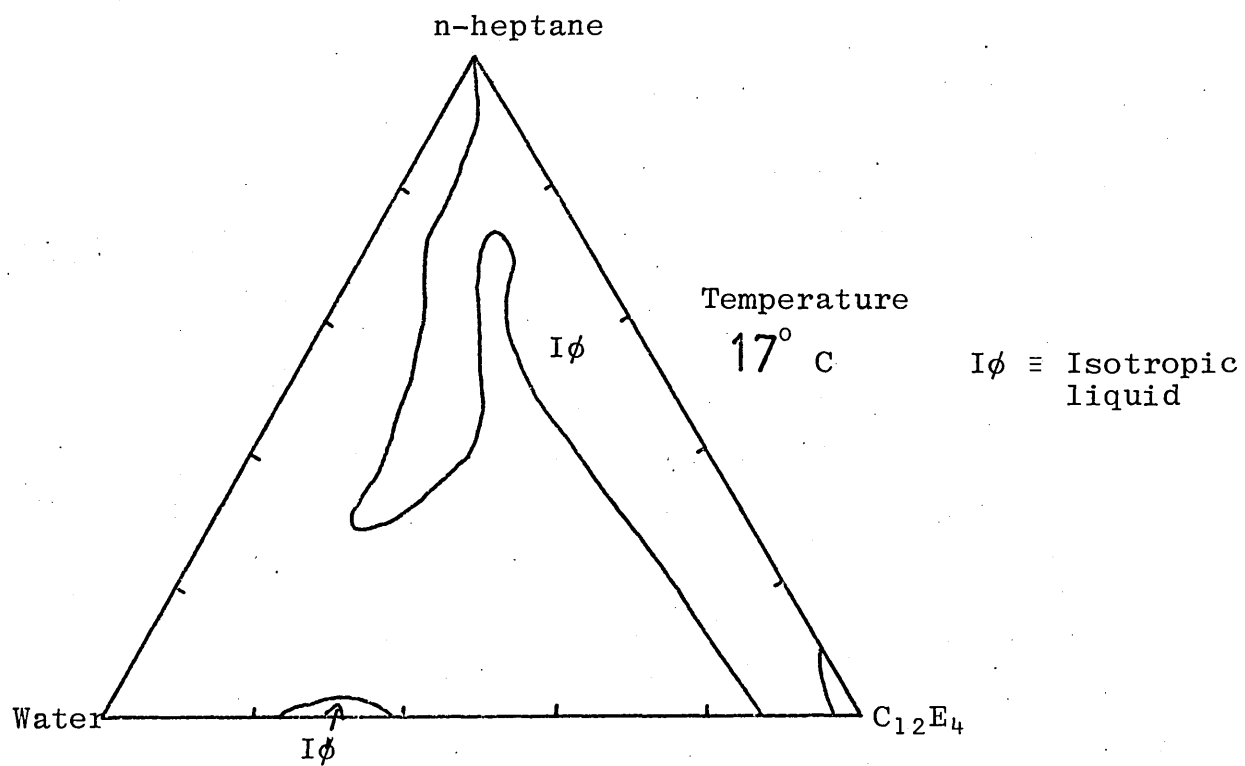
FIGURE 48

Isotropic liquid regions in ternary mixtures
of $C_{12}E_4$ with water and n-heptane
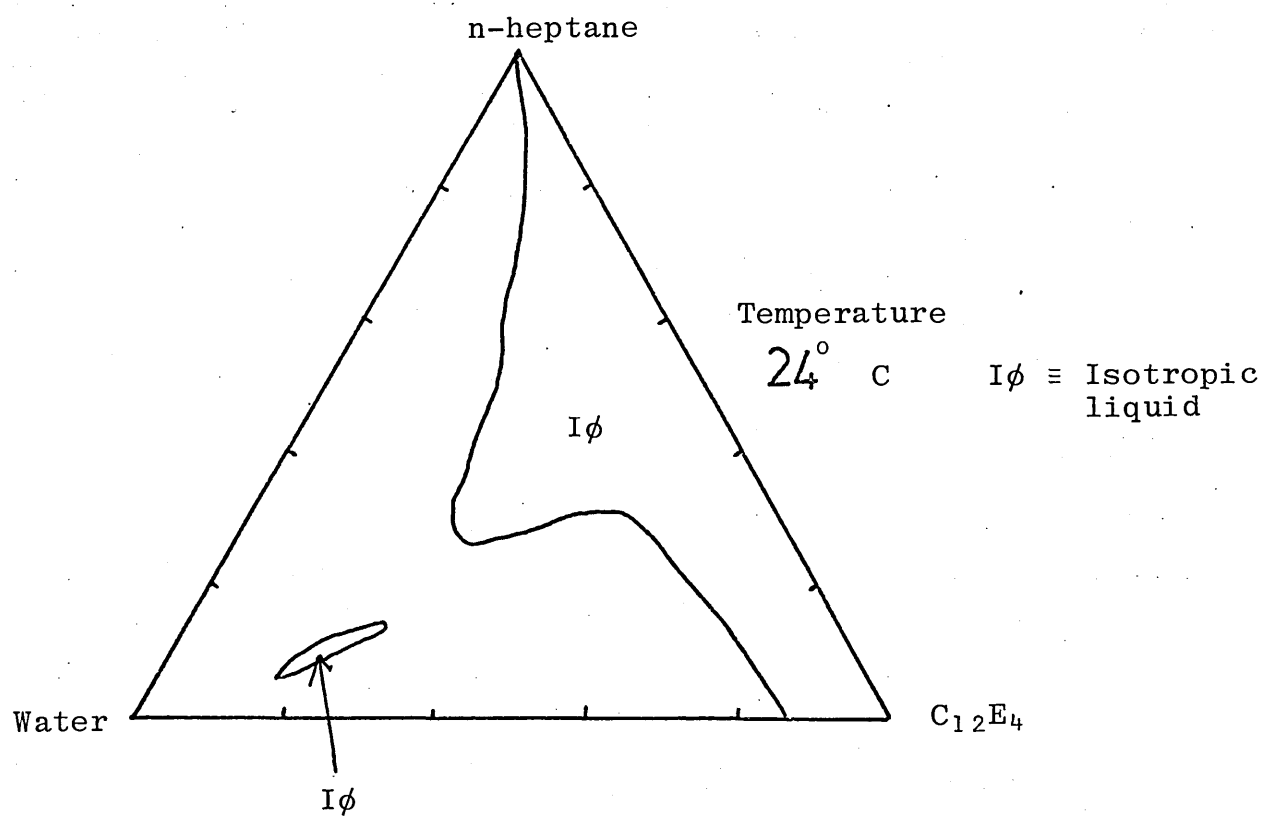
FIGURE 49

Isotropic liquid regions in n-alkane and water systems with increasing concentration of $C_{12}E_4$

Temperature /°C

Iϕ

40% n-hexadecane + 60% H_2O

Iϕ = isotropic liquid

30

15

0

10   20   % $C_{12}E_4$ (by mass)

Temperature /°C

30

Iϕ 40% n-decane + 60% H_2O

15

0

10   20   % $C_{12}E_4$ (by mass)

Temperature /°C

30

15

Iϕ 40% n-heptane + 60% H_2O

0

10   20   % $C_{12}E_4$ (by mass)

- 275 -
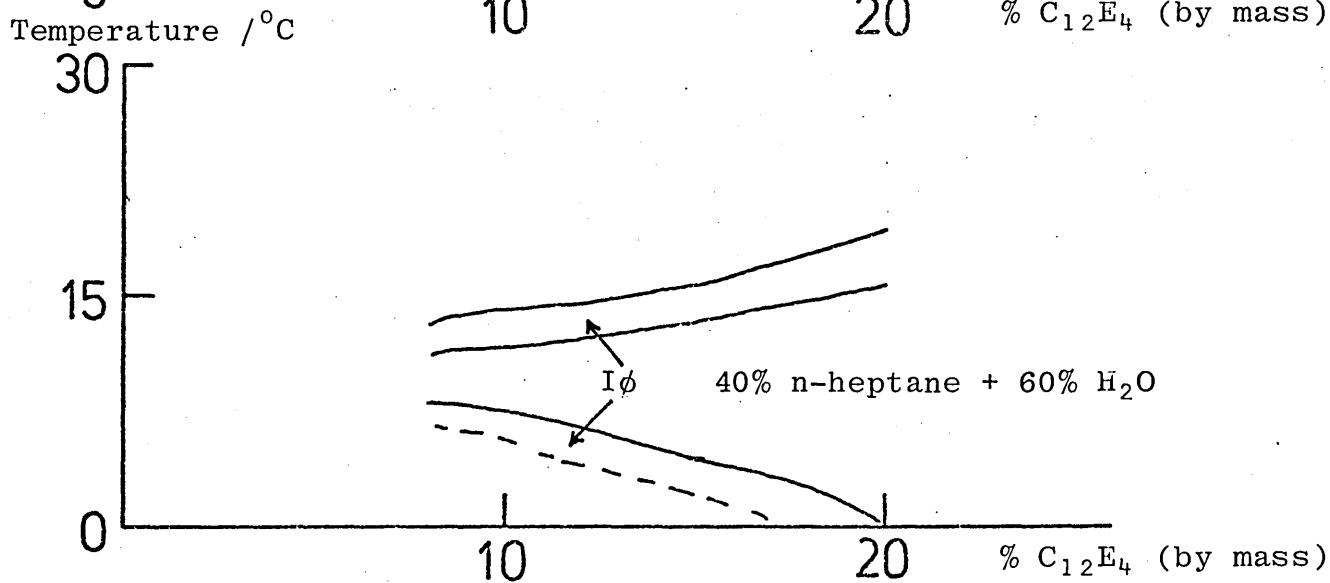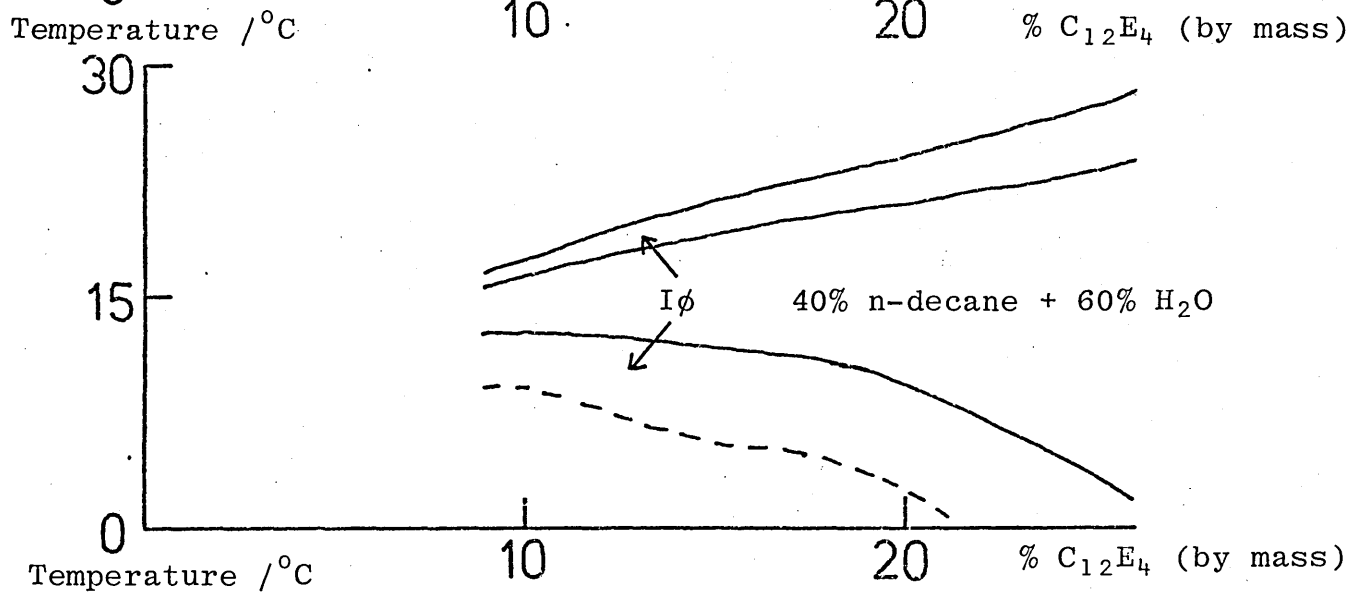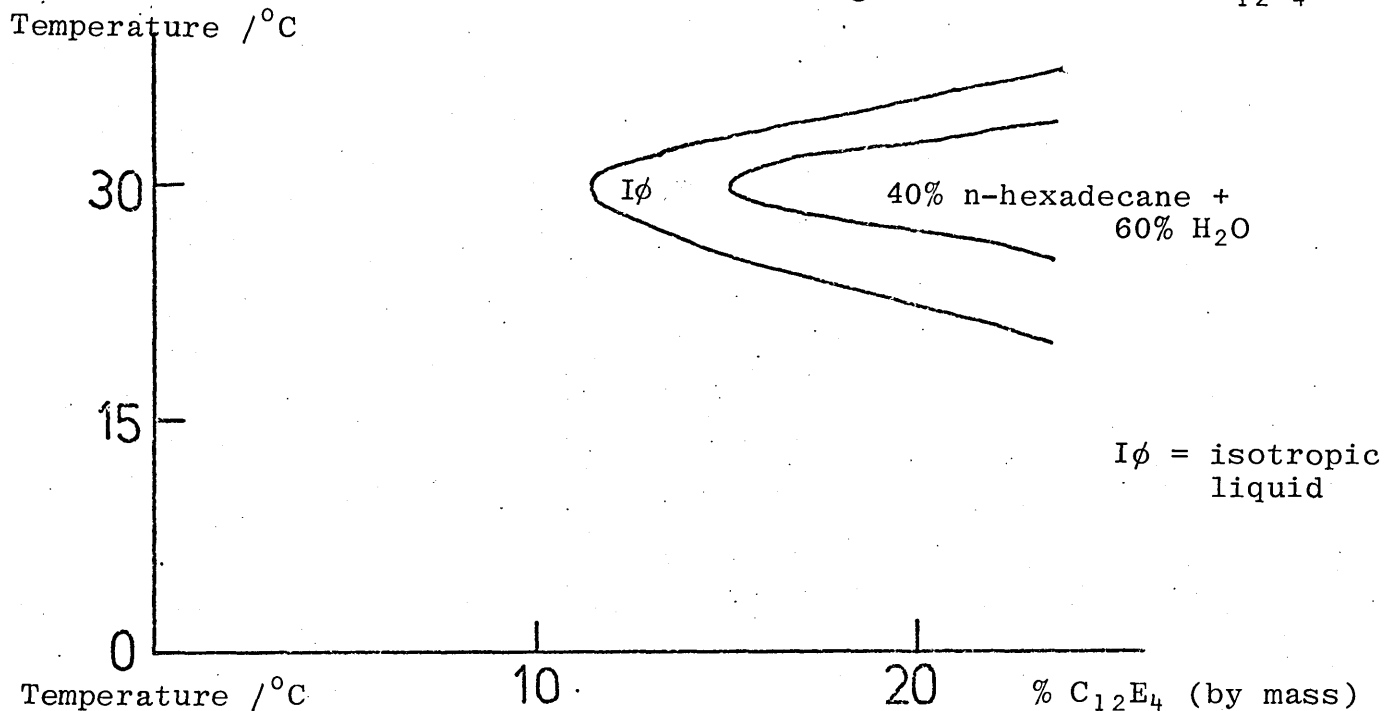
Conductivity changes with temperature in
n-alkane and aqueous 0.01 M NaCl + $C_{12}E_4$ systems

(a)

(a) 40.3% n-heptane + 49.7% aqueous 0.01 M NaCl + 10.0% $C_{12}E_4$

(b)

(b) 35.9% n-decane + 54.3% aqueous 0.01 M NaCl + 9.8% $C_{12}E_4$

(c)

(c) 34.3% n-hexadecane + 51.7% aqueous 0.01 M NaCl + 14.0% $C_{12}E_4$

(d)

(d) 32.8% n-hexadecane + 49.1% aqueous 0.01 M NaCl + 18.0% $C_{12}E_4$
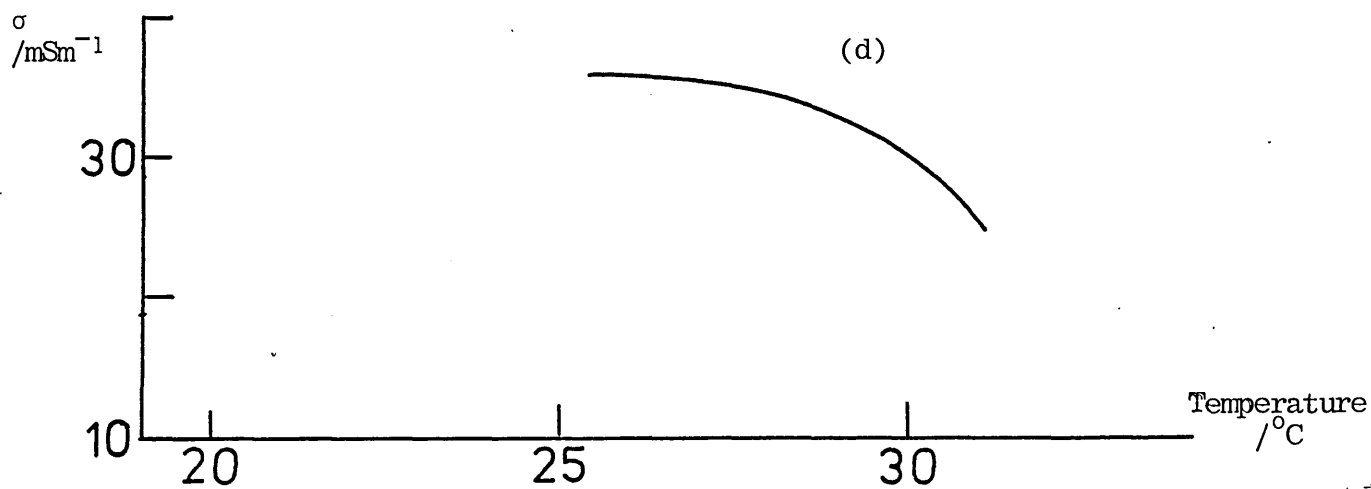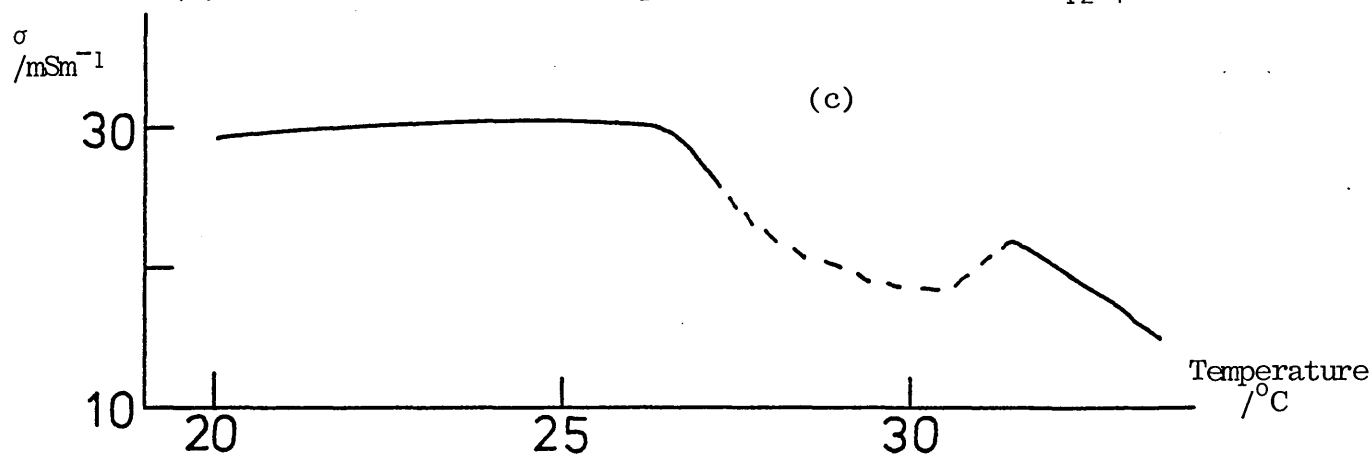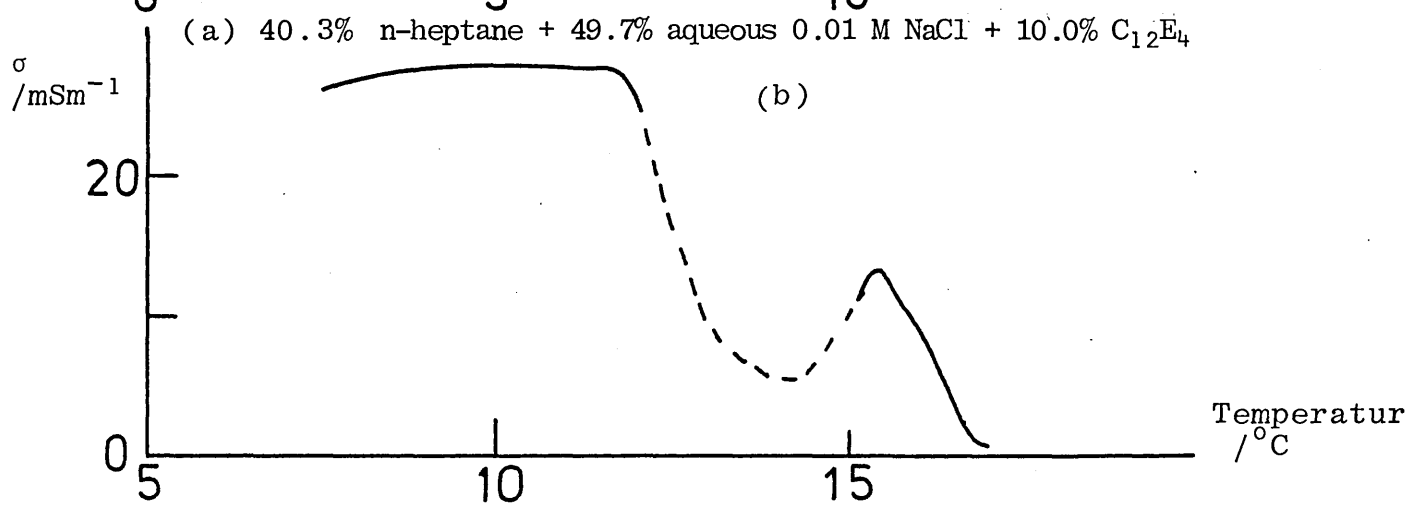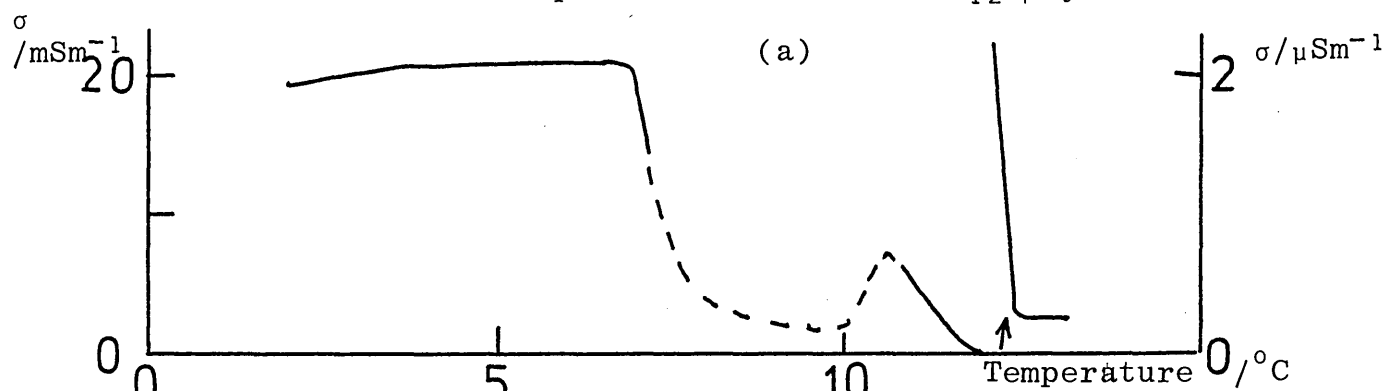
FIGURE 51

Isotropic liquid regions in ternary mixtures of
Brij 30 with water and n-heptane

n-heptane

Temperature
27° C

Iφ

Iφ ≡ isotropic liquid

Water

Brij 30

n-heptane

Temperature
20° C

Iφ   Iφ
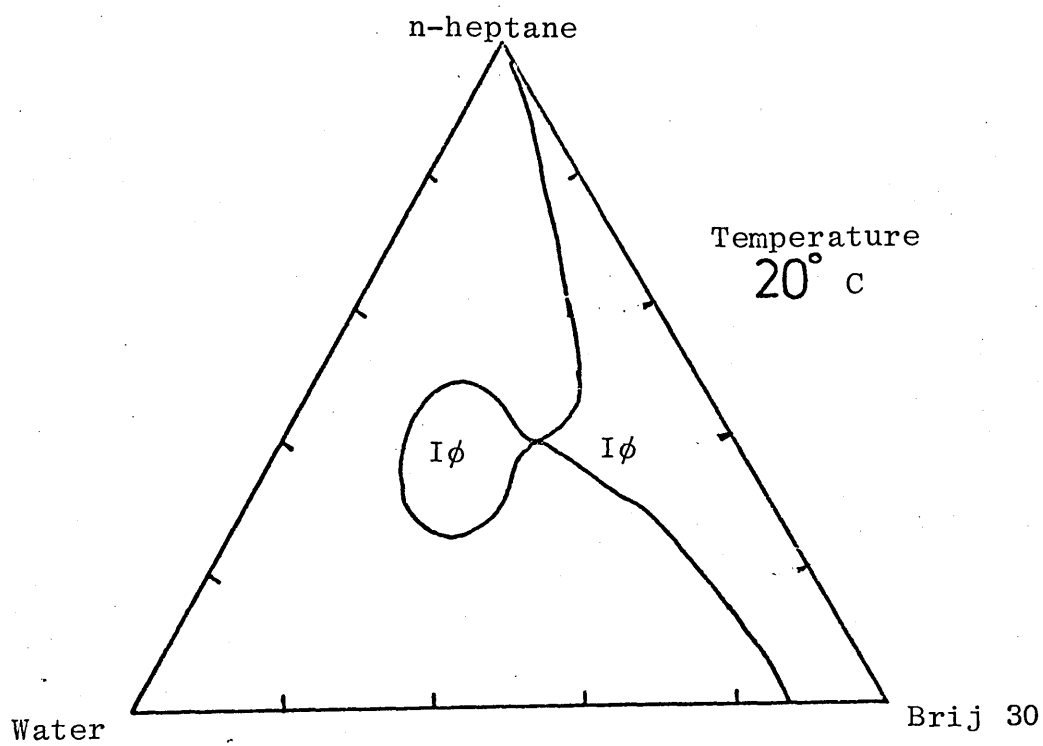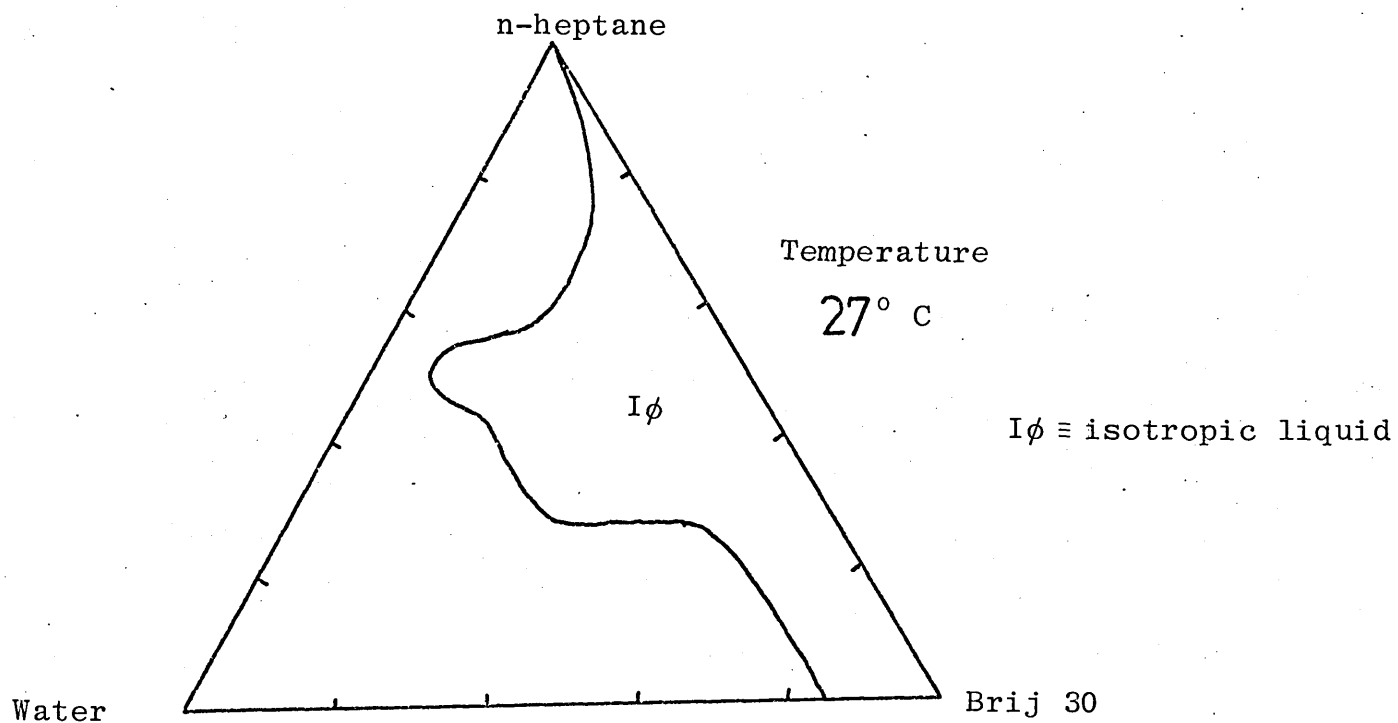
Water

Brij 30

FIGURE 52

Isotropic liquid regions in ternary mixtures
of Brij 30 with water and n-heptane

n-heptane

Temperature
40° C

Iφ ≡ isotropic liqui

Iφ
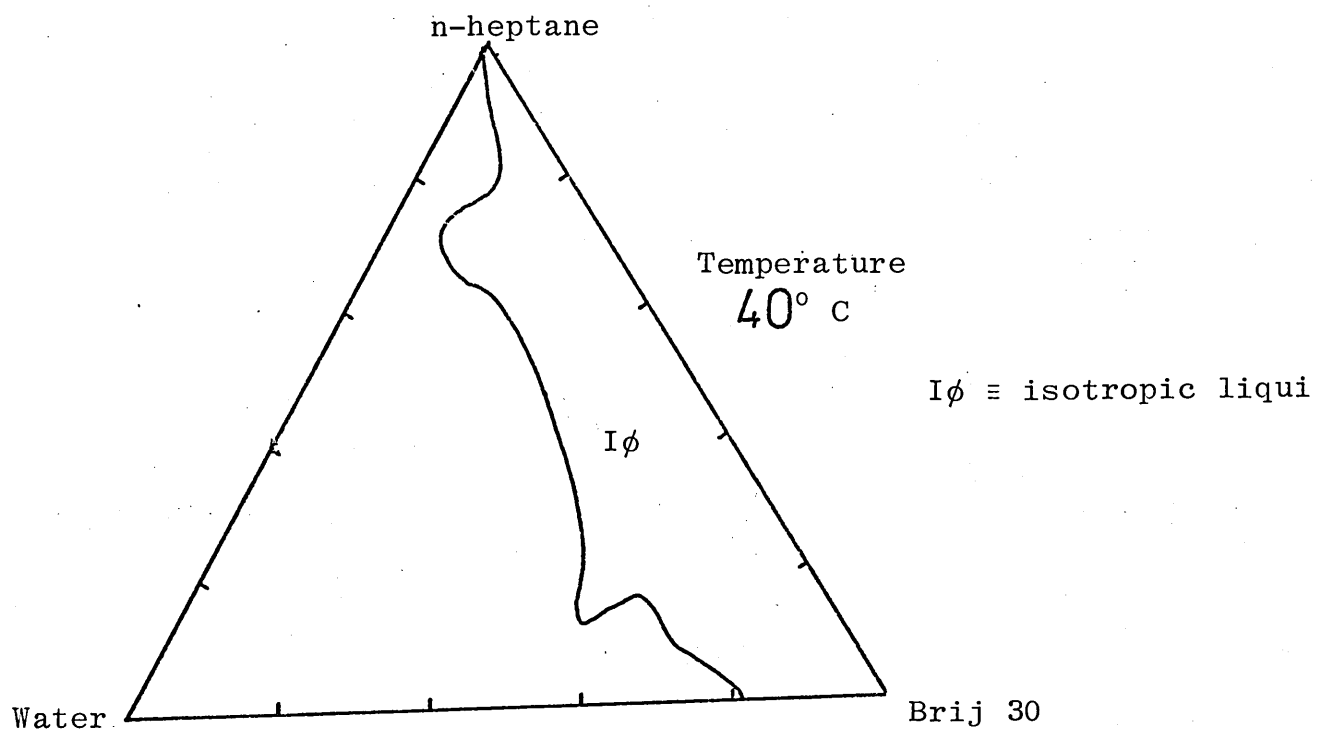
Water

Brij 30

5.6   Surfactant-water-n-alkane ternary mixtures

The isotropic liquid regions in ternary mixtures of
the surfactants $C_{12}E_4$ and Brij 30 with water and
heptane are given in Figures 46 to 48, 51 and 52.
Similar behaviour of the surfactants appears in the
regions of low water content, but differences are
evident in the regions of low surfactant content where
isotropic solutions are formed with $C_{12}E_4$ but not with
Brij 30.   As there is currently particular interest in
ternary mixtures containing low proportions of
surfactant   (microemulsions), detailed attention will be
given to such mixtures.   The isotropic liquid regions
of $C_{12}E_4$ in n-alkane + water systems with increasing
concentration of $C_{12}E_4$ for the n-alkanes hexadecane ,
decane and heptane are given in Figure 49 (p 275). For all
three n-alkanes there are two separate regions in
which isotropic liquids appear at about 15% by mass of
$C_{12}E_4$.   However, at lower surfactant concentration, the
hexadecane system displays markedly different behaviour
from the other two in that below 12% by mass of $C_{12}E_4$
no clear region occurs and between 12% and 14% of $C_{12}E_4$
the upper and lower isotropic regions appear to merge.

The dielectric properties of the ternary systems can
best be discussed by considering separately the
behaviour within and outside the temperature ranges in
which the mixtures form isotropic liquids.

5.6.1 Dielectric properties outside the temperature limits for isotropic liquids

The results given in Tables 59 to 62 and Figure 42 (p 230) show dielectric dispersion behaviour in the RF range as the temperature is lowered beyond the limit for isotropic liquids. The absence of dielectric dispersion at temperatures just above the cloud point is consistent with proposals that separation into two phases occurs at a temperature which is somewhat higher than the cloud point (11). At temperatures just above the cloud point, the mixture may still be regarded as a single phase system but with larger micelles. Since dielectric dispersion was not observed over the temperature range in which isotropic liquids are formed, similar behaviour would be expected just above the cloud point.

In contrast, at temperatures just below the lower limit for isotropic liquids very considerable structural changes occur for a very small temperature change, with separation into a two phase emulsion ((a), (b) and (c) in Figure 42) or formation of a liquid crystalline phase ((d) in Figure 42) depending on the composition of the mixture, occurring rapidly.

The observation of Cole-Cole arc type dispersion at these temperatures (Figure 42) is worthy of note, and it does appear that when dielectric dispersion occurs in emulsions, this type of dispersion is the norm. However,

it is considered incorrect to attribute observed Cole-
Cole arc type dispersion to the presence of a heterogeneous
structure as suggested by Peyrelasse et al (106) because
there are a number of examples of simple liquids which
also exhibit such dispersion, eg chlorinated diphenyls
(135).

5.6.2 Dielectric properties of ternary mixtures within temperature range for isotropic liquids

In order to attempt to explain the dielectric behaviour
of the ternary mixtures in the isotropic liquid region,
two approaches based on spherical dispersions have been
applied. In the first approach, it has been assumed
that the dielectric properties of the mixtures are due
to the water and n-alkane only and the permittivity values
for spherical dispersions have been calculated using the
equations of Rayleigh [2.14] for both W/O and O/W,
Hanai for W/O [2.31] and O/W [2.29] and Bruggeman [2.16]
for W/O.

In the second approach, the observed dielectric properties
have been considered to be due to contributions from all
three components of the mixture and the permittivity
values have been calculated using (i) the ideal mixing
equation [2.5] and (ii) spherical dispersions with shells
equations of Maxwell [2.55] and [2.56] for both W/O and
O/W dispersions.

The permittivities of the hydrocarbons heptane and decane at each measurement temperature were obtained from literature data (195). As the permittivity of hexadecane was not given, a value of 2.04 was adopted based on extrapolation of the literature values in reference 195 for the C_5 to C_{12} n-alkanes. The permittivity of water at each measurement temperature was calculated from the relation given by Malmberg and Maryott (43). The densities of the hydrocarbons were obtained from literature data (196). The densities of the hydrocarbons were all assumed to have the same temperature dependence and a value for this based on literature data for pentane (193) was used. The permittivities of the surfactants at each measurement temperature were obtained from the values given in this work.

The permittivity values given by the various mixture equations together with the experimental values for the $C_{12}E_4$ ternary mixtures are given in Table 71 and 72 and the Brij 30 ternary mixtures in Table 73.

5.6.2.1 Ternary mixtures of n-alkane–water–$C_{12}E_4$

5.6.2.1.1 Microemulsion region

Table 71

Comparison of experimental static permittivity values with values given by mixture equations.

Mass fraction of water	Mass fraction of n alkane	Mass fraction of $C_{12}E_4$	Temperature /°C	Experimental value	Rayleigh W/O	Rayleigh O/W	Hanai W/O	Hanai O/W	Brugge-man W/O	Ideal Mixing	Maxwell 3 Component W/O	Maxwell 3 Component O/W
	(1) Heptane											
0.40	0.50	0.10	4.2	20.3	4.7	24.3	7.1	20.2	6.1	27.9	5.2	21.4
0.40	0.50	0.10	13.0	7.3	4.7	23.4	7.1	19.6	6.1	26.8	5.1	20.7
	(2) Decane											
0.51	0.34	0.15	7.5	32.0	7.6	37.0	18.0	37.8	12.1	38.2	8.0	32.1
0.51	0.34	0.15	19.0	15.6	7.6	35.1	18.0	35.9	12.0	36.2	7.9	30.6
	(3) Hexa-decane											
0.49	0.33	0.18	24.3	28.1	7.9	35.0	19.4	32.4	12.3	36.3	8.1	29.2
0.49	0.33	0.18	33.3	19.2	7.9	33.7	19.4	31.3	12.2	34.9	8.0	28.2
0.52	0.35	0.13	28.4	26.3	8.0	35.2	20.7	32.4	13.0	37.8	8.2	30.7
0.52	0.35	0.13	31.4	23.1	8.0	34.7	20.7	32.0	12.9	37.3	8.2	30.3

In order to interpret the permittivity values of these
compositions, the results for the three n-alkanes studied
will be considered separately in the following sub-
sections.

(i)   n-heptane

Comparison between values given by the Hanai equations
for the mixture containing 40% by mass of water, 50%
heptane and 10% surfactant reveals very close agreement
with the Hanai equation for a spherical O/W dispersion
at the lower temperature and good agreement with the
Hanai equation for a spherical W/O dispersion at the
higher temperature. It is therefore suggested that in
this micellar mixture which can be termed a microemulsion
as the surfactant concentration was low, micellar
inversion from a normal (O/W) to an inverted (W/O)
micelle has take place between 4.2^{o} and 13.0^{o} C. Support
for such micellar inversion is given in the conductivity
data of Bostock (83), given in Figure 50, page 276.
On the basis of proposals made earlier, the agreement
with Hanai equation values suggests that the micellar
dimensions in this microemulsion are large and comparable
to those in dilute aqueous solutions of $C_{12}E_4$ which is
in agreement with the proposals on globule size in
microemulsions given by various authors (89, 90, 91).

There is evidence that deviation from spherical shape
occurs in these mixtures at intermediate temperatures

because the upper clear region appears at 10.8° C but the conductivity value does not fall to a value appropriate to that of an oil continuous phase until the temperature reaches 12° C as shown in Figure 50. In addition, the mixture exhibits streaming birefringence within the above temperature range. These observations led Bostock et al (197) to conclude that in the temperature range 10.2° to approximately 12° C the micellar aggregates have a basically lamellar structure. In view of this lamellar interpretation between 10° and 12° C, the possibility of non-spherical aggregates at the measurement temperature of 13.0° C in the dielectric studies cannot be excluded. As dielectric dispersion was not observed, it is possible that the appropriate permittivity value is given by ε_{∞} rather than ε_{s}, which with the Hanai equations is the same as the Bruggeman mixture equation value.

Use of the experimental permittivity value in the generalised Bruggeman equation derived in this work (equation $\boxed{2.64}$) gives a shape factor A_{a} = 0.27 which corresponds to prolate spheroids of axial ratio b/a = 1.2 when equation $\boxed{2.39}$ is used.

Alternatively, since deviations from the Hanai O/W equation were reported by Clausse et al (131) for O/W microemulsions with mass fractions of surfactant above about 10%, which were attributed by these authors to a

contribution by the surfactant to the dielectric
properties; it is possible that the Maxwell three
component equation may be more appropriate, even though
it is considered to be limited to relatively low volume
fractions of dispersed phase, as discussed in Chapter 2.

In order to determine the effect of spheroidal shape on
the permittivity of a three component mixture, equations
$[2.55]$ and $[2.56]$ have been modified by using the
Rayleigh equation $[2.14]$ which is the basis of $[2.55]$
and $[2.56]$ in the generalised form given by van Beek
(equation $[2.36]$). Application of this procedure gives
the following for the three component equations general-
ised to spheroidal shape:

$$\varepsilon_I = \varepsilon_{sh} \cdot \frac{\varepsilon_{sh} + [A_a(1 - \phi) + \phi](\varepsilon_2 - \varepsilon_{sh})}{\varepsilon_{sh} + A_a(1 - \phi)(\varepsilon_2 - \varepsilon_{sh})} \qquad [5.1]$$

and $$\varepsilon = \varepsilon_1 \frac{\varepsilon_1 + [A_a(1 - \phi) + \phi](\varepsilon_I - \varepsilon_1)}{\varepsilon_1 + A_a(1 - \phi)(\varepsilon_I - \varepsilon_1)} \qquad [5.2]$$

Application of these two equations to a W/O dispersion
of shape factor A_a = 0.18, which corresponds to prolate
spheroids of axial ratio a/b ≃ 2.0, gives a permittivity
value of 7.2 which agrees satisfactorily with the
experimental value of 7.3. Since small deviations from
spherical shape are not expected to be revealed by
streaming birefringence studies, prolate spheroids of
axial ratio of 1.2:1 given by the generalised Bruggeman
equation are considered to be as equally compatible with

the experimental data as a spherical shape on which the Hanai equation [2.31] is based. Although the axial ratio of 2:1 given by the three component equation is more likely to be revealed in streaming birefringence studies, this is not certain to be so and it is therefore considered that in this composition, the dielectric behaviour at the higher temperature may be satisfactorily described by the Hanai, generalised Bruggeman and generalised three component equations. The lower temperature data is satisfactorily accounted by by all three equations without the requirement of significant deviation from spherical shape.

In order to account for the conductivity behaviour of this mixture, Bostock et al (197) have proposed a model for phase inversion, in which at temperatures just below the inversion temperature the normal micellar aggregates have a lamellar shape. They proposed that under the critical interfacial energy conditions close to phase inversion, collision between two or more aggregates leads to the formation of semi-circular and eventually annular structures enclosing water. The phase inversion was suggested as arising from coalescence between these annular structures, eventually leading to the observed clear phase containing inverted micelles. The proposal of lamellar type structure formation as phase inversion is approached is supported by the predictions given by the conductivity equation [2.71] derived in the present

work because such a structure will arise from distortion from a spherical to oblate spheroidal shape which will cause the shape factor A_a to increase giving a lower conductivity. However, difficulty is encountered in justifying phase inversion on the basis of coalescence of annular structures because it would seem more probable that in coalescing the inverted micelles so formed would have an oblate spheroidal shape, which with rise of temperature, becomes spherical. This is counter to the predictions of equation $\boxed{2.75}$ which gives an increase in conductivity as the shape factor A_a reduces to the value of $\frac{1}{3}$ for spheres. In order to be compatible with equation $\boxed{2.75}$ a prolate rather than oblate spheroidal shaped inverted micelle is required.

A revised form of the proposals of Bostock et al (197) is proposed as follows. At the lower temperature, the oblate spheroidal micelles are envisaged as being distorted towards a more elongated structure. When coalescence occurs due to collision, it is suggested that as in the Bostock et al model, because the changes in curvature occur principally at the edges of these elongated spheroids, the coalescence will occur between the edges of two (or more) such spheroidal aggregates. However, because the effective collision cross-section will be greater along the 'long' side of these aggregates, it is considered more probable that this

FIGURE 53

(a)   Coalescence of oblate spheroidal normal micelles
       (shape distorted to show effect)

(b)   Coalescence of cylindrical W/O aggregates to
       form prolate spheroidal inverted micelle.

(a)

Water continuous
phase

oil

(b)

oil
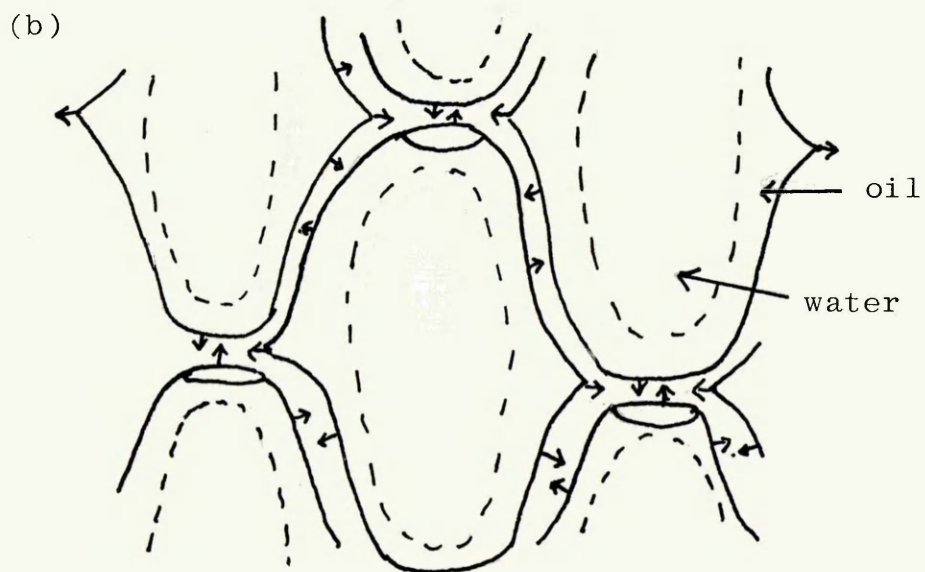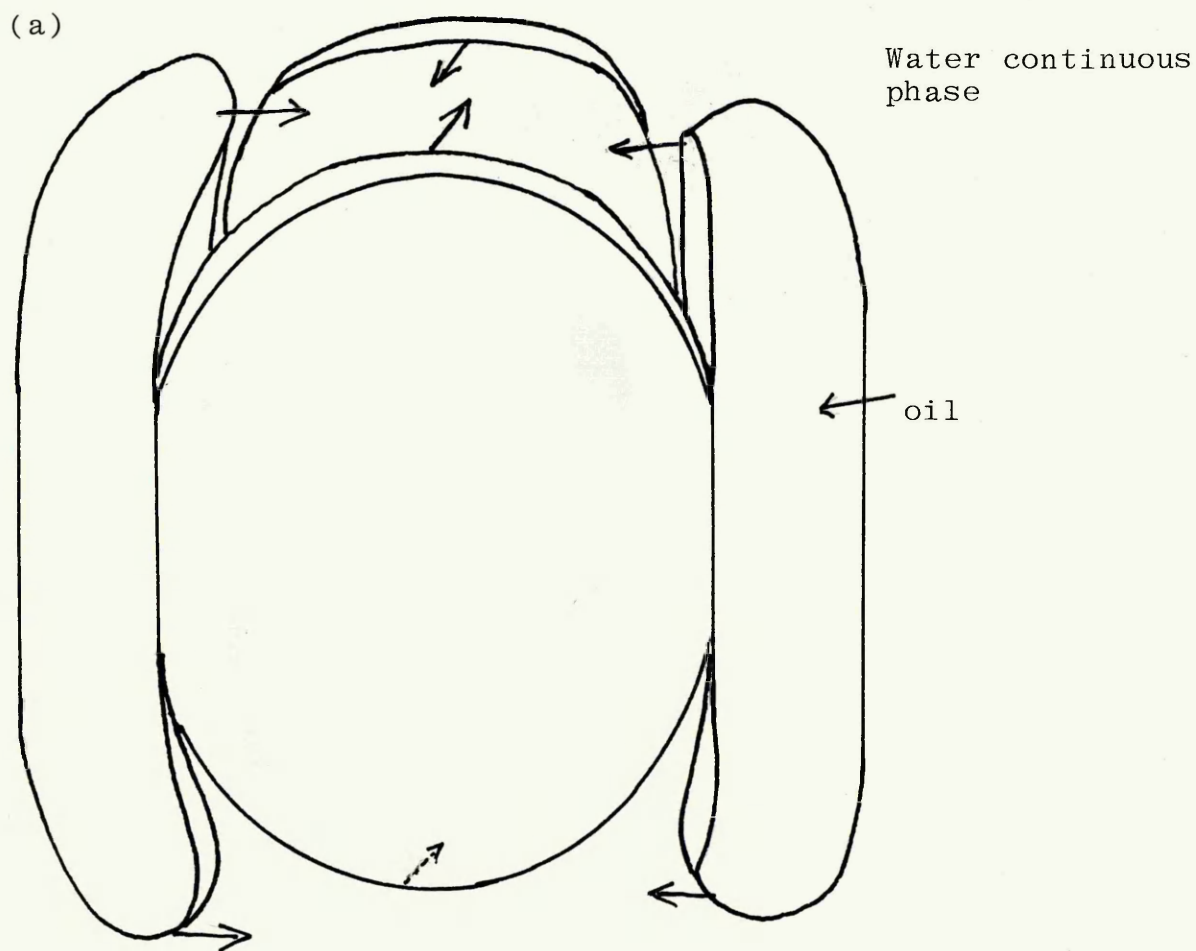
water

will lead to cylindrical rather than annular structures surrounding water. Coalescence between these cylindrical aggregates would lead to an inverted micellar structure of extended prolate spheroidal shape which with increasing temperature changes to a prolate spheroid and then a sphere. The proposed coalescence is sketched in Figure 53. The above behaviour will then be entirely compatible with predictions given by the conductivity equations [2.71] and [2.75]. These proposals are also in accord with predictions given by the permittivity equations [2.72] and [2.76] as a continuous fall in permittivity between 4.2° and 13° C was observed.

(ii) n-decane

The ternary mixture with the n-alkane decane contained a small proportion of surfactant (15% by mass) and can thus be termed a microemulsion. The mixture exhibits a marked permittivity fall between 7.5° and 19.0° which suggests that inversion from normal to inverted micelles has occurred between the two temperatures. However the Hanai O/W equation gives a permittivity value at 7.5° C which is too high and the Hanai W/O equation also gives too high a permittivity value at 19° C.

The conductivity data of Bostock (83) for this mixture (Figure 50) suggests the presence of normal micelles at the lower temperature but at the higher temperature the conductivity value is too high to justify an inter-

pretation based on inversion from normal to inverted micelles.

The lower temperature dielectric data is very satisfactorily accounted for by the three component O/W equation [2.55] and [2.56] and the higher temperature data is intermediate between values given by the Hanai W/O and Bruggeman W/O equations.

Since the surfactant concentration in the decane mixture is higher than that in the heptane one considered in (i), it is likely that effects due to the contribution of the surfactant layer to the dielectric properties will be more significant in the decane mixture. The close agreement between the three component O/W values and the lower temperature data clearly gives support to this proposal. The poor agreement between the spherical three component equation for W/O and the higher temperature data could be due to incomplete micellar inversion and be related to the presence of non-spherical micellar aggregates. Application of the generalised three component equations to the higher temperature data for an O/W dispersion of shape factor $A_a = 0.78$, which corresponds to oblate spheroids of axial ratio $b/a = 5.5$ when equation [2.40] is used, gives a permittivity value of 15.6. Alternatively for a W/O dispersion of shape factor $A_a = 0.1$, which corresponds to prolate spheroids of axial ratio $a/b \simeq 3$ when equation [2.39] is used,

gives a permittivity value of 15.6. Both values are the same as the experimental value.

It is thus possible to account for the dielectric behaviour at the higher temperature on the basis of either oblate spheroidal normal or prolate spheroidal inverted micelles.

Tanford (194) has calculated aggregation numbers for spheroidal micelles and his results show that for C_{12} surfactants an oblate spheroidal structure of axial ratio 1.25:1 has the same aggregation number as that of a prolate spheroidal structure of axial ratio 1.5:1. Assuming the micelle aggregation number is unchanged during inversion, it is proposed that when an oblate spheroidal micelle is inverted, the prolate spheroidal micelle so formed will have an axial ratio (1.5/1.25) higher than the oblate type. Thus in order to decide whether a micellar aggregate is normal or inverted, the criterion adopted will be that the axial ratio for the prolate spheroid must be less than 6/5 times that for the oblate spheroid in order that the former be selected.

Since the axial ratio in the decane mixture at the higher temperature is lower for a prolate spheroidal shape, it is suggested that the aggregates are prolate spheroidal inverted micelles.

Although the two component equations are considered to
be of more limited use in this mixture due to neglect
of the contribution of surfactant layer, it is of
interest to compare conductivity values given by the
equations for spheroidal dispersions with those given for
spherical dispersions. For oblate spheroidal normal
micelles of shape factor $A_a = 0.78$ as given above, the
conductivity of this mixture given by equation $[2.71]$
is a factor of 7 lower than that for spherical normal
micelles. For prolate spheroidal inverted micelles
of shape factor $A_a = 0.1$ the conductivity of this
mixture given by equation $[2.75]$ is a factor of 170 higher
than that given for spherical inverted micelles. The
data of Bostock reveals that the conductivity at the
higher temperature is (i) about a factor of 70 lower than
that at the lower temperature and (ii) it is about a
factor of 1,500 higher than the value obtained for the
heptane mixture in the upper clear region when inversion
is complete. As the discrepancies between the conductivity
values given by both the oblate spheroidal O/W and the
prolate spheroidal W/O equations and the experimental data
are similar, both the oblate and prolate spheroidal
shapes are about equally probable on the basis of
conductivity values. However, as these comments are based
on two component equations which are considered to be
less adequate, the prolate spheroidal shape is preferred
due to its lower axial ratio as given by the three

component permittivity equations.

(iii) <u>n-hexadecane</u>

In the ternary mixture with hexadecane containing 18%
by mass of surfactant, the dielectric data at the lower
temperature is consistent with a normal micellar inter-
pretation where, as in the decane mixture, since the
surfactant concentration is higher than the 10% used in
the heptane mixture, the contribution by the surfactant
layer to the dielectric behaviour is expected to be more
significant. This is revealed by the more satisfactory
agreement with the three component O/W equation than with
the Hanai O/W equation. At the higher temperature however,
agreement with the Hanai W/O equation is good which would
suggest the presence of spherical inverted micelles.
Such behaviour is contrary to the proposals of Bostock
who has suggested that, on the basis of conductivity
data given in Figure 50, normal micelles are present in
the lower temperature clear region whereas in the higher
temperature clear region, the conductivity is much too
high to justify an interpretation based on micellar
inversion.

Since a micellar inversion proposal cannot be maintained,
it is considered that this agreement with the Hanai W/O
is entirely fortuitious and further emphasises the
limitations of the Hanai equations in applications to
microemulsions of nonionic surfactants at higher

surfactant concentrations. As the three component
equation is the most appropriate in describing the
lower temperature behaviour, it is considered to be
also the most appropriate for the higher temperature
behaviour. The deviation between the spherical three
component equation and the experimental data is again
attributed to deviation from spherical shape, and as
in the decane mixture, there are two possibilities
(a) oblate spheroidal normal or (b) prolate spheroidal
inverted micelles. The generalised three component
equation for O/W with a shape factor A_a = 0.65, which
corresponds to oblate spheroids of axial ratio b/a = 3.3,
gives a permittivity of 19.2; whereas for W/O with a
shape factor A_a = 0.07, which corresponds to prolate
spheroids with an axial ratio a/b = 4.2, the equation
gives a permittivity of 18.8. Both permittivity values
compare satisfactorily with the experimental values
of 19.2

In this case, the axial ratio for the prolate shape is
a factor of 4/3 higher than the oblate shape. Since this
is higher than the 6/5 figure discussed earlier, it is
considered that the aggregates at the higher temperature
are more likely to be oblate spheroidal normal micelles.

In the hexadecane mixture containing 13% by mass of
surfactant, the permittivity at 28.4° C is too low to
be accounted for by any of the spherical O/W equations

and at 31.4° C is too high to be accounted for by any of the spherical W/O equations. At the lower temperature, the three layer O/W equation gives the closest agreement and at the higher temperature the Hanai W/O equation gives closest agreement.

The data of Bostock for this composition (Figure 50) reveals a progressive fall of conductivity as the temperature is increased with no evidence of phase inversion behaviour. Since the conductivity at 28.4° C is approximately 5% lower than the value at the lower limit of the clear region (25° C), it is quite possible that the micelles at 28.4°C are normal but of an oblate spheroidal rather than spherical shape as equation [2.71] gives a lower conductivity for the oblate spheroidal shape. Such a shape would account for the measured permittivity being lower than that given by any of the O/W equations. Since the three component equation is considered to be the most suitable for describing the dielectric behaviour at surfactant concentrations higher than about 10% by mass, it is presumed that this equation is the most suitable one for describing the behaviour of this mixture.

At the lower temperature for an O/W dispersion of shape factor $A_a = 0.5$, which corresponds to oblate spheroids of axial ratio $b/a = 1.9$, a permittivity value of 26.0 is obtained. This is satisfactorily close to the

experimental value of 26.3.

At the higher temperature, it is possible that the aggregates are either oblate spheroidal normal or prolate spheroidal inverted micelles. For an O/W dispersion of shape factor A_a = 0.6, which corresponds to oblate spheroids of axial ratio b/a = 2.5, a permittivity value of 22.5 is obtained. For a W/O dispersion of shape factor A_a = 0.05, which corresponds to prolate spheroids of axial ratio a/b $\simeq$ 5, a permittivity value of 22.6 is obtained. The permittivity values given for both types of micellar aggregate compare satisfactorily with the experimental value of 23.1.

It is thus again possible to account for the experimental value at the higher temperature by either normal oblate or inverted prolate micelles. However, as the axial ratio for an oblate spheroidal shape is much less than that for the prolate shape, the oblate shape is favoured.

Whilst it is not possible to be unequivocal about the micellar structure, it could be that the micellar inversion process may be due to an increasingly oblate spheroidal shape becoming less favoured than a prolate shape and then inversion occurs when the axial ratio for a prolate spheroidal inverted micelle becomes lower than that requried for an oblate spheroidal normal micelle subject to the 6/5 condition already discussed.

With the above interpretation, micelle inversion as the temperature is raised is envisaged as a continuous process involving change from spherical to oblate spheroidal to prolate spheroidal and back to spherical shape. A well-defined boundary between the transition from oblate spheroidal normal to prolate spheroidal inverted micelles would not be expected and this is in agreement with the phase diagram, conductivity and permittivity behaviour.

(iv)   Summary of microemulsion behaviour

The observed dielectric behaviour of the microemulsions formed with the n-alkanes heptane, decane and hexadecane can be satisfactorily accounted for on a model for phase inversion involving micelle shape changes : spherical normal $\rightarrow$ oblate spheroidal normal $\rightarrow$ prolate spheroidal inverted $\rightarrow$ spherical inverted. In the heptane mixture inversion is complete, ie all four changes occur, whereas with the longer alkanes the above process cannot be completed. In the decane mixture, the prolate spheroidal inverted micelle is formed but in the hexadecane mixtures, two phases are formed when the micelle is still an oblate spheroidal normal micelle.

These observations are consistent with the proposals of other workers. Particular attention has been given to the so-called "surfactant phase" observed at temperatures close to that for inversion in microemulsions of $C_{12}E_4$

with the n-alkane hexadecane (82, 84, 86, 87). Shinoda
et al (84, 87) suggested that this phase has a basically
lamellar shape. Friberg et al (86) showed that a regular
layer structurehaving constant spacing was ruled out by
the results of low angle X-ray diffraction and favoured
an interpretation based on closed structures in which
the mixture involved a rather complex mixing of spherical
aggregates together with planar structures. These authors
also suggested that deviation from spherical shape was
revealed in anomalous hydrocarbon solubilisation behaviour.
The model of phase inversion given in this work, which is
a modification of that of Bostock et al (197) is much
more detailed and more satisfactory in that deviation
from spherical shape is accounted for without the
requirement of postulating the complex "mix" of Friberg
et al (86) or the basically lamellar structure of
Shinoda et al (84, 87). The observation of streaming
birefringence behaviour indicates that the phase
inversion model of Robbins (198) which is based on
spherical micelles in unsatisfactory, whereas the
spheroidal shapes proposed in this work are consistent
with such birefringent behaviour.

Although the O/W microemulsion studies of Mackay and
Agarwal (199) were on the rather different system of
the commerical nonionic surfactant Tween with water, an
oil and n pentanol; their conductivity data, which

exhibited significant deviations from the Hanai-

Bruggeman equation, is of interest. These authors

favoured an interpretation of their data based on

increase in the size of the dispersed oil globules as

oil was added causing the microemulsion to become

polydisperse. It is not clear why polydispersity should

cause the observed conductivity behaviour.

These authors did not discuss micelle shape. If an

oblate spheroidal rather than spherical shape is adopted,

the observed conductivity behaviour can be accounted for

by using equation $[2.71]$ derived in this work because

with a shape factor $A_a = 0.6$, which corresponds to oblate

spheroids of axial ratio $b/a = 2.5$, the observed

conductivity behaviour is accurately described. Such

micelle dimensions are comparable to values given both in

this work and by Tanford et al (74).

5.6.2.1.2 Other ternary mixtures

Table 72

Comparison of experimental static permittivity values with values given by mixture equations.

Mass fraction of water	Mass fraction of heptane	Mass fraction of $C_{12}E_4$	Temperature /°C	Experimental Value	Rayleigh W/O	Rayleigh O/W	Hanai W/O	Hanai O/W	Bruggeman W/O	Ideal Mixing W/O	Maxwell 3 component W/O	Maxwell 3 component O/W
0.10	0.70	0.20	17.2	3.70	2.5	6.9	2.5	5.0	2.5	8.5	2.9	6.6
	0.60	0.30	17.7	4.29	2.5	7.4	2.6	5.3	2.5	9.0	3.3	7.2
	0.40	0.50	17.4	5.71	3.8	10.0	3.0	7.2	2.9	10.2	4.2	7.9
	0.20	0.70	17.4	7.97	3.8	17.1	4.7	13.2	4.3	11.7	5.5	9.5
0.30	0.50	0.20	16.9	7.0	4.1	19.0	5.3	15.1	4.7	21.6	4.6	16.5
0.70	0.10	0.20	20.2	32.3	20.5	60.9	329.2	60.2	41.0	54.4	17.8	47.4

The experimental data given in Table 72 for the set of
mixtures containing 10% by mass of water are more accurately
described by W/O equations for high hydrocarbon concen-
tration with the three component equation giving closest
agreement, but the measured permittivity values are higher
than those given by any of the W/O equations. This
discrepancy between the W/O equation values and experiment
increases with increasing surfactant concentration and
at 70% by mass of surfactant (20% heptane), the three
component O/W equation gives the best fit.

It is suggested that the dielectric behaviour of these
micellar solutions is consistent with a structure in
which there are inverted micelles at high hydrocarbon
concentration and normal micelles at low hydrocarbon
concentration. Inverted micelles would be more likely
at high hydrocarbon concentration and, since it has been
proposed that binary mixtures of $C_{12}E_4$ and water contain
normal micelles over the whole composition range, normal
micelles would also be expected at low hydrocarbon
concentration. The discrepancies between the experimental
data and the three component equation values are attributed
to inadequacies in this equation at higher volume fractions
of the shell component.

The temperature dependence of the permittivity $d\varepsilon_S/dT$,
of the 10% water mixtures changes from $- 9.9 \times 10^{-2}$ $^{\circ}C^{-1}$
at the highest heptane concentration (70% by mass) to an
almost concentration-independent value of $- 3.2 \times 10^{-2}$ $^{\circ}C^{-1}$

when the heptane concentration is 40% and below. The more pronounced temperature dependence at high heptane concentration would not be expected on the basis of the various mixture equations because the surfactant has a higher temperature coefficient than the heptane. The higher $d\varepsilon_S/dT$ value for the 70% heptane mixture could be due to micellar reorganisation.

The data of Bostock (83) for the 10% water mixture containing 70% heptane reveals a rapid fall in conductivity over a very small temperature range, to account for which the possibility of inversion from normal to inverted micelles has been proposed. It is suggested that the anomalously high $d\varepsilon_S/dT$ value for this mixture is due to micellar inversion behaviour.

In this mixture, it is considered that the micelles will be rather smaller than in the microemulsions and are thus less likely to deviate from spherical shape. Hence a mechanism of inversion based on change of micelle shape as proposed by Bostock et al (197) and this author for microemulsions cannot be applied here.

A tentative explanation of inversion in these mixtures may be given in terms of the dynamic equilibrium of the micelle. Winsor (200) has pointed out that micelles must be considered as structures capable of rapid breakdown and, due to the short half-life of micellar breakdown, rapid re-formation. At lower temperatures

the interfacial energies will be such that normal micelles are continuously broken and reformed. Using the formalism of Winsor (200) where the term R , defined by

$$R = \frac{\text{tendency of surfactant to become convex to oil}}{\text{tendency of surfactant to become convex to water}} ,$$

is used, normal micelles have R < 1. At higher temperatures, the micelles are inverted (R > 1), and these inverted micelles are similarly continuously broken and reformed. At the temperature corresponding to phase inversion R = 1 and in principle there is equal probability of formation of either normal or inverted micelles. It is suggested that the so called breakdown of micelles under both the R < 1 and R > 1 conditions does not involve complete micellar dissociation but rather only a number of the molecules contained in a micelle. At low temperatures where R is less than unity, the effect of increase of temperature can be regarded as causing an increase in the number of molecules being involved in the micellar breakdown process. At a critical temperature, T_c, corresponding to R = 1, there will be complete micellar dissociation and as a normal micelle dissociates it will reform as either a normal or inverted micelle depending on whether , due to local thermal fluctuations, the temperature is above or below T_c when the micelle is reformed.

As the temperature is raised fractionally above the
R = 1 temperature, the micelles will be inverted and
the number of molecules involved in the 'breakdown'
will then steadily fall as the temperature is raised
further above the R = 1 condition. With this inter-
pretation, there will be no deviation from spherical
symmetry which is consistent with the absence of
streaming birefringence effects in this 10% by mass of
water mixture (83). On the other hand, the above
interpretation is not applicable to the microemulsions
because at all compositions studied, streaming bire-
fringence behaviour is observed at temperatures close
to that for inversion (83) indicating the presence of
non-spherical aggregates.

The experimental value of 7.0 for the $C_{12}E_4$ ternary
mixture containing 30% by mass of water and 50% heptane
is not accounted for by any of the mixture equations.
As the permittivity is rather closer to values given by
W/O rather than the O/W equations, it is considered
probable that the micelles are inverted. This proposal
is consistent with the phase diagram given in Figure 47
(p 273) because at 17° C the isotropic liquid region
shows continuity to the alkane corner. In addition, the
measurement temperature is rather higher than the
temperature at which inversion occurred in the micro-
emulsion containing n-heptane.

As the surfactant concentration was 20%, the three component equation is considered the most appropriate. The discrepancy between theoretical and experimental values could be due to inadequacies in this mixture equation when the volume fraction of the surfactant shell is comparable with that of the water core, as is the case for inverted micelles in this mixture. Alternatively, because the surfactant concentration is only marginally higher than that used in the microemulsions, the discrepancy could be due to prolate spheroidal rather than spherical micelle shape as proposed for the microemulsions above the inversion temperature. If the micelles are assumed to have a prolate spheroidal shape of axial ratio $a/b \simeq 2$, there is good agreement between theory and experiment.

The experimental value of 32.3 for the $C_{12}E_4$ ternary mixture containing 70% by mass of water and 10% heptane is not accounted for by any of the mixture equations. Since the hydrocarbon concentration of 10% is very low, it is likely that the micellar structure will be very similar to that of the binary mixtures of the surfactant with water for which normal micelles are favoured. This interpretation is supported by the fairly similar permittivity values given by the binary aqueous mixtures at approximately similar proportions of surfactant and water. The poor agreement between the three component O/W equation and the experimental data is

probably due to inadequacies in the equation because
for normal micelles the volume fraction of the
surfactant shell is greater than that of the hydrocarbon
core. Alternatively there could be a contribution due
to deviation from spherical to oblate spheroidal shape,
as proposed for the binary mixtures of $C_{12}E_4$ with water
at low surfactant concentration.

5.6.2.2   Brij 30 ternary mixtures

The isotropic liquid regions are shown in Figures 51
and 52 p 277, 278.

Table 73

Comparison of experimental values with values given by mixture equations.

Mass fraction of water	Mass fraction of heptane	Mass fraction of Brij 30	Temperature /°C	Experimental Values	Rayleigh W/O	Rayleigh O/W	Hanai W/O	Hanai C/W	Bruggeman W/O	Ideal Mixing	Maxwell 3 component W/O	Maxwell 3 component O/W
0.10	0.60	0.30	27.5	3.0	2.5	7.2	2.6	5.2	2.5	8.8	3.3	7.1
	0.50	0.40	27.5	4.4	2.6	8.3	2.8	6.0	2.7	9.4	3.7	7.3
	0.40	0.50	30.0	5.0	2.8	9.6	3.1	7.0	3.0	9.9	4.2	7.7
	0.30	0.60	27.0	5.7	3.1	11.8	3.5	8.8	3.3	10.7	4.8	8.9
	0.20	0.70	23.2	7.3	3.7	16.1	4.6	12.4	4.2	11.6	5.6	9.5
	0.10	0.80	40.0	9.1	5.3	24.0	8.9	20.6	7.1	11.5	6.3	9.3
0.20	0.60	0.20	33.5	4.8	3.1	11.7	3.5	8.6	3.3	14.0	3.7	10.6
	0.50	0.30	34.5	5.6	3.3	13.0	3.9	9.8	3.6	14.7	4.1	11.3
	0.40	0.40	32.4	6.8	3.7	15.5	4.6	12.0	4.2	15.6	4.7	12.0
	0.30	0.50	30.0	7.3	4.2	19.3	5.8	15.6	5.1	16.5	5.5	12.9
	0.20	0.60	29.0	8.8	5.4	25.5	9.1	22.0	7.3	17.8	6.5	14.1
	0.10	0.70	40.0	11.3	8.3	35.5	24.1	33.1	12.7	17.5	7.4	13.8
0.30	0.50	0.20	27.5	5.5	4.0	18.2	5.4	14.8	4.8	20.8	4.6	15.9
	0.40	0.30	23.0	8.2	4.6	21.8	6.7	18.0	5.7	22.3	5.4	17.2
	0.30	0.40	26.4	9.6	5.4	25.8	9.1	22.2	7.3	23.2	6.4	18.1
0.35	0.50	0.15	27.5	6.0	4.4	20.1	6.1	16.4	5.3	23.6	4.9	18.1
0.40	0.40	0.20	21.2	7.9	5.3	26.0	8.9	22.3	7.2	28.3	6.0	22.1
	0.30	0.30	21.2	8.8	6.6	31.7	13.7	28.4	9.9	29.6	7.2	23.3

As the binary mixture studies of surfactant and
water revealed considerable differences between the
dielectric behaviour of the surfactants $C_{12}E_4$, $C_{12}E_6$
and $C_{12}E_8$, the uncertain polydispersity of Brij 30
precludes detailed interpretation of the dielectric
behaviour.

The mixtures containing 10% by mass of water are
considered to be satisfactorily accounted for by
proposing inverted micelles at high hydrocarbon
concentration and normal micelles at low concentration.
As in the $C_{12}E_4$ mixtures of similar composition
the measured permittivities are not satisfactorily
accounted for by the mixture equations. This is again
attributed to inadequacies in the equations at higher
surfactant concentrations.

The conductivity data of Bostock (83) is consistent
with an interpretation based on inverted micelles at the
higher hydrocarbon concentrations and normal micelles
at the lower concentrations. As in the $C_{12}E_4$ mixtures,
since the surfactant itself is considered to contain
normal micellar aggregates, normal micelles are to be
expected at low hydrocarbon concentrations.

The mixtures at 20% by mass of water are also considered
to contain inverted micelles at the higher hydrocarbon
concentrations and normal micelles at lower concentrations.

However, the agreement between calculated values and the experimental data at low hydrocarbon content is unsatisfactory, possibly due to polydispersity in the surfactant. At 30% by mass of water, there is encouraging agreement with the Hanai W/O values for two of the compositions, indicating that the micelles are inverted and of large size. The 35% water mixture gives similarly good agreement with the Hanai W/O equation. At 40% by mass of water, the situation is less satisfactory . A mean of the Bruggeman W/O (ie Hanai equation for ε_∞) and that of the Hanai W/O is required for the 20% Brij 30 mixture, whereas at 30% Brij 30 the Bruggeman W/O is the best. It is suggested that these mixtures contain inverted micelles.

Conductivity data of Bostock (83) is again consistent with an interpretation of the 20% water data on the basis of inverted micelles at higher hydrocarbon concentrations and normal micelles at lower concentrations. The conductivity data for the mixtures with water concentrations in the range 30 to 40% by mass at the measurement temperatures of the dielectric studies is consistent with an interpretation based on inverted micelles (83). Inverted micelles for these 35% and 40% water mixtures are considered likely on the basis of inversion temperatures because the $C_{12}E_4$ microemulsions with n-heptane exhibited inversion between 4.2° and $13.0^\circ C$. As the measurement temperatures in these Brij 30 ternary

mixtures were above 20° C, inverted micelles are to be expected.

5.7 Conclusions

5.7.1 Surfactant-water binary mixtures

For all compositions studied the micelles are normal (O/W) over the whole composition range in the temperature regions in which clear phases occur. For the shortest oxyethylene chain length surfactants, $C_{12}E_4$ and Brij 30, the static permittivity values at higher concentrations are lower than the ideal mixing equation values, and are satisfactorily described by the Hanai-Bruggeman equation for spherical dispersions. Deviations at low surfactant concentration are attributed to either oblate spheroidal micelle shape or secondary aggregation of micelles. Using equations derived in this work for concentrated dispersions of spheroidal globules, the oblate spheroidal interpretation requires an axial ratio of 3.5:1 in $C_{12}E_4$ and 2.6:1 in Brij 30 at the lowest concentrations.

The permittivity values of $C_{12}E_6$-water mixtures over most of the concentration range are satisfactorily described by the Rayleigh equation. None of the mixture equations describes the permittivity behaviour of $C_{12}E_8$-water mixtures. The dielectric behaviour of the $C_{12}E_6$ and $C_{12}E_8$ mixtures is attributed to progressively smaller micelle sizes for a given alkyl chain length as

the length of the oxyethylene chain is increased. This
leads to an increasing contribution by co-operative
molecular association between the ethylene oxide groups
and water which gives an enhanced permittivity value.
There is a basis for believing that there might be a
contribution due to prolate spheroidal micelles in the
$C_{12}E_6$-water mixtures at the lowest concentration and in
the $C_{12}E_8$ mixtures over the whole concentration range.
However in the $C_{12}E_8$ mixtures, this latter effect is
considered to be of only secondary importance.

5.7.2   Surfactant-n-alkane   binary mixtures

The dielectric behaviour of binary mixtures of Brij 30
with heptane is attributed to the presence of inverted
micelles at low surfactant concentration and normal
micelles at high concentrations. The permittivity
values are satisfactorily described by heterogeneous
mixture equations, with the Rayleigh equation being
the most suitable.

5.7.3   Surfactant-water-n-alkane ternary single phase mixtures

The dielectric behaviour of the microemulsion of $C_{12}E_4$
with water and n-heptane is satisfactorily described in
terms of a structure in which there are spherical normal
micelles at the lower temperature and spherical inverted
micelles at the higher temperature. On the basis of
equations for both the permittivity and conductivity
of a spheroidal dispersion given in this work, the

inversion behaviour can be described in terms of micelle shape changes. With increase of temperature the spherical normal micelle changes to an oblate spheroidal shape and then by coalescence of extended oblate-spheroidal aggregates, a prolate spheroidal inverted micelle is formed, which with increase of temperature, becomes spherical.

The rather different behaviour of microemulsions with the n-alkanes decane and hexadecane is attributed to the greater length of the alkyl chain causing the system to form two phases before the above inversion process can be completed. With decane this occurs when the prolate spheroidal inverted micelle has formed, whereas with hexadecane, it occurs when the aggregates are oblate spheroidal normal micelles.

The behaviour of ternary mixtures containing 10% by mass of water is considered to be satisfactorily accounted for by inverted micelles at high hydrocarbon concentration and normal micelles at low concentration. In the mixture containing 10% water, 70% heptane and 20% $C_{12}E_4$, micelle inversion has been proposed which has been interpreted in terms of the dynamic equilibrium of the micelle. Deviations between theory and experiment are attributed primarily to limitations of the mixture equations at higher surfactant concentrations.

The dielectric behaviour of Brij 30 ternary mixtures

at high water concentration is interpreted in terms of inverted micelles. At low water concentrations there are similarities with the $C_{12}E_4$ system in that the micelles are again inverted at high hydrocarbon concentrations and normal at low concentrations. The polydispersity of this surfactant precludes detailed interpretation.

5.8 Further Work

It is suggested that dielectric studies of the compositions reported in this work be performed at higher frequencies in order to determine whether or not the dielectric dispersion predicted by the generalised Hanai equations derived in this work occurs in these systems. Such studies will give more information on the applicability or otherwise of the equations to spheroidal micellar systems.

In order to gain support for proposals given in this work, it is desirable to investigate the dielectric behaviour of both binary and ternary micellar solutions of other members of the polyoxyethylene-alkyl ether series surfactants. The $C_{12}E_3$ -water system should be of value because it has a phase diagram similar to that of the $C_{12}E_4$ system (187) but the shorter oxyethylene chain will result in even larger micelles than in $C_{12}E_4$. Thus effects due to oblate spheroidal shape should be more pronounced and should enable the proposals given in

this work concerning micelle shape to be further evaluated.

The $C_{16}E_{12}$- and $C_{10}E_6$-water systems should also be of value because their phase diagrams show similarity to the $C_{12}E_8$ system in that a hexagonal liquid crystalline phase is the dominant feature at lower temperatures (187). As in $C_{12}E_8$ this will result in prolate spheroidal micelles being more probable. The relative balance between the alkyl chain and the polar headgroup for these two systems will be different from that for $C_{12}E_8$, hence the relative contributions to measured permittivity values of prolate spheroidal shape and association between headgroups and water will be different.

It would also be of interest to study the dielectric properties of microemulsions of other polyoxyethylene alkyl ether surfactants to obtain confirmation of the structural proposals given in this work.

REFERENCES

1. Pimentel G C and McClellan A L - The Hydrogen Bond

    W H Freeman and Company, San Francisco and

    London 1960

2. Vinogradov S N and Linnell R H - Hydrogen Bonding

    Van Nostrand Reinhold Company, New York 1971

3. Bordewijk P, Gransch F and Böttcher C J F

    Trans Far Soc 1970, 66, 293

4. Fletcher A N

    J Phys Chem 1972, 76, 2562

5. Dannhauser W and Flueckinger A F

    Phys Chem Liq 1970, 2, 37

6. Brink G, Campbell C and Glasser L

    J Sth Afr Chem Inst 1976, 29, 136

7. Brown A C and Ives D J G

    J Chem Soc 1962, 1608

8. Lawrence A S C, McDonald M P and Stevens J V

    Trans Far Soc 1969, 65, 3231

9. Fendler J H and Fendler E J - Catalysis in micellar

    and macromolecular systems

    Academic Press, New York and London, 1975

10. Shinoda K, Nakagawa T, Tamamushi B-I and Isemura T

    Colloidal Surfactants

    Academic Press, New York and London, 1963

11. Becher P and Schick M J - Nonionic Surfactants Ed Schick

    M J   Edward Arnold Publishers (Ltd), London, 1967

12. O'Connell J P and Brugman R J - Improved Oil Recovery
    by Surfactant and Polymer Flooding
        Eds Shah D O and Schechter R S - Academic Press
        New York and London 1977

13. Debye P - Polar Molecules
        Chemical Catalog Co, New York, 1929

14. Onsager L
        J Am Chem Soc, 1936, $\underline{58}$, 1486

15. Kirkwood J G
        J Chem Phys 1939, $\underline{7}$, 911

16. Dannhauser W and Cole R H
        J Chem Phys 1955, $\underline{23}$, 1762

17. Liszi J and Naray M
        Acta Chem (Budapest) 1974, $\underline{81}$, 11

18.. Dannhauser W and Bahe L W
        J Chem Phys 1964, $\underline{40}$, 3058

19. Garg S K and Smyth C P
        J Phys Chem, 1965, $\underline{69}$, 1294

20. Garg S K and Smyth C P
        J Chem Phys, 1967, $\underline{46}$, 373

21. Hassion F X and Cole R H
        J Chem Phys 1955, $\underline{23}$, 1756

22. Johari G P and Dannhauser W
        J Phys Chem 1968, $\underline{72}$, 3273

23. Oster G and Kirkwood J G
        J Chem Phys 1943, $\underline{11}$, 175

24. Bordewijk P, Kunst M and Rip A
        J Phys Chem 1973, $\underline{77}$, 548

25. Malecki J and Jadzyn J

      J Phys Chem 1974, $\underline{78}$, 1203

26. Campbell C, Brink G and Glasser L

      J Phys Chem 1975, $\underline{79}$, 660

27. Jakusek E and Sobczyk L - Dielectric and Related

    Molecular Processes - Vol 3

      Chemical Society, London 1977

28. Crossley J

      Adv Mol Relaxation Proc, 1970, $\underline{2}$, 69

29. Glasser L, Crossley J and Smyth C P

      J Chem Phys 1972, $\underline{57}$, 3977

30. Chekalin N V

      Zh Fiz Khim, 1971, $\underline{45}$, 452

31. Kauzmann W

      Rev Mod Phys, 1942, 14, 12

32. Bauer E

      Cahiers Phys, 1944, $\underline{20}$, 1

33. Brot C and Magat M

      J Chem Phys, 1963, $\underline{39}$, 841

34. Campbell C, Crossley J and Glasser L

      Adv Mol Relax Proc, 1976, $\underline{9}$, 63

35. Sagal M W

      J Chem Phys, 1962, $\underline{36}$, 2437

36. Hanna F F and Hakim I K

      Z Naturforsch, 1971, $\underline{26A}$, 1194 and 1972, $\underline{27A}$, 1363

37. Van den Berg J F, Michielson J C F and Ketelsar J A A

      Rec Trav Chim Pays Bas, 1974, $\underline{93}$, 104

38. Komooka H

    Bull Chem Soc Jap, 1972, <u>45</u>, 1696

39. Koshii T, Arie E, Nakamura M, Takahashi H and

    Higasi K

    Bull Chem Soc Jap, 1974, <u>47</u>, 618

40. Hasted J B - Dielectric and Molecular Processes

    Vol 1

       The Chemical Society, London, 1972

41. Hasted J B - Aqueous Dielectrics

       Chapman and Hall, London, 1973

42. Grant E H, Sheppard R J and South G P - Dielectric

    Behaviour of Biological Molecules in Solution

       Oxford University Press, Oxford, 1978

43. Malmberg C G and Maryott A A

       J Res Nat Bur Standards, 1956, <u>56</u>, 1

44. Hill N E

       Trans Far Soc, 1963, <u>59</u>, 344

45. Zafar M S, Hasted J B and Chamberlain J

       Nature, London 1973, <u>243</u>, 106

46. Afsar M N and Hasted J B

       J Opt Soc Am 1977, <u>67</u>, 902

47. Bernal J D and Fowler R H

       J Chem Phys, 1933, <u>1</u>, 515

48. Pople J A

       Proc Roy Soc, 1951, <u>A205</u>, 163

49. Bernal J D

       Proc Roy Soc, 1964, <u>A280</u>, 299

50. Haggis G H, Hasted J B and Buchanan T J

      J Chem Phys, 1952, 20, 1452

51. Eisenberg D and Kauzmann W - The Structure and

      Properties of Water

      Oxford University Press 1969

52. Pauling L - Nature of the Chemical Bond

      Cornell University Press, Ithaca, New York, 1948

53. Rahman A and Stillinger F H

      J Chem Phys, 1971, 53, 3336

54. Grant E H and Sheppard R J

      J Chem Phys, 1974, 60, 1792

55. Akerlof G

      J Am Chem Soc, 1932, 54, 4125

56. Decroocq D

      Bull Soc Chim F, 1964, 127

57. D'Aprano A

      J Phys Chem, 1974, 78, 652

58. Lippold B C and Adel B C

      Arch Pharmaz 1972, 305, 417

59. Tjia T H - Thesis

      University of Leiden, 1974

60. Hill N E, Vaughan W E, Price A H and Davies M -

      Dielectric Properties and Molecular Behaviour

      Van Nostrand, London, 1969

61. Schallamach A

      Trans Far Soc 1946, 42A, 180

62. Daumezon P and Heitz R

      J Chem Phys, 1971, 55, 5704

63. Denney D J and Cole R H

  J Chem Phys, 1955, 23, 1767

64. Chekalin N V and Shakhparonov M I

  Russ J Phy Chem, 1971, 45, 250

65. Chekalin N V and Shakhparonov M I

  Fiz Fiz Khim Zhidk, 1972, 1, 151

66. Peyrelasse J

  CR Acad Sci Ser B, 1977, 284, 185

67. Sarojini V

  Trans Far Soc, 1961, 57, 1534

68. Buck D E - PhD Thesis

  M I T 1965

69. Davies M

  Acta Phys (Pol), 1976, A50, 241

70. Shinoda K and Kunieda H

  J Colloid Interface Sci, 1973, 42, 381

71. Nakagawa T - Non-ionic Surfactants

  Ed Schick M J, Edward Arnold Publishers Ltd

  London 1967

72. Mysels K J - Introduction to Colloid Chemistry

  Wiley, New York, 1959

73. Elworthy P H, Florence A T and Macfarlane C B -

  Solubilisation by Surface Active Agents and its

  Applications in Chemistry and the Biological Sciences

  Chapman and Hall, London 1968

74. Tanford C, Nozak Y and Rohde M F

  J Phys Chem, 1977, 81, 1555

75. Tanford C

   J Phys Chem, 1974, <u>78</u>, 2469

76. Elworthy P H and Macfarlane C B

   J Chem Soc 1963, 907

77. Attwood D

   J Phys Chem, 1968, <u>72</u>, 339

78. Ottewill R H, Storer C C and Walker T

   Trans Far Soc, 1967, <u>63</u>, 2796

79. Corkill J M and Walker T

   J Colloid Interface Sci, 1972, <u>39</u>, 621

80. Staples E J and Tiddy G J T

   J Chem Soc, Far Trans I, 1978, <u>74</u>, 2530

81. Bostock T A, McDonald M P and Tiddy G J T, Discussion of
   Colloid and Interface Sci Group of Far Div of Chemical
   Society, Hull September 1978

82. Brown J B, Lapczynska I and Friberg S

   Proc Int Conf Colloid Surf Sci

   Ed Wolfram (Kiado, Budapest) Vol 1, 1975

83. Bostock T A

   (Private Communication)

84. Shinoda K and Friberg S

   Adv Coll Interface Sci, 1975, <u>4</u>, 281

85. Friberg S and Lapczynska I

   Progr Coll and Polymer Sci, 1975, <u>56</u>, 16

86. Friberg S, Lapczynska I and Gillberg G

   J Colloid Interface Sci, 1976, <u>56</u>, 19

87. Shinoda K and Kunieda H - Microemulsions Theory and
   Practice

   Ed Prince L M, Academic Press, New York and
   London, 1977

88. Schulman J H, Stoeckenius W and Prince L M

     J Phys Chem, 1959, <u>63</u>, 167

89. Shah D O, Bansal V K, Chan K and Hsieh W C -

Improved Oil Recovery by Surfactant and Polymer

Flooding

     Eds Shah D O and Schechter R S, p 293

     Academic Press, New York and London, 1977

90. Friberg S - Microemulsions

     Ed Prince L M, p 133, Academic Press, New York

     and London, 1977

91. Prince L M

     Ibid p 1

92. Kitchener J A and Mussell White P R - Emulsion

Science

     Ed Sherman P, Academic Press, London and New

     York, 1968

93. Gerbacia W, Rosano H L and Whittam J H

     Colloid and Interface Science, Ed Kerker M,

     Vol 2, p 245, Academic Press, New York, 1976

94. Prince L M

     J Colloid Interface Sci, 1975, <u>52</u>, 182

95. Eicke H F

     J Colloid Interface Sci, 1977, <u>59</u>, 308

96. Ruckenstein E and Chi J C

     J Chem Soc, Far Trans 2, 1975, <u>71</u>, 1690

97. Crooks J E

     J Colloid Interface Sci, 1978, <u>66</u>, 355

98. Shinoda K and Sagitani H

Ibid, 1978, <u>64</u>, 68

99. Shinoda K

Ibid, 1967, <u>24</u>, 4

100. Shinoda K and Ogawa T

Ibid, 1967, <u>24</u>, 56

101. Shinoda K

Ibid, 1970, <u>34</u>, 278

102. Saito H and Shinoda K

Ibid, 1971, <u>35</u>, 359

103. Kaatze U, Limberg C H and Pottel R

Ber Bunsenges Phys Chem, 1974, <u>78</u>, 561

104. Eicke H F and Shepherd J C W

Helv Chim Acta, 1974, <u>57</u>, 1951

105. Beard R B, McMaster T F and Takashima S

J Colloid Interface Sci, 1974, <u>48</u>, 92

106 Peyrelasse J, McClean V E R, Boned C, Sheppard R J
and Clausse M

J Phys D, Appl Phys, 1978, <u>11</u>, L117

107. Cavell E A S

J Colloid Interface Sci, 1977, <u>62</u>, 495

108. O'Konski C T

J Phys Chem, 1960, <u>64</u>, 605

109. Kaatze U, Göttmann O, Podbielski R, Pottel R and
Terveer U

J Phys Chem, 1978, <u>82</u>, 112

110. Kaatze U

Ber Bunsenges Phys Chem, 1978, <u>82</u>, 690

111. Tartar H V

    J Colloid Interface Sci, 1959, 14, 115

112. Anacker E W

    J Phys Chem, 1964, 68, 81

113. Schwarz G

    J Phys Chem, 1962, 66, 2636

114. Tartar H V

    J Phys Chem 1955, 59, 1195

115. Grant E H

    J Mol Biol 1966, 19, 133

116. Pennock B E and Schwan H P

    J Phys Chem 1969, 73, 2600

117. Eicke H F and Christen H

    J Colloid Interface Sci 1974, 48, 281

118. Eicke H F, Hopmann R F W and Christen H

    Ber Bunsenges Phys Chem 1975, 79, 667

119. Clausse M, Sheppard R J, Boned C and Essex C G

    Colloid and Interface Science, Vol 2, ed Kerker M

    Academic Press New York 1976

120. Hanai T

    Emulsion Science Ed Sherman P, Academic Press

    London 1968

121. Hanai T

    Kolloid Z 1961, 177, 57

122. Hanai T, Koizumi N and Gotoh R

    Kolloid Z 1962, 184, 143

123. Hanai T and Koizumi N

     Bull Inst Chem Res Kyoto Univ 1975, _53_, 153

124. Clausse M

     C R Acad Sci 1972, _274B_, 887

125. Lafargue C, Clausse M and Lachaise J

     C R Acad Sci 1972, _274B_, 540

126. Clausse M

     C R Acad Sci 1973, _277B_, 261

127. Clausse M

     Colloid and Polymer Sci 1977, _255_, 40

128. Sjöblom E and Friberg S

     J Colloid Interface Sci 1978, _67_, 16

129. Senatra D and Guibilaro G

     J Colloid Interface Sci 1978, _67_, 448

130. Senatra D and Guibilaro G

     ibid 1978, _67_, 457

131. Clausse M, Sherman P and Sheppard R J

     J Colloid Interface Sci 1976, _56_, 123

132. Peyrelasse J, Boned C, Xans P and Clausse M

     C R Acad Sci 1977, _284B_, 235

133. Fröhlich H – Theory of Dielectrics

     Oxford University Press, London 1949

134. Oster G

     J Am Chem Soc 1946, _68_, 2036

135. Cole K S and Cole R H

     J Chem Phys 1949, _9_, 341

136. Davidson D W and Cole R H

     J Chem Phys 1951, _18_, 1417

137. Powles J G

J Chem Phys 1953, 21, 633

138. Glarum S H

J Chem Phys 1960, 33, 1371

139. O'Dwyer J J and Sack R A

Aust J Sci Res 1952, A5, 647

140. van Beek K L H - Progress in Dielectrics

7, 71, Heywood, London 1967

141. Rayleigh J W

Phil Mag 1892, 34, 481

142. Wiener O

Abh sächs Akad Wiss Math-Phys Kl 1912, 32, 509

143. Runge I

Z Tech Phys 1925, 6, 61

144. Meredith R E and Tobias C W J

J Appl Phys 1960, 31, 1270

145. Bruggeman D A G

Ann Phys Lpz 1935, 24, 636

146. Looyenga H

Physica 1965, 31, 401

147. Landau L D and Lifshitz - Electrodynamics of

Continuous Media

Pergamon Press, London 1960

148. Kraszewski A, Kulinski S and Matuszewski M

J Appl Phys 1976, 47, 1275

149. Böttcher C J F - Theory of Electric Polarisation

Elsevier, Amsterdam 1952

150. Hanai T, Koizumi N, Sugano T and Gotoh R

      Kolloid Z 1960, 171, 20

151. Naiki T, Fujita K and Matsumara S

      Mem Fac ind Arts Kyoto Univ 1959, 8, 1

152. Mandel M

      Physica 1961, 27, 827

153. Maxwell J C

      Electricity and Magnetism Vol 1, Clarendon

      Press, Oxford, 1892

154. Wagner K W

      Arch Elektrotech 1914, 2, 37/

155. Hanai T and Koizumi N

      Bull Inst Chem Kyoto Univ 1976, 54, 248

156. Sillars R W

      J Inst Elec Eng 1937, 80, 378

157. Stratton J A

      Electromagnetic Theory, McGraw-Hill, New York 1941

158. Grosse C and Greffe J L

      C R Acad Sci Ser C 1976, 283, 95

159. Polder D and Van Santen J H

      Physica 1946, 12, 257

160. De Loor G P - Thesis

      University of Leiden 1956

161. De Loor G P

      J Microwave Power 1968, 3, 67

162. Pauly H and Schwan H P

      Z Naturf 1959, 14b, 125

163. Kraszewski A

    J Microwave Power 1977, <u>12</u>, 216

164. Dryden J S and Meakins R J

    Proc Phys Soc 1957, <u>70B</u>, 427

165. Chapman I D

    J Phys Chem 1968, <u>72</u>, 33

166. Le Petit J P, Delbos G, Bottreau A M, Dutuit Y

    Marzat C and Cabanas R - J Microwave Power 1977, <u>12</u>, 335

167. Reynolds J A - Thesis

    University of London 1955

168. Pradhan B P and Gupta R C

    Dielectrics 1964, <u>1</u>, 195

169. Fellner-Feldegg H

    J Phys Chem 1969, <u>73</u>, 616

170. Whittingham T A

    J Phys Chem 1970, <u>74</u>, 1824

171. Suggett A, Mackness P A, Tait M J, Loeb H W and

    Young G M

    Nature, 1970, <u>228</u>, 456

172. Loeb H W, Young G M Quickenden P A and Suggett A

    Ber Bunsenges Phys Chem 1971, <u>75</u>, 1155

173. Van Gemert M J C, De Loor G P, Bordewyk P and Suggett A

    Adv Mol Relaxation Proc 1973, <u>5</u>, 301

174. Fellner-Feldegg H

    J Phys Chem 1972, <u>76</u>, 2116

175. Van Gemert M J C,

    Philips Res Dept 1973, <u>28</u>, 530

176. Suggett A - New techniques in Biophysics and Cell
     Biology
          Ed B H Pain and B Smith, J Wiley and Sons
          London and New York 1975
177. Clark A H, Quickenden P A and Suggett A
          J Chem Soc Far Trans II 1974, 70, 1847
178. Clarkson T S, Glasser L, Tuxworth R W and
     Williams G
          Adv Mol Relax Interact Proc 1977, 10, 173
179. Giese K and Tiemann R
          Adv Mol Relaxation Proc 1975, 7, 45
180. Fellner-Feldegg H and Barnett E F
          J Phys Chem 1970, 74, 1962
181. Brehm G A and Stockmayer W H
          J Phys Chem 1973, 77, 1348
182. Shannon C
          Proc I R E 1949, 37, 10
183. Samulon H A
          Proc I R E 1951, 39, 175
184. Clarkson T S and Williams G
          Chem Phys Lett 1975, 34, 461
185. Stevens J V - PhD Thesis
          University of Sheffield 1970
186. Clunie J S, Corkill J M, Goodman J F, Symons P C
     and Tate J R
          Trans Far Soc 1967, 63, 2839
187. Tiddy G J T - Private Communication

188. Sato H, Koshii T and Takahasi H

Chem Lett 1974, 579

189. Arnoult R, Lebrun A and Boullet C

Arch Sci phys et nat (spec) 1956, $\underline{9}$, 44

190. Lebrun A,

Cahiers Phys, 1955, $\underline{60}$, 11

191. Mulley B A

Nonionic Surfactants Ed Schick M J

Edward Arnold Publishers (Ltd), London, 1967

192. Davies M, Williams G and Loveluck G D

Z Elektrochem, 1960, $\underline{66}$, 576

193. Kaye G W C and Laby T H

Tables of Physical & Chemical Constants

13th Edition, Longman, London 1971

194. Tanford C

The Hydrophobic Effect : Formation of

Micelles and Biological Membranes

John Wiley & Sons, New York & London, 1973

195. Maryott A A and Smith E R

Table of Dielectric Constants of Pure Liquids

Nat Bur Standards Circular 514, 1951

196. Handbook of Chemistry and Physics, 49th Edition

The Chemical Rubber Company, Cleveland,

Ohio, 1968

197. Bostock T A, McDonald M P, Tiddy G J T and
      Waring L

          SCI Chemical Society Symposium on Surface

          Active Agents, Nottingham, September 1979

          (Preprint)

198. Robbins M L

          ACS 48th Nat Coll Symp, Austin, 1974

          Preprints p 174

199. Mackay R A and Agarwal R

          J Colloid Interface Sci 1978, $\underline{65}$, 225

200. Winsor P A

          Chem Rev 1968, $\underline{68}$, 1

ACKNOWLEDGEMENTS

COMPUTER PROGRAM FOR FOURIER TRANSFORM (FORTRAN IV G1)

```
      DIMENSION TITLE (20)
      INTEGERZ (99)
      READ (5,1) TITLE
 1    FORMAT(20A4)
      DIMENSIONA(25),B(250), WIG(99),W(99),TC(25),TS(250)
 2R(99),C(250),D(250),UC(250),US(250),ALPHA(99),S(99),T(99)
 2EO(99),ET(99),P(250),E(250),THETA(99),PHI(99),EK(99)
 2OG(250),G(250),V(250),VC(250),VS(250),GAM(99),Y(250),RT(250)
 2DEL(250),EOR(250),ETR(250),PR(250),ER(250),OGR(250),PHIR(99)
      WRITE(6,2) TITLE
 2    FORMAT(1H1,10X,20A4//)
      WRITE(6,3)
 3    FORMAT(6X,'EO',7X,'ET',6X,"FREQ MHZ'//)
      JJ=1
      KK=1
      READ(5,10)N,X
10    FORMAT(I2,F6.3)
      WRITE(6,12)N,X
12    FORMAT(32X,'N=',I2,3X,'X/100PS=',F6.3)
      X=X/(1.E10)
      DO25I=1,N
      READ(5,20)Z(I)
20    FORMAT(I4)
      WIG(I)=Z(I)*6.2832
      W(I)=WIG(I)*1.EO6
25    CONTINUE
      READ(5,30)K,A(1)
30    FORMAT(I3,F5.2)
      WRITE(6,33)K
33    FORMAT(33X,'K=',I3)
      DO37I=2,K
      READ(5,35)A(I)
35    FORMAT(F5.2)
37    CONTINUE
      READ(5,40)M,C(1)
40    FORMAT(I3,F5.2)
      DO44I=2,M
      READ(5,42)C(I)
42    FORMAT(F5.2)
44    CONTINUE
      READ(5,45)LL,MM,KL,ML
45    FORMAT(I2,1X,I2,1X,I3,1X,I3)
46    B(JJ)=A(JJ)
47    JJ=JJ+1
48    DO50I=JJ,K
      B(I)=A(I)-A(I-1)
50    CONTINUE
      D(KK)=C(KK)
      KK=KK+1
      DO60I=KK,M
```

```fortran
      D(I)=C(I)-C(I-1)
60    CONTINUE
      JJ=JJ-1
64    DO75I=1,N
      CUM=0
      SUM=0
      L=1
      DO70J=JJ,K
      TC(J)=B(J)*(COS((L-0.5)*W(I)*X))
      TS(J)=B(J)*(SIN((L-0.5)*W(I)*X))
      CUM=CUM+TC(J)
      SUM=SUM+TS(J)
      L=L+1
70    CONTINUE
      THETA(I)=ATAN(CUM/SUM)
      R(I)=SQRT((CUM*CUM+SUM*SUM)/(2.*SIN(W(I)*X/2.))**2.)
75    CONTINUE
      KK=KK-1
      DO85I=1,N
      DUM=0
      TUM=0
      L=1
      DO80J=KK,M
      UC(J)=D(J)*(COS((L-0.5)*W(I)*X))
      US(J)=D(J)*(SIN((L-0.5)*W(I)*X))
      DUM=DUM+UC(J)
      TUM=TUM+US(J)
      L=L+1
80    CONTINUE
      TUM=ABS(TUM)
      ALPHA(I)=ATAN(DUM/TUM)
      S(I)=SQRT((DUM*DUM+TUM*TUM)/(2.*SIN(W(I)*X/2.))**2.)
85    CONTINUE
      DO100I=1,N
      T(I)=(-R(I)/S(I))
      PHI(I)=((THETA(I))-(ALPHA(I)))
      EO(I)=((1-T(I)*T(I))*(1-T(I)*T(I))-4.*T(I)*T(I)*(SIN
     (PHI(I)))*
     2(SIN(PHI(I))))/((1.+T(I)*T(I)+2.*T(I)*(COS(PHI(I))))**2.)
      ET(I)=(4.*(1.-T(I)*T(I)*T(I)*(SIN(PHI(I))))/((1.+T(I)*T(I)
     2+2*T(I)*(COS(PHI(I))))**2)
      WRITE(6,90)EO(I),ET(I),Z(I),THETA(I),ALPHA(I),R(I),S(I),T(I)
     2PHI(I)
90    FORMAT(2X,F7.3,3X,F7.3,3X,I4,3X,F7.2,3X,F7.2,3X
     2F7.2,3X,F7.2,3X,F7.2)
100   CONTINUE
      K=K-MM
      M=M-MM
      WRITE(6,120)K,M
120   FORMAT(33X,'K=',I3,4X,'M=',I3)
      IF(K.GE.LL) GO TO47
      READ(5,150,END=400)JJ,KK
150   FORMAT(I1,I1)
      IF(JJ.EQ.0) GO TO400
```

```
      WRITE(6,160)JJ,KK
160   FORMAT(34X,'JJ=',I1,3X,'KK',I1)
      K=KL
      M=ML
      GO TO46
400   READ(5,420)ES
420   FORMAT(F5.2)
      WRITE(6,422)ES
422   FORMAT(34X,'ES=',F5.2)
      WRITE(6,425)
425   FORMAT(10X,'REFCO',7X,'PERMIT'',6X,'LOG(ES-E)')
      K=KL
      DO440I=1,K
      P(I)=A(I)/C(I)
      E(I)=((1+P(I))**2)/((1-P(I))**2)
      IF(ES.GT.E(O)) OG(I)=ALOG(ES-E(I))
      WRITE(6,430)P(I),E(I),OG(I),A(I),C(I)
430   FORMAT(10X,F6.4,4X,F8.3,4X,F7.418X,F5.2,3X,F5.2)
440   CONTINUE
500   CALL EXIT
      END
```